

Aus dem Zentralinstitut für Seelische Gesundheit
Institut für Neuropsychologie und Klinische Psychologie
(Wissenschaftliche Direktorin: Prof. Dr. Dr. h.c. Herta Flor)

Evaluating Genetic Analysis and Neuroimaging Tools in Pain Research

Inauguraldissertation
zur Erlangung des Doctor scientiarum humanarum (Dr.sc.hum.)
der
Medizinischen Fakultät Mannheim
der Ruprecht-Karls-Universität
zu
Heidelberg

vorgelegt von
Kristina Geraldine Krause

aus
Düsseldorf
2017

Dekan: Prof. Dr. med. Sergij Goerd
Referentin: Frau Prof. Dr. rer. soc. Dr. h. c. Herta Flor

TABLE OF CONTENTS

Seite

ABBREVIATIONS	5
1 INTRODUCTION	1
1.1 Pain Mechanisms	1
1.2 Biomarkers, Clinical Endpoints and Surrogate Markers	5
1.3 Pain Genetics	8
1.4 Pain Phenotypes	10
1.5 Imaging Pain	13
1.6 Combining genetics and neuroimaging in search of biomarkers and mechanisms of pain and nociception – a rationale for this thesis.....	18
2 MANUSCRIPTS	21
2.1 Manuscript I: Beyond Patient Reported Pain: Perfusion Magnetic Resonance Imaging Demonstrates Reproducible Cerebral Representation of Ongoing Post-Surgical Pain	21
2.2 Manuscript II: Quantifying the test-retest reliability of cerebral blood flow measurements in a clinical model of on-going post-surgical pain: A study using pseudo-continuous arterial spin labelling	38
2.3 Manuscript III: Molecular Characterisation of blood-based Response to Surgical Trauma reveals Enriched Expression in Pain-Relevant Signaling Pathways.....	53
2.4 Manuscript IV: Negative Association Between Grey Matter Density and Sensory and Affective Pain Scores in Female Carriers of the OPRM1 118A SNP with Chronic Musculoskeletal Pain	74
3 GENERAL DISCUSSION	89
3.1 Fulfilment of quality criteria in biomarker discovery and limitations	93
3.2 General thesis conclusion	98
4 REFERENCES.....	102

5 APPENDIX	132
5.1.1 <i>Supplementary table II-1: Correlation table repeated measures interval and within-subject ICC</i>	132
5.1.2 <i>Supplementary table III-1: Differentially expressed genes post surgery</i> 133	
5.1.3 <i>Supplementary Table III-2a: ES and rank scores for genes in the osteoclast differentiation pathway</i>	148
5.1.4 <i>Supplementary Table III-2b: Es and rank scores for genes in the MAP kinase signaling pathway</i>	152
5.1.5 <i>Supplementary Table III-2c: ES and rank scores for genes in the chemokine signaling pathway</i>	159
6 CURRICULUM VITAE	164
7 DEDICATION AND ACKNOWLEDGEMENTS.....	165

ABBREVIATIONS

ACC	anterior cingulate cortex
AMY	amygdala
ASL	arterial spin labelling
BET	brain extraction tool
BOLD	blood oxygenation level dependent
BS	brain stem
CASL	continuous arterial spin labeling
CBF	cerebral blood flow
CEPH	Caucasian European, genetic HapMap population
CES-D	Center for Epidemiological Studies Depression Scale
CEU	Caucasian European, genetic HapMap population
CHB	Han Chinese Beijing, genetic HapMap population
CNS	central nervous system
CRPS	chronic regional pain syndrome
CTA	cortical thickness analysis
DFNS	German Research Network on Neuropathic Pain
DNA	Deoxyribonucleic acid
EEG	electroencephalography
FDR	false discovery rate
fMRI	functional magnetic resonance imaging
FMS	fibromyalgia syndrome
FSL	FMRIB's Software Library
GM(D)	grey matter (decreases)
GSEA	Gene Set Enrichment Analysis
GWA(S)	genome wide association (study)
HapMap	Haplotype Map; catalogue of common genetic variants in humans
HIP	hippocampus
ICC	intra-class correlation
IMPACT	Initiative on Methods, Measurement, and Pain Assessment in Clinical Trials
INS	insula
KEGG	Kyoto Encyclopedia of Genes and Genomes
LES	leading edge subset, genes before the enrichment score in GSEA
MBP	mu-opioid binding potential
MNI	Montreal Neurological Institute
MRC	Medical Research Council
MRI	magnetic resonance imaging
NICE	National Institute for Clinical Excellence
NSAID	non-steroidal anti-inflammatory drug
OPRM 1	Mu-opioid receptor 1
PAG	periaqueductal grey
pCASL	pseudo continuous arterial spin labeling
rCBF	resting cerebral blood flow
PAG	periaqueductal grey (substantia grisea centralis)
PCC	posterior cingulate cortex
PET	positron emission tomography

ROI	region of interest
S1	somatosensory cortex I
S2	somatosensory cortex II
SCL-90-R	Revised Symptom Checklist 90
SMA	supplementary motor area
SNP	single nucleotide polymorphism
STAQ	State-Trait Anxiety Questionnaire
THA	thalamus
TME	third molar extraction
ULBP	unspecific low back pain
VAS	visual analogue scale
VBM	voxel-based-morphometry

1 INTRODUCTION

The aim and purpose of this thesis was to assess the combination of genetic and neuroimaging techniques and to evaluate their utility in the exploration of mechanisms underlying pain resulting from tissue and nervous system injury. This thesis adhered to the recommendations for implementing clinical trials from a mechanism-based perspective (Woolf & Max, 2001) in designing the two studies which served as the foundation for the four manuscripts comprised in this thesis.

This thesis investigated three patient cohorts, i.e. dental patients with recurrent pericoronitis in need of third molar extraction (TME) and patients diagnosed with either fibromyalgia syndrome (FMS) or unspecific low back pain (ULBP) in a combined analysis. The first study of this thesis, which utilized TME as a model for tissue injury pain, included a micro-array gene expression analysis of ribonucleic acid (RNA) extracted from samples of peripheral whole blood taken pre and post surgery in combination with pre- and post-surgical functional magnetic resonance imaging (MRI) assessments of cerebral blood flow (CBF).

The second study analysed the effect of a common single nucleotide polymorphism (SNP) from the mu-opioid receptor 1 (*OPRM1*, rs1799971) on grey matter (GM) density in response to FMS and ULBP as a model of nervous system injury pain by means of voxel-based morphometry (VBM).

This thesis will first present an overview of the general topic by providing an introduction to the rationale behind and advances in research towards a mechanism-based classification of pain with special regard to the concept of biological markers. It will introduce essential concepts and technologies in neuroimaging and genetics research and the use of TME as a suitable model of post-surgical pain to provide a framework within which the studies conducted for this thesis can be integrated. This will be followed by the four manuscripts and a summary of the findings and a final discussion of the results.

1.1 Pain Mechanisms

The Austrian philosopher Ludwig Wittgenstein (2003) proposed a famous thought experiment:

Suppose everyone had a box and inside the box was something we call “beetle”. Nobody can peek into the box of another; and everybody claimed to know what a beetle was, from looking at their beetle. Thus it could be that everyone has something completely different in their box. One could imagine that such a thing changes constantly. But if the word “beetle” had a use? It would not be the meaning of the thing. (Wittgenstein, 2003) (§ 293.)

While Wittgenstein’s thought experiment can be applied to all cognitive phenomena, it has special resonance with reference to pain and its treatment. It highlights the inter-individual variability and subjective nature of the experience of pain and summarises the key problem for anyone involved in researching or treating it.

Pain is a highly subjective and complex sensation and emotion. The International Association for the Study of Pain defines it as a bio-psycho-social construct, “an unpleasant sensory and emotional experience associated with actual or potential tissue damage, or described in terms of such damage” (Mersky & Bogduk, 1994).

The complexity of pain manifests in the variability encountered in several aspects of pain and its measurement. In experimental settings the noxious stimuli are clearly defined and applied in different modalities such as pressure (Nussbaum & Downes, 1998), heat (Rosier, Iadarola, & Coghill, 2002; Yarnitsky, Sprecher, Zaslansky, & Hemli, 1995), cold (Chen, Dworkin, Haug, & Gehrig, 1989) and ischemic pain (Rainville, Feine, Bushnell, & Duncan, 1992), allowing for standardised measurement of the effects on the research participant.

However, more pressing problems arise in the clinical context, where the origin of the pain experience is often unclear, pain may have turned chronic, the need to resolve it is great and judgements regarding the nature of a patient’s pain experience for correct diagnosis and initiation of appropriate treatment or recommendations in disability and compensation claims are demanded.

There is a recognized need to open the lid and take snapshots of the contents of Wittgenstein’s proposed boxes (Chapman et al., 1985) that can be shared among clinicians and researchers as to independently arrive at the same classification of the individual content across medical specialties.

The beetle in the box problem in pain is most strikingly illustrated by problems in functional pain diagnoses such as fibromyalgia and irritable bowel syndrome (Nimnuan, Rabe-Hesketh, Wessely, & Hotopf, 2001), which do not feature tissue trauma or noxious stimuli. Oftentimes the differential diagnosis relies on the topography of the pain phenotype in question and the medical specialty consulted and not on the actual pathology (Woda et al., 2005). Current descriptors of categories of chronic pain such as chronic vs. acute, benign vs. malignant or the body part in which the pain occurs have limited utility in determining the real nature of the “beetle” inside the box. These shortcomings of current classification systems in pain have stimulated efforts in the late 1990s and early 2000s to move towards a mechanism-based approach in diagnostics and treatment (Woolf et al., 1998; Woolf & Max, 2001).

The search for mechanisms has special relevance with regard to the development of pharmaceutical interventions in pain. The developmental process of most pain medications in use today has followed a purely phenomenological approach (Bunge, 1963), in which the medication served as an input into a black box and pain relief was the output achieved by medications that were then successfully released onto the market. It has been argued that due to this approach most new analgesics are merely derivatives of already established drug classes such as nonsteroidal anti-inflammatory drugs (NSAIDs) and opioid analgesics (Max & Stewart, 2008b). Mechanism-oriented research could mean a move away from serendipitous findings and off label prescription of drugs approved for other disorders, such as anti-depressant use in chronic pain (Fishbain, 2000; Jung, Staiger, & Sullivan, 1997).

Only recently has the lid been lifted off the box containing the mechanisms of NSAIDs, which have been released long prior to the discovery of their mechanisms

(Sneader, 1997). The discovery of the inhibitory effects of cyclooxygenase-2 (COX-2) on pro-inflammatory mediators (Moncada, Ferreira, & Vane, 1975; Vane, 1971; Xie, Chipman, Robertson, Erikson, & Simmons, 1991) has enabled the development of a more specific type of NSAIDs, COX-2 inhibitors. However, there are still further unidentified contents in this box, which became apparent when the COX-2 inhibitor Rofecoxib was taken off the market in 2004 (Kearney et al., 2006), after findings of unwanted cardio-vascular complications in patients on this medication (Yu et al., 2012).

The mechanism-based approach also aims to increase reliability in diagnoses by using only truly functional criteria in combination with a distinct set of inclusion and exclusion criteria to deal with nosologic overlap between disorders. This problem surfaces as phenotypic heterogeneity, an issue which will be explored in more detail in the genetics section, as this is one of the major challenges in genetic association studies. To this end, the mechanism-based approach as defined by Woolf et al. (2000) proposes four distinct levels at which the pain experience can be characterised. It sets out with a disease, injury or diathesis, which affects different mechanisms. These mechanisms then determine the observable symptoms and several symptoms can then be clustered together to signify different syndromes. Treatment is applied at the mechanism level, while improvement or exacerbation can be measured at the symptom level (Woolf, 2004).

As a phenomenon that is determined by social, psychological and biological processes, pain requires a wide array of measurements at the symptom level in order to encompass all relevant facets. This is reflected by efforts to establish standardised assessment batteries by different research consortia such as German Research Network on Neuropathic Pain (DFNS) (Rolke, Baron, et al., 2006a; Rolke, Magerl, et al., 2006) or the Initiative on Methods, Measurement, and Pain Assessment in Clinical Trials (IMMPACT) (Dworkin et al., 2005; Turk et al., 2003). The latter, for example, recommends six core outcome domains consisting of (1) pain; (2) physical functioning; (3) emotional functioning; (4) participant ratings of improvement and satisfaction with treatment; (5) symptoms and adverse events; and (6) participant disposition.

These outcome domains mainly focus on physical/functional and psychological aspects of pain by making use of psychometric and psychophysical tools, which include numeric or visual analogue rating scales (Dworkin et al., 2005; Jensen, Karoly, & Braver, 1986; Price, Bush, Long, & Harkins, 1994; Victor et al., 2008) and questionnaires such as the McGill Pain Inventory (Melzack, 1975; Melzack, 2005), diagnostic questionnaires for specific disorders such as temporomandibular joint and other disorders (Diatchenko et al., 2005; Gonzalez et al., 2011). Other pain-associated psycho-social and psychological constructs such as depression (Beck, Steer, & Carbin, 1988; Weissman, Sholomskas, Pottenger, Prusoff, & Locke, 1977), fear of movement or pain (McCracken, Zayfert, & Gross, 1992; Mcneil, 1998), catastrophising and coping (Flor, Behle, & Birbaumer, 1993; Jacobsen & Butler, 1996; Sullivan, Bishop, & Pivik, 1995) and/or impact of pain on the quality of life such as the SF-36 (McHorney, Ware, & Raczek, 1993; Ware & Sherbourne, 1992) are often measured as well.

If we are to gain insight into patients' Wittgensteinian boxes and with an eye towards patient benefit in clinical trials, these outcome measures are essential in the context

of clinical endpoints, which will be defined in more detail in the following chapter. However, they have to be complemented by biological markers such as neural correlates, psychophysical parameters and molecular endpoints (e.g. genetic variants and gene expression levels), if the aim is a comprehensive search for pain mechanisms.

Examples of psychophysiological measures include measurements of pain thresholds and tolerance for different pain modalities such as pressure pain (Ohrbach & Gale, 1989a, 1989b), heat pain (Yarnitsky et al., 1995) and the use of comprehensive quantitative sensory testing batteries (Hansson, Backonja, & Bouhassira, 2007; Juhl, Jensen, Norholt, & Svensson, 2008; Rolke, Baron, et al., 2006b; Rolke, Magerl, et al., 2006).

The genomic revolution has also opened up new technologies in the quest for biomarkers (Klapa & Quackenbush, 2003), which allow for a thorough search for pain-related genes and their effect on pain, nociception and the effects of analgesics (J S Mogil, Yu, & Basbaum, 2000; Jeffrey S. Mogil, 2009). In addition, neuroimaging techniques such as positron emission tomography (PET) (Di Piero et al., 1991; Jääskeläinen et al., 2001; Jones, Watabe, Cunningham, & Jones, 2004; Willloch et al., 2004b), MRI (Borsook, Moulton, Schmidt, & Becerra, 2007; Davis, Kwan, Crawley, & Mikulis, 1998; Davis & Moayedi, 2013; Flor, Braun, Elbert, & Birbaumer, 1997; Owen, Bureau, Thomas, Prato, & Lawrence, 2008) or electroencephalographic (EEG) studies (Malver et al., 2014; Prichep, John, Howard, Merkin, & Hiesiger, 2011; Schulz, Zherdin, Tiemann, Plant, & Ploner, 2012) promise great potential with regard to identifying neural correlates of pain and the mechanisms by which they are regulated. The aim of this study was to determine the utility of specific genetic and MRI markers in search of pain mechanisms.

Positive aspects of the new perspective opened by a mechanism-based approach are that it will potentially lead to the development of drugs that target distinct mechanisms, inform new guidelines for experimental design in clinical research, and deliver more reliable and valid diagnostic tools for clinical investigation and treatment through selecting treatments that interact with specific mechanisms.

While all of these aspects are desirable, the identification of pain-mechanisms and subsequent development of mechanism-based treatments faces several challenges: first, pain patients' suffering may arise from a mix of mechanisms, which may act in parallel or even interact. In addition, they are often diagnosed with co-morbidities, adding further confounding factors (Buse, Manack, Serrano, Turkel, & Lipton, 2010) likely to obscure potential findings in the search for pain-specific mechanisms. This issue greatly affects the search for pain genes and will be explored in more detail in the genetics chapter, where the concept of polygenicity and a distinction between disease and pain susceptibility genes will be elucidated.

However, once identified and met by a suitable intervention, application of this intervention would bring relief to sufferers across different disorders in which that same mechanism is at work. The ability to identify the contribution of any one mechanism might enable the reduction of the number of contributors in multi-mechanism pain scenarios and thus aid the discovery of further underlying mechanisms.

The disentanglement of different pain mechanisms is most likely to be achieved if sound quality criteria are rigorously incorporated into studies in search of pain mechanisms. These criteria include reliability, which means that the patient can be sure that the disorder and its underlying mechanisms are given the same diagnosis by different clinicians. Further quality criteria also include first generalizability, where the same mechanism is recognized for the same diagnosis in mild as well as severe forms and second comprehensiveness, which allows for every necessary diagnosis to be included in a classification system. The last quality criterion is validity, which is defined as the degree of achieving the objective of a study (Büttner, 1997) and pertains to the ability with which a diagnostic measure can answer a medical question. Usually this is achieved by employing a gold standard model of a disorder. However, since many of the mechanisms underlying pain are yet unknown, alternatives to a gold standard model can be found in studies of biological markers, history and treatment response and symptom clusters.

1.2 Biomarkers, Clinical Endpoints and Surrogate Markers

This section will describe different concepts of biomarker research and their associated strengths and limitations in general and in the context of pain. For this purpose this chapter will start with definitions and move on to biomarker classifications and the associated advantages and caveats.

Definitions

The term biomarker is a commonly used contraction for a biological marker. The biomarker concept is usually discussed in association with two other concepts: the clinical endpoint and surrogate endpoint.

Atkinson et al. (2001) defined a biomarker as “a characteristic that is objectively measured and evaluated as an indicator of normal biologic processes, pathogenic processes, or pharmacologic responses to a therapeutic intervention.” This definition has also been adopted by the National Institute of Health Biomarkers Definitions Working Group and represents the narrowest definition of the concept (Lesko & Atkinson, 2001).

A clinical endpoint fulfils the same requirements as a biomarker with regard to objectivity and quantifiability of biological processes, but it also takes into account, how a participant in a clinical trial feels, functions or survives (Lesko & Atkinson, 2001). It is thus more comprehensive, because in addition to biological and physiological features it also refers to psycho-social characteristics of a given disorder. The aforementioned IMMPACT criteria are an example of such clinical endpoints. It follows, that research using clinical endpoints is more likely to yield the most reliable results in search of pain mechanisms. Ideally biomarkers and/or surrogate markers should be derived from the study of clinical endpoints. However, acquiring extensive data sets with detailed clinical endpoints in large clinical trials is expensive and time consuming.

The surrogate endpoint represents a compromise between a clinical endpoint and a biomarker. It is defined as a biomarker, which is used as an outcome in a clinical trial with the intent to serve as a substitute for a clinically meaningful endpoint. The

purpose here is to predict the effect of a therapeutic intervention (Lesko & Atkinson, 2001).

This is justified, if a biomarker consistently and accurately predicts a clinical outcome. It can thus be used as a stand-in for a clinical endpoint, which has several advantages associated with it. For example, a surrogate endpoint may occur more frequently than a bona fide clinical endpoint such as survival or total remission. Hence, the use of a surrogate endpoint allows for smaller sample sizes, more efficient studies and interim analyses, while a larger dataset is being acquired (e.g. within the framework of a longitudinal, cross-generational study) (Aronson, 2005).

Biomarker classification

Further differentiation between three types of biomarkers has been suggested (Frank & Hargreaves, 2003). Here biomarkers can range from type zero to type two. Within this classification, type 0 biomarkers are defined as measures of the natural history of disease (i.e. symptoms, which manifest over the full range of disease states), which also correlate longitudinally with clinical symptoms or indices. Type I biomarkers determine the biological effect of a therapeutic intervention with regard to the mechanism of action. However, the exact nature of the mechanism's association with clinical outcomes may not be known. Type II biomarkers are defined in differentiation from clinical endpoints. They are considered surrogate endpoints, because a change in a type II biomarker predicts clinical benefit.

Advantages and caveats

There are several advantages, but also caveats to the use of biomarkers. The promise of biomarkers is, that they achieve a reduction in complexity and enable an intervention at the mechanism level, even before the actual pathology mechanism is fully understood. Thus, the biomarker concept is considered to be most useful in the early phases of drug development, where measurement of clinical endpoints may be too time-consuming, cost-intensive or difficult.

Biomarkers offer an economical alternative to a full clinical trial with regard to proof of concept or dose-ranging information in the early stages of drug and intervention development (Frank & Hargreaves, 2003) by reducing ever increasing opportunity costs (DiMasi, Hansen, & Grabowski, 2003). This reduction may free funds for the development of so called orphan drugs and other interventions for rare disorders of low interest for the private sector from a commercial perspective (Stevens et al., 2011).

At the point of care, biomarkers can help reduce the cost for diagnostic assessment for example by monitoring them in blood from routine blood screens and thus help patients forego more hazardous medical examinations such as exposure to ionizing radiation as part of some imaging techniques (Huckins et al., 2013).

Biomarkers also serve as a screening tool for primary prevention and pre-symptomatic treatment. An example of this is a germline mutation in *BRCA1*, which predicts an 83% cumulative risk of onset of breast cancer by the age of 70 and subsequent ovarian cancer in its female carriers (Ford, Easton, Bishop, Narod, & Goldgar, 1994). Biomarkers can also be used in the evaluation of drugs and other

therapeutic interventions. If appropriately validated biomarkers demonstrate them to be effective, they can be tested more extensively in a standard clinical trial procedure. In pain research one such example is the melanocortin-1 receptor, which was first validated as a pain-relevant genetic locus in mice (Mogil et al., 2003).

Caveats of the biomarker approach stem from two sources. One is inherent in the approach itself: the reduction of complexity of the biomarker concept is its greatest advantage, but at the same time its greatest limitation. It potentially bears risks of producing false negative and false positive results in comparison to using conventional clinical endpoints.

Another caveat is found in potential legal issues regarding intellectual property in collaborative efforts between industry and academia with regard to patenting and licensing, where royalties for use of patented biomarkers or biomarker identification procedures may be due. This may hamper or drive up the cost of biomarker research and development of drugs or interventions (Esmond, 2001; Stevens et al., 2011).

A further caveat is a potential discrepancy between changes in biomarkers or surrogate endpoints and the true clinical outcome, where either false positive or false negative findings are possible challenges.

In case of a false positive result the biomarker or surrogate endpoint does not necessarily predict useful clinical outcomes with regard to wellbeing or functioning of a patient or group of patients. There may be a positive association between the biomarker and the intervention, but it may fail to translate into a clinical benefit. As previously mentioned, the melanocortin-1 receptor was identified as a relevant biomarker for the efficacy of kappa-opioidergic analgesics in rodents and demonstrated similar effects in humans. Tachykinin NK₁ receptor antagonists, which demonstrated inhibition of pain behaviour in rodents, however, have failed to demonstrate inhibitory effects on pain transmission in human (Hill, 2000).

Two strategies have proven useful in controlling for these scenarios: First, biomarker research would ideally be designed to simultaneously measure both surrogate outcomes and true clinical endpoints or derive biomarkers from the study of clinical endpoints in demonstrating that a treatment was effective at achieving its aim and purpose. However, this would eliminate the time- and cost-effectiveness advantage of the biomarker approach.

Another method for controlling for false positive and false negative results is for research involving biomarkers or surrogate endpoints to incorporate panels of biomarkers that can reflect more adequately the full spectrum of relevant potential therapeutic and/or harmful effects. A panel of biomarkers can increase the effectiveness of prediction of pathology and inform treatment allocation. One such example is found in the evaluation of a panel of demographic, blood serum and electrocardiographic biomarkers, which was evaluated with regard to chest pain as an indicator of an impending major adverse cardiac event (Than et al., 2011). This biomarker panel served to prioritise patients with regard to and correctly identify patients suitable for timely discharge and those who require more extensive treatment to prevent serious health problems.

The purpose of this thesis was an evaluation of a combination of genetic and neuroimaging biomarkers with regard to their potential to increase the probability of uncovering mechanisms relevant to pain and nociception. The following sections will provide an overview of the genetic and neuroimaging techniques and technologies used to provide a framework for the actual studies included in this thesis.

1.3 Pain Genetics

Overall, medical research has embraced the concept of genes as biomarkers and genetic methodologies and has eagerly incorporated them into their investigative efforts. In cancer research for example; more than 3,000 microarray studies alone were published in this field in 2003 (Brentani et al., 2005). Compared to cancer however, genetic methodologies in pain research slowly increased in the early 2000s (Bradshaw, Nakamura, & Chapman, 2005).

One reason for this might be the late discovery of genetic contributions to pain, which can be attributed to several factors: First, to this day pain is often viewed in terms of an accompanying symptom in the context of other disorders and health problems such as breakthrough pain in cancer patients (Portenoy & Hagen, 1990) or pain resulting from surgery (Visser, 2006). In some painful disorders such as arthritis (The Wellcome Trust Case Control Consortium, 2007) and headaches (Allegra et al., 2009; Gervil, Ulrich, Kyvik, Olesen, & Russell, 1999; Larsson, Bille, & Pedersen, 1995; Spector, Cicuttini, Baker, Loughlin, & Hart, 1996), somatic aspects such as inflammation or vascularisation take the foreground.

Second, in spite of familial clustering of some pain disorders, the pain response was generally not viewed in terms of a heritable trait until Devor and Raber first demonstrated a substantial genetic contribution to pain-related autonomy behaviours in a neuropathic mouse model of pain in 1990 (Devor & Raber, 1990).

In addition to extensive animal research, in which heritability of pain phenotypes was established in different strains of rodents (LaCroix-Fralish, Ledoux, & Mogil, 2007; Mogil et al., 1999; Jeffrey S Mogil, 2009), studies of pain in families (Turk, Flor, & Rudy, 1987) demonstrated the involvement of genetic factors in addition to environmental conditions. Twin studies in the 1990s further supported the notion of a genetic component in several painful clinical disorders and response to experimental pain stimuli (Norbury, MacGregor, Urwin, Spector, & McMahon, 2007) in humans. Heritability of 50% and more has been reported for various pain phenotypes such as back pain (Bengtsson & Thorson, 1991), dysmenorrhoea (Treloar, Martin, & Heath, 1998) and irritable bowel syndrome (Morris-Yates, Talley, Boyce, Nandurkar, & Andrews, 1998). But there was also evidence against genetic influences in some types of pain. An experimental twin study of pressure pain even arrived at the conclusion that environmental factors outweighed genetic factors (MacGregor, Griffiths, Baker, & Spector, 1997).

Devor was also the first to coin a definition for what constitutes a pain gene (Devor, 2010) (p.229): "A pain gene is a gene for which there are one or more polymorphisms (i.e. variations in the sequence of DNA base-pairs) that affect the expression or the functioning of its protein product in a way that affects pain response." This pain gene definition signifies a hypothesis-driven approach regarding the specific manifestation of a gene as a phenotype. This is appropriate for obvious targets such as genes

involved in central and peripheral nervous signal transduction and receptors for pain peptides.

However, due to the close association between diseases and pain, Devor further distinguished between “disease susceptibility genes” and “pain susceptibility genes” in addition to “pain genes”. Associations with disease susceptibility genes would enable a more accurate estimation of epidemiological risks to develop clinically relevant pain for their carriers. However, these genes might not be informative regarding the pain itself. According to Devor, a scenario in which three different disorders produce the same type of neuropathic pain (wearing constricting footwear, pressure from tumour tissue extension, and disc herniation) (Devor, 2010) is possible. Among geneticists this problem is known as locus heterogeneity (Gulcher, Kong, & Stefansson, 2001), which means that risk variants of different genes can cause the same phenotype, in this case neuropathic pain.

The field of genetics as such has made enormous progress and has taken less than 100 years from the introduction of the term “genetics” by William Bateson in 1905 (Harper, 2005) to describe general principles of heritability to the publication of the sequence of the entire human genome in 2001 (Venter et al., 2001). Today the term genotype refers to the genetic constitution of an organism, which is stored internally as deoxyribonucleic acid (DNA), a molecule that contains an organism’s genetic code and determines the hereditary potentials and limitations of that organism (Malats & Calafell, 2003).

Complementary to the concept of the genotype, the term phenotype was first introduced by Wilhelm Johannsen in 1909 to describe the manifestation of the genotype (Churchill, 1974). More precisely, the phenotype is defined as an individual characteristic or a composite of an organism’s observable characteristics or traits.

Research on the association between pain genes and pain phenotypes can be performed on different levels. The simplest distinction is made between structural and functional genetic studies, and has implications with regard to the tissues and substrates to be investigated. Structural studies are concerned with the DNA sequence and its potential variations. Functional studies investigate the dynamic translational processes that occur en route from genotype to phenotype. These studies involve differences in gene expression levels dependent on various factors such as genotype, epigenetic changes in DNA (Holliday, 2006) or events that trigger transcription changes.

Genetic material for such analyses can be gained from different sources and acquisition varies with regard to invasiveness of the sampling material and method. The least intrusive method is the use of saliva or buccal swab samples. A better yield of DNA and RNA is usually gained from blood samples, which require venepuncture, which was the sampling method employed for this thesis. RNA extracted from biopsy samples from oral mucosa have been used in previous studies to investigate gene expression changes in response to oral surgery and/or administration of Rofecoxib (Wang et al., 2007; Warburton et al., 2005). The disadvantage here is that the tissue will be (re-)traumatised, if the biopsy is taken post surgery, causing the participant discomfort in addition to the initial surgery.

Once heritability was established for pain phenotypes and samples are acquired, the next step is to identify the actual genes responsible.

There are two main modes of inheritance, which inform the choice of experimental designs. Some pain-related genes cause rare Mendelian disorders, which follow inheritance patterns first described by Gregor Mendel (Mendel, 1866). The key features of Mendelian traits are that they are determined by just one gene and that the trait occurs in all carriers of that particular gene. This is referred to as complete penetrance. If a particular gene or a specific mutation therein, is solely responsible for a disorder, this disorder is classified as a “monogenic disorder”. Examples include certain congenital insensitivities to pain (Auer-Grumbach, 2008; Lafreniere et al., 2004; Oertel & Lötsch, 2008), which are prime examples for Devor’s pain gene concept.

The other mode of inheritance is a polygenic pattern, where several genes and possible mutations therein contribute to a specific phenotype. These genes are referred to as quantitative trait loci (QTL) (Plomin & Crabbe, 2000).

In contrast to monogenic disorders, the QTL perspective postulates that phenotypes follow a normal distribution due to their polygenic origin, where several genes each make smaller contributions to a phenotype. Other than in a Mendelian one gene one disorder scenario, where a disorder is either present or absent, this mode of inheritance enables a focus on both ends of the distribution. Genes contribute to normal variation, but contributions to the extreme ends of the distribution, make them either factors for illness, disability or vulnerability or factors for health, ability and resilience.

In DNA analyses QTLs are best detected in case-control studies of unrelated individuals (Risch & Merikangas, 1996). They compare cases, i.e. patients with specific pain phenotypes, to matched healthy control participants. This approach has been used to identify risk genes in chronic pain phenotypes such as fibromyalgia, irritable bowel syndrome, migraine and rheumatoid arthritis (Sikander et al., 2010; S. Smith & Maixner, 2012; Vargas-Alarcón et al., 2009; Yu, Huang, Wu, Wu, & Tsai, 2004). In functional analyses differential expression would be expected between pain-free and painful states. However, there are some pitfalls to be avoided when selecting populations and phenotypes.

1.4 Pain Phenotypes

The phenotype is the description of the outward appearance of the contents of the Wittgensteinian boxes. The more detailed the description, the better the chances of identifying boxes with similar or identical contents and for discovering the mechanisms by which these contents operate.

The concepts of the phenotype and clinical endpoints greatly overlap, as they both measure an organism’s characteristics. However, the phenotype definition is less focused on processes than the definition of the clinical endpoint. It is often a set of relatively static characteristics such as duration of painful episodes or their frequency, age of onset and common qualitative pain descriptors (e.g. searing, burning, etc.). A phenotype can pertain to the features or symptoms of a syndrome in clinical studies of a specific disorder, but can also include response to an intervention in a treatment

study, e.g. when looking at responders vs. non-responders to various drugs. And although phenotyping and measurement of clinical outcomes are usually the most cost- and labour-intensive aspects of any study, they are also the most crucial for the success of clinical trials and genetic association studies. Measurement errors diminish overall statistical power and can prevent the detection of true associations in addition to wasting funds.

Characterisation of a phenotype should be as exhaustive as possible, in order to allow for analysis of potential mediating factors that are not rooted in the genetic make up of an individual (e.g. previous injuries and tissue trauma in CRPS patients for correct allocation to patient groups).

Another option is the use of so called endophenotypes. Endophenotypes are hereditary characteristics that are associated with some condition, but are not a direct symptom of that condition. Endophenotypes are specific variants of a biomarker in genetic epidemiology and represent intermediate phenotypes not as readily observable as the symptoms of a disorder (e.g. cerebral blood flow changes). Similar to the biomarker, the use of an endophenotype reduces complexity at the syndrome level and thus increases power to detect associated genes (Gottesman & Gould, 2003). Genetic association studies have been conducted in post-surgical pain (Kim & Lee, 2009; Kim, Lee, Rowan, Brahim, & Dionne, 2006), CRPS (Huehne et al., 2010), Fibromyalgia (Solak et al., 2014; Vargas-Alarcón et al., 2007) and other pain disorders.

In addition, complex pain syndromes harbour potential risk of missing suitable genetic targets in search of mechanisms due to other confounding factors: Pain is usually experienced as a symptom of various diseases and disorders, thus making it difficult to identify pain genes as defined by Devor. The difficulty lies in distinguishing genes associated with a disease from those specific to the pain experience.

In order to break down the level of phenotype complexity, another strategy is to employ standardised, evoked painful stimuli and compare patients or participants and their responses by genotype. For example, associations between pain phenotypes such as pressure sensitivity, thermal, ischemic, and mechanical stimuli with SNPs from the Catechol-O-methyl transferase (*COMT*) and *OPRM1* genes (Diatchenko et al., 2006; Roger B Fillingim et al., 2005) have been reported. In some cases quantitative sensory (QST) assessments such as laser evoked potentials allow identification of subpopulations within patients with the same diagnosis (i.e. peripheral and central neuropathic pain (Cruccu et al., 2004)) and thus help to discover the genetic diversity underlying different types of pain.

Particular attention needs to be paid to the concept of population stratification, a term that describes systematic differences in allele frequencies between subpopulations in a population due to different ancestry, known as genetic admixture. This concept is particularly relevant in the context of association studies with participants from ethnically diverse populations (Devlin & Roeder, 1999; Devlin, Roeder, & Wasserman, 2001). An example of this is a finding in Pima and Papago Native Americans with and without diabetes. The difference was the result of genetic admixture in the control participants from European ancestry in which these genetic variants are less frequent for other reasons than these genes, but in whom diabetes

is also less frequent than in Native Americans (Knowler, Williams, Pettitt, & Steinberg, 1988).

The population stratification can be controlled for by utilising markers for which ethnicity-dependent differences in frequencies have been demonstrated in genomic studies, which are referred to as ancestry informative markers (Halder, Shriver, Thomas, Fernandez, & Frudakis, 2008). Subsequently, one can either correct statistically for this effect or include only one specific ethnicity in the analysis or perform separate analyses for each subpopulation. In candidate gene studies participants should be selected from ethnically uniform backgrounds.

Genetic technologies have different profiles with regard to scope and resolution of a planned study. At the low resolution end of the spectrum, linkage studies indicate the location of a target gene within a section of the genome (Roberts, MacLean, Neale, Eaves, & Kendler, 1999) and at the high resolution end of the spectrum sequencing technologies provide the exact sequence of the entire genome (Mardis, 2008).

What type of genetic technology to use, depends on the study design. The majority of genetic studies in pain have used selected candidate genes, because they were driven by specific hypotheses. For example, extensive work has been conducted on *OPRM1* and, in particular, on a SNP at position 118 in the gene coding for this receptor. This SNP is considered to be a functional SNP, because it causes a substitution of the wild-type A-allele by the G-allele, which effects a difference in the amino acid chain of the receptor molecule (Lötsch, Geisslinger, & Tegeder, 2009a; Mura et al., 2013).

As a primary target site for various opioid ligands, questions regarding the consequences of this functional change in *OPRM1* have been addressed by employing several pharmacodynamic and pharmacokinetic phenotypes on opioid potency (Lötsch, Stuck, & Hummel, 2006), including metabolite toxicity, pupil dilation (Lötsch, Zimmermann, et al., 2002) and receptor affinity (Bond et al., 1998a).

Modern high throughput microarray technology has enabled the transition beyond small sets of candidate genes towards a more exhaustive whole genome approach for both DNA and RNA in man and animals (Gillet, de Longueville, & Remacle, 2006; Nijman, Kuipers, Verheul, Guryev, & Cuppen, 2008). This is an advantage with regard to investigating common pain disorders and their progression, which are most likely of a poly-mechanistic and polygenic nature with many yet unidentified genes.

However, due to the cost, only two of the many possible phenotypes to date, rheumatoid arthritis and postsurgical pain have been examined in large genome wide association (GWA) studies (Gregersen et al., 2009; The Wellcome Trust Case Control Consortium, 2007). The use of microarrays is more frequent in pharmacogenomic studies of RNA, where an intervention is expected to affect more than one marker of interest and use of panels of biomarkers for other clinical endpoints such as cytokines are common (Slade et al., 2011).

With regard to clinical practice the study of genetic variation potentially promises individualised, allele-specific medicine with genotype-informed diagnoses and drug prescription practices. Ethnicity-dependent differences in the frequency of polymorphisms in genes encoding enzymes and drug transporters have been shown

to affect pharmacokinetic phenotypes such as metabolic capacities for various drugs. Hence some drugs (e.g. opioids, debrisoquine, etc.) are less effective in some populations than others. These pharmacogenetic differences already inform prescription recommendations for some medications in the USA and Japan (Ozawa et al., 2004).

In summary, if one is to discover “true pain-related genes”, careful conceptualisation of genetic studies is of utmost importance and hinges on several components. Parameters to be considered when designing a genetic study include population, tissues, substrate, phenotype selection and scope. An endophenotype/biomarker approach promises reduced phenotype complexity and increased power for discovery of pain and pain susceptibility genes.

1.5 Imaging Pain

Wittgenstein’s box analogy and the inability of introspection to capture objective features of a phenomenon resonated with the view of the behaviourists of the early 20th century, who considered the brain a black box, since there were no technologies to observe the inner workings of the brain in action and in vivo apart from reaction (time) experiments (Watson, 1913).

Today’s definition of pain includes the subjective experience not by simple introspection, but by employing a wide variety of imaging modalities to study neural correlates of pain in combination with psychometric measures. Neuroimaging techniques can be used to explore functional and/or anatomical aspects of pain processing, even though this had not been the express purpose at the time of their development. They have opened up new vistas of the brain during the experience of pain (Schweinhart & Bushnell, 2010).

The use of neuroimaging techniques has undergone a development similar to that of genetic technologies in the context of pain research. The brain as a central component in pain perception had been neglected, because during the first half of the 20th century it was believed that pain did not have any important cortical representations beyond the somatosensory cortex (Head & Holmes, 1911; Wilder Penfield & Boldrey, 1937). The parietal operculum and posterior insula, both brain areas which are involved in generating painful sensations in response to electrical stimulation, and the thalamus received some attention (Mazzola, Isnard, Peyron, & Mauguire, 2012), but inspired no further interest in brain-related pain research.

Neuroimaging techniques have evolved from Electroencephalography (EEG), initially developed in the 1920s by Hans Berger (Berger, 1938). With few EEG studies in pain in the 1950s, investigating headaches and migraine (Apley, Lloyd, & Turton, 1956; Ulett, D, & O’Leary, 1952). EEG has high temporal, but low spatial resolution and is less informative with regard to subcortical structures. Then Positron Emission Tomography (PET) emerged in the late 1950s (Bonte, 1976) and employs a glucose analogue marked with a radioactive tracer. The first functional neuroimaging study in pain used a heat pain paradigm in healthy volunteers in combination with functional magnetic resonance imaging (fMRI) for better stereotactic localisation (Talbot et al., 1991). Other radioactive tracers have enabled the study of brain functions in pain, such as cortical activation in response to pressure pain (Wey et al., 2014), acute pain post dental extraction (Derbyshire, Jones, Collins, Feinmann, & Harris, 1999), pain threshold testing (Vogt, Derbyshire, & Jones, 1996), opioid-binding in central post

stroke pain (Willoch et al., 2004b) and the role of the dopaminergic system in chronic pain (Jääskeläinen et al., 2001). However, this technology has low temporal resolution, because it takes a certain amount of time for tracer fluids such as flourodeoxyglucose to be absorbed by the body and to accumulate in brain areas, where the glucose is metabolised in response to activation (Engel et al., 1996). The tomographic device registers the positrons emitted by the decaying tracer. The use of radioactive tracers also limits the number of applications of PET as prolonged hazardous exposure to ionizing radiation needs to be avoided. Hence, this method is unsuitable for the repeated monitoring of chronic pain conditions for extended periods of time.

Imaging post-surgical pain

Acute pain is defined in contrast to chronic pain. In clinical practice three months is the most widely used point of division between the two (Sternbach, 1974). Furthermore, pain which persists past the normal time of healing is also labelled as chronic pain (Bonica, 1953). Within the mechanism-based taxonomy of pain the label “acute” can be allocated to two types of pain. In most cases the label acute pain refers to transient pain, which is nociceptive pain, defined as a response to a noxious stimulus, which does not produce long-term sequelae (Woolf, 2004). Within a clinical setting the label acute pain can also include tissue injury pain such as postoperative pain (Pogatzki-Zahn, Zahn, & Brennan, 2007; Clifford J. Woolf, 2004), which subsides once the tissue has healed. In experimental studies other on-going pain induced by saline solution injection (Zubieta et al., 2001b) or application of capsaicin (Iannetti et al., 2005) has been investigated.

To date BOLD imaging is the most frequently used fMRI technique in pain research. It makes use of neurovascular coupling, which was first discovered by Roy and Sherrington in 1890 to describe the fact, that brain activity increases the activity-related blood flow into the active brain regions (Roy & Sherrington, 1890). This response creates a local surplus in oxygen which represents the foundation of the BOLD signal, which stems from the proportion of oxy- to deoxy-haemoglobin in the blood (Ogawa & Lee, 1990), since oxygenated haemoglobin does not affect the magnetic field.

BOLD fMRI has led to the identification of a distributed network of brain areas with distinct roles in pain and nociceptive processing for each brain region. These areas include the somatosensory cortex I and II (S1 & S2), anterior cingulate (ACC), midcingulate cortex (MCC) and insula (Apkarian, Bushnell, Treede, & Zubieta, 2005), prefrontal cortex (PFC), motor cortex, supplementary motor area (SMA) (Friebel, Eickhoff, & Lotze, 2011), and subcortically the basal ganglia, thalamus and brainstem (Peyron, Laurent, & García-Larrea, 2000). The most frequently used study designs in this context are event-related and block designs, where transient noxious stimuli are given and withheld.

However, BOLD imaging has been largely unsuccessful in characterising background or on-going pain and is suffering from a range of other limitations, which diminish its usefulness in the context of biomarker research, as they pertain to reliability. In addition, loss of statistical power for BOLD fMRI studies stems from extensive signal variations between subjects as well as across sessions (Aguirre, Zarahn, & D'esposito, 1998) for reasons yet unknown (Miezin, Maccotta, Ollinger, Petersen, &

Buckner, 2000). Arterial Spin Labelling on the other hand provides a biologically meaningful quantitative measure of perfusion without exposure to ionizing radiation (Apfelbaum, Chen, Mehta, & Gan, 2003).

ASL represents a class of MRI scanning sequences that captures tissue perfusion. The tracer used in ASL is the body's own magnetically labelled blood water, which exchanges rapidly between intravascular (IV) and extravascular (EV) tissue water compartments. The longitudinal magnetisation of the arterial blood water is modified by radiofrequency (RF) pulses in the carotid and vertebral arteries en route to the target tissue. After it reaches the tissue, the label is observed as an alteration of the tissue magnetization. The label decays with time constant T_1 , which is 1650 milliseconds at 3T, the field strength used in this thesis (Owen et al., 2008). Due to the high EV to IV ratio in the brain, the average time for arterial water to traverse from arterial to venous side, as opposed to a red blood cell, which takes about 1 second and remains intravascular, is tens of seconds. Transit delay describes the travel time of the blood from the labelling location to the target tissue and takes approximately one second and competes with T_1 . The key trade-off between these two factors constitutes the ASL measurement, as T_1 favours a short delay between label application and image acquisition, while transit delay favours a long delay for complete tracer delivery prior to image acquisition. The tracer is delivered by the regular blood stream to capillary beds and tends to accumulate in the tissue water of the surrounding tissues before it becomes venous and decays (Chen, Wang, & Detre, 2011).

The ASL variant used in the fMRI study of this thesis was pseudo-continuous arterial spin labelling (pCASL) due to several advantages. The first is the elimination of potentially large magnetisation transfer effects in pCASL, which is the transfer of longitudinal magnetisation from the hydrogen nuclei of restricted water bound to a larger molecule to the hydrogen nuclei of water that moves unrestricted in cytosol. This effect frequently occurs in CASL.

Finally, pCASL allows for mapping of vascular territories by making use of the time gaps between RF pulses and applying gradient pulses, thus modulating the labelling across vessels within the labelling plane. In addition, pCASL has a higher signal to noise ratio than other forms of ASL and allows for direct control over bolus duration. The trade off is increased sensitivity to resonance offsets (i.e. change of phase due to an applied field or inhomogeneity of field between two RF pulses, or from one pulse to the next), to which pCASL is more sensitive than CASL.

In practice pCASL uses a long series of short RF and gradient pulses instead of continuous pulses and an approximately 10 times higher gradient amplitude during the RF pulse in addition to a slice selective RF pulse, which provides excitation at the labelling plane, where the tracer is induced (Wong, 2014). The ASL signal, is directly proportional to the local CBF, because the amount of tracer in a bolus of labelled arterial blood delivered upstream, is deposited in each voxel of the scanned target tissue. Thus perfusion in ASL is a measure quantified by the amount of blood delivered to the tissue per time unit, per unit of volume or mass of tissue for which reliability has been established (Tracey & Johns, 2010a; Xu et al., 2011). Thus unlike BOLD it is a direct and physiologically meaningful CBF measure, but comes at the price of lower temporal resolution, as the scan is acquired over a period of approximately six minutes.

Imaging morphological changes induced by chronic pain

This thesis also investigated genotype-dependent morphodynamic changes in response to chronic musculoskeletal pain. In addition to short-term changes in blood flow and electrical activity, it has been demonstrated that the repeated or on-going experience of pain may have morphodynamic effects on the brain (May, 2008).

Here the term morphodynamic is used in similar fashion to the geological concept of morphodynamics, which describes the effect of environmental gradients, such as tidal range, wave exposure and sediment type on the shape of a landscape (Carter & Woodroffe, 1997). In this thesis chronic musculoskeletal pain serves as a gradient. The term morphodynamic is not used in the traditional biological sense, where it pertains to embryonal development (Keller, Schmidt, Wittbrodt, & Stelzer, 2008).

Grey matter generally decreases with age and is associated with a decline in cognitive capability (Ceko, Bushnell, Fitzcharles, & Schweinhardt, 2013). Morphological changes of the brain have been demonstrated in grey matter as well as white matter (Ceko et al., 2013). An inverse relationship independent of pathology between grey matter density and pain sensitivity with accompanying changes in resting state network activity has been demonstrated in participants undergoing a heat pain challenge (Emerson et al., 2014). Apkarian et al. (Apkarian et al., 2004) were the first to demonstrate grey matter decreases in response to chronic back pain. Since then decreases in grey matter have been demonstrated in several other chronic pain disorders such as FMS (Lutz et al., 2008; Robinson, Craggs, Price, Perlstein, & Staud, 2011), temporomandibular disorder (Moayedil et al., 2012), chronic low back pain (Schmidt-Wilcke et al., 2006) and tension type headaches (Schmidt-Wilcke et al., 2005).

These decreases were initially thought to represent permanent atrophy. However, this view has been challenged by reports of grey matter recovery after cessation of chronic pain following reconstructive surgery (Rodriguez-Raecke, Niemeier, Ihle, Ruether, & May, 2013a), indicating that GM density changes could potentially serve as a biomarker for the success of clinical interventions.

The majority of studies have demonstrated decreases in grey matter in areas associated with persistent pain processing, whose extent corresponds to the duration of the pain experience. However, there are additional factors such as affect. When comparing three groups of 29 age-matched participants – healthy controls, FMS patients with affective disorder and FMS patients without affective disorder- Hsu et al. (Hsu et al., 2009) demonstrated no significant GM differences between the healthy controls and FMS patients without affective disorder.

In addition, the findings of decreases also seem counterintuitive (Moseley & Flor, 2012) considering the results from training studies, where GM volume increased in response to frequent use of the activated region (e.g. hippocampal areas in taxi drivers). It could be expected that structures involved in the perception of pain would increase in GM density in response. Corresponding findings were reported for striatal grey matter, which was increased in FMS patients in comparison to healthy controls (Schmidt-Wilcke et al., 2007). A recent study suggests that the relationship between pain and grey matter density may be more complex. Ceko et al. (2013) investigated

GM density in female FMS patients and divided the sample by age. The younger patients demonstrated GM density increases, which were interpreted as an adaptive reaction resulting in amelioration of pain, while older patients demonstrated decreases and increased pain indicating that the plasticity changes had turned maladaptive.

So far, little is known about the molecular factors driving these morphodynamics. While genetic markers are associated with changes in sensitivity to pain, genetic variation may also serve as a risk or protective factor for plasticity changes in pain patients. A recent study on the genetic contribution of the catechol-O-methyltransferase val158met polymorphism in female migraine sufferers (Liu et al., 2015) highlighted a significant disease by genotype interaction in the hippocampus, where GM was increased in val-homozygote migraine patients.

This thesis took a novel approach in analysing the effects of SNP rs1799971 from the gene encoding mu-opioid receptor 1 on grey matter density.

Voxel based morphometry (VBM) has become the methodology of choice (Ashburner & Friston, 2000) due to its convenience in comparison to the other two methodologies. It has been used to investigate differences in cortical volumes between groups affected by chronic mental illness such as schizophrenia and healthy controls (Wright et al., 1995) as well as London taxi drivers in comparison to regular drivers and demonstrated increases in grey matter in the posterior hippocampus in the taxi drivers as a result of repeatedly performing the spatial task of navigating through London (Maguire et al., 2000).

VBM analysis uses four distinct steps: spatial normalisation, segmentation, smoothing and statistical analysis. During spatial normalisation the individual MRI images are registered to the same template image to create a template. The aim is to create a template consisting of the average of a large number of MR images registered in the same stereotactic space. First transformation parameters are estimated to map the individual MRI images to the template (Ashburner & Friston, 1997). Second, global nonlinear shape differences are accounted for by minimising the residual squared difference between the image and the template and maximizing the smoothness of the anatomical differences between template and participant scan.

During segmentation the normalised images are segmented into the different tissue types: grey matter, white matter, cerebrospinal fluid and three non-brain partitions. Then a priori probability maps of different tissues in normal subjects are combined with voxel intensity distributions of particular tissue types. Images then are corrected for intensity non-uniformity and the resulting tissue class images are binarised to allocate each voxel to its most probable tissue class (Ashburner & Friston, 2000). Images are then smoothed by an isotropic Gaussian kernel to ensure that each voxel in the images contains the average amount of grey or white matter from the radius of the smoothing kernel, to increase the validity of subsequent parametric statistical tests by creating more normally distributed data and to compensate for the remaining inaccuracies of the spatial normalisation (Mechelli, Price, Friston, & Ashburner, 2005). The data is then ready for statistical analyses such as group comparisons.

In summary, so far neuroimaging techniques have afforded us new vistas into the neuronal processes that generate the sensation of pain by highlighting brain regions previously considered inconsequential in pain processing (e.g. nucleus accumbens, striatal areas). Apart from the intuitive targets such as the somatosensory cortex I and II, a network of brain areas has been proposed and is often referred to as the pain matrix or neuromatrix of pain (Melzack, 1999, 2001). The concept of the pain matrix however, has also sparked some controversy with regard to which areas are included in this network. There has also been critique regarding an oversimplified approach by treating the components of the pain matrix similar to specialised structures in the visual cortex for example (Iannetti & Mouraux, 2010; Legrain, Iannetti, Plaghki, & Mouraux, 2011), when many areas such as the anterior cingulate cortex and the thalamus for example also play important roles in other processes such as attention (Luerding, Weigand, Bogdahn, & Schmidt-Wilcke, 2008)

1.6 Combining genetics and neuroimaging in search of biomarkers and mechanisms of pain and nociception – a rationale for this thesis

Both genetics and neuroimaging have undergone similar, yet, mostly separate progressions in the development and recent application of technologies in pain. The past 25 years have seen a rapid proliferation of genetic and imaging techniques in pain research and have, also through combination, opened up new seams for mining in search of pain biomarkers and mechanisms.

To date imaging and genetic approaches have rarely been used in combination with a few notable exceptions. There are three candidate gene studies, of which one focused on opioidergic signalling in the brain in the presence of a mutation within *OPRM1* A118G. The first focused on genotype-dependent differences in pain-related brain activation measured with fMRI after administration of short pulses of gaseous CO₂ to the nasal mucosa using the same SNP (Oertel, Preibisch, Wallenhorst, Hummel, Geisslinger, Lanfermann, & Loetsch, 2008). The study demonstrated decreased linear activation in relation to alfentanil concentrations in brain regions associated with the processing of the sensory intensity of pain, which was significantly less pronounced in *OPRM1* 118G carriers.

Two other studies investigated the effect of the *COMT* val158met polymorphism in combination with neuroimaging phenotypes. First, an fMRI study on structural and functional changes in the hippocampus in female migraine patients (Liu et al., 2015) revealed a significant disease by genotype interaction effect, which corresponded to disease-related increase of GM in val/val carrying migraineurs in a VBM analysis. Here increased GM and decreased connectivity between the hippocampus and the medial prefrontal cortex was only found in val homozygote migraine patients without aura compared to val homozygote healthy control volunteers. In another study (Zubieta et al., 2003) women underwent a PET scan using the mu-opioid receptor-selective radiotracer [¹¹C]carfentanil in the presence of an on-going pain stimulus during the early follicular phase of their menstrual cycle. The study demonstrated diminished regional mu-opioid system responses to pain in carriers of the met158met genotype of *COMT* compared with heterozygotes, and higher sensory and affective ratings of pain in addition to a more negative internal affective state.

This thesis consisted of two studies in which one used genetic and imaging analyses in parallel and one combined both endpoints to evaluate their utility in establishing

novel biomarkers in search of mechanisms underlying different types of pain. The VBM study was driven by a specific biological hypothesis based on previous insights into the effects of SNP rs1799971 in *OPRM1*. It investigated the effect of this SNP on GM density in chronic musculoskeletal pain patients, for which grey matter changes in comparison to healthy age and gender matched control participants have been demonstrated (May, 2008; Schmidt-Wilcke et al., 2005; Schmidt-Wilcke, 2008).

The hypothesis that *OPRM1* influences GM density was based on previous observations that its G-allele seems to serve as a protective factor against pain in general and FMS in particular (Solak et al., 2014; Walter & Lötsch, 2009b). GM decreases in response to chronic pain have been reported for various pain conditions (Lutz et al., 2008; May, 2008). In addition, opioidergic signalling is altered in FMS and ULBP patients (Baraniuk, Whalen, Cunningham, & Clauw, 2004; Harris et al., 2007), thus making *OPRM1* most likely a pain gene in line with Devor's definition and larger GM decreases more likely in A-allele carriers.

The other study analysed RNA from peripheral whole blood and used microarrays for comprehensive genomic coverage. It assessed the changes in cerebral blood flow by means of ASL and analysed gene expression levels from peripheral whole blood pre and post surgery in response to TME. It employed a data-driven analysis approach in search for pain susceptibility genes using pre-post comparisons as well as Gene Set Enrichment Analysis (GSEA) to identify known molecular pathways in the context of post-surgical pain.

TME reliably produces on-going moderate to severe post-surgical pain (Moore, Edwards, & McQuay, 2005). The most common indication for TME in accordance with NICE guidelines is recurrent pericoronitis, repeated bouts of inflammation of the tissues surrounding the impacted wisdom tooth (NICE/NHS, 2000). A benefit of the TME model is that study participants can be assessed pain-free during asymptomatic periods, providing useful 'baseline' information. Patients also commonly present with bilateral, similarly positioned wisdom teeth requiring extraction. Similar morphology between left and right teeth provides a matched level of surgical difficulty and resulting post-surgical pain. This makes TME ideal for analgesic trials employing a crossover design and thus allowing for assessment of reliability, one of the key requirements in a biomarker.

This study aimed at establishing blood as an easily accessible tissue as a proxy for pain-related molecular changes. It evaluated the potential of RNA derived from peripheral whole blood as a substrate for biomarker discovery in pain research. Blood is already used for immune monitoring in response to vaccines for example has been implemented by means of mRNA real-time polymerase chain reaction (PCR) (Stordeur et al., 2003) and cyclooxygenase activity (Brideau et al., 1996) among other indicators. Blood is routinely taken in many clinical settings in pain treatment and would thus lend itself well as an easily accessible substrate for biomarker generation in pain.

Gene expression profiling has previously been applied in the context of TME and potentially enables extrapolation to other forms of post-surgical pain (Barden, Edwards, McQuay, & Moore, 2004). Performed in otherwise healthy volunteers, it allows for assessment of on-going pain without the plasticity changes encountered in chronic pain patients. Together, the studies were designed to provide coverage of as

many of the different aspects of successful establishment of biomarkers and pain measurement as possible, rooted in a mechanism-based classification of pain.

Both studies were performed in humans to enable the assessment of cognitive components of the pain experience such as sensory and affective ratings of pain. These are difficult to operationalise in animals (Max & Stewart, 2008b), but are essential components of the human pain experience. The mechanism-based taxonomy of pain proposed by Woolf et al. (Woolf et al., 1998) distinguishes between stimulus-dependent and stimulus-independent pain, which this thesis addressed by investigating pain subsequent to TME with TME serving as pain stimulus. This type of pain also falls into the category of adaptive pain in the mechanism-based taxonomy, which further distinguishes between adaptive and maladaptive pain. Post surgical pain aids the recovery of tissue from surgical trauma and usually subsides once the tissue has healed.

The second study of patients with chronic musculoskeletal pain suffering from FMS and ULBP represented a model of stimulus-independent pain, since no external event to precipitate its onset was identifiable. It is also classified as maladaptive, since it neither indicates impending tissue damage nor serves any other adaptive purpose such as tissue recovery. In this scenario the pain is the disease and both patient cohorts were grouped under the category of nervous system injury pain brought on by maladaptive CNS processing (Woolf, 2004) even though FMS and ULBP are diagnosed as separate disorders in current clinical practice (WHO, 2010).

The sample in the VBM candidate gene study consisted entirely of female participants based on the fact that the majority of patients are female. The other study consisted entirely of male participants to exclude known effects of the menstrual cycle (Teepker, Peters, Vedder, Schepelmann, & Lautenbacher, 2010). Based on clinical experience of the surgeons involved in the study, the recruitment of post-menopausal females is near impossible, since third molars are usually removed by the age of 35 in most patients. Both studies were conducted in Caucasian participants to prevent population stratification or and to control for its potential effects on gene expression.

This thesis aimed to achieve an assessment with well-characterised, controlled, clinically relevant pain endophenotypes that are robust, yet relatively easy to acquire. This was done with the intention to maximise the chances of identifying genetic targets for clarifying the underlying molecular mechanisms and to generate suitable tools for the development of diagnostic procedures and evaluation of therapeutic success.

2 MANUSCRIPTS

2.1 Manuscript I: Beyond Patient Reported Pain: Perfusion Magnetic Resonance Imaging Demonstrates Reproducible Cerebral Representation of Ongoing Post-Surgical Pain¹

Reference:

Howard MA, Krause K, Khawaja N, Massat N, Zelaya F, Schumann G, et al. (2011) Beyond Patient Reported Pain: Perfusion Magnetic Resonance Imaging Demonstrates Reproducible Cerebral Representation of Ongoing Post-Surgical Pain. PLoS ONE 6(2): e17096. doi:10.1371/journal.pone.0017096

Abstract

Development of treatments for acute and chronic pain conditions remains a challenge, with an unmet need for improved sensitivity and reproducibility in measuring pain in patients. Here we used pulsed-continuous arterial spin-labelling [pCASL], a relatively novel perfusion magnetic-resonance imaging technique, in conjunction with a commonly-used post-surgical model, to measure changes in regional cerebral blood flow [rCBF] associated with the experience of being in ongoing pain. We demonstrate repeatable, reproducible assessment of ongoing pain that is independent of patient self-report. In a cross- over trial design, 16 participants requiring bilateral removal of lower-jaw third molars underwent pain-free pre-surgical pCASL scans. Following extraction of either left or right tooth, repeat scans were acquired during post-operative ongoing pain. When pain-free following surgical recovery, the pre/post-surgical scanning procedure was repeated for the remaining tooth. Voxelwise statistical comparison of pre and post-surgical scans was performed to reveal rCBF changes representing ongoing pain. In addition, rCBF values in predefined pain and control brain regions were obtained. rCBF increases (5–10%) representing post-surgical ongoing pain were identified bilaterally in a network including primary and secondary somatosensory, insula and cingulate cortices, thalamus, amygdala, hippocampus, midbrain and brainstem (including trigeminal

¹ Author contributions listed the author of this thesis for three types of contributions: “Performed the experiments”, where she contributed 80% of recruitment, phone and psychometric screenings, MRI data acquisitions, sample collection, storage, randomisation and shipping arrangements and liaison with the lab that processed RNA and micorarrays. “Analyzed the data” included manual check of all acquired slices for artefacts for 20 participants * 5 visits * 6 cASL scans, pre-processing including brain extraction and mask generation from T1 scans for inclusion in the main analysis (40%). “Wrote the paper” included contributing passages to the introduction, methods section and discussion (10%).

ganglion and principal-sensory nucleus), but not in a control region in visual cortex. rCBF changes were reproducible, with no rCBF differences identified across scans within-session or between post-surgical pain sessions. This is the first report of the cerebral representation of ongoing post-surgical pain without the need for exogenous tracers. Regions of rCBF increases are plausibly associated with pain and the technique is reproducible, providing an attractive proposition for testing interventions for ongoing pain that do not rely solely on patient self-report. Our findings have the potential to improve our understanding of the cerebral representation of persistent painful conditions, leading to improved identification of specific patient sub-types and implementation of mechanism-based treatments.

Introduction

As many as 80% of individuals experience moderate to severe post-operative pain (Apfelbaum et al., 2003) and intractable pain in patients with cancer, diabetes and HIV is a major healthcare concern (Pöpping et al., 2008). The breadth of available treatments for pain control remains limited with an over-reliance on opiate-based medication (Woodcock, Witter, & Dionne, 2007). Without a record-able biological marker for pain, decades of analgesic trials have relied largely on patients' own reports to describe location, intensity and quality of their pain. Standardised psychometric techniques have been developed, but inter-individual variability in pain reporting has often been incorrectly viewed as artefactual (Chizh, Priestley, Rowbotham, & Schaffler, 2009), rather than representing true differences in pain experience. According to a bio-psychosocial interpretation of pain (Melzack & Casey, 1968), individual differences in pain response are likely to include effects of concurrent pathophysiology, cognitive and affective strategies and confounding effects of co-medications (Coghill, McHaffie, & Yen, 2003). Compounded by a failure to report null findings, the search for novel analgesics remains slow and expensive. It has been suggested that performance issues inherent in traditional analgesic development have been stymied by continuing to use the "evaluation tools and infrastructure of the last century to develop this century's drug therapy" (Woodcock et al., 2007). With this in mind, novel indices for measuring pain are required; ideally they should relate to an underlying aspect of pain transduction, take account of bio-psycho-social factors and translate between human and preclinical studies (Coghill et al., 2003).

Modern neuroimaging techniques, such as Positron Emission Tomography (PET) and functional Magnetic Resonance Imaging (fMRI), show great promise in the development of novel measurement techniques, allowing non-invasive investigation of the cerebral mechanisms underpinning the pain experience. Many imaging studies to date, however, have relied on 'experimental pain' models using healthy volunteers to derive brain responses to acute, repeated, short-duration nociceptive stimuli (reviewed in (Apkarian et al., 2005; Peyron et al., 2000)). For ethical reasons, human experimental pain paradigms are often expressly designed to provide a highly controllable, psychophysically constrained stimulus that minimises tissue damage. As a result, brain responses to such stimuli are highly unlikely to account for the physiological changes that result from tissue trauma (Pogatzki-Zahn et al., 2007). In addition, neurological sequelae that relate uniquely to individual chronic pain conditions (Apkarian et al., 2004; Maihofner, Handwerker, Neundorfer, & Birklein, 2004; May, 2008) are largely impossible to represent in experimental models of pain in healthy controls; a fact reflected in the increasing reports of neuroimaging

investigations in patients with persistent pain (Tracey & Bushnell, 2009b). Both post-traumatic pain and chronic painful conditions are perceived as having an ongoing painful component. By contrast, the majority of pain-imaging studies have relied on the statistical comparison of a repeated nociceptive event with interspersed 'rest' or 'control' states derived within the same experimental session. As a result, many of these studies to date have been ill-suited to investigation of ongoing pain that cannot be modulated under experimental control within-session (Tracey & Johns, 2010b).

Compared to studies examining responses to evoked pain, there are relatively few neuroimaging reports describing the cerebral representation of ongoing pain; fewer still describe clinical ongoing pain. There are several reports using PET, for example (Derbyshire et al., 1994; Derbyshire & Jones, 1998; Derbyshire et al., 1999; Di Piero et al., 1991; Jääskeläinen et al., 2001) but rather than examining the ongoing clinical pain per se, several of these studies have examined CBF changes in response to an experimentally-derived nociceptive stimulus in addition to any ongoing background pain. Further, safety considerations, availability, expense, small group sizes and inferior temporal and spatial resolution (compared to fMRI), have limited the impact of their findings. Similarly, reports using Blood Oxygenation Level Dependent [BOLD] fMRI, for example (Apkarian, Krauss, Fredrickson, & Szeverenyi, 2001; Pogatzki-Zahn et al., 2010), have examined the relationship between changes in participants' self-reported pain and BOLD signal intensity, rather than examination of the BOLD signal alone, producing results confounded by motor responses underpinning participants' continuous online pain ratings. Others have used BOLD fMRI to examine inter-relationships in resting-state BOLD signal time series information between brain regions, known as functional connectivity analysis (Cauda et al., 2009; Cauda et al., 2009). Perhaps most importantly, conventional BOLD-fMRI paradigms are most sensitive to signal changes over several seconds and are less suitable for examining pain responses lasting many minutes (Thunberg et al., 2005) or for monitoring long-term treatment effects (Cahana, Carota, Montadon, & Annoni, 2004). By contrast, perfusion MRI methodologies such as arterial spin labelling (ASL) (Petersen, Zimine, Ho, & Golay, 2006; Williams, Detre, Leigh, & Koretsky, 1992) may be preferable for the study of behaviours or states over the course of minutes as opposed to seconds. ASL has already been documented as an ideal methodology for the central investigation of ongoing, non-paroxysmal pain (Tracey & Johns, 2010b). The methodology provides quantitative, reproducible rCBF measurements throughout the brain and has superior noise-power characteristics, compared to fMRI, in within-subject designs with a task periodicity of 120 seconds or greater (Aguirre, Detre, Zarahn, & Alsop, 2002). The application of ASL to the study of pain remains in its infancy (Owen et al., 2008; Owen, Clarke, Ganapathy, Prato, & St. Lawrence, 2010); to the best of our knowledge there has yet to be a report of the application of ASL to ongoing, clinically-relevant pain.

Here we assess the validity of pulsed-continuous ASL [pCASL] (Dai, Garcia, De Bazelaire, & Alsop, 2008) as a quantitative, reproducible marker of ongoing post-surgical pain. We applied the most commonly employed clinical pain model used in trials of analgesics such as non-steroidal anti-inflammatory drugs and opiates, the third molar extraction (TME) model (Barden et al., 2004; Chen, Elliott, & Ashcroft, 2004). In the TME model, healthy participants, with no prior history of chronic painful disease other than recurrent, intermittent pericoronitis of their third molars, are recruited. As a result, participants are unaffected by confounding variables such as heterogeneity in pain distribution, concomitant medication and pathology and

participants can be initially assessed while asymptomatic and completely pain-free. Often bilateral, similarly-positioned wisdom teeth require extraction that are matched for surgical difficulty, resulting in reproducible amounts of moderate- to-severe post-surgical pain following each unilateral extraction (Szmyd, Shannon, & Mohnac, 1965). Reproducibility of pain response renders the model ideal for 'cross-over' placebo-controlled analgesic trials. In addition a recent meta-analysis reported that TME-derived assessments of analgesic efficacy could be extrapolated to other forms of post- surgical pain (Barden et al., 2004), demonstrating the broad utility of the model.

In this study we applied pCASL to the challenge of representing the cerebral basis of ongoing pain. We imposed three constraints, namely that the ongoing pain experience was induced by genuine tissue damage, could not be modulated by the experimenter within a single session, and that assessments of ongoing pain could be repeated to fulfil the requirements of a cross-over trial design. We demonstrate quantitative, reproducible rCBF increases that represent the experience of being in ongoing pain following TME including those in a network of brain regions specified a priori. Further, we provide novel insights into the central representation of post-surgical trigeminal pain in humans. Our findings are discussed in terms of their potential impact on development of novel interventions for treatment of acute and chronic pain conditions and how the pCASL technique might be utilised in translational research.

Ethics Statement

This study was approved by Kings College Hospital Research Ethics Committee (REC Reference 07/H0808/115).

Subjects and Materials

16 right-handed, healthy male volunteers aged 20–41, (mean=26.4 years) provided informed consent to participate in the study. Females were excluded due to potential variability in the phase of the menstrual cycle affecting reproducibility of the response to post-surgical pain (Teepker et al., 2010). All participants presented with bilateral recurrent pericoronitis and fulfilled NICE guidelines for extraction of lower-jaw left and right third molars (NICE/NHS, 2000).

Experimental Design

Participants were scanned on five separate occasions (S1–S5); screening/familiarisation (S1), pre-surgical (S2) and post-surgical sessions (S3) for the first extraction and pre-surgical (S4) and post- surgical (S5) sessions for the second extraction. An interval of at least two weeks separated S3 and S4, following complete recovery from the first surgery. Order of left and right tooth extraction was balanced and pseudo-randomised across the group. At each session, pulse rate and blood pressure were recorded, an alcohol and drug-screen performed and a psychometric assessment completed. Analgesic medication (1000 mg paracetamol & 400 mg ibuprofen) was provided to participants immediately following scanning during S3 & S5.

Procedure

At S1, standardised screening questionnaires were administered to assess presence of any pain and baseline psychometric information (see Baseline Psychometry). A short MR examination was performed for familiarisation with the imaging environment and participants received training on using a computerised, joystick-operated visual analogue scale (VAS). MR examinations during sessions S2–S6 were identical, each comprised of six separate consecutive pCASL scans, each lasting six minutes. Participants were instructed to lie still with their eyes open. Prior to and following acquisition of each rCBF map, participants subjectively rated pain intensity and alertness using a computerised VAS.

Baseline Psychometry

Baseline psychometric screening assessments were performed for all participants prior to scanning at S1. Screening for depression was performed using the Centre for Epidemiological Studies Depression Scale [CES-D] (Weissman et al., 1977), and trait and state anxiety using the State-Trait Anxiety Questionnaire [STAQ] (Spielberger, 1983). Changes in state anxiety relating to surgery were assessed at the beginning of each session. Screening for general mental health status was assessed using the Revised Symptom Checklist 90 [SCL-90-R] (Derogatis, 2005), and for alcohol and drug abuse using sections 11 and 12 of the Schedules for Clinical Assessment in Neuropsychiatry [SCAN] (Wing et al., 1990). Finally, the Cognitive Coping Strategies Inventory [CCSI] (Butler, Damarin, Beaulieu, Schwebel, & et al, 1989) was administered in order to assess participant coping strategies for pain. Participants with psychometric data outside published normative limits for each test were not included in the study.

Surgery

Unilateral TME was performed under local anaesthesia (4.4 ml Lignospan Special, Septodont) using a standardised technique. Surgical difficulty was rated on a 1-5 scale (Renton, Smeeton, & McGurk, 2001). Following surgery, participants were supervised for up to six hours before their post-surgical scan, during which time ratings of pain intensity were recorded using a pen-and-paper 100mm VAS. Scanning commenced when three consecutive VAS scores greater than 30/100 mm were provided within a 30-minute period.

Imaging Procedure

Imaging was performed on a 3 Tesla Signa HDx whole-body MR imaging system (General Electric, USA) fitted with an 8-channel, phased-array receive-only head coil. High-resolution T1- and T2-weighted MR structural sequences were acquired for radiological assessment and image registration. Resting-state rCBF measurements were made using pCASL (Dai et al., 2008), using an irradiation time of 1.5 s and post-labelling delay of 1.5 s. pCASL images were acquired using a single-shot, Fast Spin Echo readout resulting in whole-brain blood flow maps, with a spatial resolution of 16163 mm.

Image Preprocessing

Preprocessing and analysis were performed using FSL v4.1.0 [<http://www.fmrib.ox.ac.uk/fsl>] (Smith et al., 2004). Preprocessing prior to voxelwise analysis using a General Linear Model (GLM), consisted of skull stripping [BET], registration to the Montreal Neurological Institute (MNI) template [FLIRT] and a non-linear noise-reduction algorithm [SUSAN] to improve signal-to-noise ratio and condition the data for statistical analysis.

Surgical and Behavioural data analysis

All surgical and behavioural data analyses were computed using GenStat v11.1 (<http://www.vsnl.co.uk/>). Variability in perceived surgical difficulty and surgery-to-scan time between left and right tooth extractions were assessed using student's t-tests. VAS estimates of pain and alertness were fitted to a mixed effect model, with Participant and Participant-by-Session as random effects, and Session-pair (Pair 1[S2,S3]/Pair 2[S4,S5]), Surgery (Pre-surgery/Left/Right tooth post-surgery), Timepoint, and Surgery by Timepoint as fixed effects. A first-order auto-regressive (AR(1)) covariance structure was specified for the repeated measures Timepoint. Significance thresholds for all behavioural analyses were at the $p < 0.05$ level.

Whole brain voxel-wise analysis

Statistical analysis of pCASL data was applied at two levels using a voxelwise optimised GLM [FLAMEO]. First-level analyses were computed for each subject to create grey-matter only mean and variance images of the six individual pCASL scans acquired at each of sessions S2–S6. These images were used in a higher-level mixed effects analysis with Participant, Surgery (Presurgery/Left/Right tooth surgery) and Session-pair (Pair 1[S2,S3]/Pair 2[S4,S5]) as model terms, to assess changes in rCBF relating to post-surgical pain and rCBF differences following left, compared to right TME. Z-statistic images were thresholded using clusters determined by $Z > 2.3$ and a corrected cluster-significance threshold of $p = 0.05$ according to random field theory (Worsley, Evans, Marrett, & Neelin, 1992).

ROI Creation

Anatomical ROIs in MNI-template space were derived from Harvard-Oxford Cortical/Subcortical and Juelich-Histological Atlases. Based on a priori information regarding brain activation related to pain, ROIs were created for anterior cingulate cortex [ACC], primary [S1], and secondary [SII] somatosensory cortices, insula [INS], thalamus [THAL], amygdala [AMY] and hippocampus [HIP] in each cerebral hemisphere. Finally, an ROI was created for V5/MT, an a priori-defined, comparably-sized control ROI involved in visual motion perception and eye movements (Born & Bradley, 2005). We hypothesised that rCBF in V5/MT would not be modulated by post-surgical pain.

ROI Data Extraction

Two ROI datasets were created. In both datasets, the mean of the 20% voxels with greatest CBF values was computed (Mitsis, Iannetti, Smart, Tracey, & Wise, 2008) as a summary measure. In set one, ROIs were extracted from each individual CBF map

acquired at for each participant at each session; these data were used to examine temporal variation in rCBF response to post-surgical pain. In set two, ROIs for each hemisphere at each session were extracted from mean images created following first level voxelwise analyses.

ROI Analysis

All ROI analyses were performed using GenStat v11.1. Temporal variation within-session rCBF values extracted from set one were plotted to examine temporal variation in rCBF value within a single session. For each ROI in each hemisphere, rCBF estimates from each pCASL scan were fitted to a mixed effect model, with Participant, Participant-by-Session, Participant-by-Session-by-Time and Participant-by-Session-by-Hemisphere as random effects, Session-Pair (Pair 1/Pair 2) as fixed effect, and a 3-way factorial of Surgery (Pre-surgery/Left/Right tooth Post-surgery) Hemisphere (Left/Right) and Timepoint (1–6). P-values were Bonferroni corrected for multiple comparisons.

Pre/Post-surgical differences

For each ROI in each hemisphere, rCBF values for each subject in each session were fitted to a mixed effect model. Participant and Participant-by-Session were fitted as random effects, and Surgery (Pre-surgery/Left/Right-tooth post-surgery), Session-pair (Pair 1[S2,S3]/Pair 2[S4,S5]) and Hemisphere (Left/Right) were fitted as fixed effects. Significance thresholds were imposed after Bonferroni correction.

Correlation Analysis

For each ROI, an ANCOVA model was fitted to rCBF values obtained from each hemisphere in set two. Subject was fitted as a fixed effect and VAS estimate of pain [VAS] fitted as a covariate. The model was used to calculate intra-subject correlation co-efficients (rw) for each ROI (Bland & Altman, 1995). Due to the exploratory nature of these correlation analyses, multiple comparison correction was not employed.

Results

Surgical Outcome

There were no differences relating to site of surgery (left versus right). Perceived surgical difficulty and time taken from local anaesthesia to first CBF map did not differ between left and right surgeries (Difficulty: Left = 3.29, Right = 3.47; paired-t, $p = 0.44$; Time taken: Left = 210 minutes, Right = 204 minutes; paired-t, $p = 0.738$).

Psychometric Outcomes

Mean alertness ratings did not differ between pre- and post-surgical MRIs (Pre-surgery = 62.36, Post-surgery = 66.4; $p = 0.35$), (Figure 1a). There was no session order effect ($p = 0.592$). Mean post-surgical pain ratings were increased compared to pre-surgical visits (Figure 1b) (Pre-surgery = 1.8, Post-surgery = 56.5; $F[1,39.6] = 432.99$, $p < 0.001$), but there were no differences following extraction of left, compared to right, third molars ($p = 0.97$). There was no session order effect ($p = 0.55$).

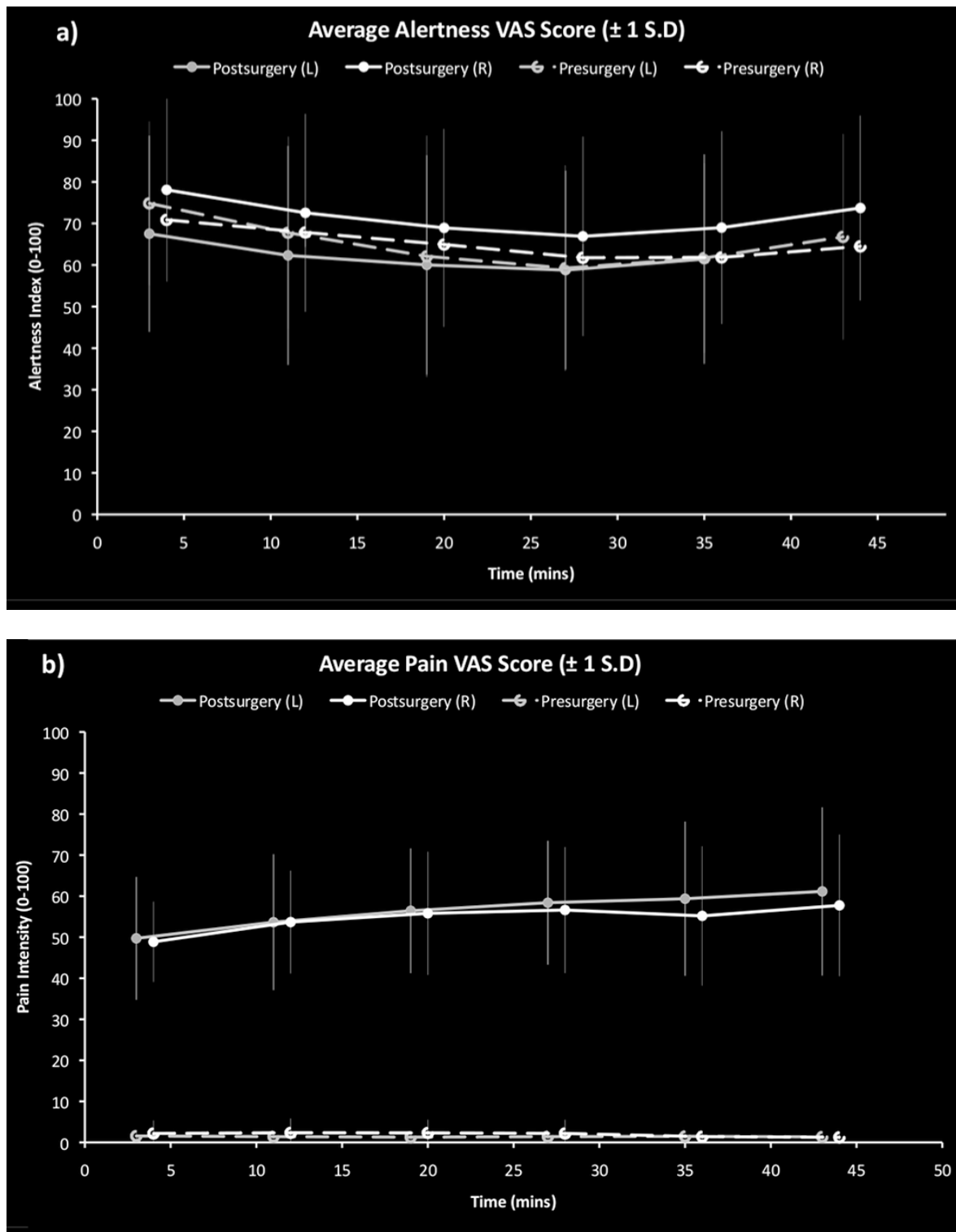


Figure I-1: Within-scanner time courses of VAS indices of (a) perceived alertness and (b) pain experienced pre/post each pCASL scan. Each visit is plotted separately (Left tooth = Grey, Right Tooth = White; Filled circles = Post-surgical visit, Unfilled circles = Pre-surgical visit; Error bars indicate ± 1 Standard Deviation.

Neuroimaging

A distributed network of brain regions demonstrated significant increases in rCBF relating to pain following extraction of left and right third molars, compared to pain-free pre-surgical periods in the same subjects. Table 1 details each cluster in brain regions we hypothesised a priori would demonstrate CBF changes during post-surgical pain; for brevity, only clusters with highest Z-scores per anatomical region have been reported. We did not observe any post-surgical decreases in CBF in these regions or elsewhere. In particular, bilateral increases in rCBF during post-surgical pain were identified in postcentral gyrus, specifically the somatotopic region of S1 relating to the face/jaw (Penfield & Rasmussen, 1950; Weigelt, Terekhin, Kemppainen, Dörfler, & Forster, 2010) (Figure 2; 3a), in SII (Figure 3b), extending ventrally towards posterior insula cortex and in mid/anterior insula cortices, extending towards the frontal operculum.

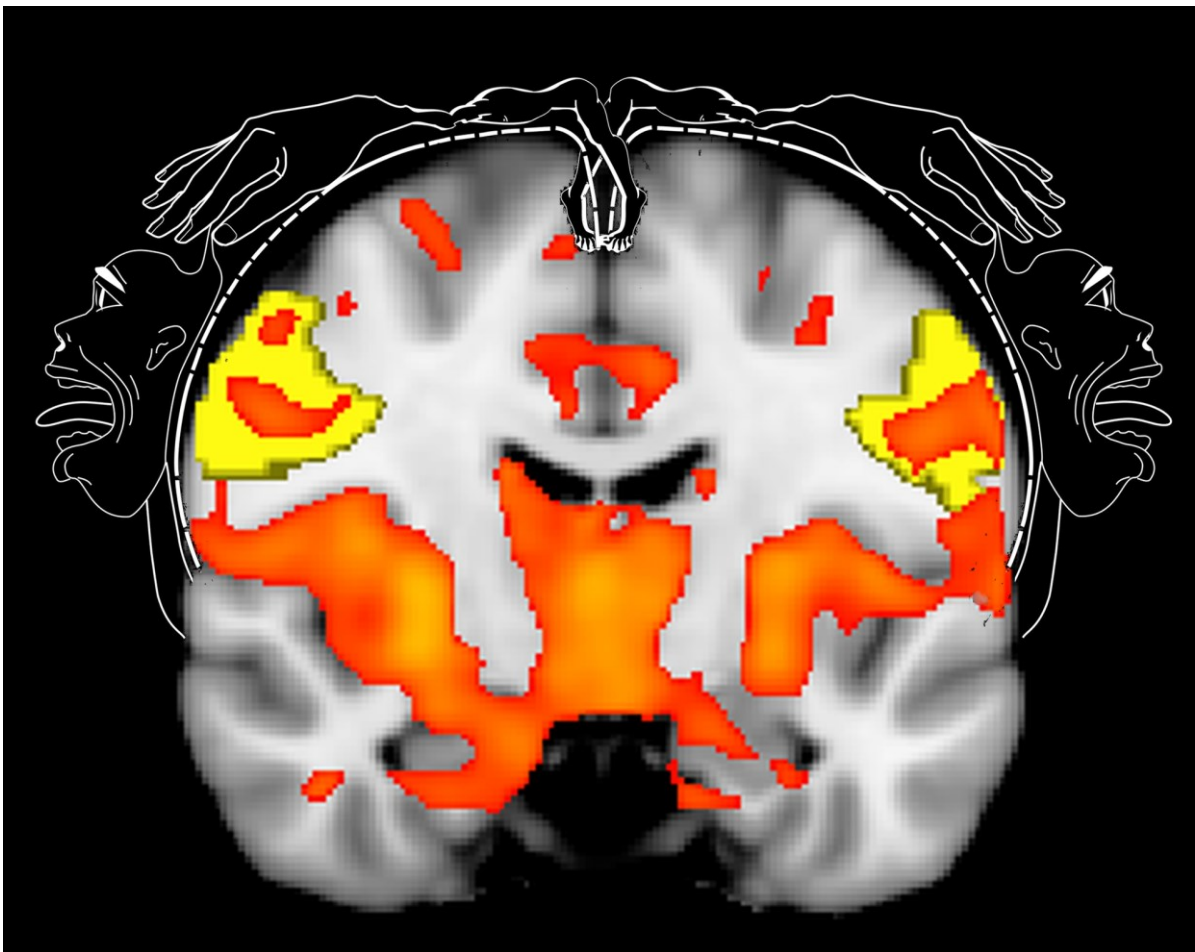


Figure I-2: Post-surgical CBF changes in S1 relate to the classical somatotopic representation of the jaw (adapted from (Weigelt et al., 2010)). CBF increases coded in red illustrates mask image of clusters significant at the $p < 0.05$ (corrected) level. Yellow mask illustrates S1 ROI in left and right cerebral hemispheres.

Structure	Left Hemisphere				Right Hemisphere			
	Zstat	x	y	z	Zstat	x	y	Z
Primary Somatosensory Cortex	3.41	-62	-16	42	3.17	42	-16	42
Secondary Somatosensory Cortex	3.29	-56	-14	14	3.36	54	-14	16
Thalamus	3.46	-20	-28	16	3.76	16	-36	6
Pons	2.98	-18	-28	-32	3.11	14	-30	-26
Trigeminal System					3.53	-18	-18	-32
Midbrain	3.22	-16	-22	-8	3.54	4	-24	-14
Posterior Cingulate Gyrus	3.02	-8	-64	12	3.38	24	-70	6
Cingulate Gyrus	3.03	-4	-32	24	3.25	10	-42	26
Mid-anterior Cingulate Gyrus	3.26	-12	6	36	3.38	14	-12	44
Anterior Cingulate					3.13	6	36	6
Hippocampus/Parahippocampus	4.05	-28	-50	-6	4.00	26	-44	-4
Amygdala	3.80	-30	2	-26	4.32	24	0	-14
Insula	3.47	-44	-10	6	4.10	40	-12	14

Table I-1: Regions of increased post-surgical CBF specified *a priori* to underpin cerebral processing of pain.

At midline, clusters were observed bilaterally in mid-anterior cingulate cortices, (Figure I-3c) extending towards perigenual cingulate cortex, and in posterior cingulate gyrus close to the splenium of the corpus callosum. In the temporal lobe, clusters were identified in amygdala (Figure I-3d), extending dorsally through hippocampal/parahippocampal cortices (Figure I-3e). In the thalamus, a single, bilateral interconnected cluster was identified which included pulvinar, ventral posterior, ventromedial and anterior regions at midline, extending inferiorly to include the hypothalamus (Figure I-3f).

ROI	Estimated Means		Marginal Pre-surgery vs. Post-surgery				Post-surgery (left vs. right)				Hemisphere Session Pair			
	Pre-surgery	Post-surgery	Post-surgery	Mean difference	F-ratio	p	Mean difference	F-ratio	p	F-ratio	p	F-ratio	P	
AMY	56.6	60.2	61.3	4.2	14.45	0.00	1.1	0.47	0.49	18.87	0.00	0.04	0.85	
HIP	59.3	62.1	63.4	3.5	10.47	0.00	1.3	0.73	0.40	0.57	0.45	0.08	0.78	
Insula	81.0	85.4	87.5	5.4	10.38	0.00	2.1	0.79	0.38	27.23	0.00	0.00	0.99	
S1	66.6	71.2	71.2	4.6	5.28	0.03	0	0.00	0.99	69.58	0.00	0.01	0.91	
S2	71.9	76.2	77.2	4.8	11.02	0.00	1.1	0.27	0.61	32.05	0.00	0.04	0.85	
ACC	93.3	97.0	100.2	5.3	6.80	0.01	3.2	1.27	0.27	4	0.00	0.12	0.73	
PCC	103.1	105.7	108.6	3.9	4.01	0.05	2.9	1.11	0.30	73.98	0.00	0.01	0.92	
Thalamus	67.4	71.5	74.2	5.5	15.35	0.00	2.8	1.98	0.17	18.34	0.00	0.03	0.85	
V5	76.4	77.3	77.9	1.2	0.39	0.53	0.6	0.04	0.84	8	0.00	0.01	0.91	

Table I-3: Summary table: Pre and post-surgical estimated means, and ANOVA outputs for each pre-specified ROI.

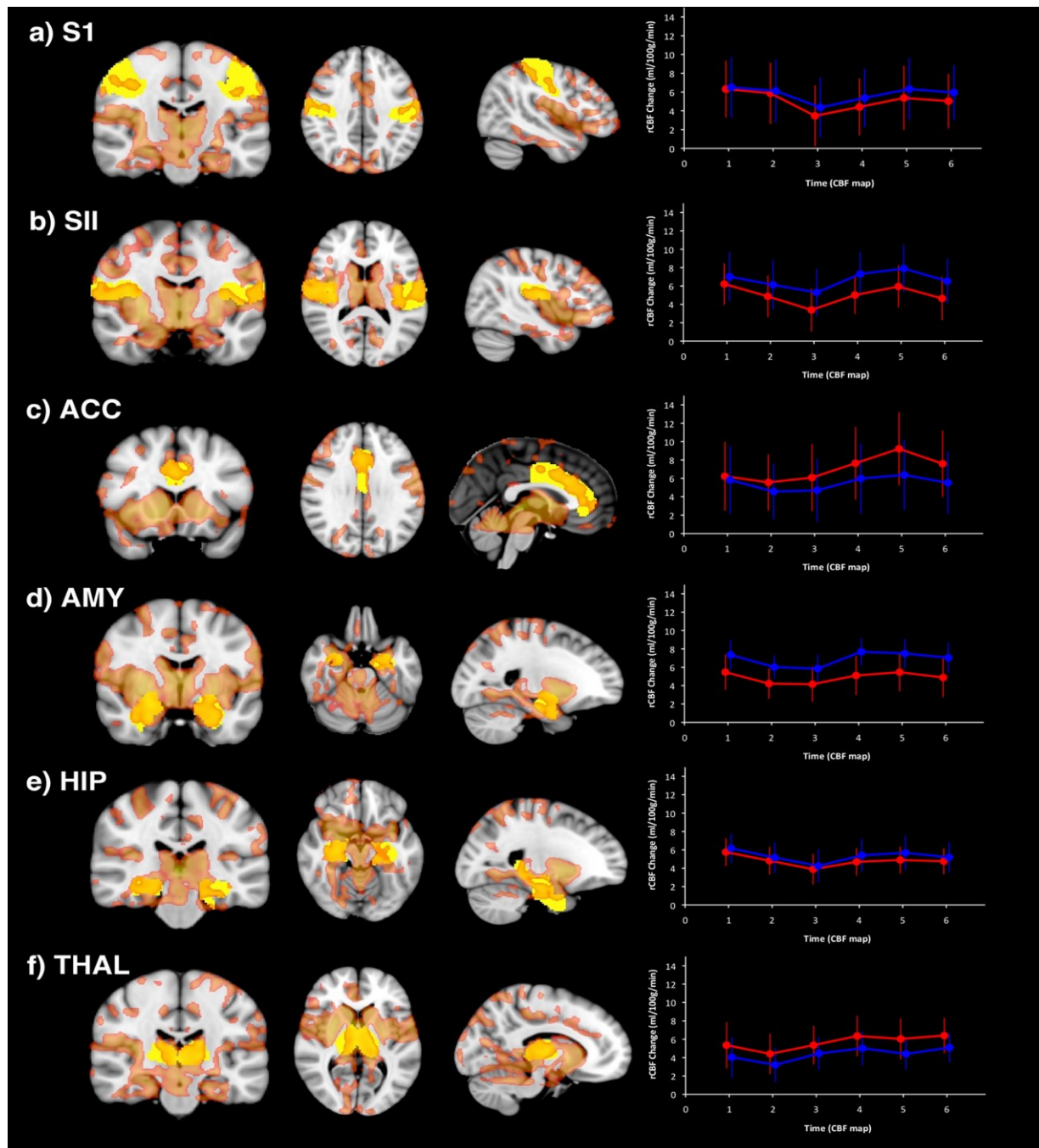


Figure I-3: (a–f) Time courses of post-surgical rCBF increases relating to pain in each a priori-defined ROI. Cluster-corrected ($p < 0.05$) Z-statistic map (red) indicates regional post-surgical increases in CBF relating to pain. In each row, a priori ROI masks are outlined in yellow. Plots at far right of each row indicate time courses of post-surgical increases in CBF (ml/100 g/min) for each ROI extracted from each individual pCASL scan (Red = left hemisphere, Blue = right hemisphere; Error bars represent ± 1 Standard Error).

Further regions of increased post-surgical rCBF (Table 2) were identified in addition to those specified a priori. In the frontal lobe, clusters were identified in superior, middle, medial and orbital-frontal cortices, in precentral gyrus and superior and inferior parietal lobules bilaterally. In the temporal lobe, bilateral regions of increased CBF were identified in superior, middle inferior temporal and fusiform gyri, and in the lingual gyrus and precuneus in the occipital lobe. In the basal ganglia, clusters were identified in caudate and lentiform nuclei bilaterally. In the brainstem, increased post-surgical CBF was identified bilaterally adjacent to the lateral mid-pons, approximating

to the trigeminal ganglion/ roots (Figure 4), with further continuous regions of increased rCBF in mid-pons identified as principal sensory trigeminal nucleus (Vp), extending posteriorly towards bilateral anterior cerebellar hemispheres and vermis. Superior to Vp, a single cluster was observed encompassing the pontine reticular formation, ascending superiorly into midbrain reticular formation including much of the tectum including substantia nigra, ventral tegmental area and red nucleus, and tectum including quadrigeminal body and periaqueductal grey.

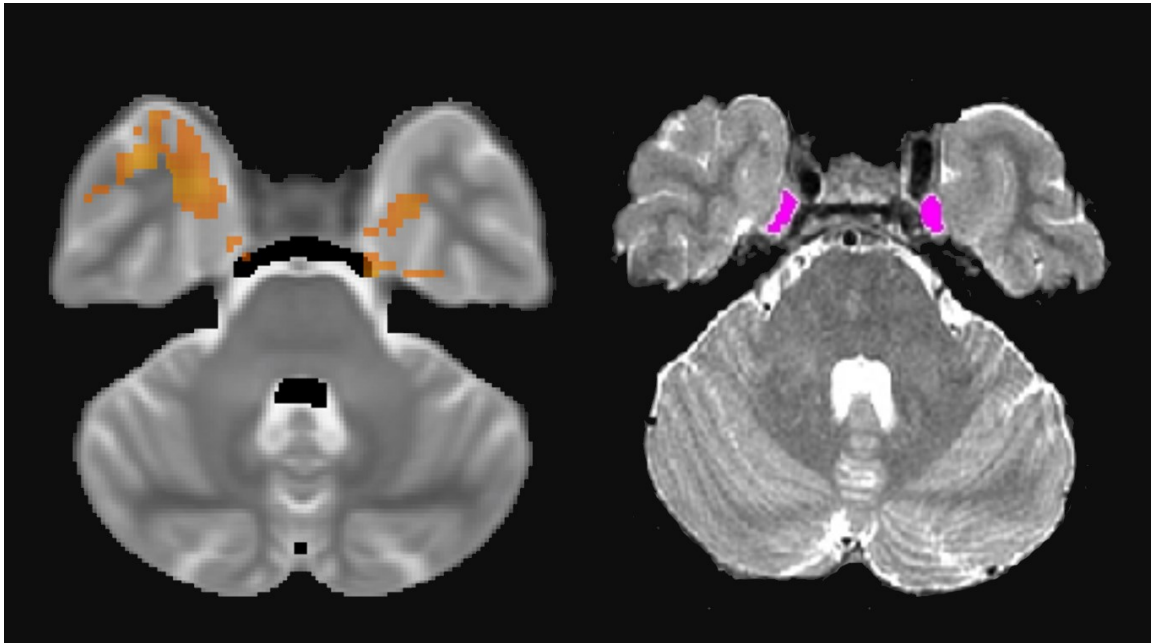


Figure I-4: Anatomical and Functional Localisation of the Trigeminal Ganglion. (left) High resolution axial T2-weighted image illustrates Meckel's cave (magenta), the anatomical location of the trigeminal ganglion. (right) Post-surgical rCBF increases in trigeminal ganglion.

ROI Analysis: Temporal Variation Within Session

The anatomical location of each ROI, post-surgical CBF change and associated time courses is illustrated in Figure I-3 (a2f). Mixed effect model analyses in each a priori ROI demonstrated that no significant variation in rCBF across scans (Time) was identified within a single session. There were no other significant second or third order interactions of Time with Hemisphere, or Surgery, indicating that within-session temporal variation across pCASL scans did not differ between cerebral hemispheres, either in pre-surgical or post-surgical scanning sessions following either left or right TME. In the light of these findings, assessment of between session variation in rCBF was studied using ROIs derived from set two, the average of all 6 cASL maps acquired within a single session.

Pre/Post surgery differences

Mixed effect models were computed for all pain and control ROIs. Main effects and interactions for ROIs are summarised in Table I-3. In each pain-related ROI, rCBF increases between 5-10% were identified following TME. Following correction for multiple comparisons, significant increases in post-surgical rCBF were observed in AMY, HIP, SII, THAL, & INS ROIs, with strong trends in the same direction identified in S1 and ACC, but not in control region V5/ MT. There was no effect of side of first tooth removal. A main effect of hemisphere was observed in all ROIs, including control region V5/ MT but excluding HIP, which indicated that both pre- and post-

surgical rCBF values for ROIs were increased in right, compared to left hemisphere. There were no significant interactions of hemisphere with surgery side across all ROIs, meaning that surgery effects had the same impact on each hemisphere independently of whether left or right third molar was removed.

Structure	Left Hemisphere				Right Hemisphere			
	Zstat	x	y	z	Zstat	x	y	z
Medial Frontal Gyrus	2.66	-12	38	24	2.71	8	-8	60
Superior Frontal Gyrus	2.74	-20	-4	68	2.91	34	56	28
Middle Frontal Gyrus	3.12	-34	2	66	2.78	24	-2	46
Inferior Frontal Gyrus	3.77	-36	8	-16	3.20	42	32	-12
Orbital Gyrus					2.95	4	42	-22
Rectal Gyrus					2.95	12	42	-18
Rectal Gyrus					2.86	6	32	-24
Precentral Gyrus	3.92	-60	10	0	3.49	64	8	10
Postcentral Gyrus	2.70	-28	-48	72	3.22	22	-34	66
Paracentral Lobule	3.46	10	-32	62	3.15	6	-42	72
Superior Parietal Lobule	2.92	-22	-60	56	3.20	26	-66	56
Inferior Parietal Lobule	2.64	-2	-94	26	3.35	24	-62	30
Superior Temporal Gyrus	3.78	-64	-6	4	3.77	36	8	-20
Middle Temporal Gyrus					3.25	64	-40	-10
Inferior Temporal Gyrus					3.49	38	-6	-28
Fusiform Gyrus	3.32	-36	-34	-22	3.61	36	-40	-18
Supramarginal Gyrus					2.84	-28	-46	38
Superior Occipital Gyrus					2.74	34	-88	22
Precuneus	3.22	-18	-62	30	3.42	22	-86	42
Lingual Gyrus	2.68	-20	-78	-4	3.69	18	-84	-6
Lentiform Nucleus	4.55	-26	2	-4	4.24	30	-12	2
Caudate	3.78	-10	20	6	4.71	6	4	2
Internal Capsule	4.26	-18	20	-6	4.49	30	6	-4
Clastrum					4.31	32	0	8
Cerebellum	3.25	-20	-46	-32	3.23	12	-56	-26
Cerebellar Lingual					3.90	2	-46	-24
Declive					3.29	50	-50	-26
Cuneus	3.17	-14	-74	16	3.01	0	-100	4
Culmen	3.20	-12	-70	-12	3.68	12	-44	-24

Table I-2: Additional regions of increased post-surgical CBF not specified a priori to underpin central processing of pain.

Relationships Between VAS Pain Estimates and rCBF

Within-subject correlation co-efficients (r_w) were computed for each ROI in each hemisphere to assess the relationship between post-surgical pain rCBF and patients' self-reported pain VAS scores. Significant linear relationships were identified in AMY, HIP, S1, SII, THAL, INS, PCC & ACC ROIs, (Table I-4) but not in control region V5/MT.

ROI Structure	Left Hemisphere		Right Hemisphere	
	ρ_w	F-prob	ρ_w	F-prob
Amygdala	0.41	0.004	0.51	0.000
Brainstem	0.40	0.005	0.44	0.002
Hippocampal Formation	0.42	0.003	0.46	0.001
Insula	0.35	0.014	0.48	0.001
S1	0.36	0.011	0.41	0.003
S2	0.38	0.008	0.46	0.001
ACC	0.37	0.009	0.37	0.009
Thalamus	0.47	0.001	0.46	0.001
V5	0.15	0.304	0.23	0.122

Table I-4: Within-subject correlation co-efficients (ρ_w) between mean rCBF in each region in each hemisphere and mean self-reported pain.

Discussion

Using pCASL, we have demonstrated reproducible, rCBF- derived markers of ongoing, clinically-relevant pain. Increases in rCBF were established following surgery, compared to pain-free pre-surgical periods, in an unbiased voxel-wise analysis and in a priori hypothesised regions inherent in the central processing of pain, but not in control brain regions hypothesised to be unchanged by pain. rCBF assessments were stable within a single session and there were no between-session differences in post- surgical rCBF following extraction of left, compared to right, teeth, indicating a viable test-retest paradigm. Post-surgical CBF changes correlated with VAS estimates of self-reported pain, but only in brain regions known to underpin the processing of pain and not in a control brain region. Quantitative changes in rCBF that represent ongoing pain have potential as markers of treatment efficacy for acute and persistent painful conditions.

Our findings of rCBF increases during pain following TME provide valuable new insights into the representation of ongoing post-surgical trigeminal pain. Independently of site of removal, the pain resulting from tooth extraction is represented by a largely bilateral pattern of rCBF changes throughout the brain. No hemispheric differences in rCBF changes related to extraction were found. These findings differ from earlier pain studies using PET imaging, which have largely

reported rCBF changes contralateral to the painful body-site, for example, contralateral increases in rCBF in PFC, insula cortex, and lentiform nucleus were reported following a composite third molar extraction and thermal heat pain challenge (Derbyshire et al., 1999). To the best of our knowledge, this is the only other neuroimaging study of pain following third molar extraction, but is difficult to relate to our findings due to the confounding effect of a nociceptive heat stimulus applied to the hand contralateral to the extracted tooth. Two recent reports using experimental pain models have highlighted the potential of ASL in pain research (Owen et al., 2008; Owen et al., 2010). Several findings in those studies were concordant with our own, namely, similar magnitude of CBF values in grey matter and resulting rCBF changes in response to pain in bilateral insula cortex, SII, cingulate cortex and supplementary motor area, as well as responses in S1 and thalamus. However, contrary to our own findings, responses to a tonic painful hypertonic saline stimulus produced a CBF decrease in S1, while several additional regions demonstrated a reduction in magnitude of the CBF change over the time course of the saline infusion. We speculate that such CBF decay characteristics may relate to differences not only in physiological response but also in terms of the threat value of an experimentally evoked stimulus, compared to a genuine post-surgical tissue trauma (Pogatzki-Zahn et al., 2010; DD Price, 1999; Weigelt et al., 2010). Differences in ASL implementation in those studies precluded further examination of CBF changes inferior to the thalamus and provided a lower spatial resolution than reported here, and further comparisons are difficult due paradigm design, body-site differences, and potentially confounding CBF changes relating to patient introspection and movements derived from providing VAS estimates of perceived pain throughout image acquisition.

Our finding of bilateral post-surgical rCBF increases in S1 is supported by primate electrophysiological studies of S1 neurones with bilateral receptive fields (Lin, Murray, & Sessle, 1993), and other imaging reports of evoked painful and non-painful stimulation of the trigeminal nerve, e.g. (Jantsch, Kemppainen, Ringler, Handwerker, & Forster, 2005; Weigelt et al., 2010). Our observations of bilateral rCBF changes in thalamus most likely relate particularly to representation of pain by the trigeminal system. In particular, crossed and uncrossed somatosensory and nociceptive afferents project from the trigeminal ganglion, via the principal sensory nucleus and nucleus caudalis respectively, terminating at the ventral medial and lateral posterior regions of the thalamus. Both these thalamic regions contain bilateral representations of the intra-oral cavity (Nieuwenhuys, Voogd, & Van Huijzen, 2008). In addition, extensive interconnections in thalamus and hypothalamus (Pogatzki-Zahn et al., 2007) are likely to underpin bilateral changes in post-surgical thalamic rCBF and may represent changes in arousal as well as the experience of ongoing pain (De Leeuw, Albuquerque, Okeson, & Carlson, 2005).

Demonstration of local increases in CBF in Vp during post- surgical, ongoing trigeminal pain echo recent reports of changes in brain activation in Vp in preclinical studies (Dessem, Moritani, & Ambalavanar, 2007), following hypertonic saline injection to the masseter muscle (Nash, Macefield, Klineberg, Murray, & Henderson, 2009) and following noxious electrical stimulation of the tooth pulp (Weigelt et al., 2010). These findings challenge the traditional belief that Vp is associated only with somatosensation, with nociceptive trigeminal afferents processed only via nucleus caudalis of the trigeminal nerve (Nieuwenhuys et al., 2008) and provide evidence that Vp plays a role in pain processing. We could not identify rCBF changes in trigeminal nucleus caudalis; this region of hindbrain was inferior to the ASL imaging volume

prescribed. Further methodological development is required to include these regions within the imaging volume. We speculate that extended brainstem coverage is likely to improve our ability to detect significant bilateral post-surgical CBF increases in the trigeminal ganglion (TG). While we report a cluster of significant CBF increase in left TG only, CBF increases in right TG were slightly below statistical cluster threshold and are likely to be explained by type-II error. Our findings of CBF changes in response to pain in the mandibular branch of TG are contrary to a recent report using BOLD-fMRI, which reported signal changes in the maxillary branch of TG only (Weigelt et al., 2010).

Taken together, our findings have potential to impact positively upon the role of neuroimaging in assessing novel treatments for pain (Borsook et al., 2008). We conjecture that in future, pCASL-derived rCBF measures might be used as prospective independent endpoints for pain assessment, rather than an adjunct to patient self-reported pain. We acknowledge such a statement is likely to provoke considerable controversy within the field (Derbyshire, 2006). In common with previous reports, for example (Derbyshire et al., 1997), our findings of correlations between post-surgical rCBF and VAS estimates of self-reported pain, limited only to brain regions known to underpin the pain experience, demonstrate that our results are physiologically plausible and relate (at least in part) to the pain experience. Caution should be exercised, however, in over-interpretation of VAS pain-estimate relationships with individual ROIs; first, given the multi-dimensional nature of the pain experience (Melzack, 2001) multivariate regression analyses are likely to provide better predictions of verbal response (Marquand et al., 2010); secondly, seeking only to replicate patient-self reported endpoints using neuroimaging obviates its use. Arguably imaging-based markers of ongoing pain should be considered in terms of their ability to add value over and above self-report (Borsook et al., 2008).

Our finding of reproducible rCBF data, within and between sessions, makes 'cross-over' assessments of pain treatments tenable. A critical next step to develop ASL as a methodology for assessing modulation of ongoing pain will be to demonstrate pain-related CBF changes that are attenuated by an analgesic of known efficacy. Successful demonstration of analgesic-modulated CBF changes should provide the evidence necessary to refine decision-making techniques for assessing efficacy of novel interventions. We envisage several potential uses for the pCASL methodology (Borsook et al., 2008); central effects of pain medications unrelated to their analgesic action could be assessed in pain-free participants (Wagner et al., 2001); putative mechanisms of action for novel analgesics might be investigated and possible new indications for existing compounds in related therapeutic areas uncovered; examinations of differential efficacy across pharmacological classes and doses could be realistic applications. In addition, availability of ASL in preclinical MRI should facilitate translational research; ASL studies might potentially illustrate new insights in ongoing pain in preclinical cohorts in which examination of simple behavioural endpoints in response to evoked pain has predominated to date (Mogil, 2009).

Improved knowledge of acute ongoing pain should impact upon understanding the central representation of chronic pain; bridging this gap might facilitate developing new medications for intractable pain conditions that are often resistant to currently approved analgesics (Kupers & Kehlet, 2006). Given increasing evidence for changes in brain function and structure relating to chronicity of pain (May, 2008), a better understanding of disease-specific 'neurosignatures' will be imperative. The

ROI-based methodology described here is appropriate to examining post-surgical pain in healthy volunteers, but cannot be applied universally to all persistent pain states; instead, selecting a set of a priori ROIs based on previous knowledge of the specific pain condition should be preferred. While we believe ASL has utility in analgesic trials, the method should be equally applicable to assessing changes in ongoing pain in other, non-pharmaceutical scenarios; for example, pain modulation following cognitive behavioural therapy (Eccleston, Williams, & Morley, 2009). Additional applications might include assessing pain in individuals less able to verbalise self-reported pain, for example children (Eccleston et al., 2012) or potentially, patients with consciousness disorders (Owen & Coleman, 2008).

In summary, using perfusion MRI, in concert with the TME model, we have described a network of rCBF increases representing ongoing post-surgical pain. Post-surgical CBF changes are reproducible within- and between sessions. Our findings represent the beginning of a novel approach to measure ongoing pain as an alternative to self-report. The approach is stable and provides robust, repeatable results in a relatively small group of participants, compared to conventional studies solely using self-reported pain as endpoints (Moore, Gavaghan, Tramèr, Collins, & McQuay, 1998). Reduction in study numbers is likely to provide benefits in the early phase assessment of putative analgesics and other interventions, both in terms of cost and time. While we have focussed upon assessment of acute, ongoing post-surgical pain, we believe that developing the methodology for examining pain in patients with persistent painful conditions will be valuable for pioneering much-needed new therapies.

Author Contributions

Conceived and designed the experiments: Howard, M.A., Huggins, J.P., Williams, S.C.R., Renton, T.F., Schumann, G., Performed the experiments: Howard, M.A., Krause, K., Khawaja, N., Renton, T.F., Analysed the data: Howard, M.A., Krause, K., Massat, N., Williams, S.C.R., Contributed reagents/materials/analysis tools: Howard, M.A., Zelaya, F., Massat, N., Wrote the paper: Howard, M.A., Krause, K., Khawaja, N., Massat, N., Zelaya, F., Schumann, G., Huggins, J.P., Vennart, W., Williams, S.C.R., Renton, T.F. .

Conflict of interest

The collection of the data was funded by Pfizer Global Research and Development UK. MAH and KK were paid on grant income from this source. JPH and WV were employees of Pfizer.

Acknowledgements

The authors would like to thank Owen O'Daly, Sheelah Harrison, Mick Thacker, Ailsa Morrison, Steve Smith, Mark Woolrich, Trevor Smart, Caroline Wooldridge, and David Alsop for their comments and suggestions.

2.2 Manuscript II: Quantifying the test-retest reliability of cerebral blood flow measurements in a clinical model of on-going post-surgical pain: A study using pseudo-continuous arterial spin labelling²

Reference:

Hodkinson, D. J., Krause, K., Khawaja, N., Renton, T. F., Huggins, J. P., Vennart, W., ... Howard, M. a. (2013). Quantifying the test–retest reliability of cerebral blood flow measurements in a clinical model of on-going post-surgical pain: A study using pseudo-continuous arterial spin labelling. *NeuroImage: Clinical*, 3, 301–310. <http://doi.org/10.1016/j.nicl.2013.09.004>

Abstract

Arterial spin labelling (ASL) is increasingly being applied to study the cerebral response to pain in both experimental human models and patients with persistent pain. Despite its advantages, scanning time and reliability remain important issues in the clinical applicability of ASL. Here we present the test–retest analysis of concurrent pseudo-continuous ASL (pCASL) and visual analogue scale (VAS), in a clinical model of ongoing pain following third molar extraction (TME). Using ICC performance measures, we were able to quantify the reliability of the post-surgical pain state and Δ CBF (change in CBF), both at the group and individual case level. Within-subject, the inter- and intra-session reliability of the post-surgical pain state was ranked good-to-excellent (ICC N 0.6) across both pCASL and VAS modalities. The parameter Δ CBF (change in CBF between pre- and post-surgical states) performed reliably (ICC N 0.4), provided that a single baseline condition (or the mean of more than one baseline) was used for subtraction. Between-subjects, the pCASL measurements in the post-surgical pain state and Δ CBF were both characterised as reliable (ICC N 0.4). However, the subjective VAS pain ratings demonstrated a significant contribution of pain state variability, which suggests diminished utility for inter-individual comparisons. These analyses indicate that the pCASL imaging technique has considerable potential for the comparison of within- and between-subjects differences associated with pain-induced state changes and baseline differences in regional CBF. They also suggest that differences in baseline perfusion and functional lateralisation characteristics may play an important role in the overall reliability of the estimated changes in CBF. Repeated measures designs have the important advantage that they provide good reliability for comparing condition effects because all sources of variability between subjects are excluded from the experimental error. The ability to elicit reliable neural correlates of ongoing pain using quantitative perfusion imaging may help support the conclusions derived from subjective self-report.

² Author Contributions to Idea/Experimental Hypothesis: 5%, Experimental Design: 5% Data Collection: 80%, Data Analysis: 20%, Writing: 5%, Interpretation: 5%

Introduction

Pain is a complex, multidimensional experience that includes sensory and affective components. Within this context, pain is subjective and is not readily quantifiable. For humans, pain assessment strategies may include self-rating scales, observational scales, and other behavioural tools (Katz & Melzack, 1999). One of the most commonly used methods for assessing pain in the clinic is the visual analogue scale (VAS). While this assessment is by definition, highly subjective, these scales are of most value when looking at changes within individuals, and are of less value for comparing across a group of individuals at one particular time (Steingrimsdóttir, Vøllestad, Røe, & Knardahl, 2004; Victor et al., 2008). Critically, there is an acknowledged, unmet need for more reliable endpoints of the pain experience (Kupers & Kehlet, 2006). The identification of robust and quantifiable measurement tools is likely to improve the diagnosis and management of chronic pain conditions, and help provide a better evaluation of the mechanisms of analgesic drugs.

Neuroimaging techniques have demonstrated that a large, distributed brain network underpins nociceptive processing. In the past, authors have referred to this network as the “pain matrix” (Brooks & Tracey, 2005); however this concept has been challenged, as relevant salient or behavioural stimuli have been shown to engage a similar network (Downar, Mikulis, & Davis, 2003; G. D. Iannetti & Mouraux, 2010). For acute pain experiences, commonly activated areas include the primary and secondary somatosensory cortices, insular, anterior cingulate, prefrontal cortex, and the thalamus (Apkarian et al., 2005; Tracey & Bushnell, 2009a). Depending on the nociceptive stimulus and experimental paradigm, other brain regions including the basal ganglia, cerebellum, amygdalae, hippocampus, and areas within the parietal and temporal cortices may also be recruited. By contrast, the mechanisms that contribute to the generation and maintenance of chronic clinical pain states are more complex. Several groups have reported consistent activation in the pre-frontal, frontal, and anterior insular cortices that may be important in the maintenance of chronic pain conditions (Apkarian, Baliki, & Geha, 2009; Howard et al., 2012; Schweinhardt & Bushnell, 2010; Wasan et al., 2011). However, it is still unclear if these markers of activity directly predict the underlying clinical pathology, or represent other contextual aspects of the patients' experiences.

Owing to the advent of arterial spin labelling (ASL) MRI techniques, the representation of ongoing or spontaneous pain states has rightly received attention in neuroimaging (Howard et al., 2011; Maleki, Brawn, Barmettler, Borsook, & Becerra, 2013; Owen et al., 2008; Owen et al., 2010; Tracey & Johns, 2010b). Our group recently reported a study using pseudo-continuous ASL (pCASL) (Dai et al., 2008), in conjunction with a commonly used post-surgical model, to demonstrate changes in regional cerebral blood flow (CBF) associated with the experience of being in ongoing pain after third molar extraction (TME) (Howard et al., 2011). This study identified a number of the anatomical regions consistent with pain response patterns detected using ASL in other experiments (reviewed in Maleki et al., 2013 (Maleki et al., 2013)). Pain following TME has become the most frequently used model in acute pain trials, particularly for regulatory purposes (Barden et al., 2004). However, in the present literature, there is limited information available on the reliability of quantitative perfusion measures for the study of ongoing pain in experimental volunteers and patients using ASL methodologies.

A well-established measure of reliability is the intra-class correlation coefficient (ICC) (Shrout & Fleiss, 1979). ICC has classically been described in the context of consistency or agreement between ratings given by different judges; however, it can also be used to assess the reliability of ratings across different testing sessions and to assess the reliability of imaging methods over time (Bennett & Miller, 2010; Caceres, Hall, Zelaya, Williams, & Mehta, 2009). Several groups have conducted reliability studies of resting CBF measurements employing different ASL labelling schemes (Çavuşoğlu, Pfeuffer, Uğurbil, & Uludağ, 2009; Y. Chen et al., 2011; Floyd, Ratcliffe, Wang, Resch, & Detre, 2003; Gevers, Majoie, Van Den Tweel, Lavini, & Nederveen, 2009a; Gevers et al., 2011; Hermes et al., 2007; Jahng et al., 2005; Jain et al., 2012; Jiang et al., 2010; Parkes, Rashid, Chard, & Tofts, 2004; Petersen, Mouridsen, & Golay, 2010; Tjandra et al., 2005; Xu et al., 2010; Yen et al., 2002). These studies converge on the conclusion that ASL reliability is comparable to other perfusion imaging techniques such as PET or SPECT; however, the extracted CBF values are often constrained to the cortical grey matter (GM), flow territories, brain lobes, or targeted regions-of-interest (ROIs). Two recent studies assessed the feasibility of ASL for pharmacological research, conducting test–retest evaluations of citalopram and fentanyl drug challenges (Klomp, Caan, Denys, Nederveen, & Reneman, 2012; Zelaya et al., 2012). To our knowledge, there have been no reports confirming the reliability of ASL-based perfusion measurements for the study of ongoing pain states in experimental volunteers or chronic pain patients. Similarly, there have been no ‘head-to-head’ comparisons of the ASL technique with traditional behavioural assessments of pain.

To confidently compare CBF values across different cohorts of a population (i.e. pain patients vs. healthy controls) and across repeated measurements on the same individual (such as in longitudinal cross-over studies and drug trials), it is important to consider the between- and within-subject variability. In this study, we sought to quantify the test–retest reliability of concurrent pCASL and VAS in a clinical model of ongoing pain following TME. Reliability was examined at three levels; (1) inter-subject, (2) inter-session, and (3) intra-session. Within each of these categories, we calculated the ICCs for the pre- and post-surgical states, together with the change in CBF (Δ CBF) between conditions. The principal aim of this work was to inform on the reliability of the pCASL technique versus VAS subjective pain ratings, and help provide a framework to support future use of ASL methodologies for the study of chronic pain conditions and experimental ongoing pain states.

Methods

Ethical approval and consent

All procedures were approved by the Kings College Hospital Research Ethics Committee (REC Reference 07/H0808/115). Informed, written consent was provided by all participants.

Inclusion criteria

Sixteen right-handed, healthy male volunteers (age range: 18– 50 years) were selected for the study. Participants presented with bilateral recurrent pericoronitis and fulfilled NICE guidelines for extraction of lower-jaw left and right third molars (NICE/NHS, 2000). Females were not included in the study due to potential variability

in the phase of the menstrual cycle affecting reproducibility of the post-surgical pain (Teepker et al., 2010).

Study design

Data were pooled from the previously published work of Howard et al. (2011) (Howard et al., 2011). Briefly, sixteen subjects were assessed on five separate occasions, screening/familiarisation (S1), pre-surgical scan (S2), post-surgical scan following the first tooth extraction (S3), pre-surgical scan (S4), and postsurgical scan following the second tooth extraction (S5) (Fig. 1). Scanning commenced at S3 and S5 when three consecutive VAS scores greater than 30/100 mm were provided within a 30-minute period. Order of left and right tooth extraction was balanced and pseudo-randomised across the group. A minimum of two-week interval separated S3/S4, and participants were assessed based on individual report of pain cessation to ensure complete recovery from the surgery. The rescue medication of 1000 mg paracetamol/400 mg ibuprofen was provided to participants immediately following scanning during S3 & S5. Full alcohol and drug-screens were performed at every visit, including psychometric assessment.

Perfusion MRI

Participants were scanned on a 3 T whole-body MRI scanner (GE Signa HDX) fitted with a receive-only 8-channel, phased-array head coil. For image registration purposes, a high resolution T2-weighted Fast Spin Echo (FSE) image was acquired. Perfusion measurements were made using a pseudo-continuous arterial spin labelling (pCASL) sequence (Dai et al., 2008). Labelling was performed using a train of Hanning RF pulses; 500 μ s duration, peak-to-peak gap 1500 μ s, and a total labelling duration of 1.5 s. After a post-labelling delay of 1.5 s, the image was acquired with a 3D FSE inter-leaved spiral readout (8 shots, TE/TR = 32/5500 ms, ETL = 64, 3 tag-control pairs). Pre-saturation of the image volume, followed by selective inversion pulses for background suppression, was also acquired in order to minimise the static signal. Two reference images (fluid suppressed and both fluid and white matter suppressed); as well as a coil sensitivity map, were used for the computation of the CBF maps in physiological units (ml blood per 100 g of tissue per min). The ASL time series comprised 6 pCASL scans, lasting 6 min each. Participants were instructed to lie still with their eyes open. Full details of the pCASL sequence and absolute quantification of CBF are available in Supplementary information.

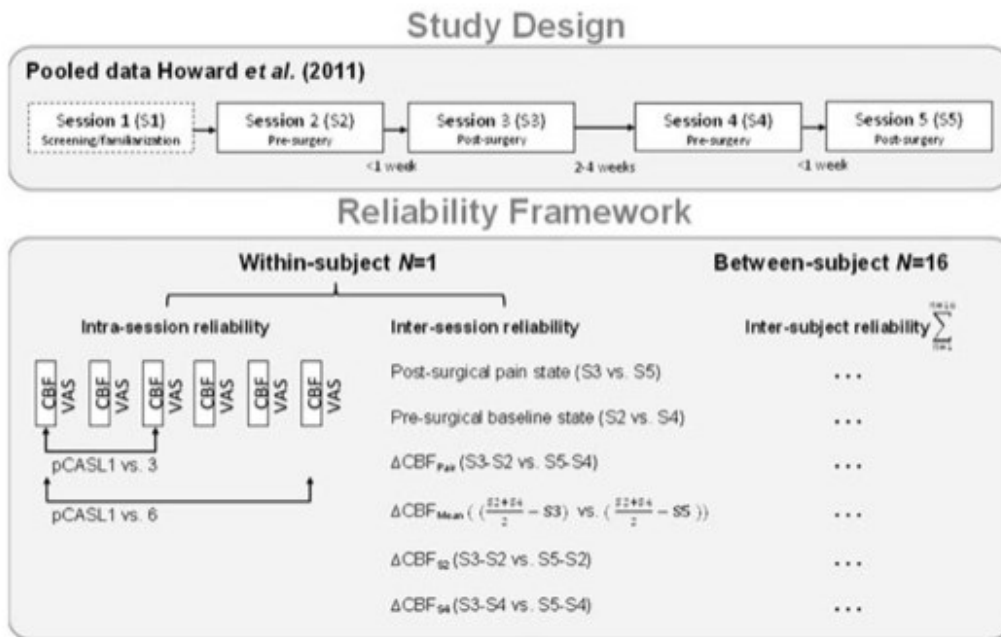


Figure II-1: Study design for the assessment of reliability of the pCASL and VAS modalities in the clinical model of ongoing post-surgical pain. The data was pooled from two pre- and post- surgical visits to assess group-level inter-subject consistency, and the within-subject inter- and intra-session reliability.

Visual analogue scales

Concurrent with the MRI examination, subjects were asked to rate their perceived levels of pain and alertness using a visual analogue scale (VAS). The VAS measurements were performed according to an established protocol (Howard et al., 2011) which consisted of a computerised line anchored with “no pain”/“worst imaginable pain” and “very sleepy”/“wide awake”. Participants subjectively rated their experience following each of the six pCASL scans using a computerised VAS and button-box.

Image pre-processing

The quantitative CBF data were pre-processed using FSL (<http://www.fmrib.ox.ac.uk/fsl>) (S. M. Smith et al., 2004). The pipeline consisted of skull stripping [BET], affine registration of each subject's T2 to the Montreal Neurological Institute (MNI) ICBM152 non-linear asymmetric T2- weighted template with resampling to $2 \times 2 \times 2\text{ mm}^3$ [FLIRT], and non-linear noise reduction [SUSAN: $\lambda = 5\text{ mm}$ full-width half maximum]. Statistical analysis was performed under the framework of the general linear model (GLM) [FLAMEO]. First-level analyses were computed for each subject to create grey-matter (GM) only mean images of the six individual pCASL scans acquired at each of the sessions S2–S5. For the second-level analysis, changes in the CBF relating to post-surgical pain were obtained using a mixed-effects two-way ANOVA of the combined session-pairs (i.e. Pair 1[S2,S3]/Pair 2[S4, S5]) and a t-threshold equivalent to $p < 0.01$ ($z = 2.3$, $t = 2.41$, $\text{dof} = 45$). Factorial designs are powerful, because the interaction between various cognitive components (factors) is explicitly modelled in the analyses (Friston et al., 1996). However, an anticipated problem with calculating the change in CBF between pre- and post-surgical states (ΔCBF) is that arithmetic subtraction between these two

conditions will not take account of the error variance. To examine these effects, images of ΔCBF (change in CBF) were calculated in four separate ways: (1) arithmetic subtraction of the pre- and post-surgical session- pairs ($\Delta\text{CBFPairs}$), (2) subtraction of the post-surgical sessions from the combined mean of the pre-surgery sessions ($\Delta\text{CBFMean}$), (3) subtraction of the post-surgical sessions from the first pre-surgery session only (ΔCBFS2), and (4) subtraction of the post-surgical sessions from the second pre-surgery session only (ΔCBFS4). The same contrast images, for the pre- and post-surgical sessions only, were used to extract the reliability of the independent states (see Figure II-1).

Regions of interest

To assess CBF reliability between subjects and sessions, regions of interest (ROIs) were defined a priori based upon previously implicated areas in pain processing measured with arterial spin labelling (reviewed in Maleki et al. (2013) (Maleki et al., 2013)). ROIs were anatomically defined in standard MNI space from the Harvard–Oxford cortical and subcortical structural atlases, with probabilistic images thresholded at 20% and binarised to create exclusive ROI masks. These were anterior cingulate cortex (ACC), posterior cingulate cortex (PCC), anterior insula (aINS), posterior insula (pINS), somatosensory cortex (primary, S1 and secondary, S2), thalamus (THAL), hippocampus (HIP), amygdala (AMY), and brainstem (BS).

Statistical methods

To systematically evaluate the test–retest performance of the TME post-surgical pain model, we examined the inter-subject, inter-session, and intra-session variability of CBF and VAS measurements (Fig. II-1). These reliability estimates were calculated using the third ICC defined by Shrout and Fleiss (1979) (Shrout & Fleiss, 1979)

$$\text{ICC}(3,1) = \frac{\text{BMS} - \text{EMS}}{\text{BMS} + (k - 1)\text{EMS}}$$

where BMS is the between-targets mean square, EMS is the error mean square, and k is the number of repeated sessions (here two). All ICC values were calculated in MATLAB 7.1 (The Mathworks Inc.) and the statistical toolbox produced by (Caceres et al., 2009) (ICC Toolbox is available for download at:

<http://www.kcl.ac.uk/iop/depts/neuroimaging/research/imaginganalysis/Software/ICC-Toolbox.aspx>). We denote ICC values < 0.4 as poor, $0.4\text{--}0.59$ as fair, $0.60\text{--}0.74$ as good, and > 0.75 as excellent (Fleiss, Levin, & Paik, 2003). However, these ranges should be interpreted with caution as they do not take into account the confidence intervals of the ICC.

Coefficient of variation (CV) is defined as the ratio of the standard deviation σ to the mean μ := $\frac{\sigma}{\mu}$.

Reliability of the behavioural measures

We examined behavioural changes using the VAS self-report of subjective alertness and pain. Inter-subject consistency was compared using all ratings from the post-surgical pain sessions. Within-subjects the VAS measurements from left and right-side post-surgical pain sessions were used to assess inter-session reliability. Intra-session stability was evaluated using the six VAS measures from either left or right-

side post-surgical sessions independently. The parameter Δ VAS (change in VAS) could not be assessed due to a floor effect (i.e. scores of zero) in the pre-surgery VAS condition.

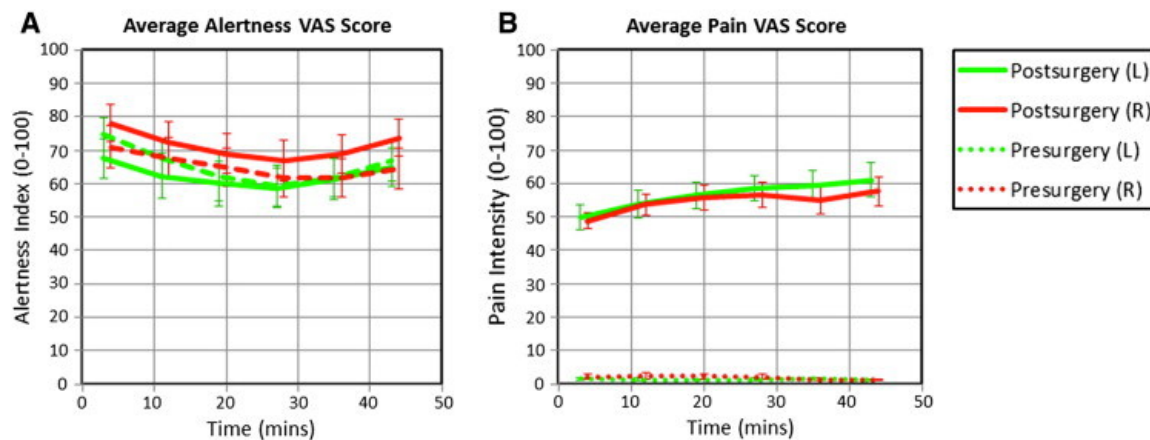


Figure II-2: Concurrent VAS ratings of perceived alertness (A) and pain (B). Participants subjectively rated their experience following each of the six pCASL scans. Data represents the mean (\pm S.E.M.) of all subjects' ratings.

Inter-subject reliability of the CBF measurements

Inter-subject consistency of the ASL data was compared using an ICC approach previously described in the literature (Caceres et al., 2009). This was performed as a voxel-wise calculation of ICC, based upon the medians of ICC distributions (med ICC). We demonstrate the reliability of the pain network, whole GM volume, and targeted ROIs.

Inter- and intra-session reliability of the CBF measurements

Inter- and intra-session reliability of the ASL data was compared using an intra-voxel ICC measurement (ICCv) (Caceres et al., 2009; Raemaekers et al., 2007; Specht, Willmes, Shah, & Jancke, 2003). This was calculated by extracting the CBF amplitudes of each voxel, and assessing the distribution of ICC values across voxels of each ROI (Caceres et al., 2009). Comparisons between the session pairs were used to assess inter-session reliability. For intra-session reliability, the CBF values of the first and third, and first and sixth pCASL scans were examined independently. These scans were chosen as they represent the start, mid-point, and end of the dynamic time-series, hence should reflect any temporal variations in CBF between the repeated measurements.

Results

Behavioural results

The VAS self-reported measures of alertness and pain are shown in Figure 2. There were no significant differences in alertness between the pre- and post-surgical sessions ($p = 0.35$), indicating that voluntary attention was consistent across the group. Participants' subjective ratings of pain were significantly higher in the post-surgical sessions as compared to the pre-surgical sessions ($p < 0.001$). There were

no significant differences in the VAS scores relating to the left or right third molar extraction ($p = 0.97$). The ICC performance measures of alertness and pain VAS ratings demonstrated the highest reliability within-subjects. Both inter- and intra-session ICCs were consistently above 0.6 and 0.8 with a low coefficient of variation (CV), indicating that the test–retest reliability of the pain and alertness ratings was good-to-excellent. At the group level, inter-subject VAS ratings of alertness indicated a good level of reliability (ICC = 0.664). However, the pain ratings demonstrated only fair reliability between-subjects (ICC = 0.456), which indicates a significant contribution of pain state variability. The ICC results are summarised in Table II-1.

VAS reliability								
Visual analogue scales	Inter-subject		Inter-session		Intra-session			
	ICC	CV	Left vs right		Left		Right	
ICC			CV	ICC	CV	ICC	CV	
Pain intensity	0.456	0.285	0.602	0.200	0.830	0.300	0.861	0.267
Alertness	0.664	0.359	0.640	0.203	0.800	0.390	0.940	0.320

Table II-1: Reliability measures for the subjective behavioural ratings of pain and alertness. ICC, intraclass correlation coefficients; CV, coefficient of variation.

Group-level inter-subject consistency of the CBF measurements

Univariate GLM analysis of the pre- and post-surgical sessions showed significant CBF increases in the respective anatomical target regions (Figure II-3) (see Supplementary information Table II-1 for ROI values).

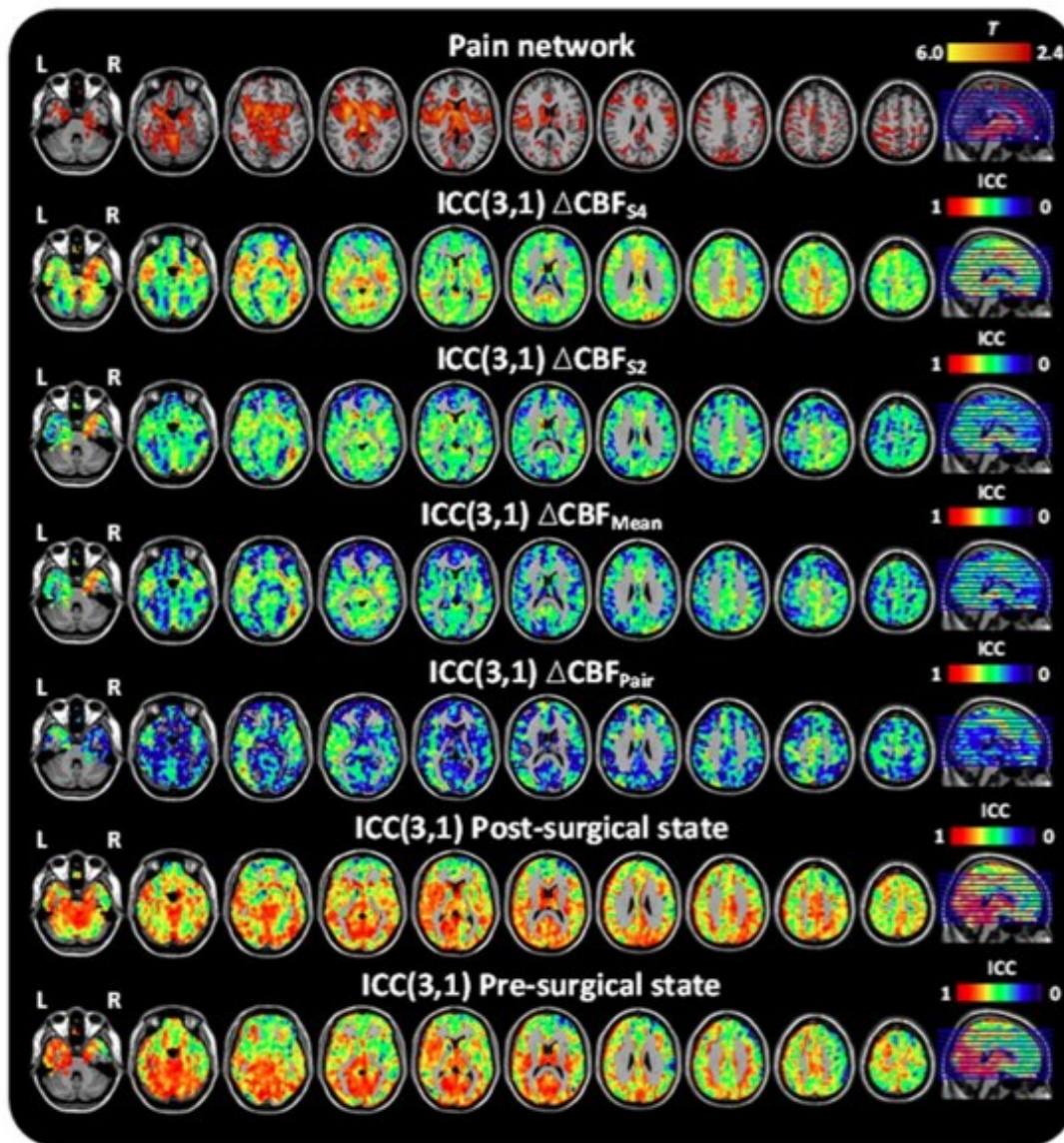


Figure II-3: Group-level univariate and ICC analysis of pre- and post-surgical sessions, and ΔCBF .

Having confirmed that a network of rCBF increases is present during pain processing in the TME model, these data were used to assess the reliability of the pre- and post-surgical states together with the stability of the observed pain response (ΔCBF). The resulting ICC (3,1) maps for these conditions are depicted in Fig. II-3. ICC values across the pre- and post-surgical states were high (0.763/0.746 and 0.744/0.731; [pain network/total GM]), which confirms high reliability across the individuals. Estimates of the reliability associated with the different ΔCBF calculations were less consistent: the between-subjects ICC was smallest in the $\Delta\text{CBF}_{\text{Pair}}$ (0.325/0.343), slightly higher using the mean of the two pre-surgical sessions ($\Delta\text{CBF}_{\text{Mean}}$ 0.469/0.440), and greatest with the $\Delta\text{CBF}_{\text{S}_2}$ (0.542/0.494) or $\Delta\text{CBF}_{\text{S}_4}$ (0.604/0.589). The voxel-wise ICC values for individual ROIs can be found in Fig. II-4A.

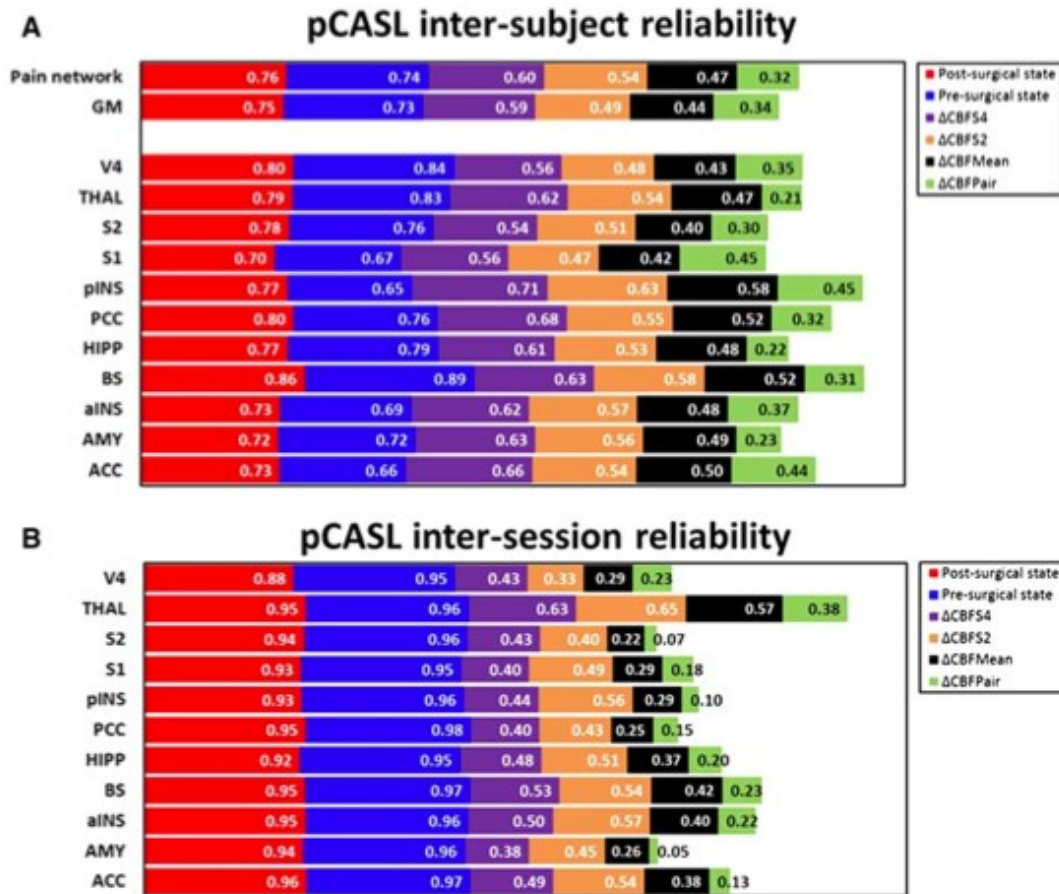


Figure II-4. Inter-subject (A) and inter-session (B) reliability for the cortical grey-matter (GM), pain network, and targeted ROIs. Stacked columns represent the reliability magnitude including labels inside end. ICC values were calculated at a voxel-wise level. Abbreviations: amygdala (AMY), hippocampus (HIPP), brainstem (BS), thalamus (THAL), anterior insula (aINS), posterior insula (pINS), somatosensory cortex (primary, S1 and secondary, S2), posterior cingulate cortex (PCC), anterior cingulate cortex (ACC).

Examining the ICC distributions, plots of the relative number of voxels against ICC score are shown in Fig. II-5. The profiles of the pre- and post-surgical states (Fig. II-5A) both demonstrate a pronounced negative skew in the ICC distribution, with the mass of the distribution concentrated on the right of the figure. There were relatively few low ICC values. For the parameter ΔCBF (Fig. II-5B), the profiles of the four baseline calculation methods were considerably different. The negative skew was largest with $\Delta\text{CBF}_{\text{S}_2}$ or $\Delta\text{CBF}_{\text{S}_4}$, slightly smaller with the $\Delta\text{CBF}_{\text{Mean}}$, and smallest with the $\Delta\text{CBF}_{\text{Pair}}$ baseline. Importantly, in the $\Delta\text{CBF}_{\text{S}_2}$ or $\Delta\text{CBF}_{\text{S}_4}$ comparisons, voxels of the pain network were visibly more detached from the ICC values of the total GM volume.

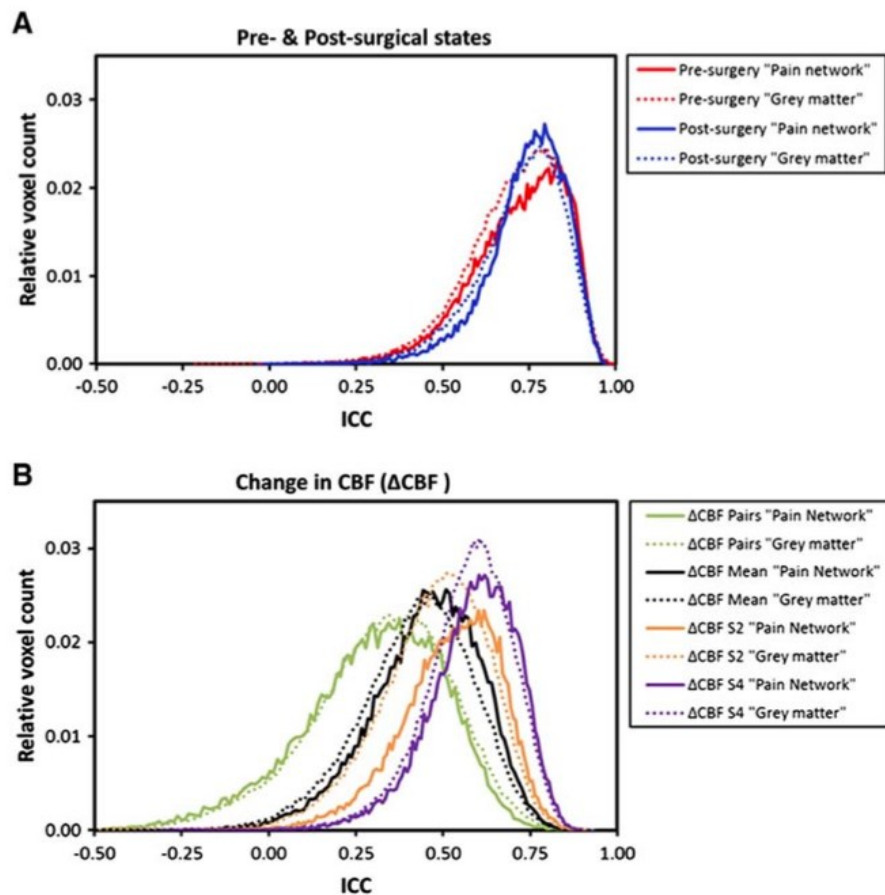


Figure II-5. ICC distributions of the pre- and post-surgical states (A) together with the Δ CBF (change in CBF) (B). Plots show the relative number of activated voxels against ICC score for the grey matter (dotted lines) and activated pain network (solid lines).

Within-subject inter-session reliability of the CBF measurements

Figure II-4B shows the regional inter-session ICC values for the pre- and post-surgical states together with the change in CBF (Δ CBF). For the pre- and post-surgical states, a high level of agreement was found in all ROIs of the pain network. These voxel-based ICCs (ICC_v) were consistently above 0.90 for each subject, demonstrating that the rCBF measurements have excellent inter-session reproducibility. By contrast, the ICC values for the Δ CBF images were much more varied with the Δ CBF_{Pair} and Δ CBF_{Mean} ranking poor-to-fair reliability, and Δ CBF_{S2} or Δ CBF_{S4} classified as fair to good.

Within-subject intra-session reliability of the CBF measurements

Intra-session reliability was reported for the post-surgical states. Sequential comparisons of the pCASL scans revealed that the voxel-based ICCs in all ROIs were consistently above 0.90 for every subject (irrespective of surgery-side) (Table II-2). This suggests that the CBF measurements have excellent time-course reproducibility, and are stable from scan-to-scan.

pCASL intra-session reliability								
ROI	Left-side post-surgical state				Right-side post-surgical state			
	pCASL 1 vs 3		pCASL 1 vs 6		pCASL 1 vs 3		pCASL 1 vs 6	
	CC _v	SEM	ICC _v	SEM	ICC _v	SEM	ICC _v	SEM
ACC	0.965	0.006	0.962	0.006	0.968	0.003	0.966	0.006
AMY	0.937	0.009	0.921	0.017	0.944	0.004	0.938	0.007
aINS	0.967	0.005	0.959	0.004	0.970	0.005	0.964	0.004
BS	0.974	0.003	0.970	0.004	0.974	0.003	0.970	0.002
HIPP	0.931	0.008	0.923	0.010	0.938	0.004	0.938	0.004
PCC	0.974	0.007	0.973	0.007	0.977	0.005	0.972	0.006
pINS	0.958	0.005	0.951	0.007	0.963	0.003	0.961	0.005
S1	0.957	0.004	0.952	0.007	0.953	0.008	0.947	0.007
S2	0.974	0.004	0.968	0.003	0.976	0.003	0.971	0.004
THAL	0.955	0.006	0.945	0.012	0.957	0.005	0.955	0.012

Table II-2: Intra-session reliability of the representative pain ROIs. ICC values are compared between first and third, and first and sixth pCASL scans in the post-surgical pain states (ICC_v; the intra-voxel reliability; SEM, standard error from measurement).

Discussion

Summary

In the current literature there is very limited information available on the reliability of quantitative cerebral perfusion measures for the study of ongoing pain in experimental volunteers and patients. Here we present the test–retest analysis of concurrent pCASL and VAS measurements in a clinical model of ongoing pain after third molar extraction (TME).

The key findings of this study are:

- 1) Within-subject, the inter- and intra-session reliability of the post-surgical pain state was ranked good-to-excellent across both pCASL and VAS modalities. The parameter Δ CBF (change in CBF between pre- and post-surgical states) performed reliably, provided that a single baseline condition (or the mean of more than one baseline) was used for subtraction.
- 2) Between-subjects, the pCASL measurements in the post-surgical pain state and Δ CBF were both characterised as reliable. However, the subjective VAS pain ratings demonstrated a significant contribution of pain state variability, which suggests diminished utility for inter-individual comparisons.

Reliability at the behavioural level

Of the various methods for measuring pain, the visual analogue scale (VAS) is regarded the most sensitive. In the present study, inter- and intra-session reliability of VAS was consistently above 0.60, which indicates good-to-excellent levels of sensitivity to the changes in pain intensity within-subjects. As anticipated, the group-level pain scores demonstrated only fair reliability, reflecting a significant contribution of pain state variability. A likely reason for this numerical discrepancy is that the ICC measures are particularly sensitive to the small number of observations. One could argue that higher numbers of subjects may be required to detect a more robust behavioural response to pain. However, the VAS measures of alertness appeared not to suffer from this affect, suggesting that the variation in reliability could be explained by the influence of other contextual aspects of the patients' environment,

which are known to separately influence pain perception (Tracey, 2010). A potential weakness of pain VAS is that each scale is one-dimensional and does not capture the full complexities of an individual's pain experience (Schiavenato & Craig, 2010). This remains a contentious issue in pain research (Davis, Racine, & Collett, 2012; Robinson, Staud, & Price, 2013); however our paper focuses on the opportunities afforded through combining novel neuroimaging endpoints of pain with subjective self-report.

Group-level inter-subject consistency of the CBF measurements

Reliability and agreement are important issues in the conduct of clinical studies as they provide information about the amount of error inherent in any diagnosis, score, or measurement. In the present study, ICC values for the pre- and post-surgical states were characterised as good-to-excellent, while the reliability of Δ CBF ranged from poor-to-good depending on the method of Δ CBF calculation. These findings support the use of perfusion MRI measures for the study of ongoing pain states and induced CBF responses. However, we demonstrate that measurement of more than one pre- and post-surgical CBF map has a profound effect on the reliability of the Δ CBF parameter.

ICC reliability indexes are not fixed characteristics of a measurement instrument. Factors associated with the study design (e.g. time-intervals between sessions and session order), the study cohort (e.g. age, gender, emotional status, and cognitive level), surgical interventions, etc., might all influence the magnitude of the variance between subjects as well as the error variance. To minimise the impact of these effects, we employed a counterbalanced within-subject study design, including strict inclusion and exclusion criteria as a means of establishing precision in the cohort. However, our reliability tests suggest that the cognitive or physiological contexts of the pre- and post-surgical states are not entirely independent or free of both functional and psychological interactions. Issues with pure insertion are common in studies that employ cognitive subtraction, and it has been shown that factorial designs are generally more powerful in the analysis of cognitive processes (Friston et al., 1996). These effects were recently demonstrated by Klomp et al. (2012), who reported issues in detecting reliable drug-induced CBF changes with ASL using the test–retest method. With this in mind, we demonstrate that using a single baseline condition (or the mean of more than one baseline) may give more precise estimations of ICCs, and we suggest taking this innovation into account when designing future test–retest studies involving repeated measures, particularly in the context of a drug study.

We also observed that the high ICC values do not necessarily follow the high values of t (see Figure II-3). This discrepancy may originate from differences in the spatial distribution of the CBF response to pain, or from differences in intrinsic physiological factors between the individuals. Under normal resting conditions, perfusion has the potential to fluctuate considerably (Petersen et al., 2010) depending on the level of brain activity (Wenzel et al., 1996). Also, variations in blood T1, neuronal density or number, and arousal (Parkes et al., 2004) may cause individual differences in the perfusion estimate. Given that we carried out pCASL measurements at 3 T rather than 1.5 T, we had the advantage of longer T1, higher SNR, and improved spatial and temporal resolution. Uncertainties regarding the cerebrovascular kinetics or blood equilibrium magnetisation might potentially bias the calculation of absolute CBF

values; however, this would not affect the conclusions of the current paper regarding reliability of the on-going pain state. The ICC is clearly dependent on the heterogeneity of the sample and fluctuations in physiology induced by the pain state. We therefore conclude that any spatial non-uniformity of reliability in the CBF measurements may be driven by physiological variability rather than potential limitations of the pCASL technique. Further reliability studies in patient populations relevant for pain clinical trials will be important for the future use of ASL methodologies for assessing the cerebrovascular response to pain. Our results provide a framework for such assessments.

Within-subject inter-session reliability of the CBF measurements

Within-subject reliability is principally a longitudinal phenomenon. In the current study, the pre- and post-surgical states demonstrated excellent levels of reliability following a minimum two week interval in the TME model (see Figure II-4), which is comparable with previous studies into the longitudinal reliability of ASL in healthy volunteers (Chen et al., 2011; Gevers et al., 2009a; Gevers et al., 2011; Jain et al., 2012; Parkes et al., 2004) and neurological patients (Xu et al., 2010). The reliability of ΔCBF was acceptable depending on the method of the ΔCBF calculation. More specifically, the ICC values were smaller with $\Delta\text{CBF}_{\text{Pair}}$ and $\Delta\text{CBF}_{\text{Mean}}$ than with $\Delta\text{CBF}_{\text{S2}}$ or $\Delta\text{CBF}_{\text{S4}}$. We suggest that this highlights once again the inadequacy of the simple insertion model, which may be an intrinsic problem with testing reliability by the test–retest method at the individual subject level. It must be stressed that our study design did not allow us to perform the pre-surgical scans immediately before surgery, but were instead performed on different days. This limitation was considered when interpreting the results of this reliability assessment; however we found no relationship between interval length and ICC values (see Supplementary information — Figure II-S2).

There may also be intrinsic physiological differences in lateralisation of anatomy and/or function within-subjects. Initial assessments of lateralisation (Howard et al., 2011) revealed that the surgical pain appeared to have the same impact on each hemisphere, independent of whether the left or right third molar was removed. Bilateral activations in S1, S2, and the insular cortex have also been reported in two previous studies employing painful (Jantsch et al., 2005) and non-painful (Ettlin et al., 2004) dental stimulations. This has important implications for follow-up studies and crossover trials, as the ability to demonstrate low variation across repeated measures enables the detection of small alterations in CBF indices to monitor disease progression or the effect of therapeutic interventions. Other advantages of the ASL technique are that it is less invasive and less expensive than existing perfusion imaging approaches using radioactive tracers or paramagnetic contrast agents (Petersen et al., 2006). As ASL sequences become more widely used, evaluations of their reliability across the course of longitudinal studies will be important for understanding the advantages they offer in clinical pain research.

Within-subject intra-session reliability of the CBF measurements

Potential variability in the CBF measurements could be attributed to temporal variation. The temporal stability of the ASL signal was investigated with respect to the duration of scanning for each subject. Since the pCASL scans were repeated without repositioning, the potential error from aligning the acquisition and labelling plane was

averted. Theoretically, this should minimise the operator-related variability, and begin to approach reproducibility values that are completely physiology dependent. As anticipated, the ICC values between pCASL scans were higher than those between sessions (Figure II-4 & Table 2), confirming that the CBF measurements within the on-going pain state have excellent time-course stability. The relative stability of these perfusion measurements to sustained temporal effects makes pCASL an attractive method to study naturalistic responses to pain. Furthermore, it allows within-subject investigations of spontaneous fluctuations in pain state, over relatively long-time intervals.

Conclusion

Here we present the test–retest analysis of concurrent pCASL and VAS measurements in a clinical model of on-going pain after third molar extraction (TME). Using ICC performance measures, we were able to quantify the reliability of the pain response and the on-going pain state, both at the group and individual case level. Within-subject, the inter- and intra-session reliability of the post-surgical pain state was characterised as good-to-excellent across both pCASL and VAS modalities. The parameter Δ CBF (change in CBF between pre- and post- surgical states) performed reliably, provided that a single baseline condition (or the mean of more than one baseline) was used for subtraction. Between-subjects, the pCASL measurements in the post-surgical pain state and Δ CBF were both characterised as reliable. However, the subjective VAS pain ratings demonstrated a significant contribution of pain state variability, which suggests diminished utility for inter-individual comparisons. These analyses indicate that the pCASL imaging technique has considerable potential for the comparison of within- and between-subjects differences associated with pain-induced state changes and baseline differences in regional CBF. They also suggest that differences in baseline perfusion and functional lateralisation characteristics may play an important role in the overall reliability of the estimated changes in CBF. Repeated measures designs have the important advantage that they provide good reliability for comparing condition effects, because all sources of variability between subjects are excluded from the experimental error. The ability to elicit reliable neural correlates of ongoing pain using quantitative perfusion imaging might help support the conclusions derived from subjective self-report.

Conflict of interest

The collection of the data was funded by Pfizer Global Research and Development UK. MAH and KK were paid on grant income from this source. JPH and WV were employees of Pfizer. DJH was paid with grant income from the MRC.

Acknowledgements

The authors would like to thank Dr David Alsop for providing us with the 3D pCASL sequence used for this work. We also thank Nick Spahr, Kate Jolly, Duncan Sanders, and Owen O'Daly for their comments and suggestions. This work was supported by the award of a Developmental Pathway Funding Scheme from the Medical Research Council (MRC). SW would also like to thank the National Institute for Health Research (NIHR), Biomedical Research Centre for Mental Health at South London and Maudsley NHS Foundation Trust and [Institute of Psychiatry] King's College London, the Wellcome Trust and EPSRC (under grant no. WT088641/Z/09/Z) for their continued infrastructure support of our neuroimaging research.

2.3 Manuscript III: Molecular Characterisation of blood-based Response to Surgical Trauma reveals Enriched Expression in Pain-Relevant Signaling Pathways³

Reference:

Krause, K., Sticht, C., Witt, S., Johnston, G., Huggins, J. P., Vennart, W., Williams, S. C. R., Lourdasamy, A., Howard, M.A., Khawaja, N., Renton, T.F., Schumann, G., Flor, H. (in preparation). Molecular Characterisation of the blood-based Response to Surgical Trauma Reveals Enriched Expression in Pain-Relevant Signalling Pathways.

Abstract

Genome-wide gene expression levels in peripheral whole blood pre- and post third molar extraction with added bioinformatic pathway analysis yielded a list of potential biomarkers in inflammatory post-surgical pain in humans. Several of the genes showed numerous associations with various pain disorders and coded for members of protein groups with known pain modulatory functions (e.g. zinc finger proteins, interleukins and enkephalinases). The high number of associations with various pain phenotypes might facilitate future identification of shared mechanisms between pain disorders of different clinical manifestations and promote the development of novel analgesics and drug classes within a mechanism based framework of pain and its treatment.

Introduction

To date genotyping individuals with rare Mendelian disorders has led to the discovery of genes, which dramatically affect the pain response by causing severe insensitivity to pain (Auer-Grumbach, 2008; Einarsdottir et al., 2004; Lafreniere et al., 2004; Wada et al., 2002). In addition, several candidate gene studies have investigated various single nucleotide polymorphisms (SNPs) in specific pain populations or experimental pain paradigms (Diatchenko et al., 2006; Kim, Mittal, Iadarola, & Dionne, 2006; Vargas-Alarcón et al., 2007) based on prior knowledge about pain physiology. For example, in the clinical context the effects of opioid analgesics in conjunction with their primary target, the mu-opioid receptor and mutations therein, have received much attention (J Lötsch & Geisslinger, 2006; Walter & Lötsch, 2009a).

The majority of pain disorders seen in clinical practice, however, is most likely of polygenic origin (Kalow, 2006; Max & Stewart, 2008a) with genes from a target selection whose full extent is still undetermined. The genes involved may also vary between disorders, since our knowledge of molecular pain mechanisms is still

³ Author Contributions to Idea/Experimental Hypothesis: 40%, Experimental Design: 40%, Data Collection: 80%, Data Analysis: 20%, Writing: 90%, Interpretation: 80%

incomplete (Max, 2000; Woolf & Max, 2001). A pure candidate gene approach is time-consuming and prone to overlook potentially relevant targets.

Recent advances in genomic technologies have enabled the simultaneous assessment of the expression patterns of a multitude of genes. These technologies are increasingly employed in a wide range of clinically relevant pain disorders and nociception (Galicia, Henson, Parker, & Khan, 2016; Sjöstrand et al., 2006).

This study assessed gene expression patterns at whole-genome level in human participants pre and post third molar extraction (TME) in order to identify genes indicated in acute inflammatory pain. TME represents a clinically relevant pain challenge and has been utilised successfully in genetic association studies in humans in association with gene expression in oral mucosa wound repair (Warburton et al., 2005), in a DNA association study on post-surgical pain tolerance (Kim, Ramsay, Lee, Wahl, & Dionne, 2009) and has also produced useful results in the assessment of inflammatory pain (Barden et al., 2004). Results are also likely to translate to other post-surgical pain experiences (Hyungsuk Kim et al., 2009). This investigation used gene expression levels in peripheral whole blood as a clinical endpoint in search of candidate genes for post-surgical pain in a TME paradigm. Blood was selected due to its involvement in pain modulation by delivering inflammatory mediators to damaged tissues such as histamine, bradykinin and opioid-peptides from leukocytes (Busch-Dienstfertg & Stein, 2010; Dray, 1995).

TME tissue trauma triggers several cascades of molecular responses including an immune response in order to protect the body from pathogens likely to enter through the lesion, tissue repair functions to restore protective tissue boundaries and a nociceptive response to alert the organism to this threat, prevent further damage and to modify behaviour in order to support the latter two responses. As a result an extensive list of differentially expressed genes with involvement in these different responses emerges in comparisons of samples collected in painful and pain-free states. The particular challenge was to identify those genes differentially expressed after surgery with a primary association with post-surgical pain.

Gene Set Enrichment Analysis (GSEA) of gene expression data takes into account prior biological knowledge in evaluating microarray data by operating at the level of gene sets rather than individual genes or gene lists simply ordered by statistical significance and fold change (Mootha et al., 2003; Subramanian, Tamayo, & Mootha, 2014). These gene sets are organised maps generated manually from current scientific literature on molecular interaction and reaction networks. One such database is the Kyoto Encyclopedia of Genes and Genomes (KEGG), which provides seven different categories of pathways (1. metabolism, 2. genetic information processing, 3. environmental information processing, 4. cellular processes, 5. organismal systems, 6. human diseases and a structure relationship map for 7. drug development). This study used GSEA to test for significant enrichment of the list of genes with significant up- and down-regulation post surgery in any of the established KEGG pathways.

GSEA potentially facilitates the discovery of known molecular pathways in novel contexts with post-surgical pain. In addition, novel sets of genes might emerge, which could highlight hitherto unknown molecular pathways and mechanisms of pain regulation. This in turn might enable a much needed expansion in the number of molecules that have so far been considered targets in pain treatment (Belfer et al.,

2004; Max & Stewart, 2008a) and may thus improve analgesic development, treatment allocation and increase patient benefit (Max, 2000; Woolf et al., 1998).

Methods

Ethics Statement

This study was approved by Kings College Hospital Research Ethics Committee (REC Reference 07/H0808/115).

Subjects and Materials

Informed consent was provided by all participants prior to study procedures. Removal of both wisdom teeth in the lower jaw was necessitated by bilateral intermittently recurring pericoronitis, diagnosed in accordance with NICE guidelines (NICE/NHS, 2000). Impact of the wisdom teeth on the second molars and gum tissue was confirmed by an experienced clinician based on x-ray images. Surgeries were performed while pericoronitis was in remission and participants were pain-free.

In total 22 right-handed, healthy male volunteers aged 20–41, (Mean=26.44, SD=5.49) were assessed. Since the study was conceived as a proof of concept study, potential variability was controlled for by excluding female participants as menstrual cycle status interferes with reproducibility of the post-surgical pain response (Teepker et al., 2010).

Study Design & Procedure

Teeth were removed separately on two of a total of one familiarisation and five study visits (T2 & T4). This created a cross-over study design with pain-free baseline measurements to use in contrast the post-surgical measurements (see figure III-1). Due to the similar placement and surgical difficulty level, the surgery on the side opposite to the initial surgery site can be used akin to a repeated measure. A modified version of this design was used in a follow up study to compare the effect of a drug vs. placebo (Hodkinson, Khawaja, et al., 2015b).

Time point	Labels	description
T0	Sample A	familiarisation
T1	Sample B	non-surgical baseline
T2	Sample C1	pre tooth extraction
T2	Sample C2	post tooth extraction
T3	Sample D	non-surgical baseline
T4	Sample E1	pre tooth extraction
T4	Sample E2	post tooth extraction
T5	Sample F	non-surgical baseline

Table III-1: Sampling time points and labels

The order of left and right tooth extraction was balanced and pseudo-randomised across the group, to account for occasions where one tooth had to be removed before the other due to clinical need. There was a minimum of three weeks between T2 and T3 to allow for recovery from the first surgery such that participants did not report any on-going pain at T3. The same interval was applied for post-surgical recovery from T4 before T5. For each tooth there was a minimum of a week and a

maximum of three weeks between pre-surgical and post-surgical sessions. Peripheral whole blood was collected on each of the visits.

A total of eight peripheral whole blood samples were taken from each subject, out of which seven per participant were included in the analysis (T1-T7). Baselines B, D and F were taken after the MRI assessment on T1, T4 and T5. Pre-surgical samples C1 and E1 were taken before surgery on T2 and T4. Post-surgical samples C2 and E2 were taken after the MRI assessments on the same visits. Table III-1 contains an overview of the all sampling time points and labels. A sample was taken after the scan on the familiarisation session T0 was not included in the analysis due to lack of corresponding MRI data.

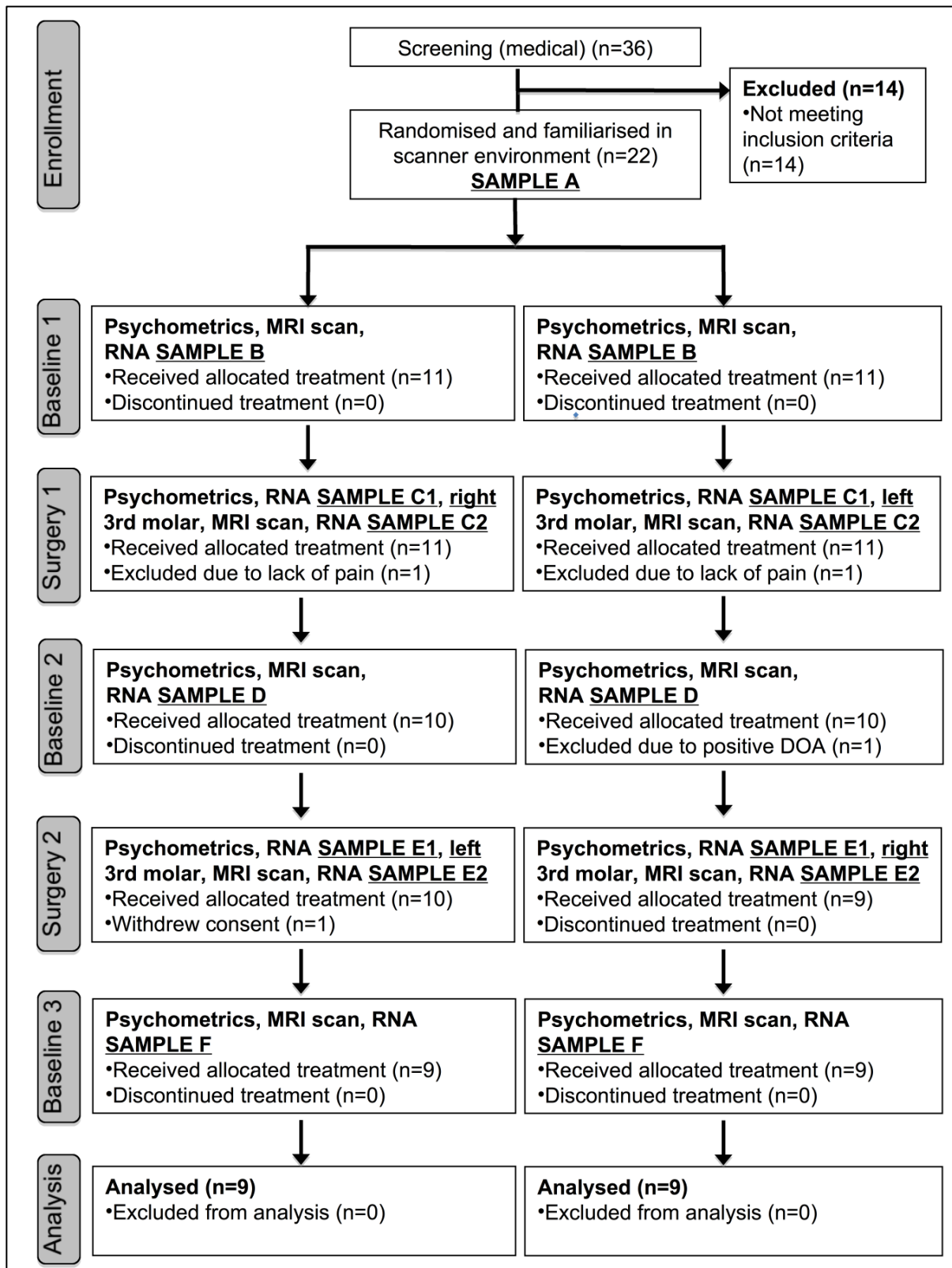


Figure III-1: Flow chart for study recruitment & analysis of the gene expression samples

Baseline Psychometry

Baseline psychometric screening assessments were performed for all participants at T0 to ensure participants scored within normal limits in measures of mental health, as depression, substance use and chronic anxiety are known to alter response to

painful stimuli (Bair, Wu, Damush, Sutherland, & Kroenke, 2008; Carr, Thomas, & Wilson-Barnet, 2005). For a full list of screening questionnaires and interviews see Howard et al., 2011 (Howard et al., 2011).

Surgeries

Unilateral TME under local anesthetic was performed by one of three experienced oral surgeons using a frequently performed, standardised technique (NICE/NHS, 2000; Renton et al., 2001). Briefly, local anesthetic was administered via an inferior alveolar block and long buccal infiltration using 4.4ml lignospan (2% lidocaine, 1:80,000 adrenaline). A buccal mucoperiosteal flap was raised and a gutter of bone buccal to the lower third molar removed using a fissure bur. Following decoronation and root sectioning with a fissure bur, tooth fragments were elevated and extracted. The surgical site was closed using 1-2 vicryl 3/0 rapide sutures. Surgical difficulty was rated by the surgeon on a 1-5 scale (Renton et al., 2001).

Following haemostasis and issuing of post-operative instructions, patients were escorted back to the MRI facility and supervised for up to six hours before returning to the MRI scanner for a post-surgical MRI scan. During the supervision period, participants provided ratings of pain intensity every 30 minutes using a pen-and-paper 100mm VAS (Katz & Melzack, 1999). The frequency of VAS responses increased to every ten minutes at the first indication of a VAS score greater than 20 out of 100 mm. Scanning commenced when three consecutive VAS scores greater than 30 out of 100 mm were provided by the participant.

RNA Extraction and Array Hybridisation

Peripheral blood for RNA extraction and a full blood count (FBC) were sampled using one 4.5ml EDTA K3 tube and two 2.5ml PAXgene tubes at each time point. RNA was sampled immediately after each MRI scan, and further samples were obtained before administration of the local anesthetic on each of the surgical visits. PAXgene tubes were left at room temperature for 2 hours to allow fixation of the transcripts in the stabiliser solution and were then stored at -80 degrees Celsius until further processing.

RNA extractions

Samples were randomised prior to shipping on dry ice to prevent batch effects. The cooling chain was uninterrupted. Total RNA was isolated from PAXgene-collected blood samples by Asuragen, Inc., according to the company's standard operating procedures.

A pilot of ten samples, randomised across the different conditions, was run to ensure the quality of the automated extraction protocol by extraction reagents manufacturer NuGen Inc. . The protocol was implemented on a robot for the first time at the lab. RNA integrity, cDNA conversion and hybridisation results on the Exon arrays yielded acceptable results and hybridised arrays passed standard quality controls.

The purity and quantity of total RNA samples were determined by absorbance readings at 260 and 280 nm using a NanoDrop ND-1000 UV spectrophotometer. The integrity of total RNA was qualified by Agilent Bioanalyzer 2100 capillary

electrophoresis. RNA integrity numbers (RIN) were reported and 11 samples fell short of the standard of 7.0. Replication tubes were shipped on dry ice for a second extraction. All samples were used for hybridisation onto Affymetrix Exon 1.0 ST arrays. Final RIN for the repeat samples were between 5.4 and 7.4. All samples were included and arrays with RNA of an RIN of less than 7 were flagged up for additional quality control. None of the arrays showed signs of errors attributable to low quality RNA.

Gene expression profiling

Biotin-labeled sense strand cDNA was prepared from 50 ng total RNA per sample using the WT-Ovation Pico RNA amplification system, WT-Ovation Exon Module, and FL-Ovation cDNA Biotin Module V2, according to the manufacturer's protocols (NuGEN, Inc.). Intermediate cRNA and resulting cDNA yields were quantified by spectrophotometry. Fragmentation and labeling of cDNA was performed using 5 µg for Exon Arrays. Hybridisation to arrays was carried out at 45°C for 16 hours in an Affymetrix Model 640 hybridisation oven. Affymetrix Human Exon 1.0 ST arrays were washed and stained on an Affymetrix FS450 fluidics station. The arrays were scanned on an Affymetrix GeneChip Scanner 3000 7G. For every array scanned, .DAT, .CEL, .GRD, .jpg, and .xml flat files were provided. In addition, robust multi-chip average (RMA) normalised data was provided for the core dataset and the corresponding QC information. RMA data captures metrics including Area Under the Curve (AUC) and polyA spikes generated using Affymetrix Expression Console.

Statistical and Pathway Analysis

Statistical analysis was performed using JMP Genomics (http://www.jmp.com/en_us/software/jmp-genomics.html) developed for SAS software, version 9.1.3 of the SAS System for Windows. GSEA and visualisations were performed using the GSEA software suite by the Broad Institute (Mootha et al., 2003; Subramanian et al., 2014) (<http://software.broadinstitute.org/gsea/index.jsp>). Pathway visualisations were rendered in the R/Bioconductor package <https://www.bioconductor.org/pub/RBioinf/> Pathview (Luo & Brouwer, 2013).

Array Pre-processing and Normalisation

Probe intensities of 126 Exon Arrays (18 individuals, 7 RNA arrays from T1 through T5) were normalised using quantile normalisation and summarised to gene level expression intensities using the robust multi-chip average (RMA) (Bolstad et al., 2003; Irizarry, Bolstad, et al., 2003; Irizarry, Hobbs, et al., 2003). Gene definition was implemented by applying the definition of the core probeset provided by the Affymetrix annotation system. Quality assessment and exploratory analysis of 126 chips were within normal limits, thus all samples were included in the analysis.

Array Data Analysis

Normalised gene level expression intensities were $-\log_{10}$ transformed. A repeated measures ANOVA was implemented to identify the differentially expressed transcripts across the samples contrasting all samples from non-surgical visits with those acquired at the two post-surgical sampling time points, when participants

emerged from the MRI scanner and reported a VAS-score of 3/10 or above. False discovery rate (FDR) was applied and p-values were corrected for multiple comparisons at $FDR < 0.05$.

Results

Gene expression results

The repeated measures ANOVA identified 837 probesets that were significantly differentially expressed between the non- and post-surgical conditions (see supplementary materials for gene list).

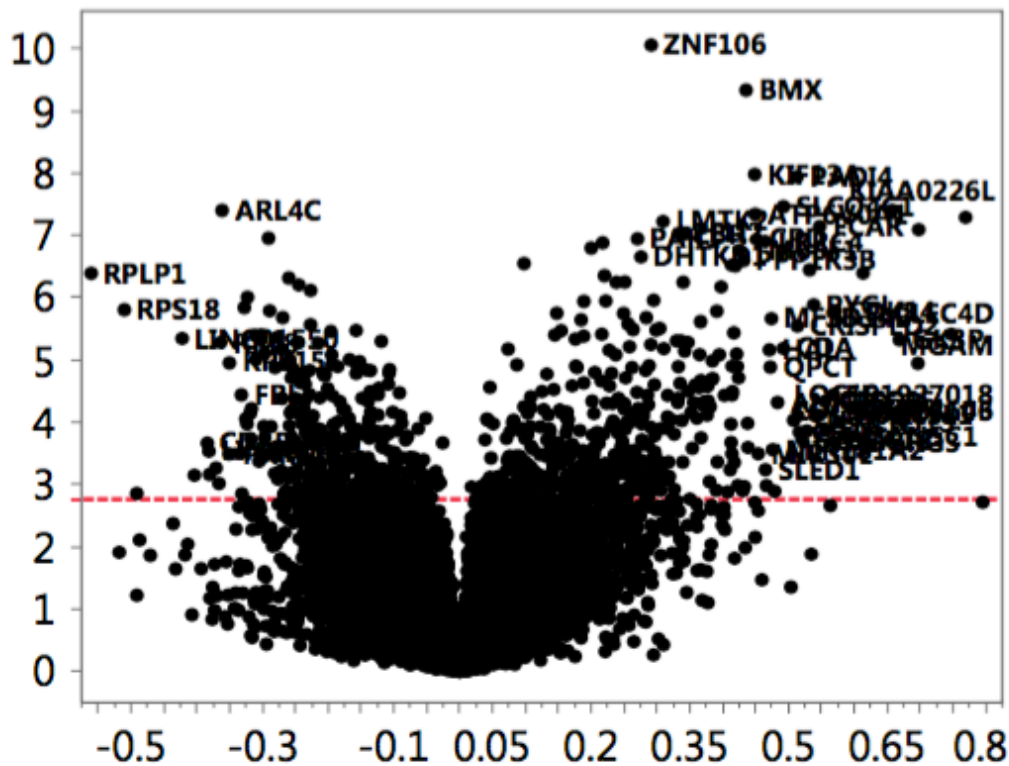


Fig III-2: Plot of differences in gene expression levels between non- and post-surgical samples: The X-axis represents log-transformed expression levels, while the Y-axis displays the p-values at $-\log(10)$; a horizontal reference line was drawn at $-\log(10) = 2.764$

Examining the top 20 genes with the most significant differences in expression revealed eight genes with explicit associations in the context of pain and nociceptive signaling (see table III-2). ZNF106 emerged as the most significantly up-regulated gene post surgery, but has no prior associations with phenotypes in pain or nociception. As a group of proteins 11 additional zinc finger proteins (ZNF 37A, 319, 337, 438, 460, 573, 586, 655, 705G, 829 and 844) demonstrated significant differential expression post surgery.

Gene	Gene name		Associated pain phenotypes or mechanisms
ZNF106	zinc finger protein 106	UP	No previous association with pain or nociception,
		UP	Signaling and control processed during the proliferation of cells (Chau et al., 2002), involvement in chronic inflammation and angiogenesis in the skin via cytokine-mediated recruitment of inflammatory cells (Paavonen et al., 2004), rheumatoid arthritis (Palmer, Mutch, Page, Horwood, & Foxwell, 2008)
BMX	BMX non-receptor tyrosine kinase		
PADI4	peptidyl arginine deiminase, type IV	UP	Association with susceptibility to rheumatoid arthritis in Asian populations (Gandjbakhch et al., 2009).
ARL4C	ADP ribosylation factor like GTPase 4C	DOWN	Association with and positive predictor for Chronic Fatigue Syndrome (CFS), which is accompanied by pervasive with joint and muscle pain (Frampton, Kerr, Harrison, & Kellam, 2011; Kerr, 2008).
LMTK2	lemur tyrosine kinase 2	UP	Interacts with Cyclin-Dependent Kinase 5 (CDK5) (Kesavapany et al., 2003), which phosphorylates TRPV1 (Chalovich & Eisenberg, 2009) and is expressed in nociceptive neurons (Pareek et al., 2006)
MME	membrane metallo-endopeptidase	UP	One of the major enzymes for enkephalin degradation, cleaves peptides at the amino side of hydrophobic residues and inactivates pain-relevant peptides such as enkephalins, substance P, neurotensin, oxytocin, and bradykinin.(Comings et al., 2000)
PAK1	p21 protein (Cdc42/Rac)-activated kinase 1	UP	Its expression is increased by Lidocaine and inhibits fibroblast multiplication, which may interfere with wound healing (Desai, Kojima, Vacanti, & Kodama, 2008).
PELI2	pellino E3 ubiquitin protein ligase family member 2	UP	Shown to promote microglia-mediated CNS inflammation by regulating Traf3 degradation (Xiao et al., 2014).
LRRC4	leucine rich repeat containing 4	UP	MAP kinase signalling influenced by competitive inhibition of MEK/ERK activation in glioma cells by D domain of LRRC4, (Z. Wang et al., 2016)(Ji, Gereau, Malcangio, & Strichartz, 2009)

Table III-2: The 20 genes with the most significant differential expression. Genes from exclusive association profiles with previous associations in pain and nociception

Gene Set Enrichment Analysis

GSEA demonstrated significant enrichment of differentially expressed genes from this analysis in a total of 280 significant KEGG pathways out of which 171 were up-regulated and the remaining 109 were down-regulated. Across six of the seven main pathway categories, categories 1, 5 and 6 (metabolism, organismal systems and human diseases) revealed the largest number of significantly enriched gene sets (see Figure III-3a).

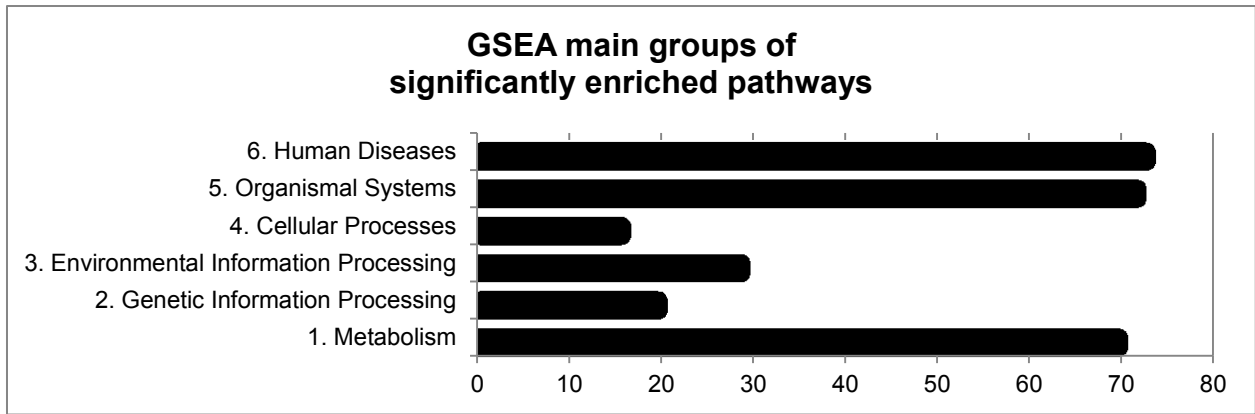


Fig III-3a: Main groups of significantly enriched pathways: Total number of significantly enriched pathways within each main group

The subgroups within the metabolism pathways enriched for differentially expressed genes were subgroups involved in glycan biosynthesis and metabolism (N=11), and lipid (N=13), carbohydrate (N=14) and amino acid metabolism (N=11) (Figure III-3b). The subgroups of organismal systems pathways with significantly enriched pathways were the endocrine (N=19), immune (N=16), digestive (N=9) and nervous system (N=10) (Figure III-3c). The subgroups within the main group of human diseases pathways with the greatest number of significantly enriched pathways were the pathways for specific cancers (N=14) and infectious bacterial diseases (N=10) (Figure III-3d).

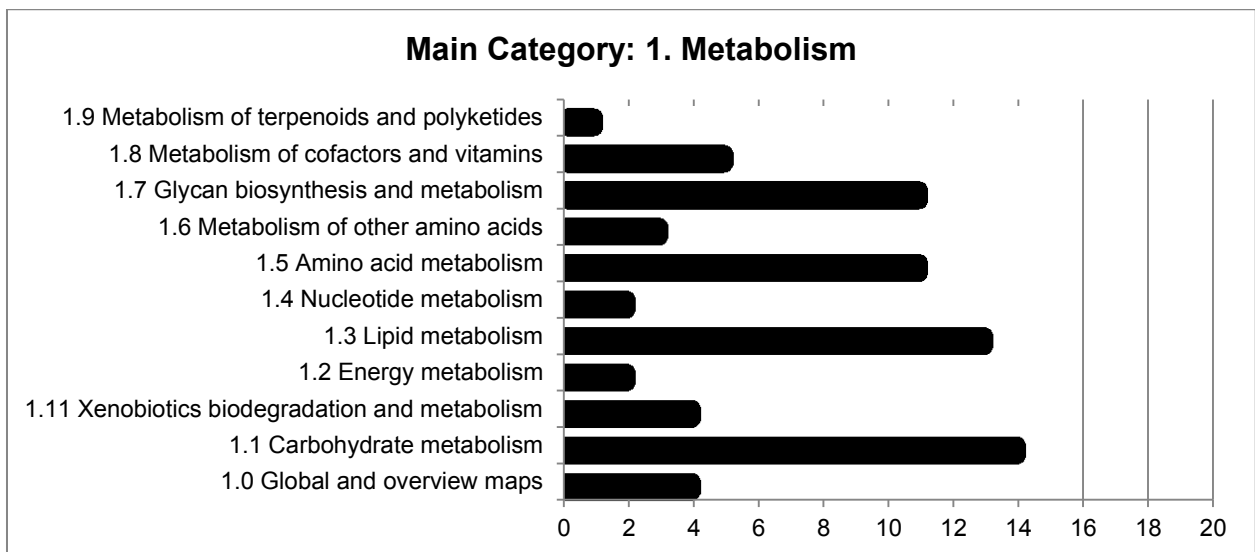


Fig III-3b: Main category: 1. Metabolism. Number of metabolism pathways subgroups enriched with genes differentially expressed between non- and post-surgical samples

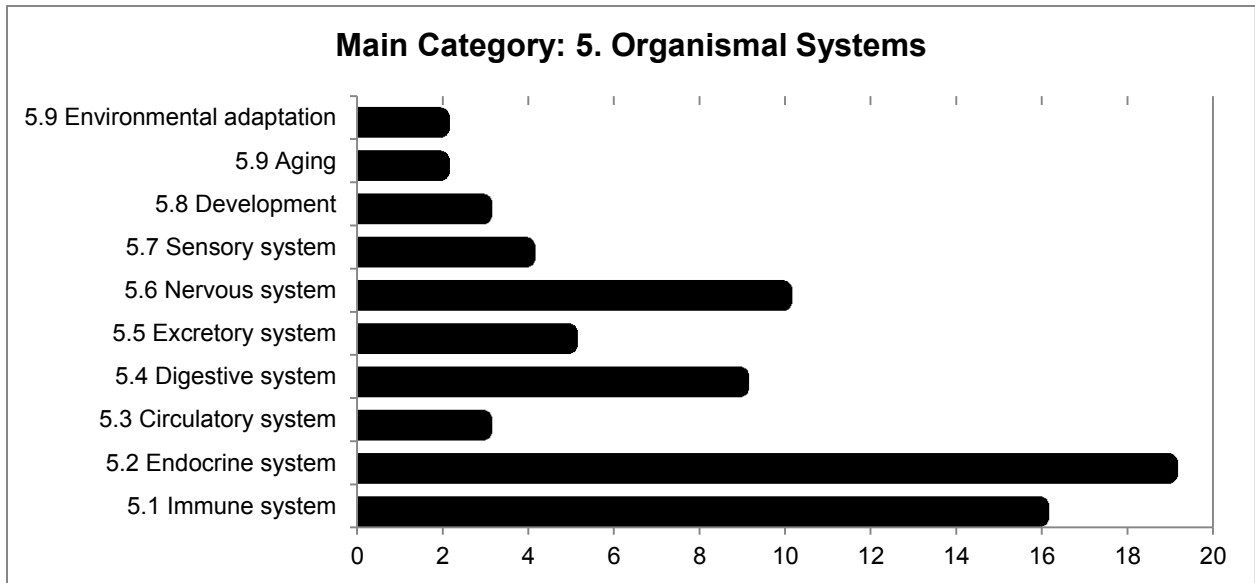


Fig III-3c: Main category: 5. Organismal Systems. Number of organismal systems pathways subgroups enriched with genes differentially expressed between non- and post-surgical samples

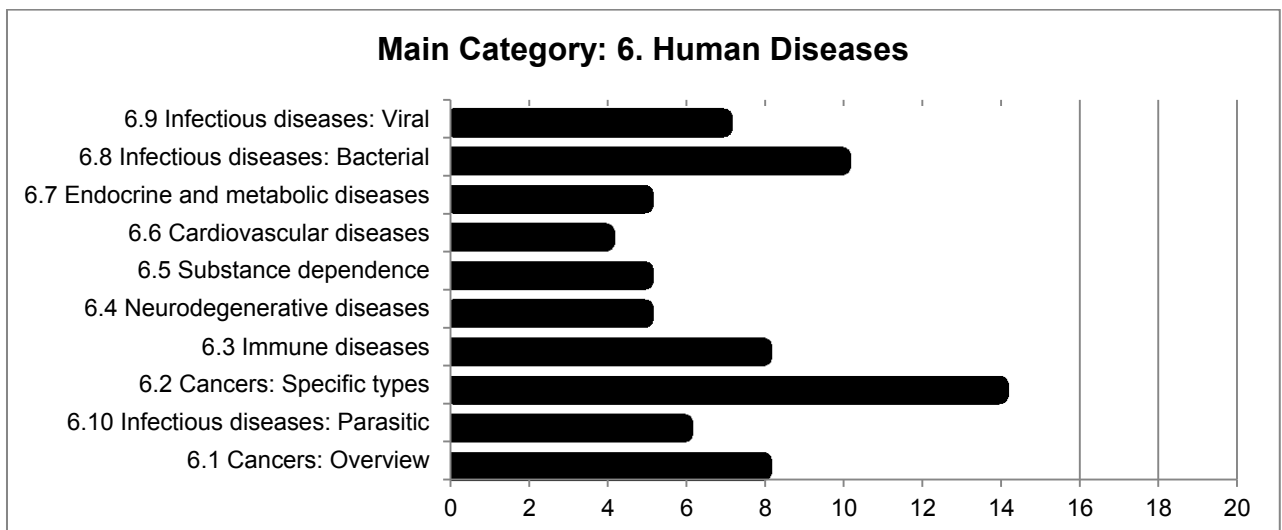


Fig III-3d: Main category: 6. Human Diseases. Number of human disease pathways subgroups enriched with genes differentially expressed between non- and post-surgical samples

GSEA revealed pronounced up-regulation of genes involved in the MAP Kinase (enrichment score (ES) = 0.348; normalised enrichment score (NES) = 1.479; nominal p-value = 0.002; FDR q-value = 0.129) and chemokine signaling pathways (ES = 0.397; NES = 1.632; nominal p-value = 0.0; FDR q-value = 0.058), and osteoclast differentiation pathway (ES = 0.517; NES = 2.003; nominal p-value = 0.0; FDR q-value = 0.007) in peripheral whole blood in patients in pain compared to the pain-free condition.

Enrichment plots illustrated the running ES for each of the pathway-specific gene ontologies as the analysis went down each of the ranked lists of differentially expressed genes. The peak value of the running ES represented the final ES. Genes before the ES contain the leading edge subset (LES) correlated with painful post-surgical state.

The heatmaps illustrated that samples from both post-surgical sampling time points revealed an expression pattern across patients that was markedly different from the non-surgical time points for the MAP Kinase and chemokine signaling pathways, and osteoclast differentiation pathway (see Figure III-6a-c). Tables listing genes with their individual ranks within the list, rank metric score and running ES are listed in the appendix (Supplementary tables III-2a-c).

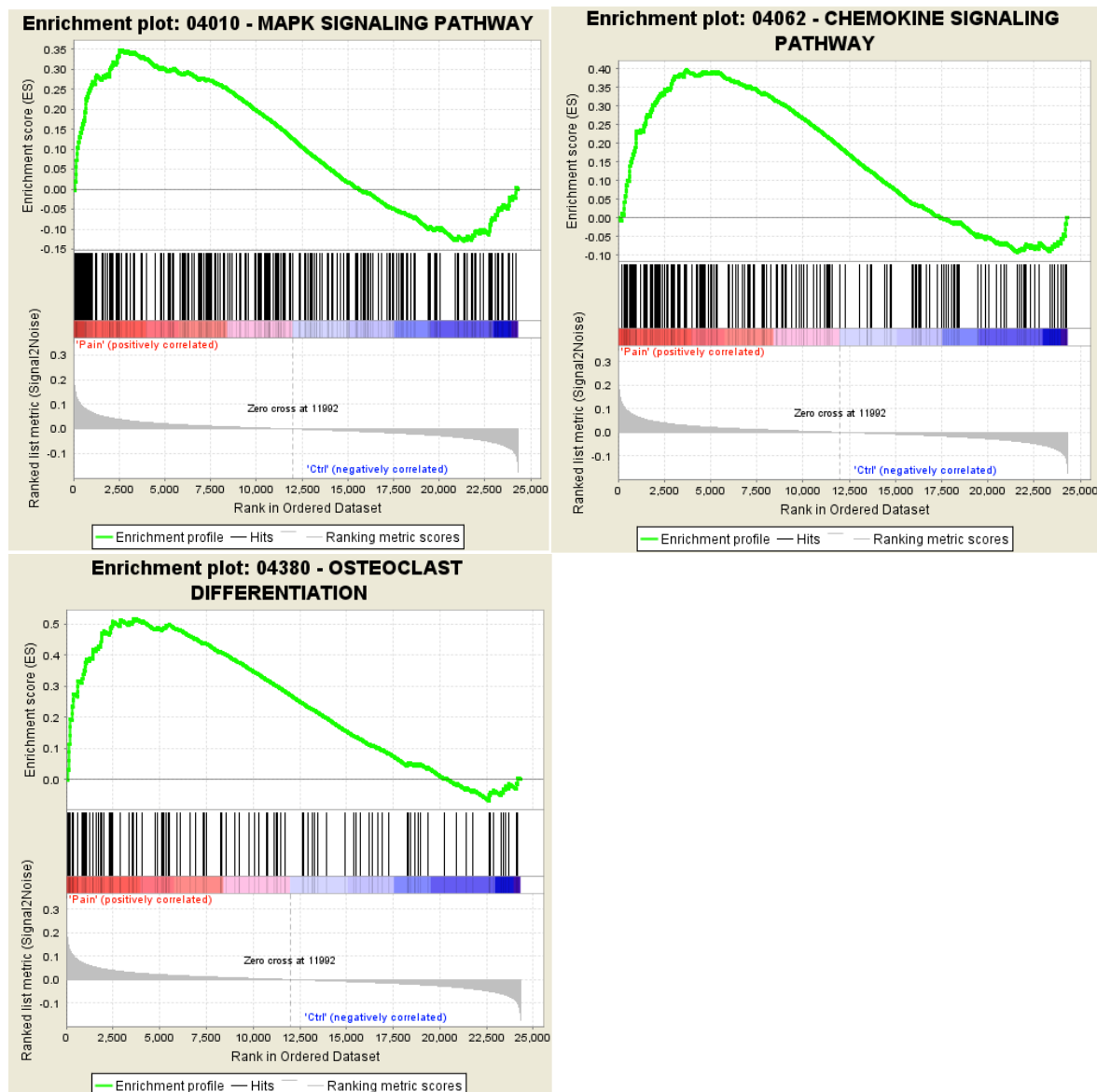


Figure III-4a-c: Enrichment plots for the MAP Kinase and chemokine signaling pathways, and osteoclast differentiation pathway. Profile of the running ES and positions of gene set members on the rank ordered list. Green line: running ES for pathway-specific gene ontologies. The peak value of the running ES represents the final ES. Genes before the ES represent the Leading Edge Subset correlated with painful post-surgical state.

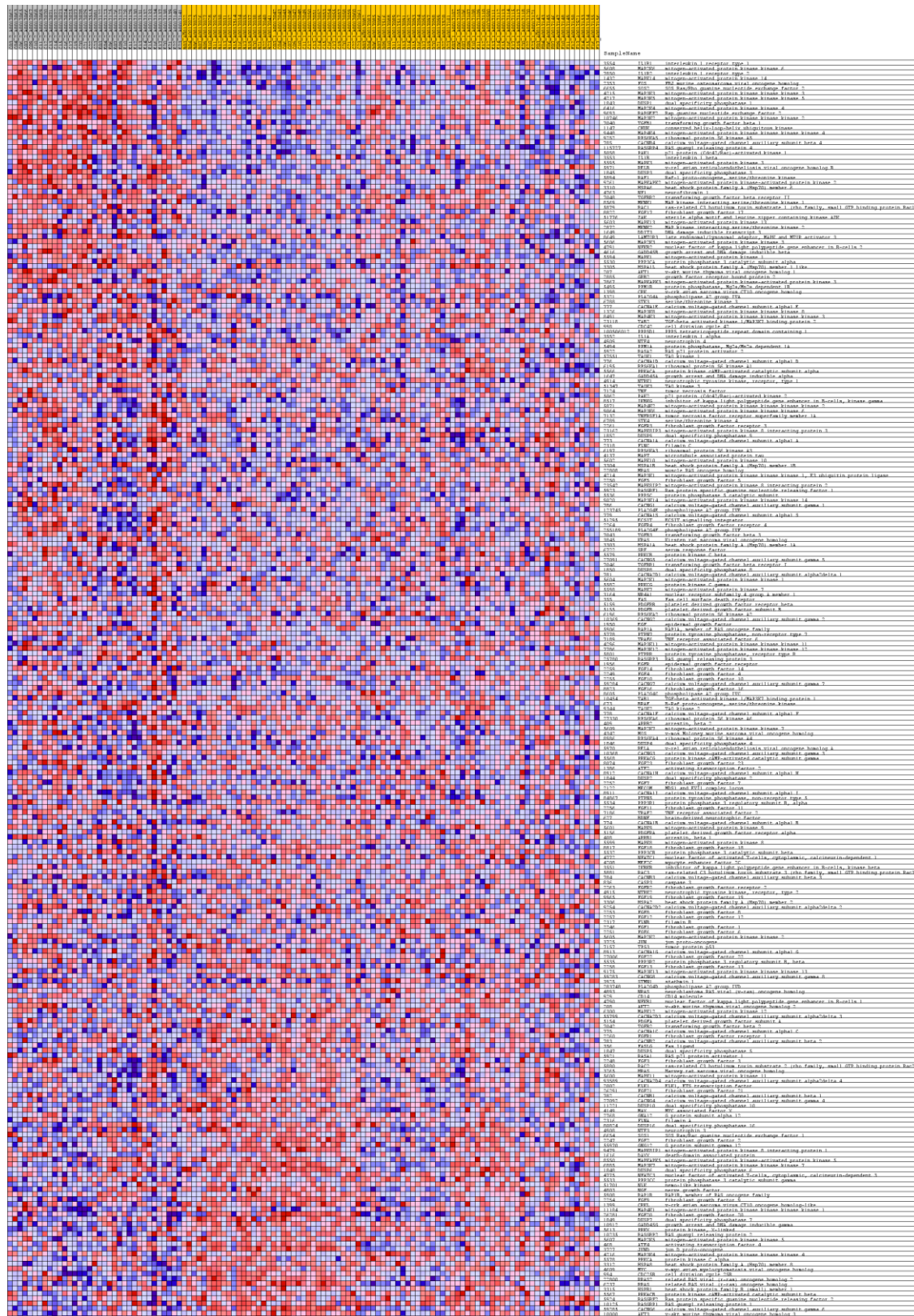


Figure III-5a: Non- and post-surgical expression intensities for gene set members of the MAP Kinase Signaling Pathway. Samples post-surgery (Samples C2 and E2) for all 18 participants are highlighted in grey, while non-surgical samples (Samples B, C1, D, E1 & F) for all 18 participants are highlighted in yellow. A full list of the genes and expression values is found in the appendix (see Table III-2a).

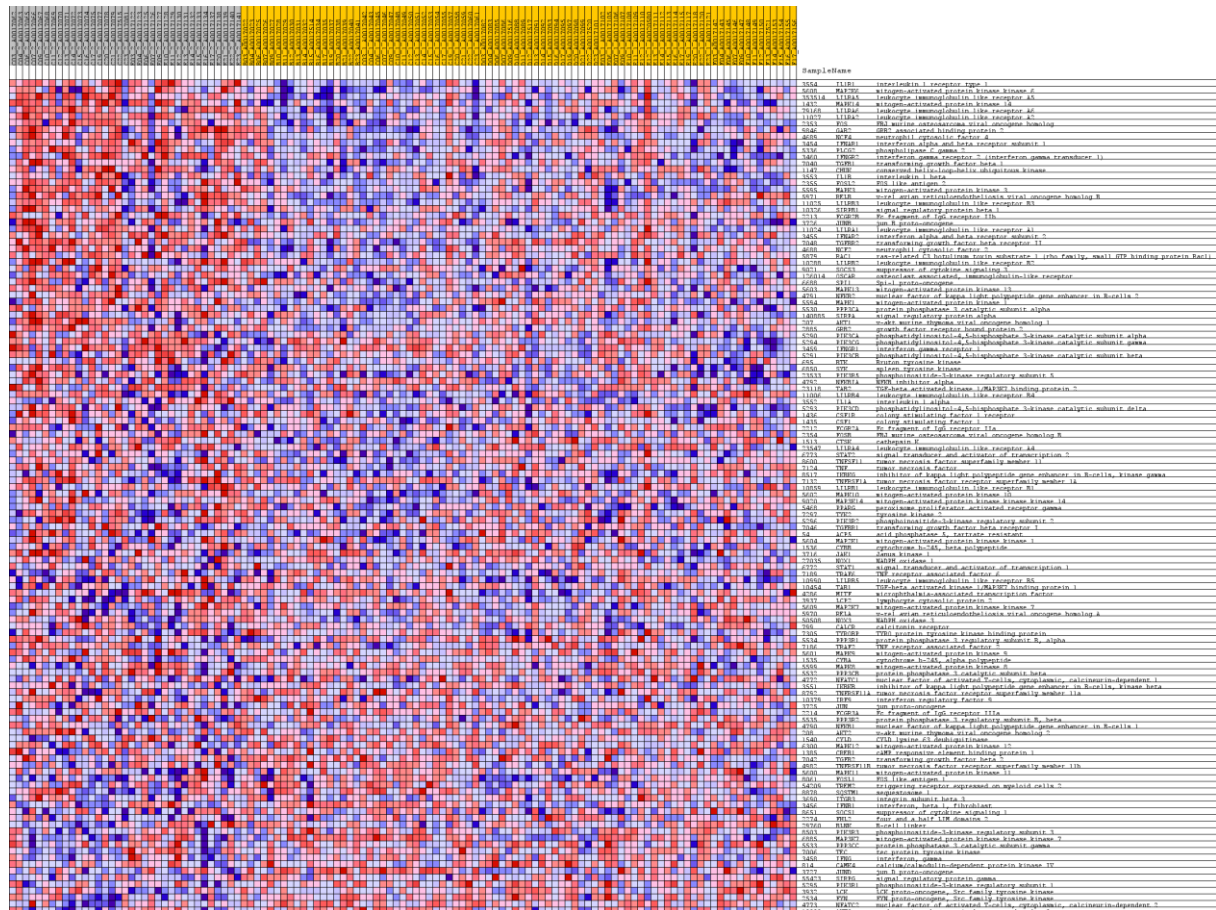


Figure III-5b: Non- and post-surgical expression intensities for gene set members of the Osteoclast Differentiation Pathway. Samples post-surgery (Samples C2 and E2) for all 18 participants are highlighted in grey, while non-surgical samples (Samples B, C1, D, E1 & F) for all 18 participants are highlighted in yellow. A full list of the genes and expression values is found in the appendix (see Table III-2b).

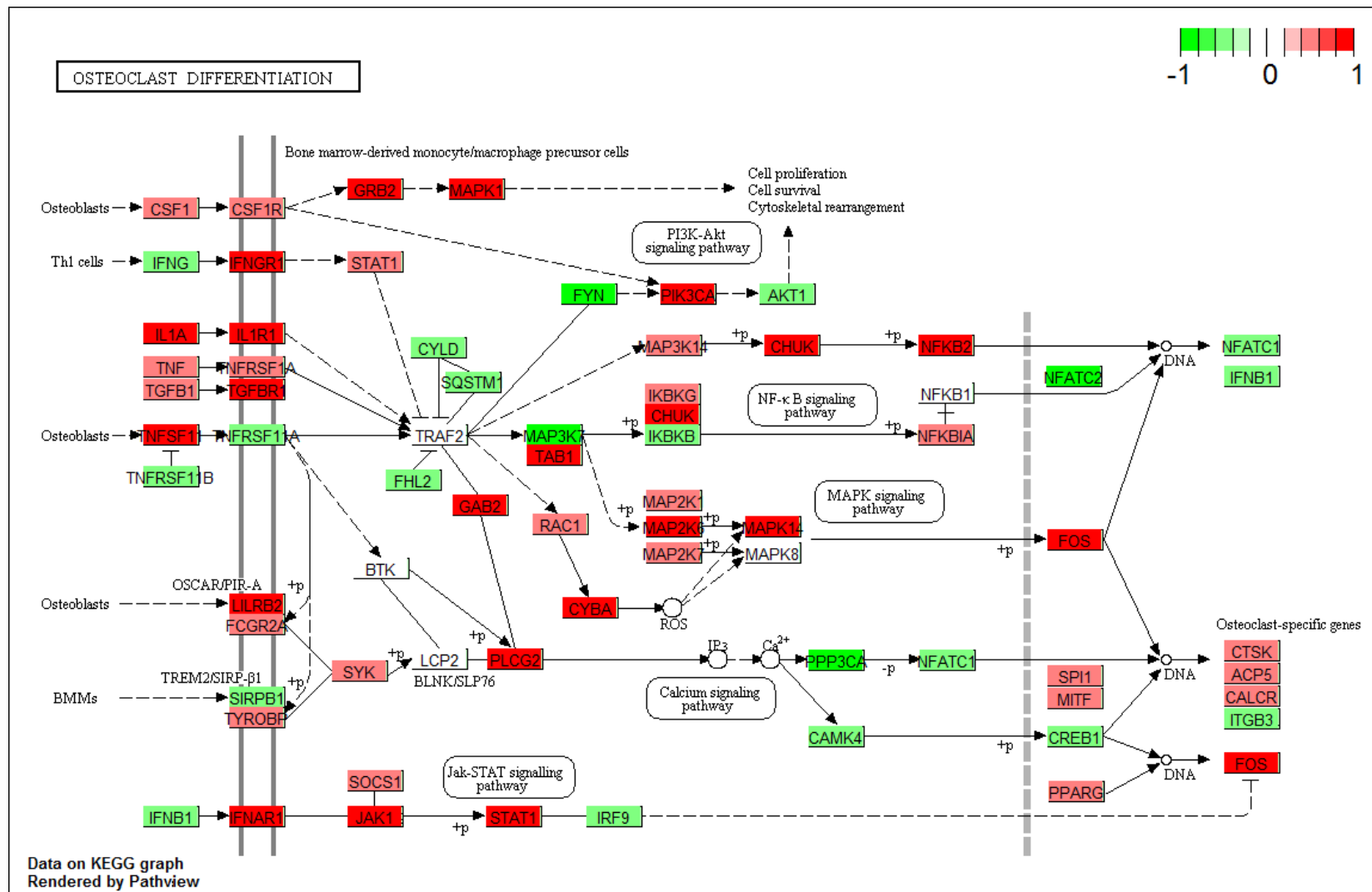


Figure III-6a: KEGG Pathway results: Osteoclast differentiation (genes highlighted in green dark red = up-regulated genes at $p < 0.05$, light red = up-regulated genes at $p > 0.05$, dark green = down-regulated genes $p < 0.05$, light green = down-regulated genes $p > 0.05$); Other maps connected to this pathway include Pi3K-Akt-, NF kappa B-, MAP Kinase-, Calcium- and Jak-STAT signaling pathways.

Discussion

The aim of this study was to evaluate the augmentation of the utility of the TME paradigm beyond mere psychometric assessment of nociception, pain and discomfort post surgery. For this purpose this study employed TME in combination with a gene expression phenotype in the assessment of inflammatory post-surgical pain. It investigated RNA extracted from peripheral whole blood in conjunction with biological pathway enrichment analysis in search of potential pain- and nociception-related biomarkers.

A significant surgery effect on gene expression levels in peripheral whole blood was established. When checking the first 20 genes on the list of differentially expressed genes ordered by significance, nearly half of them featured explicit previous associations with various pain- and nociception related phenotypes. Furthermore, GSEA highlighted gene sets from known pathways with significant enrichment for the differentially expressed genes from this study. Among the pathways of particular importance were the osteoclast differentiation, MAP Kinase signaling, chemokine signaling and inflammatory mediator regulation of TRP channels pathways.

In particular, the osteoclast differentiation pathway makes for a very biologically plausible result as restructuring of the bone occurs following tooth extraction. Osteoclasts are involved alveolar crest resorption in the mandible, while the fundic part of the bony socket fills with connective tissue and bone (Pietrokovski & Massler, 1967; Schropp, Wenzel, Kostopoulos, & Karring, 2003). Participants anecdotally commented on the speed at which the „hole“ left in the jaw post surgery disappeared at the follow up visits. To be able to show this pathway in blood without the use of tissue from the surgery site, where one might rather expect to see an increase in this cell type (Boyle, Simonet, & Lacey, 2003), could represent an opportunity to investigate mechanisms over the course of the healing process in traumatised tissue without having to re-traumatise it with biopsies.

Surgical trauma causes inflammatory pain, but also triggers gene expression events related to other biological processes such as tissue repair and immune response functions, which due to genetic pleiotropy may or may not be relevant to inflammatory pain. Hence, the challenge was to extract a list of candidate genes with primary relevance with regard to inflammatory pain signalling and processing. The large number of pathways relevant in metabolism represented an additional activated class of biological pathways concurrently activated with pain- and nociception-related pathways. Their strong representation can be attributed to a factor inherent in the design, which created considerable variability in food intake. Although patients were instructed to eat a light breakfast before the surgery, some patients reported that they were too anxious or were afraid of queasiness during the surgery to eat. Even though participants were offered a standardised soft lunch, several participants declined the lunch for fear of perturbing the sutures, biting into anaesthetised mucosal tissue or lack of appetite. In addition, the study did not adhere to a sampling schedule with fixed time intervals, but was event-related where scans were initiated in response to the patients' reported pain levels of at least 30/100. Thus the metabolism-related differences would have persisted in spite of fixed time points for food intake as the timing of the increases in VAS ratings varied between patients and could not be predicted reliably.

The most significantly up-regulated gene in this study (ZNF106) has no prior associations with other nociception and pain phenotypes. It encodes a zinc finger protein, a class of proteins, which bind to DNA, RNA and can serve as transcription factors. Due to their regulative functions, engineered zinc finger-based factors have been discussed as novel therapeutics in humans (Gommans, Haisma, & Rots, 2005; Papworth, Kolasinska, & Minczuk, 2006). Zinc-finger proteins also play an essential role in mu-opioid signalling (Rodríguez-Muñoz & Garzón, 2013). In neuropathic pain, myeloid zinc finger protein 1 has been shown to increase excitability in dorsal root ganglion (DRG) neurons by altering KCNA2 antisense RNA expression (Zhao et al., 2013) and ZNF641 is involved in MAP Kinase-mediated signalling (K. Luo et al., 2006).

Further convergent evidence for the validity of the approach in this study arose from the fact zinc finger protein genes also featured strongly in two other studies, which also employed the TME model. One investigated gene expression in oral mucosa tissue (Warburton et al., 2005) and one performed a GWAS in DNA (Hyungsuk Kim & Lee, 2009). The later used the maximum post-operative pain rating, post-operative pain onset time and the analgesic onset time after administering ketorolac as phenotypes of pain and analgesia and found a significant association with a SNP (rs2562456) from an uncharacterised gene in linkage disequilibrium with ZNF 429. The other study demonstrated differential gene expression in ZNF 9 and ZNF36, C3H type-like1 post surgery. However, there was no overlap between zinc finger protein genes from the two other studies using TME, which may also be due to the differences in substrates and sampling time points.

Highly prominent among the enriched known pathways was the MAP Kinase pathway, which is an umbrella term for three major subgroups of kinase pathways including extracellular signal-regulated kinases (ERK), p38, and c-Jun N-terminal kinase (JNK) (Ji et al., 2009). Out of these p38 MAP Kinase has already received attention as a target for a specific inhibitor (Anand et al., 2011).

The lack of gene sets specific to various pain phenotypes was not so much a limitation of the applied analysis strategy, but highlights the demand of further research into pain- and nociception-specific molecular signalling cascades. The inflammatory mediator regulation of TRP channels pathway was not part of the KEGG database, but a custom designed pathway. However, considering that genetic research in pain and nociception is still in the early stages (Bradshaw et al., 2005), the relatively large number of genes with specific associations with pain (e.g. rheumatoid arthritis (Alsaleh et al., 2010; Joosten et al., 2006)) and nociceptive signalling from the top of the gene list retrieved in this study strongly supports the validity of this approach. Reliable establishment of pain and nociception-specific pathways will benefit from the use of replication samples and larger sample sizes (Tsai, Wang, Chen, & Chen, 2005).

GSEA-based gene expression analysis has been applied to research on painful pulpal inflammation, which compared pulpal tissue from pulpitis patients with pulpal tissue from teeth extracted for other medical reasons (Galicia et al., 2016). This between-subjects comparison revealed a specific pattern of pathway activations involved in immune response activation, maintaining cellular function and cell-to-cell interaction. An additional advantage of the TME model is, that it enables within-subject comparisons, which could be applied in future studies of additional samples

taken after successful application of an analgesic to further specify their impact on blood-borne inflammatory mediators and their molecular mechanism of action.

Similar gains might be achieved from analysing data from the participants who fail to experience relevant pain post surgery. However, since this only applied to two participants in this study, no separate analysis was performed. An extension of the model to other types of surgery beyond TME might highlight shared pain-mediating molecular pathways.

One of the greatest criticisms of analgesic development has been, that analgesics released in the past decades are merely variations of existing classes of analgesics such as opioids and NSAIDs (Max, 2000; Woolf & Max, 2001). Further research will have to demonstrate if inhibitors of membrane metalloendopeptidase (MME) for example, an enzyme which cleaves enkephalins, is a suitable target in analgesic development. Thus, instead of introducing agonists and antagonists such as synthetic opioids, which bind to pain and nociception-relevant receptors, a new class of drugs which achieves analgesic effects by promoting the body's own peripheral opioid and cannabinoid analgesia, might emerge. This type of analgesic would increase the levels of inhibiting the enzymes that inactivate enkephalins. Similar drugs are already being tested. The two main groups - dual enkephalinase inhibitors, which inactivate neprilysin (NEP) and aminopeptidase N (APN) and fatty acid amide hydrolase (FAAH) inhibitors- have demonstrated analgesic effects in various models of inflammatory and neuropathic pain (Roques, Fournié-Zaluski, & Wurm, 2012). APN and NEP are provided by peripheral nerves and leukocytes in inflamed tissue (Schreiter et al., 2012), a cell type also abundant in peripheral whole blood.

Overall, this study represents another step towards a more comprehensive molecular characterisation of phenotypes in pain and nociception. It also ties in with other efforts to utilise genome-wide mapping approaches in finding pain-relevant pathways (Neely et al., 2012) and to employ data science approaches for identification of candidate genes (Ultsch, Kringel, Kalso, & Mogil, 2016). The findings support the use of RNA derived from peripheral blood as an economically viable substrate in pain- and nociception-related biomarker research.

Conflict of interest

The collection of the data was funded by Pfizer Global Research and Development UK. MAH and KK were paid on grant income from this source. GJ, JPH and WV were employees of Pfizer.

2.4 Manuscript IV: Negative Association Between Grey Matter Density and Sensory and Affective Pain Scores in Female Carriers of the OPRM1 118A SNP with Chronic Musculoskeletal Pain⁴

Reference:

Krause, K., Clarke T. C., Witt, S., Thieme, K., Diers, M., Ridder, S., Josef Frank, J., Rietschel, M., Schumann, G., Flor, H. (in preparation). Negative Association Between Grey Matter Density and Sensory and Affective Pain Scores in Female Carriers of the *OPRM1* 118A SNP with Chronic Musculoskeletal Pain.

Abstract

In this study a genotype-specific voxel-based morphometric (VBM) investigation of chronic musculoskeletal pain in relation to the single nucleotide polymorphism rs1799971 (118A/G) in the gene coding for mu-opioid receptor 1 (*OPRM1*) was performed. A total of 22 patients with either fibromyalgia syndrome (FMS) or unspecific lower back pain (ULBP) – with both groups reporting comparable levels of pain - were combined for analysis assuming a shared mechanism of maladaptive plasticity of the central nervous system. A genotype-dependent permutation-based comparison of grey matter density (GMD) revealed an inherent risk of relative hypertrophy in pain processing regions of the brain associated with the A-allele of SNP rs1799971. These effects became more pronounced when controlling for age and duration of pain. Findings potentially indicate a compensatory response to genotype-specific impairment of endogenous endorphine-mediated analgesia. A correlation analysis showed inverse relationships between mean GMD in pain-relevant regions of interest (e.g. putamen, pallidum, paracingulate, posterior cingulate) and sensory and affective pain scores. The inverse associations were more numerous for the 118A-carriers than for the 118G-carriers. There were no significant relationships when carriers of the 118A- and G-carriers were entered into the correlation analysis together. The putative mechanism of action may be rooted in impaired endogenous opioid binding in 118A-carriers, which suggests the 118A allele as a risk factor and informative biomarker for chronic musculoskeletal pain in female patients.

Introduction

⁴ Author contributions included Idea/Experimental Hypothesis: 50% for SNP selection, Experimental Design: 70% for set up of the VBM analysis in conjunction with genotype, Data Collection: 10% shipping and arrangement with genotyping facility in London, Writing: 80%, Interpretation: 70%.

Opioid signalling is a key modulator of pain-suppression. Pain is modulated by means of endogenous opioid peptide release (e.g. beta-endorphins, enkephalins and dynorphin (Basbaum & Fields, 1978)) in response to noxious stimulation (Zangen, Herzberg, Vogel, & Yadid, 1998; Zubieta et al., 2001a). Mu-opioid receptor-mediated neurotransmission is also activated as part of the placebo effect (Zubieta et al., 2005). Reduced opioid binding (Harris et al., 2007; Maarrawi et al., 2007; Willoch et al., 2004a) and elevated levels of opioid peptides in patients' cerebro spinal fluid (Baraniuk et al., 2004) have been demonstrated in different chronic pain patient cohorts. This is indicative of altered opioidergic signalling in the CNS of these populations. The exact explanations for these findings are yet to be determined, but a decrease in opioid receptor bearing neurons (Jones et al., 2004) has been discussed and is in line with findings of decreases in grey matter density (GMD) in various populations of chronic pain patients in contrast to age and sex matched control subjects in morphometric studies of the brain (Apkarian et al., 2004; May, 2008; Schmidt-Wilcke et al., 2005, 2007). In order to obtain a more comprehensive understanding of the role of opioid mechanisms in chronic pain, it is important not only to look at morphological changes, but also to try to combine morphometric endpoints with other endpoints such as genetics.

This study investigated the influence of a common genetic polymorphism (118A>G, rs1799971) and its effects on GMD in the presence of prolonged pain by means of voxel based morphometry (VBM) (Ashburner & Friston, 2000). This was implemented in a cohort of unmedicated female chronic musculoskeletal pain patients suffering from either FMS or ULBP. Said SNP is part of the gene that encodes *OPRM1*, which is a target site for endogenous opioid ligands and various opioid analgesics

FMS is characterised by chronic widespread pain, fatigue and tenderness at specific body sites. Prevalence is relatively high with diagnoses given to more than 10% of patients attending general medical clinics and higher numbers in rheumatology clinics. The patients are predominantly female and onset typically occurs in middle age before age 50 (Wolfe et al., 1990). ULBP is a common problem in industrialised countries with a lifetime prevalence between 58% to 85%. Annual prevalence is between 20% to 40% and again more women than men are affected by this pain disorder (Werber & Schiltenswolf, 2012).

This study contrasted genotypes at the whole brain level and an additional region of interest (ROI) analysis focused on brain regions with known involvement in various persistent pain conditions often summarised as the pain neuromatrix (Legrain et al., 2011). ROIs included the caudate, pallidum and putamen, which form part of the basal ganglia (Chudler & Dong, 1995; Downar et al., 2003; Starr et al., 2011). GMD increases in the basal ganglia in chronic low back pain patients emerged in comparison to healthy controls (Schmidt-Wilcke et al., 2006). Furthermore, the amygdala and nucleus accumbens, were selected as areas in which decreased mu-opioid receptor binding potential has been established to be negatively correlated with affective pain ratings in FMS patients (Harris et al., 2007).

Reduced GMD in the hippocampus has been demonstrated in chronic back pain and chronic regional pain patients along with other hippocampal abnormalities in rodents following spared nerve injury (Mutso et al., 2012). Additionally a hyperactive state of the parahippocampal gyrus, amygdala and anterior insula were observed in

somatoform pain disorder patients in response to a heat pain stimulus (Gündel et al., 2008). Additional regions involved in pain processing included thalamus, somatosensory cortex I and II (SI & SII), anterior cingulate, posterior cingulate and paracingulate. A previous study had demonstrated an inverse relationship between GMD in the posterior cingulate cortex, the adjacent precuneus and SI and pain sensitivity in participants undergoing a heat pain challenge (Emerson et al., 2014).

Gene characterisation

The 118A>G polymorphism in *OPRM1* is located on chromosome 6q24-q25 and spans over 200 Kb. It comprises at least 9 exons and can encode for 19 different splice variants under the control of multiple promoters (Pasternak, 2010; Shabalina et al., 2009). In Caucasians the minor G-variant of rs1799971 is found in 11-17% of the population (dbSNP Short Genetic Variations database of the American National Center for Biotechnology Information; NCBI, Bethesda, MD, USA, Accessed Aug 15, 2013).

The 118A>G SNP has received much attention due to its functional consequences, which affect opioidergic signalling (Lötsch, Skarke, et al., 2002; Wand et al., 2002). It causes an amino acid substitution from asparagine to aspartic acid at position 40 of the protein, a putative N-glycosylation site in the extracellular domain. Although the gene has been championed as a possible target for concepts in personalised medicine in the context of pharmacokinetic and pharmacodynamic effects on opioid medications (Hernandez-Avila, Wand, Luo, Gelernter, & Kranzler, 2003; Lötsch, Geisslinger, & Tegeder, 2009b; Mura et al., 2013), a meta-analysis of the data so far indicates only mild effects (Walter & Lötsch, 2009a). However, some studies point towards clinical relevance of the SNP in unmedicated populations. For example, non-Hispanic white carriers of the 118A-allele exhibit increased thermal and ischemic pain sensitivity (Hastie et al., 2012). Also the prevalence of the 118A allele was higher in female Turkish FMS patients, than in the general population (Solak et al., 2014).

The 118G mutation is associated with increased sensitivity to endogenous opioids through higher receptor binding affinity for beta-endorphins (Bond et al., 1998a). This could leave unmedicated pain patients carrying the wild-type A-allele at a disadvantage. In support of this assumption an EEG study of noxious and olfactory stimulation of the nasal trigeminal system demonstrated that ERP amplitude N1 is greater in 118A carriers in response to the noxious stimuli than in 118G carriers (Lötsch et al., 2006).

The aim of this study was to determine the effect of the 118A-allele on GMD in pain-associated brain regions independent of age and pain duration in combination with psychometric assessments of pain. Age and pain duration were controlled for as the extent of GMD increases as age and pain duration increase (Apkarian et al., 2004; Tisserand et al., 2004) The hypothesis was that the A-allele serves as a risk factor or diathesis for pain-related GMD in the presence of chronic pain.

Methods

The study was designed in accordance with the guidelines from the Helsinki declaration and ethics approval was obtained from the local ethics committee. Participants completed informed consent forms prior to all procedures.

Participants

The musculoskeletal pain patients in this study were diagnosed either with fibromyalgia syndrome (FMS) or unspecific low back pain (ULBP). Patients were recruited from the Mannheim and Heidelberg area, Germany. All participants suffered from their pain disorder for at least 12 months. None of the participants were on regular medication at the time of testing. T1-weighted structural MRI scans were obtained from 22 Caucasian female patients out of which 18 [Mean age=49.94yrs. (SD=11.33)] were diagnosed with FMS and four with ULBP (Mean age=46.75yrs. (SD=12.92)). There were no significant differences with regard to age ($U(18,4)=19.5$, $p<.388$) and duration of pain ($U(19,3)=13$, $p<.131$) between patient groups (see table IV-1). Homozygosity for the A-allele was established in 19 participants, three carried the AG genotype and none of the participants were homozygous for the G-allele.

Genotyping

Whole blood was collected in Saarstedt EDTA tubes during the first study visit. DNA was extracted from these samples according to standard protocol. Genotyping for rs1799971 was first performed on a SNPlex platform (Applied Biosystems Warrington, UK), which uses oligonucleotide ligation/polymerase chain reaction and capillary electrophoresis to analyse bi-allelic SNP genotypes (Tobler et al., 2005). The sample was re-genotyped by means of TaqMan SNP genotyping essays (Life Technologies, USA). Hardy-Weinberg-Equilibrium for rs1799971 was confirmed in PLINK (Purcell et al., 2007). Call rates for all samples were above .98 and there were no discrepancies in genotypes between the samples processed on the different platforms.

MRI image acquisition, pre-processing and analysis

T1-weighted images (MPRage) were acquired on a Siemens Magentome MRI scanner at a field strength of 3 Tesla. Images were assembled from .ima archive file format with dcm2nii (Rorden & Brett, 2000). Pre-processing, segmentation and smoothing was performed using VBM8 from the SPM8 toolbox (Mechelli et al., 2005).

A mean image across all participants was created with fslmaths in FSL v5.0 (www.fmrib.ox.ac.uk/fsl). There were no significant correlations between genotype, participant age ($r=-.17$, $p>.46$) and pain duration ($r=.31$, $p>.16$). Nevertheless, in order to avoid potential suppressor effects, a fixed effects model was implemented to control for these variables. In addition, age-related decreases in GM were controlled for, since the age of participants ranged from 33 to 64 years and also for years of ongoing pain, since it has been shown, that GMD become more extensive the longer pain persists (Apkarian et al., 2004).

Region of Interest Correlations

Regions of interest (ROI) for analysis were selected from pain-relevant brain areas and included the amygdala, caudate, hippocampus, pallidum, putamen, paracingulate, anterior and posterior cingulate, anterior and posterior parahippocampus, somatosensory cortex I and II, thalamus and nucleus accumbens. Thresholds for ROI masks were set to include only voxels with at least a 25% probability of being part of the respective ROI. ROI masks were created in FSLview for left and right hemisphere separately for the following bilateral structures: anterior and posterior parahippocampus, somatosensory cortex I and II, insula, nucleus accumbens, amygdala, caudate, hippocampus, pallidum, putamen, and thalamus. Three additional masks were created for the paracingulate, posterior and anterior cingulate gyrus. Mean values for each were calculated in FSL using the `fslmeants` function. Correlations were performed in SPSS (IBM SPSS Statistics, version 22).

Comparison of AA vs. AG carriers

The original mean image was thresholded at .15 and a binarised mask was created for use in the `randomise` function in FSL (Bullmore et al., 1999; Nichols & Holmes, 2002).

The carriers of the G allele were compared to carriers of the wildtype allele by carrying out a non-parametric t-test with up to 5,000 permutations. In this analysis the critical threshold was met at 1,540 permutations. The `randomise` function was implemented with the additional options to carry out Threshold-Free Cluster Enhancement (TFCE) and variance smoothing with `std` set to 2mm, which is recommended for small sample sizes (Hayasaka & Nichols, 2003). Cluster corrected thresholds were set to $p < 0.05$. Peaks, locations and voxel cluster sizes were extracted from the Harvard-Oxford and Juelich atlases.

Psychometrics

The participants' pain experience was assessed by means of the pain experience scale (Schmerzempfindungs-Skala, SES (Geisser, 1996)), a German adaptation of the McGill Pain Questionnaire (Melzack, 1975) - a multimodal pain assessment scale used to quantify the affective and sensory dimensions of the pain experience.

An independent-samples t-test was performed to assess possible differences between the FMS and ULBP patient cohorts and between AA and AG carriers with regard to age and quality and duration of pain.

Results

Psychometrics

There were no significant differences between age, duration and the different dimensions of the SES for the FMS and ULBP cohorts (see Table IV-1). In addition, there were no significant genotype-dependent differences in the SES scores, age and duration between the carriers of the AA- and AG-genotypes (see Table IV-2).

	Genotype	H	Mean rank	Value	Exact significance (2* one-tailed)
SES sensory pain	FMS	18	12.61	16	.638
	ULBP	4	6.5		
SES affective pain	FMS	18	11.81	30.5	.088
	ULBP	4	10.13		
SES local intrusion	FMS	18	12.75	13.5	.053
	ULBP	4	5.88		
SES rhythmicity	FMS	18	12.33	21	.189
	ULBP	4	7.75		
SES temperature	FMS	18	11.83	30	.600
	ULBP	4	10		
Age	FMS	18	12.17	24	.306
	ULBP	4	8.5		
Pain Duration	FMS	18	12.53	17.5	.109
	ULBP	4	6.88		

Table IV-1: Two sample Mann-Whitney-U-Test for SES scores, pain duration and age by diagnosis

	Genotype	H	Mean rank	Value	Exact significance (2* one-tailed)
SES sensory pain	AA	19	12.34	18.5	.124
	AG	3	8.17		
SES affective pain	AA	19	12.03	12.5	.337
	AG	3	6.17		
SES local intrusion	AA	19	11.5	28.5	1.000
	AG	3	11.5		
SES rhythmicity	AA	19	11.87	21.5	.491
	AG	3	9.17		
SES temperature	AA	19	12.42	11	.086
	AG	3	5.67		
Age	AA	19	11.97	19.5	.388
	AG	3	8.5		
Pain Duration	AA	19	12.32	13	.131
	AG	3	6.33		

Table IV-2: Two sample Mann-Whitney-U-Test for SES scores, pain duration and age by genotype

Region of Interest Correlations

For the overall sample including the AA and AG carriers, no significant correlations were observed between mean GM densities for any of the extracted ROIs with the SES scores for affective and sensory pain (see Table IV-3). However, when stratified by genotype, significant negative correlations emerged for the AA carriers for the SES sensory score with the posterior cingulate ($r=-.46$, $p=.047$), left putamen ($r=-.51$, $p=.025$) and left pallidum ($r=-.47$, $p=.047$). Significant negative correlations were also noted for the SES affective score with the posterior cingulate ($r=-.51$, $p=.027$), paracingulate ($r=-.46$, $p=.049$), left pallidum ($r=-.49$, $p=.039$) and left putamen ($r=-.59$, $p=.008$) (see Figure IV-1). For the 118G carriers negative correlations between GM density and SES affective pain scores emerged for the caudate ($r=-1.0$, $p=.018$) and SES sensory scores and GM density of the left amygdala ($r=-1.0$, $p=.008$) (see Figure IV-2).

Genotype	Total (N=22)				AA (N=19)				AG (N=3)			
	left		right		left		right		left		right	
ROI/SES score	SES sensory	SES affect	SES sensory	SES affect	SES sensory	SES affect	SES sensory	SES affect	SES sensory	SES affect	SES sensory	SES affect
Nucleus accumbens	.156	.000	.022	-.052	.087	-.119	-.047	-.165	.737	-.756	.939	-.450
	.488	.999	.923	.820	.724	.629	.848	.499	.472	.454	.224	.703
Amygdala	-.021	.007	.048	-.116	-.149	-.239	-.009	-.267	-1.00*	.102	-.811	-.488
	.924	.974	.830	.606	.541	.324	.972	.270	.008	.935	.398	.675
Caudate	-.036	-.077	-.153	-.162	-.122	-.220	-.252	-.335	.143	-1.00*	-.234	.993
	.872	.735	.498	.471	.619	.365	.298	.161	.909	.018	.850	.077
Hippocampus	.011	.118	-.017	.094	-.117	-.105	-.190	-.184	-.866	.596	-.584	.874
	.960	.600	.939	.679	.633	.670	.436	.450	.333	.593	.603	.324
Pallidum	-.217	-.151	.001	-.023	-.474*	-.490*	-.120	-.228	-.971	.350	b	b
	.344	.513	.995	.921	.047	.039	.626	.348	.154	.772		
Putamen	-.317	-.302	-.169	-.213	-.513*	-.588**	-.320	-.434	.991	.017	.884	-.566
	.151	.172	.452	.341	.025	.008	.181	.063	.084	.989	.310	.617
Thalamus	-.038	.132	.011	.202	-.174	-.043	-.109	.052	.990	.028	.929	.262
	.866	.560	.960	.367	.475	.860	.658	.831	.091	.982	.242	.831
Anterior Parahippocampus	.131	.245	-.087	-.002	.072	.143	-.190	-.169	.000	.993	.210	.947
	.560	.272	.699	.994	.769	.560	.435	.490	1.00	.073	.866	.208
Posterior Parahippocampus	.000	-.136	.008	-.198	-.068	-.306	-.017	-.336	-.871	-.388	-.973	-.118
	.998	.547	.972	.376	.783	.203	.944	.160	.327	.747	.149	.925
Insula	.008	.203	.081	.264	-.123	.019	-.048	.080	-.982	.300	-.812	.673
	.970	.366	.720	.235	.617	.939	.846	.745	.121	.806	.396	.530
Somatosensory Cortex I	-.097	-.160	.049	-.023	-.107	-.200	-.018	-.137	-.933	-.249	-.178	-.957
	.668	.478	.827	.918	.664	.412	.942	.576	.234	.840	.886	.187
Somatosensory Cortex II	.365	.033	.368	.073	.397	.068	.334	-.025	.639	.690	-.548	-.768
	.095	.886	.092	.745	.093	.782	.163	.920	.558	.515	.630	.443
Paracingulate	-.225	-.341			-.294	-.456*					-.265	-.927
	.315	.120			.222	.049					.829	.244
Anterior Cingulate	-.157	-.263			-.258	-.397					.359	-.968
	.485	.237			.286	.093					.766	.161
Posterior Cingulate	-.244	-.194			-.460*	-.506*					-.610	-.717
	.274	.387			.047	.027					.582	.491

Table IV-3: Correlation table genotype and ROI (by hemisphere); b = could not be calculated

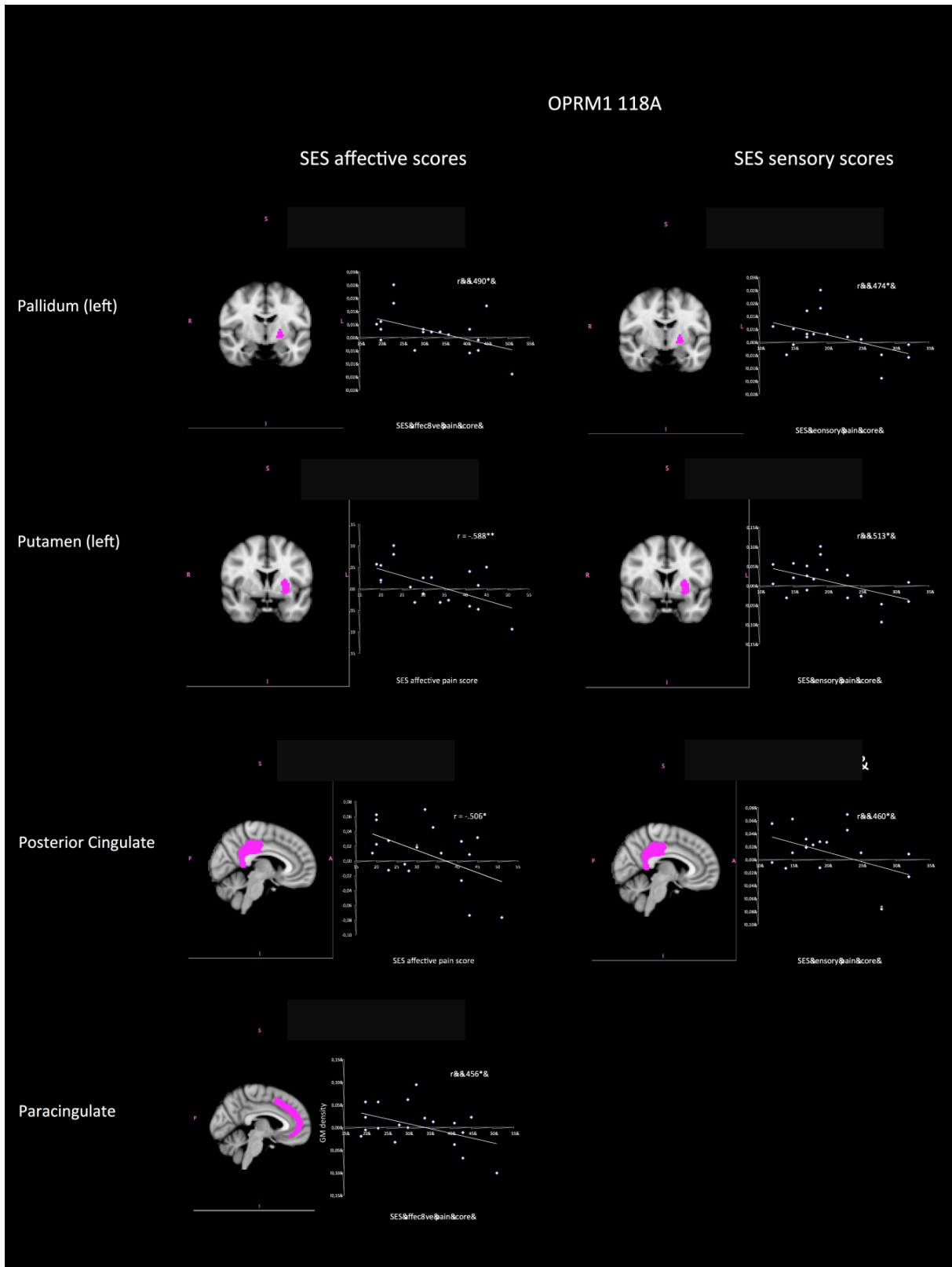


Figure IV-1: Negative correlations between SES sensory and affective scores and GM density in AA carriers in two structures of the basal ganglia and posterior and paracingulate cortex

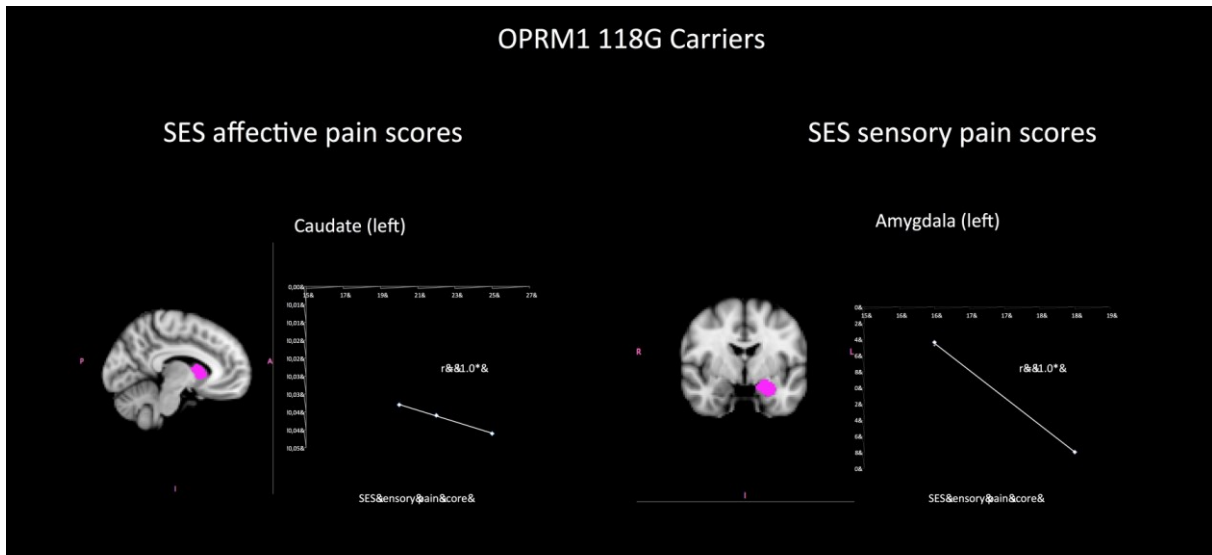


Figure IV-2: Negative correlations between GM density and SES sensory score in the amygdala and affective scores in the left caudate in AG carriers

Comparison of AA vs. AG carriers

The results image from the permutation-based GLM in randomise revealed consistently greater GM densities in AA than AG carriers after FWE correction. When comparing the patients by genotype alone, significant GM reductions were noted only in the right inferior frontal gyrus pars opercularis (local maximum = .959, no. of voxels = 84, MNI coordinates(x,y,z) = 37, 15, 25).

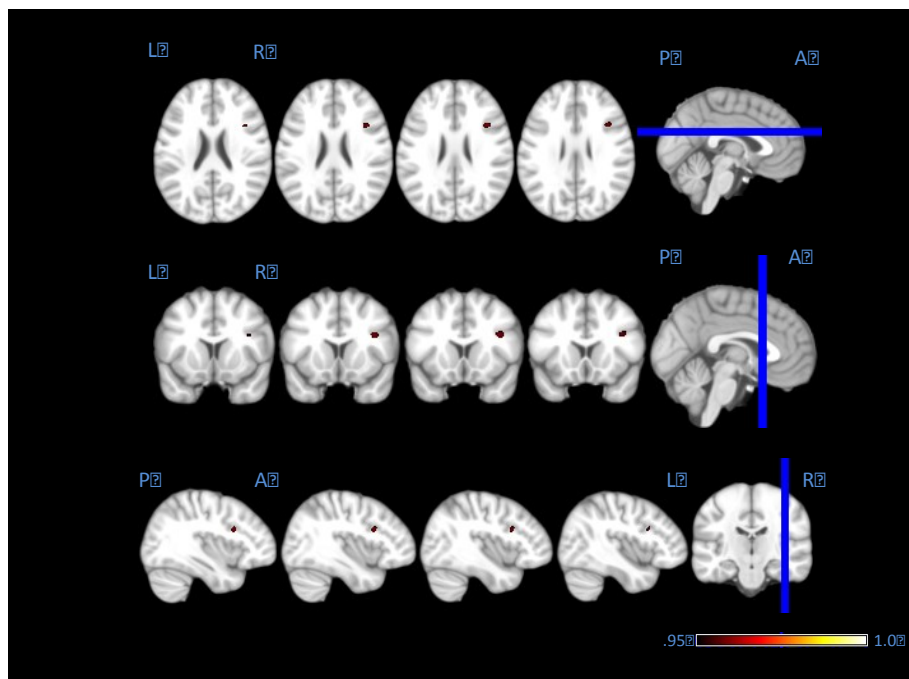


Figure IV-3: Uncorrected for age and duration of pain: GM decreases emerged in 118G carriers compared to 118A carriers

After images were controlled for age and pain duration several, significant reductions in GM density in 118G carriers in contrast to 118A carriers were noted in the right

hippocampus and parahippocampal gyrus, left amygdala and bilaterally in the secondary somatosensory cortex (see Table IV-4).

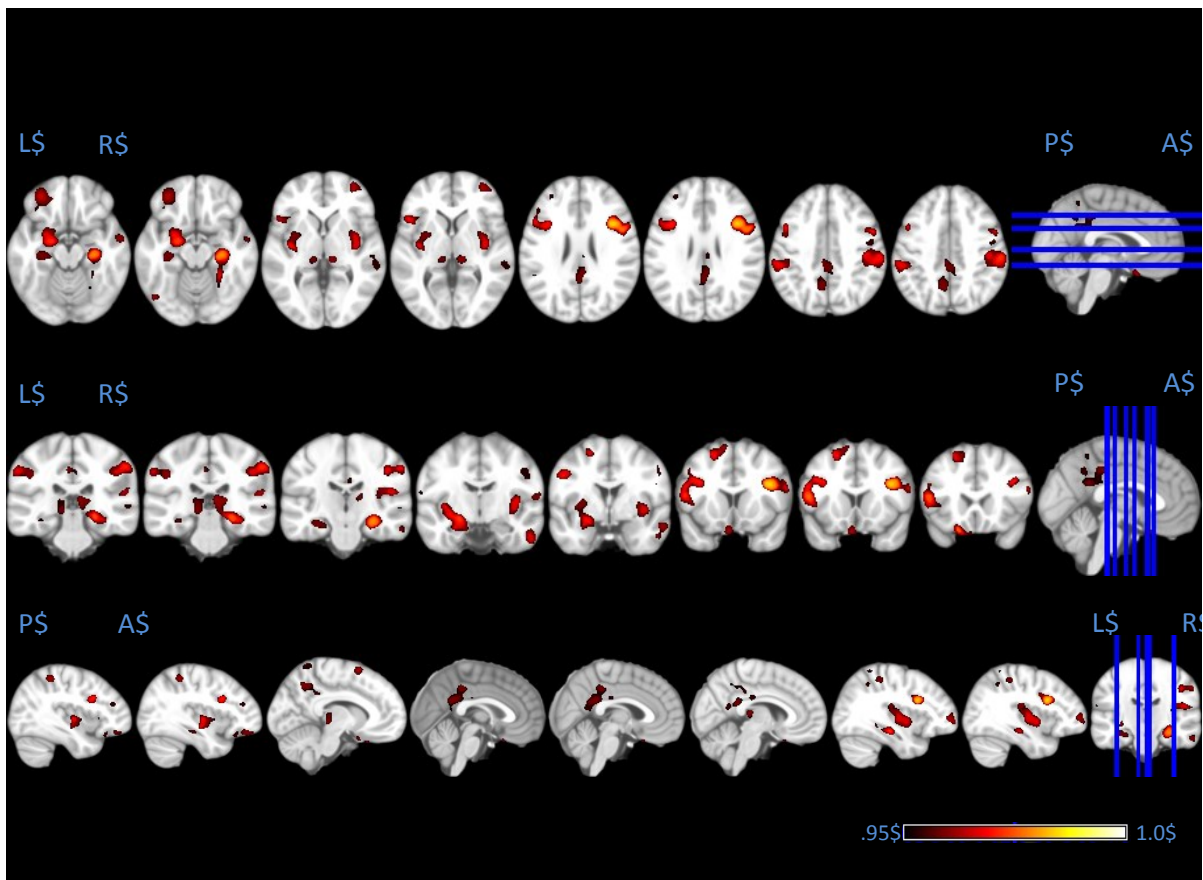


Figure IV-4: Corrected for age and duration of pain, GM decreases emerged in 118G carriers compared to 118A carriers in bilateral posterior insula, left amygdala, posterior cingulate and parahippocampus

Structure	Left Hemisphere					Right Hemisphere				
	Local max.	No. of voxels	x	y	z	Local max.	No. of voxels	x	y	z
Amygdala	0.974	373	25	-30	-9					
Caudate	0.966	7	-33	-15	-10	0.966	9	33	-25	-9
Cingulate Gyrus	0.958	359	-6	-52	42	0.958	441	1	-36	43
Cingulate Gyrus (central)	0.958	87	0	-36	37					
Clastrum	0.969	112	-33	-12	-4	0.966	133	36	-10	4
Culmen						0.953	4	27	-45	-16
Declive						0.950	8	25	-58	-16
Extra-Nuclear	0.974	817	-21	-6	-10	0.974	540	28	-24	-9
Fusiform Gyrus						0.966	359	27	-48	-12
Inferior Frontal Gyrus	0.981	1565	-18	27	-22	0.980	1144	45	13	25
Inferior Occipital Gyrus	0.966	30	-42	-72	-10					
Inferior Parietal Lobule	0.968	1249	-54	-33	42	0.969	434	58	-31	45
Inferior Temporal Gyrus						0.966	361	55	-13	-25
Insula	0.969	198	-27	-10	1	0.966	961	48	-19	18
Lentiform Nucleus	0.971	299	-21	-6	-9	0.966	26	31	-18	-9
Medial Frontal Gyrus	0.959	54	-6	10	-22					
Middle Frontal Gyrus	0.969	1327	-22	16	58	0.978	737	40	16	30
Middle Occipital Gyrus	0.971	190	-48	-72	-12					
Middle Temporal Gyrus						0.962	481	58	-1	-19
Orbital Gyrus	0.980	115	-16	25	-25					
Paracentral Lobule	0.953	12	-6	-49	60					
Parahippocampal Gyrus	0.974	968	-19	-6	-13	0.979	1101	30	-22	-13
Postcentral Gyrus	0.968	710	-55	-31	40	0.973	1561	58	-24	45
Posterior Cingulate	0.955	9	-1	-46	24	0.958	240	4	-39	24
Posterior Cingulate (central)	0.958	11	0	-48	24					
Precentral Gyrus	0.977	294	-48	18	10	0.971	616	60	-22	43
Precuneus	0.959	651	-7	-60	46	0.955	44	1	-49	30
Precuneus (central)	0.956	6	0	-49	30					
Rectal Gyrus	0.962	169	-4	15	-24	0.958	14	4	18	25
Sub-Gyral	0.969	620	-37	15	28	0.984	906	40	13	25
Subcallosal Gyrus	0.966	74	-22	3	-13					
Superior Frontal Gyrus	0.969	1249	-21	18	57	0.962	73	36	57	1
Superior Parietal Lobule	0.952	36	-12	-61	67	0.951	43	34	-51	63
Superior Temporal Gyrus						0.962	113	57	-28	16
Thalamus	0.958	291	-10	-27	0	0.961	458	16	-24	12
Transverse Temporal Gyrus	0.953	7	-63	-12	13	0.961	43	63	-10	13
Uncus	0.962	42	-15	-6	-24					

Table IV-4: MNI coordinates of local maxima comparing OPRM1 118AA > 118AG

Discussion

The aim of this study was to determine the effect of the *OPRM1* 118A-allele on GMD in female chronic musculoskeletal pain patients. Overall, we found increased grey matter density (GMD) in pain processing regions in the A-allele carriers compared to G-allele carriers. This effect became more pronounced when controlling for age and duration of pain and could indicate a compensatory response to genotype-specific impairment of endorphine-mediated analgesia. Although we found no significant correlations between pain reports and GMD when considering the complete sample, significant associations were found when computing correlations separately for A- and G-allele carriers. Indeed, numerous inverse relationships between mean GMD in pain-relevant regions of interest (e.g. putamen, pallidum, paracingulate, posterior cingulate) and sensory and affective SES pain scores were found in 118A-carriers, and to a lesser extent also for the 118G-carriers. These findings will be discussed in detail below.

As stated above, we found negative associations between GMD and pain reports when conducting analyses separately for the two genotypes, which provides further evidence for rs1799971 genotype-specific effects in different ROIs. These negative associations were in line with general findings of an inverse relationship between GMD and pain sensitivity (Emerson et al., 2014; May, 2008). Studies comparing patients with healthy controls frequently highlight an inverse relationship between GMD and reported pain (May, 2008). Based on GMD reductions, one would expect higher pain ratings in the G-carriers. The absence of this difference is suggestive of a mild protective effect of the G-allele (Walter & Lötsch, 2009b), and may thus be a resilience factor against FMS, not only in Turkish women (Solak et al., 2014).

Associations between SES and mean GMD manifested in subcortical ROIs from the basal ganglia and in the amygdala, in which opioid receptor density is high (Sprenger, Berthele, Platzer, Boecker, & Tölle, 2005) and where increased opioid-binding results in down-regulation of affective and sensory response aspects of pain (Zubieta et al., 2001b). Hence, genotype-dependent decreases in opioid-binding efficacy in A-allele-carriers would lead one to expect adaptive GM increases in these structures or similar pain ratings in spite of smaller GMD in G-allele-carriers.

Significant negative correlations for the 118A carriers in the left putamen, left pallidum and posterior cingulate with their sensory as well as affective SES scores and a significant correlation between mean GM volume of the paracingulate and the affective SES scores were in line with previous findings (Emerson et al., 2014; Schmidt-Wilcke et al., 2007). Given the prominent role of these areas in motor responses (Alexander, 1990), a function which is particularly affected in patients with musculoskeletal pain disorders, altered processing in these areas might be involved in the perception of (widespread) pain in patients suffering from FMS and ULBP.

The role of the caudate in chronic pain was investigated in an fMRI study using SPECT, which demonstrated lower rCBF in the caudate in FMS patients (Mountz et al., 1995) and a BOLD study highlighted signal decreases in comparison to healthy controls while performing a Stroop colour word task (Martinsen et al., 2014). In addition, there is strong evidence for a special role of the opioid peptide system in pain inhibition in the caudate from a study of microinjection of morphine into the head of caudate in rats (Li & Tun, 1990). A PET study by Zubieta et al. (Zubieta et al., 2005) found significant activation of endogenous opioid transmission and mu-opioid

receptors in the basal ganglia in response to a sustained pain stimulus and after administration of placebo. While the above mentioned study was not analysed by genotype, a possible mechanism at work might be that allostatic overload caused by chronic musculoskeletal pain (McEwen & Gianaros, 2011) results in reduced down-regulation of pain in 118A carriers due to decreased endogenous mu-opioid binding capacity. Increased SES ratings and the associated decreases in mean GM volume are in support of this. However, this study did not assess mu-opioid binding potential.

In spite of the power limitations due to the small number of 118G carriers, the negative associations between left amygdala and the SES sensory scores and the left caudate and the SES affective scores correspond to previous findings of opioid-binding studies. Zubieta et al. (Zubieta et al., 2001b), reported a negative correlation between mu-opioid binding in the amygdala and the sensory dimension of the McGill Pain Inventory. However, they did not perform a genotype specific analysis, which would allow conclusions regarding genotype specific mu-opioid binding. The reduced GMD in G-carriers in comparison to AA homozygotes, when corrected for age and duration of pain, is suggestive of greater pain ratings in G-carriers. However, in spite of the smaller average GMD and a negative association between mean amygdala GMD and reported sensory pain, the G-allele appears to confer some protection against sensory pain as indicated by the difference in SES sensory scores between the AA and AG carriers possibly mediated by the G-carriers' greater mu-opioid binding potential (Bond et al., 1998b).

In summary, finding that the majority of *OPRM1*-dependent correlations between GM reductions and increases in affective and sensory pain ratings were reported within structures from the basal ganglia is plausible in light of the fact that the basal ganglia possess a high opioid-receptor density (Sprenger et al., 2005). Thus genotype-mediated differences in sensitivity to endogenous opioids are likely to have effects on pain processing and consequent changes in brain plasticity.

The results of the permutation-based GLM at whole brain level, which compared the AA and the AG carriers revealed no significant differences in GM density when comparing the patients by genotype alone except for the right inferior frontal gyrus pars opercularis, which forms part of the secondary somatosensory cortex. It is also one of the few regions that elicits a pain sensation, if stimulated electrically (Head & Holmes, 1911). When corrected for age and duration of pain, smaller GMD for 118G carriers emerged in the bilateral posterior insula, primary somatosensory cortex, hippocampus and parahippocampus, posterior cingulate and left amygdala which have been described as part of a network of pain-relevant structures (Iannetti & Mouraux, 2010).

Since age and pain duration were controlled for in this study, the differences between the two groups might not represent relative GMD reductions in G-allele carriers, but hypertrophy in the A-allele carriers in order to compensate for genotype-mediated reduced effectiveness of endorphine-mediated analgesia.

Overall, the results for the 118A carriers are in line with findings for case-control studies, in which reduction of GM volume corresponds to increased pain intensity when correlating the SES scores for affect and sensory aspects of pain.

Mu-opioid binding potential (MBP) in the nucleus accumbens and thalamus was shown to be negatively associated with both the affective and sensory McGill Pain Questionnaire scores. Negative correlations were also shown between MBP in the amygdala and the sensory pain ratings and in the anterior cingulate with the affective dimension of pain (Zubieta et al., 2001b). In another study of differential opioid action on sensory and affective pain processing, somatosensory cortex I and II and posterior insula were found to be associated. Homozygous 118A carriers revealed pain-related activation in the somatosensory cortex I and II, parahippocampus, amygdala temporal pole, anterior cingulate and supplementary motor area in response to a pain challenge (Oertel, Preibisch, Wallenhorst, Hummel, Geisslinger, Lanfermann, & Lötsch, 2008).

The fact that correlations do not occur in all pain-relevant ROIs indicates a brain region-specific effect of rs1799971 on opioidergic signalling, which has also been demonstrated in SII and thalamus (Oertel, Preibisch, Wallenhorst, Hummel, Geisslinger, Lanfermann, & Loetsch, 2008). The study by Oertel et al. applied a synthetic opioid, while participants in this study were unmedicated, leaving only endorphin-mediated pain regulation. The effect of rs1799971 may thus be determined by a combination of factors including disorder, sex (Mogil et al., 2003), age, genotype and brain region. Reduced mu-opioid binding has been demonstrated in FMS patients (Harris et al., 2007) and symptoms are exacerbated in AA carriers.

While a larger number of 118G carriers would have made for a more robust comparison, the results are in line with previous findings. In addition, the permutation-based GLM was implemented due to known robustness when applied to small sample sizes. Apart from the computational aspects the emergence of functionally and biologically plausible structures with only three heterozygote patients points toward an even stronger effect in homozygotes for the G-allele.

Potential criticism might be directed at the combination of the separate clinical diagnoses ULBP and FMS on the assumption that both disorders are rooted in maladaptive CNS plasticity. There were no systematic differences between age, duration and SES scores between the participants of both diagnoses. Both from an angle of shared mechanism of disorders (Woolf et al., 1998; "Woolf Central Sensitization Pain and Plasticity," n.d.) and that both disorders affect the patients' musculoskeletal system, a combined analysis appears justifiable.

Previous studies indicated a sex-specific effect of exacerbated pain in female carriers of 118G (Olsen et al., 2012), which justifies the exclusive recruitment of female participants for this study. The fact that both disorders are more frequent in women than men might also be indicative of a sex-effect.

However, a future replication of this study should also include a sufficiently large number of male participants to further explore possible sex effects. Additionally, it would be also desirable for future studies to include all three possible allele combinations and gender, age and genotype matched controls. This would allow for a dose response analysis to ascertain whether patients homozygous for the G-allele will indeed show the smallest GM densities in comparison to AA carriers. It would also allow determination of the effect of genotype in healthy controls in relation to sensory and affective pain scores, if a sensory testing battery were included.

Overall, this study highlighted a unique genetic contribution of *OPRM1* to GMD changes in chronic musculoskeletal pain patients. While the direct mechanism of action remains elusive, the results highlighted the *OPRM1* 118A allele as a risk factor and biomarker for chronic musculoskeletal pain in female patients.

Acknowledgements

The authors would like to thank Dr Gareth Barker and Dr Bertram Walter for assistance with the assembly of the .ima-files. We also thank Ged Ridgway for advice on threshold selection for generation of the binarised mask. Funding was provided by the central project of KFG 107.

3 GENERAL DISCUSSION

This chapter provides an evaluation of the results obtained through applying genetic and neuroimaging methodologies in two specific painful clinical conditions. It will then evaluate how well the methodologies used in this thesis adhered to quality criteria for biomarker development specified in the introduction and discuss the studies' limitations before providing a final summary with future directions.

With regard to the neuroimaging components, the ASL-based rCBF measures demonstrated potential as independent endpoints for pain assessment, rather than an adjunct to patient self-reported pain. The comparison between rCBF measures following surgery and those obtained during the pain-free pre-surgical periods demonstrated rCBF increases in an unbiased voxel-wise analysis as well as in a priori hypothesised regions inherent in the central processing of pain. Associations of the post-surgical rCBF and VAS estimates of self-reported post-surgical pain were found in brain regions known to underpin the pain experience, but not in a pain-unrelated control region, thus adding to the results' physiological plausibility.

Stability for rCBF assessments was established within a single session and demonstrated robustness with regard to between-session differences in post-surgical rCBF following extraction of left, compared to right teeth. Bilateralism is of particular relevance within the context of the trigeminal system (Jantsch et al., 2005; Weigelt et al., 2010) where evoked painful and non-painful stimulation of the trigeminal nerve may elicit bilateral rCBF changes in the thalamus. Crossed and uncrossed somatosensory and nociceptive afferents project from the trigeminal ganglion to the thalamus and terminate at its ventral medial and lateral posterior regions, which contain bilateral representations of the oral cavity (Nieuwenhuys et al., 2008). Through its interconnections with the hypothalamus (Pogatzki-Zahn et al., 2007) bilateral changes in post-surgical thalamic rCBF may represent aspects of the on-going pain experience, but also changes in arousal (De Leeuw et al., 2005). Findings of bilateral rCBF increases in S1 post surgery match findings in bilateral receptive fields of primates (Lin et al., 1993).

Further analysis addressed issues regarding the reliability of quantitative cerebral perfusion measures in research on ongoing pain. It demonstrated that pain following TME could be assessed with good-to-excellent inter- and intra-session reliability across both pCASL and VAS modalities within-subject. It also capitalised on the advantage of repeated measures designs to limit variability between subjects due to experimental error and thus provide good reliability for comparing condition effects and thus enable implementation of reliable quantitative perfusion imaging biomarkers of ongoing pain to supplement the use of subjective self-report measures.

The importance of careful baseline selection was highlighted, which increased the reliability of the Δ CBF parameter (an indicator of change in CBF between pre- and post-surgical states) by demonstrating that either a single baseline condition or alternatively the mean of more than one baseline produced a higher degree of reliability. Hence, this study highlighted that ASL-based studies should be designed with several factors in mind to ensure appropriate reliability and to avoid previous

issues in detecting reliable drug-induced CBF changes with ASL using the test–retest method (Klomp et al., 2012).

An additional achievement of this study was its provision of a framework for future use of ASL-based assessments of the cerebrovascular response to pain. Since the publication of these results, ASL has successfully revealed altered perfusion patterns in other pain populations (e.g. migraineurs without aura and osteoarthritis (Hodkinson, Veggeberg, et al., 2015; Sanders et al., 2015)). The ASL technique thereby highlighted disease-specific functional deficits in neural pain processing pathways (Hodkinson, Veggeberg, et al., 2015), thus adding value above and beyond patient self-report (Borsook et al., 2008) and taking us closer to discovering potential underlying mechanisms such as adaptive or maladaptive functional plasticity. Furthermore, the pCASL rCBF signature demonstrated utility in successful differentiation between patients and healthy controls and in assessment of the effects of analgesics versus placebo (Hodkinson, Khawaja, et al., 2015a; Hodkinson, Veggeberg, et al., 2015; Howard et al., 2012; Sanders et al., 2015). Since no experimental augmentation of pain (Owen et al., 2012; Wasan et al., 2011) was needed as CBF changes manifested in patients at rest, transfer of ASL-based imaging protocols into standard clinical practice similar to those in neurological disorders such as dementia and stroke could be used in diagnostics and the monitoring of treatment progress.

The following factors in this study proved helpful in achieving reliability: first, acquisition of more than one pre- and post-surgical CBF map. Second, a counterbalanced within-subject study design and implementation of strict inclusion and exclusion criteria to minimise the impact of confounding factors. Reliability tests in this study indicated that both functional and psychological interactions occurred despite strict adherence to a balanced study protocol and thus demonstrated additional volatility factors in the assessment of the pre- and post-surgical states. Third, factorial designs have proven more powerful in the analysis of cognitive processes (Friston et al., 1996) and should thus be implemented.

Independent of whether the left or right third molar was removed, TME appeared to be represented in S1, S2, and insula ipsi- as well as contralateral to the surgery site (Howard et al., 2011), which replicated findings from previous investigations employing painful (Jantsch et al., 2005) and non-painful (Ettlin et al., 2004) dental stimulations. Such low variation across repeated measures facilitates the detection of small alterations in CBF. Hence this study demonstrated the suitability of ASL indices in the monitoring of disease progression and therapeutic intervention effects, since there is no need for contrast agents (Petersen et al., 2006).

Longitudinal reliability of ASL in this study was in line with findings from previous studies in healthy volunteers (Chen et al., 2011; S. Gevers et al., 2009a; Gevers et al., 2011; Jain et al., 2012; Parkes et al., 2004) and neurological patients (Xu et al., 2010). There was no relationship between interval length and ICC values, even though the study design did not acquire the pre-surgical scans immediately before surgery, but on different days. Still further research on reliability of perfusion-based measures across the course of longitudinal studies is desirable, even though time-course stability of the CBF measurements within the ongoing pain state was excellent in this study as indicated by higher ICC values between pCASL scans than ICC values between sessions. In addition, potential variability in the CBF measurements

due to temporal variation was investigated with respect to the duration of scanning for each subject. Operator-related variability was deemed to be low and reproducibility values to be predominantly physiology dependent as pCASL scans within-session did not require repositioning. Hence, potential error from aligning acquisition and labelling planes should be minimal. The resulting relative stability of this type of perfusion measurement over relatively long-time intervals makes it an attractive method to study naturalistic responses to pain, allowing within-subject investigations of spontaneous and intervention-dependent fluctuations in pain state.

With regard to the gene expression component, this study demonstrated the utility of gene expression analysis in peripheral whole blood after TME by generating a list of target genes in which the top 20 most significantly differentially expressed genes demonstrated high potential of being pain and nociception biomarkers, as almost half of them had previously been indicated in studies of various pain phenotypes. At the same time, the use of a data driven approach utilising pathway and interaction data from known functional pathways enabled a better discrimination of genes primarily concerned with other biological functions such as digestion, which could be treated with less priority in follow up studies on particular candidates.

The particular challenge met by this study was to implement a viable strategy to identify candidate genes and molecular pathways with primary relevance in pain and nociceptive signalling and processing rather than mere tissue repair and immune functions in response to the tissue damage. It demonstrated that the data science approach was able to condense the long list of genes to smaller groups with significant enrichment of genes from this study in established molecular pathways and a custom-designed pathway for inflammatory mediator regulation of TRP channels.

Such studies open a potential avenue to combat one of the greatest criticisms directed at analgesic development, that all currently available analgesics are merely variations of existing drug classes (e.g. opioids and NSAIDs (Max, 2000; Woolf & Max, 2001)). Instead of introducing synthetic agonists and antagonists, which bind to pain and nociception-relevant receptors, clarifying the role of genes such as membrane metalloendopeptidase (*MME*) for example, might enable the therapeutic modulation of the body's own analgesic and anti-nociceptive capacities. Inhibiting cleavage of enkephalins, which are often provided by leukocytes in inflamed tissue (Schreiter et al., 2012), but are also abundant in peripheral whole blood, might result in an analgesic effect.

Some such inhibitory drugs have already been tested, the two main groups being dual enkephalinase and fatty acid amide hydrolase (FAAH) inhibitors, in a model of inflammatory and neuropathic pain (Roques et al., 2012). Ideally such mechanism-based treatments would eliminate the irksome aspects of pain, while leaving adaptive aspects such as facilitation of tissue repair undisturbed. The multitude of associations with a range of different pain phenotypes fosters hope that effects of future interventions developed as a result of a biomarker-based approach, are effective across different pain pathologies, which might manifest in different phenotypes, but share similar mechanisms. Future comparisons of expression profiles from patients in pain and upon achieving pain relief might also help in further characterising the mechanisms of action inherent in commonly used analgesics.

The VBM study featured a combined analysis, thus making it an imaging genetics study. The overwhelming majority of studies on GM irrespective of genotype in populations suffering from chronic or ongoing pain have highlighted an inverse relationship between GM density and pain intensity (Emerson et al., 2014; May, 2008). Only one report on chronic back pain patients versus healthy controls demonstrated increases in GM density in the basal ganglia (Schmidt-Wilcke et al., 2006), albeit uncorrected for small volumes. Thus the difference in GM density is more likely to represent GM hypertrophy in carriers of the wild-type allele. This likely represents a compensatory response to the on-going pain, than pain-induced GMD in G-carriers, since all participants in this study suffered from musculoskeletal pain. Possible mechanisms behind this might be the G-allele's facilitative effect on opioid binding, which suggests decreased endorphine-mediated analgesia in A-carriers (Walter & Lötsch, 2009b). Further support for an ameliorating influence of the G-allele are findings that the G-allele is less frequently found in female FMS patients (Solak et al., 2014) and has been shown to enhance the ability to maintain positive affect even on days with higher pain (Finan, Zautra, Davis, & Lemery-chalfant, 2011).

However, a pattern of inverse relationships between GMD and sensory and affective SES scores did emerge mostly for the 118A-carriers in several ROIs with known involvement in pain and nociception, but not in an analysis of the overall sample.

Plausible reductions in mean GMD in the 118A-carriers for the left putamen, left pallidum and posterior cingulate with their sensory as well as affective SES scores and a significant negative correlation of paracingulate mean GMD and the affective SES score were in line with previous findings of an inverse relationship between GMD and sensory pain ratings in essential neural hubs of the default mode network (Buckner, Andrews-Hanna, & Schacter, 2008; Fox et al., 2005) and networks regulating somatosensory processing, direction and shifting of attention (Emerson et al., 2014; Schmidt-Wilcke et al., 2007). Previous findings of altered activation of the posterior cingulate cortex in low back pain (Kobayashi et al., 2009) and in response to painful stimulation (Adler et al., 1997; Coghill et al., 1994; Vogt et al., 1996) added further plausibility.

Significant negative correlations in ROIs of high opioid receptor density (Sprenger et al., 2005) such as the basal ganglia and amygdala pointed toward impaired down-regulation of pain through opioid-binding (Zubieta et al., 2001b) in the A-carriers and affirmed the role of the selected ROIs in motor response (Alexander, 1990), nociception (Starr et al., 2011) and integration of somatosensory and motoric information (Bingel, Gläscher, Weiller, & Büchel, 2004). The higher prevalence of significant negative correlations in A- rather than G-allele-carriers can be viewed as further evidence for genotype and brain region-specific effects of rs1799971 (Oertel, Preibisch, Wallenhorst, Hummel, Geisslinger, Lanfermann, & Loetsch, 2008). However, the number of G-carriers in this sample was limited.

In the light of a mechanism-based approach to the study and classification of pain, the absence of significant differences in SES ratings between the two diagnoses supported the assumption of a shared underlying mechanism between FMS and ULBP. The areas revealed in this study overlapped with pain-related activation in response to a pain challenge in a genotype-specific study of differential opioid action on sensory and affective pain processing, with a pronounced effect in homozygous

118A carriers (Oertel, Preibisch, Wallenhorst, Hummel, Geisslinger, Lanfermann, & Lötsch, 2008).

Despite the known effects of this SNP on endogenous opioid binding and opioidergic transmission in brain regions of high opioid-receptor density (Sprenger et al., 2005) (e.g. basal ganglia (Zubieta et al., 2005)), the exact nature of the underlying mechanism remains elusive without concomitant assessment of genotype-specific opioid-binding. Reduced mu-opioid binding has previously been demonstrated in FMS patients (Harris et al., 2007). Here impaired endogenous mu-opioid binding capacity in 118A carriers most likely resulted in reduced down-regulation of pain and in turn lead to allostatic overload with exacerbated symptoms, especially in AA carriers (McEwen & Gianaros, 2011).

The results also indicated, that the genotype-specific effects can be masked by other factors such as age and duration of pain as relative GMDs by genotype alone only appeared in the right inferior frontal gyrus pars opercularis. After correction for age and duration of pain (Iannetti & Mouraux, 2010) more extensive GMDs for the 118G carriers emerged.

This study demonstrated genotype-specific effects on brain plasticity in patients with chronic musculoskeletal pain, highlighting an inherent risk of relative hypertrophy in pain processing regions of the brain associated with the A-allele of SNP rs1799971 in *OPRM1*. These effects became more pronounced when controlling for age and duration of pain and represent a compensatory response to genotype-specific impairment of endorphine-mediated analgesia. While the direct mechanism of action remains elusive, results identified the *OPRM1* 118A allele as a risk factor and informative biomarker for chronic musculoskeletal pain in female patients.

3.1 Fulfilment of quality criteria in biomarker discovery and limitations

Adherence to commonly used quality criteria was used as a yardstick for the critical evaluation of the utility of neuroimaging and genetic technologies in search of biomarkers of pain and nociception in this thesis. High reliability, sensitivity, specificity, generalizability, comprehensiveness and validity enhance the potential for successful identification of novel genetic and neuroimaging biomarkers, clinical and surrogate endpoints and will be discussed in the following chapter along with the accompanying limitations.

Reliability

The issue of reliability was highlighted in the TME study for both the neuroimaging and the gene expression endpoints in baseline selection when calculating the differences between pre- and post-surgical gene expression and rCBF levels. Both gene expression and rCBF are subject to considerable volatility in response to environmental and/or internal factors, which put particular emphasis on the choice of a baseline in both endophenotypes.

For the rCBF data to yield good-to-excellent reproducibility the best baseline was implemented by either the use of a single baseline condition or the mean of more

than one pain-free baseline scan in order to increase the precision of ICC estimations. Similarly, the gene expression data included two pain-free baseline samples for every post-surgical sample obtained on control MRI scanning days and immediately before the surgery, and one baseline follow-up sample.

The amelioration of the effects of fluctuations in rCBF levels could be attributed to many factors such as differences in intrinsic physiological factors between the individuals, the overall level of brain activity (Wenzel et al., 1996), variations in blood T1, neuronal density or number, and arousal (Parkes et al., 2004). A definite advantage was the implementation of the pCASL measurements at 3T rather than 1.5T, which yielded improved spatial and temporal resolution due to the longer T1 and a higher signal to noise ratio (Chen et al., 2011; Tjandra et al., 2005).

Further confidence in sufficient control for variability between testing days in the ASL data stemmed from several sources: First, the pCASL -in comparison to the BOLD signal- is known to be less volatile across different time points (Gevers, Majoie, Van Den Tweel, Lavini, & Nederveen, 2009b; Gevers et al., 2011). This can be attributed to the lower temporal resolution of pCASL as it represents the sum of several measurements across a period of several minutes. In addition, pCASL-derived rCBF is mapped to parenchyma and thus less sensitive to large draining vein contributions since signal loss due to T1 recovery has reduced venous blood labeling by the time the blood arrives at the draining veins (Duong et al., 2002). This was complemented by the physiological meaningfulness of the measure, while BOLD measures of neural activity are a more implicit measure of neural activity (Wong, 2014). Further support for the meaningful application of pCASL was drawn from previous studies of differential rCBF using ASL in different pain states and disorders (Maleki et al., 2013; Owen et al., 2012).

Within the context of the VBM study, reliability was more difficult to assess. Morphometric changes are less dynamic than those observed in neural perfusion and gene expression. The method of choice in most VBM studies of pain has been a case-control design, which results in a between-subjects comparison (Apkarian & Hashmi, 2012; Lutz et al., 2008; Schmidt-Wilcke et al., 2007). Alternatively, repeated measure designs allow for a within-subject comparison thus minimising between-subject error as applied in a study of osteoarthritis patients which compared GMD before and after hip joint endoprosthetic surgery (Rodriguez-Raecke, Niemeier, Ihle, Ruether, & May, 2013b). Here, patients served as their own controls between pain-free and painful state. However, pre-morbid structural scans of FMS and ULBP patients are rarely available and there is a lack of prospective cohort studies of musculoskeletal pain, which include MRI data, due to the late onset of FMS and ULBP. One of the reasons for this might be that technological advances impede comparisons across different measurement time points. Structural data acquired on an older scanner of low(er) field strength (e.g. 1.5T) and structural data acquired a contemporary scanner with field strengths of 3T or above would be incompatible for joint analysis. In addition, comparability between scans from different manufacturers may be limited.

While genotyping DNA has become a highly reliable standardised procedure, reliability for the *OPRM1* A118G genotype data was ascertained by cross-validating genotyping results on two different platforms. The high concordance of results indicated high quality thereof.

With regard to gene expression studies the issue of reliability was more complex. Reliable detection of relatively abundant transcripts has been established for the existence and direction of expression changes. However, the magnitude of expression changes cannot be assessed accurately by microarrays (Draghici, Khatri, Eklund, & Szallasi, 2006). In addition, probe sets vary across microarray platforms and the resulting summary values for genes may not correspond with PCR-based measures of gene expression.

Sensitivity within the biomarker concept is defined as the ability of a biomarker or a change therein to be measured with adequate precision. This requires sufficient magnitude of change in order to identify meaningful alterations in important clinical endpoints (Lesko & Atkinson, 2001). The pCASL data revealed rCBF increases between 5-10% following TME, which can be considered a huge effect, considering that the majority of fMRI studies use BOLD imaging, which in studies of cognitive effects yield changes in an order of magnitude between 1-5% (Aguirre et al., 1998; Glover, 1999).

VAS estimates of pain have been a staple in pain assessment and aided in establishing association between painful sensations and significant increases in response to TME. However, simple VAS intensity ratings fall short on assessing the multi-dimensional character of pain, as they do not allow for further differentiation of specific aspects of pain processing (R. Melzack, 1975). In the VBM study additional aspects such as sensory and affective ratings of pain from the SES were included also based on previous knowledge of a differential influence of opiodergic signalling on these aspects (James, 2013; B. G. Oertel, Preibisch, Wallenhorst, Hummel, Geisslinger, Lanfermann, & Loetsch, 2008).

Specificity –the third quality criterion to be discussed within the biomarker concept– is defined as the ability of a biomarker or a change in biomarker to distinguish patients who are responders to an intervention from those who are non-responders in terms of changes in clinical endpoints. Since none of the study designs included an analgesic intervention the criterion of **generalizability** was emphasized.

Generalizability i.e. the ability of an underlying mechanism to cause a mild as well as a severe form of a disorder, highlighted some minor and some broader limitations of this thesis. For example, participants in TME study were excluded, if the VAS ratings of pain remained below 3 out of 10 after the lidocaine had worn off, thereby excluding very mild manifestations of inflammatory pain. Although analysis of non-responders bears fascinating prospects, in the context of this thesis, the small number of participants would have left such an analysis profoundly underpowered. While generalizability is desirable, there is a tendency to focus on the pathological and less on the resilient end of the spectrum. Since the resilient individuals are of little interest for interventional research and do not represent a burden for healthcare systems, studies are designed to often exclude those individuals with mild manifestations of a disorder to enable better detection of statistical effects in small pilot studies due to the cost of this type of research.

With regard to the VBM study an additional reference population of age, genotype and gender matched healthy controls would have been preferable. This thesis examined the differences in GMD between *OPRM1* 118A- and 118G-carriers

suffering from FMS and ULBP, but did not include healthy control participants. Hence the general effects of this genotype on GMD warrant further examination.

Overall an analysis for a dose-response relationship for both homozygous and the heterozygous groups would have made a much stronger point with regard to the hypothesis of this study. Furthermore, replication of the age-dependent effects on GMD demonstrated by Ceko et al. (Ceko et al., 2013) in association with genotype would have been of interest as well, since GMD differences between OPRM 1 118A- and 118G-carriers became more pronounced after controlling for age and duration of pain.

The criterion of **comprehensiveness**, is defined as providing as many diagnoses as necessary within a categorical system of pathology to sufficiently classify manifest disorders. It touches upon the most divisive point between phenomenological and mechanism based classifications of pain. Even though a disorder might present with very heterogeneous phenomenology (with ULBP and FMS being diagnosed as separate disorders in current clinical practice (WHO, 2010)), the same classification as a maladaptive CNS plasticity syndrome may apply due to a shared underlying mechanism (Yunus, 2008). In a mechanism-based classification of pain, both disorders are counted among the central sensitivity syndromes i.e. nervous system injury pain brought on by maladaptive CNS processing (Woolf, 2004). Support for a shared mechanism was found in the VBM study in that both FMS and ULBP patients demonstrated exacerbated sensory and affective pain levels and relative GMD reductions mediated by the presence of the A-allele of rs1977791.

A similar line of reasoning applies with regard to gender. Previous studies demonstrated a gender specific effect of exacerbated pain in female carriers of 118G (Olsen et al., 2012), which justifies the exclusive recruitment of female participants for this study. The fact that both disorders are more frequent in women than men might also be indicative of a sex-effect. The exclusive use of female participants was well justified by the higher frequency rates of FMS and ULBP (Werber & Schiltewolf, 2012; Wolfe et al., 2010) in women and while the exclusive use of men in the TME study allowed for control of hormonal variations at the price of limiting extrapolation of the results to female TME patients. Although men were recruited for the VBM study, the number of male data sets was too small to allow for gender-specific analysis. This is apparent gender bias is a general concern in medical research. Pharmacological studies and clinical trials are predominantly conducted in men (Gluud, 2006; Herz, 1997). Female participants are mostly post-menopausal women due to the aforementioned hormonal variation, but also to exclude potential teratogenic effects in women of child-bearing age (Ramasubbu, Gurm, & Litaker, 2001; Ruiz & Verbrugge, 1997). With regard to pain this is particularly unsatisfying since the majority of pain conditions affect more women than men and there is evidence that pain affects women differently as well (Fillingim, 2000; Greenspan et al., 2007). This thesis included both male and female participants. However, they split into an all male sample in the TME study and an all female sample for the VBM study.

In addition, both studies were also subjected to an inherent age bias, which was rooted in the typical prevalence and age of onset of the clinical phenotypes. The potential risk here is that results are subject to limitations when extrapolating to the respective opposite sex for both studies or to older or younger age cohorts. Studies of ASL have demonstrated a decline in overall rCBF levels in older patients (Parkes et al., 2004), which is attributed to the well-established age-related decline in grey

matter (Ge et al., 2002). For the TME study, extrapolation to other types of surgery-induced pain or older populations with worse overall health status, comorbidities or on concomitant medication due to age-related conditions might be impeded as well.

While age-related grey matter decrease has been controlled for in the VBM study, the small sample size and limitation to female subjects has slightly greater implications for the VBM study, where the small number of participants resulted in a lack of gender, age and genotype matched controls.

In spite of the small sample size, the criteria for Hardy-Weinberg equilibrium were met. Hence, reasonable confidence could be placed in a lack of systematic differences in genotype distribution. Although the minor allele is less common than the wild-type allele, the fact that there are hardly any GG carriers in most studies of this genotype and in particular in FMS patients, is also making an implicit statement with regard to the protective properties of the G-allele and is in line with previous findings (Solak et al., 2014).

Validity in biomarker research is defined as the degree of achieving the objective of a study and pertains to the ability with which a diagnostic measure can answer a medical question (Büttner, 1997). Clinical relevance is thus an important cornerstone of biomarker evaluation and has strong bearing on the (ecological) validity of a biomarker.

The most commonly used approach in increasing validity is employing a gold standard model of a disorder. While many of the mechanisms underlying pain and nociception are yet unknown to date, the TME model currently represents a gold standard model for inflammatory pain. It has been used in combination with genetic, QST and other phenotypes in addition to its applications in determining the efficacy of analgesics (Flores & Mogil, 2001; Hargreaves, Schmidt, Mueller, & Dionne, 1987; Juhl et al., 2008; Wang et al., 2007). The TME model also allows a direct comparison between a pain-free and a painful state in patients without confounding comorbidities as is the case in most chronic pain disorders, where there is often little reliable information regarding the pre-morbid state.

The VBM study in patients with chronic musculoskeletal pain suffering from FMS and ULBP represented a model of stimulus-independent pain, since no external event to precipitate its onset was identifiable. Hence there is no intervention such as a surgery to precipitate the pain. Here a gold standard would be to perform a prospective study to identify factors, which lead to participants developing the pathology later in life, which is impeded by the aforementioned difficulties of high drop out rates for longitudinal cohort studies and MRI platform incompatibilities.

In further support of validity, both studies were performed in humans and in actual clinical cohorts. Hence, both studies adhered to recommendations for studying common genes that contribute to human pain. Hence, minimising the risk of failure often associated with animal model-derived genetic targets in the treatment of human disorders (e.g. tachykinin NK1 receptor antagonists (Hill, 2000)) and to increase the chance of a return of the results from bench to bedside (Mitchell B Max, 2008).

An advantage of working with human participants was that it enabled the assessment of cognitive components of the pain experience such as sensory and affective ratings of pain, which are essential components of the human pain experience, but difficult to

operationalize in animals (Max & Stewart, 2008b). Another aspect pertained to the ecological validity of the study designs. The TME model offered a pain stimulus with a higher threat value than many experimental pain stimuli, with the threat component being an essential part of the pain definition (Mersky & Bogduk, 1994).

While nociception and pain are universal in humans, pharmacogenomics have demonstrated different efficacies of the same medications in different ethnicities based on genetic variation (Argoff, 2010; Roses, 2000; Wang, Zhang, He, & Fang, 2006). The same might apply in the case of rs1799971 with regard to the prevalence of FMS and ULBP due to the different distributions of the minor allele frequency across ethnicities. Low prevalence for FMS has been reported in Chinese populations (Zeng et al., 2008), where in some cases the A- and not the G-allele can be the minor allele. There are general differences with regard to the frequency of the G-allele, which is present in 5-10 % of Africans, 10-20% Caucasians and 40-60% Asians. Whether the findings in this study replicate in other populations remains to be proven and requires further research in FMS patients of different genetic backgrounds.

Participants in the VBM and TME study were screened for depression prior to inclusion and none of the participants had clinically relevant scores. With regard to the VBM study, future inclusion of depressed pain patients might reveal additional effects on affective pain scores. *OPRM1* has demonstrated effects on pain-related affect and consistency of GMD differences when controlling for affective disorders (Finan et al., 2011; Hsu et al., 2009).

Particular attention was drawn to the spatial non-uniformity of reliability in the CBF measurements. ASL measures have demonstrated spontaneous CBF fluctuations in resting state (Petersen et al., 2010) and in response to brain activation at different levels in previous studies (Wenzel et al., 1996). While ICC is clearly dependent on the heterogeneity of the sample and fluctuations in physiology induced by the pain state, the seeming independence of distribution of high ICC values and high values of *t* may be rooted in differences in the spatial distribution of the CBF response to pain. Another explanation of these findings might be differences in intrinsic physiological factors between the individuals, attributable to physiological variability without being a limitation of the pCASL methodology.

Yet another explanation for individual differences in the perfusion estimate may depend upon variations in blood T1, neuronal density, and arousal (Parkes et al., 2004). Here acquisition of CBF data at higher field strengths provided the advantage of longer T1 and enhanced signal to noise ratio in addition to improved spatial and temporal resolution.

3.2 General thesis conclusion

This final section will evaluate potential of the application of genetic analysis and neuroimaging tools in the quest for new insights into the mechanisms underlying pain and nociception.

The bottom-up approach (Mogil & McCarson, 2000) used in the TME study demonstrated the utility of gene expression data from peripheral whole blood in combination with a data science approach in highlighting differentially expressed

genes with raised potential of being relevant in pain and nociception. In the future this approach will become more refined as new pathways will be added to reference databases and more information will become available on transcripts, genes and their interactions, which are poorly characterised to date.

At the same time a combination of genetic and neuroimaging techniques was utilised in a top-down approach, where the effects of a common genetic variant from the gene encoding mu-opioid receptor 1 on grey matter density was assessed at the whole brain level, and the relationship between mean GMD and psychometric ratings of sensory and affective pain in important nodes of neural pain processing networks were assessed. The results revealed greater GMD in the carriers of the wild-type allele in comparison to carriers of the minor allele. At the same time there were significant negative genotype-dependent associations between GMD and sensory and affective pain ratings pointing towards relative hypertrophy in the wild-type allele carriers. However, the exact mechanism by which this maladaptive process is initiated and sustained warrants further investigation.

By adapting an augmented multi-level approach to a mechanism-based classification of pain disorders in lieu of the traditional phenomenological approach, it was possible to implement viable strategies involving well-characterised, controlled, clinically relevant biomarkers in pain and nociception that are robust, yet relatively easy to acquire.

It enabled the investigation of three clinical pain conditions (i.e. FMS, ULBP and TME induced post-surgical pain) at the symptoms level by using the classical phenomenological descriptors such as intensity, location and duration in conjunction with additional physiological measures i.e. gene expression and rCBF levels, GM volume and genotype closer to the biological underpinnings of the disorders under investigation. These were used as additional (endo-)phenotypes to refine identification of possible biomarkers in search of mechanisms and biological diatheses, which govern pain and nociception in the abovementioned clinical pain states and to maximise the chances of generating suitable targets for further investigation with regard to developing therapeutic and diagnostic procedures.

Neuroimaging and genetic biomarkers demonstrated utility in both a stimulus dependent prolonged pain experience as implemented in the TME study, as well as stimulus-independent musculoskeletal pain conditions. The idea of disease-specific 'neurosignatures' beyond a single universally active pain matrix (Iannetti & Mouraux, 2010; Iannetti, Salomons, Moayedi, Mouraux, & Davis, 2013; Tracey & Johns, 2010a) can be tested and implemented in the context of activation and perfusion measures, but also with regard to structural changes depicted as variations in grey matter density. Hence, selecting a set of a priori ROIs based on previous knowledge of a specific pain condition instead of a universally applied approach to all persistent pain states appears preferable. Since ROIs with known high *OPRM1* density emerged from the analysis in this study, these might lend themselves as preferred targets for future investigation.

While the decline in GMD in various pain populations in comparison to healthy controls is well established (Emerson et al., 2014; May, 2008; Robinson et al., 2011), the study of *OPRM1* genotype-dependent differences in GMD highlighted the need to investigate adaptation and coping responses to on-going pain and the potentially

modulating effects of factors such as age and gender in addition to genotype. If conditions such as FMS and ULBP are characterised by an initial increase in GMD in younger patients (Ceko et al., 2013) and if these increases are more pronounced depending on genotype this might facilitate the development of screening methods for detection of risk as well as resilience factors, but also the development of new treatments targeting a reversal of these maladaptive neural processes. Repeated MRI-based assessments of patients and volumetric analyses might then be used in monitoring diseases progression or treatment success respectively.

Similarly, the pCASL methodology (Borsook et al., 2008) lends itself to investigation of central effects of pain medications and their effects in pain-free participants (Wagner et al., 2001). It also enables future exploration of the effectiveness and putative mechanisms of action for novel analgesics and novel indications for existing compounds as well as differential efficacy across pharmacological classes and doses in preclinical studies and should facilitate translational research, thus becoming a valuable addition to simple behavioural endpoints which have predominated to date (Mogil, 2009). Additional applications might include the assessment of pain in individuals with reduced capacity for self-report such as children (Eccleston et al., 2012) or patients with consciousness disorders (Owen & Coleman, 2008).

Another possible application would be research into resilience factors, which promote protection against maladaptive pain states such as ULBP and FMS or excessive suffering post surgery. While pharmacological research focuses on non-responders to treatment interventions, little is known regarding non-responders to painful procedures such as surgery. Such patients may go undetected in clinical practice either because they have been administered analgesics pre-emptively or because they go undetected as they do not initiate further contact with the medical system, unlike those with further complaints. The exception are cases, where the inability to experience any pain at all becomes a life threatening condition, as is the case with hereditary sensory and autonomic neuropathies caused by rare ion channel mutations (Cox et al., 2006; Einarsdottir et al., 2004; Lafreniere et al., 2004; Minde et al., 2004; Oertel & Lötsch, 2008).

With regard to genetics, future studies on pain-relevant genotypes would apply the quantitative trait loci approach to disorders by focusing on the end of the distribution with increased resilience, i.e. those patients who fail to experience relevant pain post surgery. Two participants examined in the context of this thesis failed to develop clinically relevant levels of pain post surgery. While these numbers were too small to perform separate analyses, further use of the TME model as implemented in this thesis, will potentially generate more data sets of this kind. In addition, an extension of the model to other types of surgery beyond TME might achieve similar results. Incorporation of follow up appointments might also generate data with the ability to predict which patients move on to develop chronic pain conditions post surgery as well as identify particularly resilient patients.

Differences in gene expression patterns between those who did and those who did not develop clinically significant levels of pain would be of future interest. Further validation of parallel and joint application of genetic and neuroimaging techniques could be derived from their application in the context of analgesic trials. Analysis of patterns of co-variation in gene expression, subjective pain ratings by means of VAS and questionnaire measures and as rCBF levels within TME model might generate

strong leads towards potential additional mechanisms and treatments. This in turn might enable progress beyond the serendipitous discoveries of effective analgesic compounds with later discovery of the actual mechanism – as was the case with NSAIDs such as acetyl salicylic acid (Sneader, 1997) for example. A rational top-down approach to the development of pharmacological and other types of interventions (e.g. bio-feedback) would become possible with increasing knowledge of the actual mechanisms of pain and nociception.

Ultimately, the findings generated by the combination of neuroimaging and genetic methodologies may generate analgesics and therapies, where the same medication proves to be effective in disorders, which present with heterogeneous clinical features, but which share an underlying mechanism. At the same time it may facilitate the discovery of very specific mechanisms and the development of drugs targeted towards them. This may result in more individualised medications and prescription practices, with some drugs being gender-specifically prescribed, taking into account sexual dimorphisms in pain (Craft, Mogil, & Maria Aloisi, 2004; Joseph & Levine, 2003).

Until we are able to inspect the contents of the boxes within the bigger box, the use of biomarkers represents the most valuable tool in researching pain and the development of possible interventions. In particular the pCASL-derived markers met the majority of criteria for a meaningful biomarker. Within a classification of biomarkers gene expression levels and pCASL results represent type I biomarkers. This type determines the biological effect of a therapeutic intervention with regard to the mechanism of action, even though the exact nature of the mechanism's association with clinical outcomes may still be unknown.

Establishing peripheral whole blood as an easily accessible tissue to use as a proxy for pain-related molecular changes is a first step towards facilitating the use of this technology within pain research akin to the use of the commonly used blood counts and chemistry analyses in many clinical settings. In the future proliferation of genetic and neuroimaging techniques and further advances in the development of bioinformatic tools such as genome browsers and databases of molecular pathways (Hillman-Jackson et al., 2007; Rhead et al., 2009) will help to better discriminate between pain and nociception-related and pathways and those concerned with pain-unrelated functions. This will also increase general knowledge of genes, the proteins they encode and their specific functions and interactions.

Even though a biomarker by definition represents a reduction in complexity, their implementation with strong adherence to biomarker quality criteria in actual clinical pain conditions has definite advantages over the purely phenomenological approach in search of novel components and circuit in pain and nociceptive regulation. The combination of tools to generate genetic and neuroimaging biomarkers for parallel and joint analyses explicitly investigating phenotypes in pain and nociception thus represents an important step towards uncovering the mechanisms underlying pain and nociception. Knowing the contents of the Wittgensteinian box that contains the pain experience will help us to think outside the box when revising new treatments and interventions.

4 REFERENCES

- Adler, L. J., Gyulai, F. E., Diehl, D. J., Mintun, M. a, Winter, P. M., & Firestone, L. L. (1997). Regional brain activity changes associated with fentanyl analgesia elucidated by positron emission tomography. *Anesthesia and Analgesia*, *84*(1), 120–126. <http://doi.org/10.1097/00000539-199701000-00023>
- Aguirre, G. K., Detre, J. A., Zarahn, E., & Alsop, D. C. (2002). Experimental design and the relative sensitivity of BOLD and perfusion fMRI. *NeuroImage*, *15*, 488–500. <http://doi.org/10.1006/nimg.2001.0990>
- Aguirre, G. K., Zarahn, E., & D'esposito, M. (1998). The variability of human, BOLD hemodynamic responses. *NeuroImage*, *8*(4), 360–369. <http://doi.org/10.1006/nimg.1998.0369>
- Alexander, G. E. (1990). Functional architecture of basal ganglia circuits: neural substrated of parallel processing. *Trends in Neuroscience*, *13*(7), 266–271.
- Allegra, C. J., Jessup, J. M., Somerfield, M. R., Hamilton, S. R., Hammond, E. H., Hayes, D. F., ... Schilsky, R. L. (2009). American society of clinical oncology provisional clinical opinion: Testing for KRAS gene mutations in patients with metastatic colorectal carcinoma to predict response to anti-epidermal growth factor receptor monoclonal antibody therapy. *Journal of Clinical Oncology*, *27*(September 2006), 2091–2096. <http://doi.org/10.1200/JCO.2009.21.9170>
- Alsaleh, G., Sparsa, L., Chatelus, E., Ehlinger, M., Gottenberg, J.-E., Wachsmann, D., & Sibilia, J. (2010). Innate immunity triggers IL-32 expression by fibroblast-like synoviocytes in rheumatoid arthritis. *Arthritis Research & Therapy*, *12*(4), R135. <http://doi.org/10.1186/ar3073>
- Anand, P., Shenoy, R., Palmer, J. E., Baines, A. J., Lai, R. Y. K., Robertson, J., ... Chizh, B. a. (2011). Clinical trial of the p38 MAP kinase inhibitor diltmapimod in neuropathic pain following nerve injury. *European Journal of Pain*, *15*, 1040–1048. <http://doi.org/10.1016/j.ejpain.2011.04.005>
- Apfelbaum, J. L., Chen, C., Mehta, S. S., & Gan, and T. J. (2003). Postoperative Pain Experience: Results from a National Survey Suggest Postoperative Pain Continues to Be Undermanaged. *Anesthesia & Analgesia*. <http://doi.org/10.1213/01.ANE.0000068822.10113.9E>
- Apkarian, A. V., Baliki, M. N., & Geha, P. Y. (2009). Towards a theory of chronic pain. *Progress in Neurobiology*. <http://doi.org/10.1016/j.pneurobio.2008.09.018>
- Apkarian, A. V., & Hashmi, J. (2012). Pain and the brain: Specificity and plasticity of the brain in clinical chronic pain. *Changes*, *29*, 997–1003. <http://doi.org/10.1016/j.biotechadv.2011.08.021.Secreted>
- Apkarian, A. V., Krauss, B. R., Fredrickson, B. E., & Szeverenyi, N. M. (2001). Imaging the pain of low back pain: functional magnetic resonance imaging in combination with monitoring subjective pain perception allows the study of clinical pain states. *Neuroscience Letters*, *299*(1–2), 57–60. [http://doi.org/10.1016/S0304-3940\(01\)01504-X](http://doi.org/10.1016/S0304-3940(01)01504-X)
- Apkarian, A. V., Sosa, Y., Sonty, S., Levy, R. M., Harden, R. N., Parrish, T. B., & Gitelman, D. R. (2004). Chronic back pain is associated with decreased prefrontal and thalamic gray matter density. *The Journal of Neuroscience: The Official Journal of the Society for Neuroscience*, *24*, 10410–10415. <http://doi.org/10.1523/JNEUROSCI.2541-04.2004>
- Apkarian, A. V, Bushnell, M. C., Treede, R. D., & Zubieta, J. (2005). Human brain mechanisms of pain perception and regulation in health and disease. *European Journal of Pain (London, England)*, *9*, 463–484. Retrieved from

- papers://9bc3ccc5-d4d6-4a3c-9d0c-c415d2355c98/Paper/p1944
- Apley, J., Lloyd, J. K., & Turton, C. (1956). Electro-encephalography in children with recurrent abdominal pain. *Lancet*, *270*(6911), 264–5.
- Argoff, C. E. (2010). Clinical implications of opioid pharmacogenetics. *The Clinical Journal of Pain*, *26 Suppl 1*(1), S16–S20. <http://doi.org/10.1097/AJP.0b013e3181c49e11>
- Aronson, J. K. (2005). Biomarkers and surrogate endpoints. *British Journal of Clinical Pharmacology*, *59*, 491–494. <http://doi.org/10.1111/j.1365-2125.2005.02435.x>
- Ashburner, J., & Friston, K. (1997). Multimodal image coregistration and partitioning--a unified framework. *NeuroImage*, *6*(3), 209–217. <http://doi.org/10.1006/nimg.1997.0290>
- Ashburner, J., & Friston, K. J. (2000). Voxel-based morphometry--the methods. *NeuroImage*, *11*, 805–821. <http://doi.org/10.1006/nimg.2000.0582>
- Auer-Grumbach, M. (2008). Hereditary sensory neuropathy type I. *Orphanet Journal of Rare Diseases*, *3*(Hsn I), 7. <http://doi.org/10.1186/1750-1172-3-7>
- Bair, M. J., Wu, J., Damush, T. M., Sutherland, J. M., & Kroenke, K. (2008). Association of depression and anxiety alone and in combination with chronic musculoskeletal pain in primary care patients. *Psychosomatic Medicine*, *70*(8), 890–897. <http://doi.org/10.1097/PSY.0b013e318185c510>.Association
- Baraniuk, J. N., Whalen, G., Cunningham, J., & Clauw, D. J. (2004). *Cerebrospinal fluid levels of opioid peptides in fibromyalgia and chronic low back pain*. *BMC musculoskeletal disorders* (Vol. 5).
- Barden, J., Edwards, J. E., McQuay, H. J., & Moore, R. A. (2004). Pain and analgesic response after third molar extraction and other postsurgical pain. *Pain*. <http://doi.org/10.1016/j.pain.2003.09.021>
- Basbaum, A. I., & Fields, H. L. (1978). Endogenous pain control mechanisms: review and hypothesis. *Annals of Neurology*, *4*, 451–462. <http://doi.org/10.1002/ana.410040511>
- Beck, A. T., Steer, R. a., & Carbin, M. G. (1988). Psychometric properties of the Beck Depression Inventory: Twenty-five years of evaluation. *Clinical Psychology Review*, *8*, 77–100. [http://doi.org/10.1016/0272-7358\(88\)90050-5](http://doi.org/10.1016/0272-7358(88)90050-5)
- Belfer, I., Wu, T., Kingman, A., Krishnaraju, R. K., Goldman, D., & Max, M. B. (2004). Candidate Gene Studies of Human Pain Mechanisms. *Anesthesiology*, *100*(6), 1562–1572. <http://doi.org/10.1097/00000542-200406000-00032>
- Bengtsson, B., & Thorson, J. (1991). Back pain: a study of twins. *Acta Geneticae Medicae et Gemellologiae: Twin Research*, *40*(1), 83–90.
- Bennett, C. M., & Miller, M. B. (2010). How reliable are the results from functional magnetic resonance imaging? *Annals of the New York Academy of Sciences*. <http://doi.org/10.1111/j.1749-6632.2010.05446.x>
- Berger, H. (1938). Das Elektroenkephalogramm des Menschen. *Nova Acta Leopoldina*, *6*(38).
- Bingel, U., Gläscher, J., Weiller, C., & Büchel, C. (2004). Somatotopic representation of nociceptive information in the putamen: An event-related fMRI study. *Cerebral Cortex*, *14*(December), 1340–1345. <http://doi.org/10.1093/cercor/bhh094>
- Bland, J. M., & Altman, D. G. (1995). Calculating correlation coefficients with repeated observations: Part 1--Correlation within subjects. *BMJ (Clinical Research Ed.)*, *310*, 446. <http://doi.org/10.1136/bmj.310.6977.446>
- Bolstad, B. M., Bolstad, B. M., Irizarry, R. a, Irizarry, R. a, □Strand, M., □Strand, M., ... Speed, T. P. (2003). A comparison of normalization methods for high density oligonucleotide array data based on variance and bias. *Bioinformatics*, *19*(2), 185–193.

- Bond, C., LaForge, K. S., Tian, M., Melia, D., Zhang, S., Borg, L., ... Yu, L. (1998a). Single-nucleotide polymorphism in the human mu opioid receptor gene alters beta-endorphin binding and activity: possible implications for opiate addiction. *Proceedings of the National Academy of Sciences of the United States of America*, *95*, 9608–9613. <http://doi.org/10.1073/pnas.95.16.9608>
- Bond, C., LaForge, K. S., Tian, M., Melia, D., Zhang, S., Borg, L., ... Yu, L. (1998b). Single-nucleotide polymorphism in the human mu opioid receptor gene alters beta-endorphin binding and activity: possible implications for opiate addiction. *Proceedings of the National Academy of Sciences of the United States of America*, *95*(August), 9608–9613. <http://doi.org/10.1073/pnas.95.16.9608>
- Bonte, F. J. (1976). Nuclear Medicine Pioneer Citation, 1976: David E. Kuhl, M.D. *Journal of Nuclear Medicine*, *17*, 518–520.
- Born, R. T., & Bradley, D. C. (2005). Structure and function of visual area MT. *Annual Review of Neuroscience*, *28*, 157–189. <http://doi.org/10.1146/annurev.neuro.26.041002.131052>
- Borsook, D., Bleakman, D., Hargreaves, R., Upadhyay, J., Schmidt, K. F., & Becerra, L. (2008). A “BOLD” experiment in defining the utility of fMRI in drug development. *NeuroImage*, *42*(2), 461–6. <http://doi.org/10.1016/j.neuroimage.2008.04.268>
- Borsook, D., Moulton, E. a, Schmidt, K. F., & Becerra, L. R. (2007). Neuroimaging revolutionizes therapeutic approaches to chronic pain. *Molecular Pain*, *3*(ii), 25. <http://doi.org/10.1186/1744-8069-3-25>
- Boyle, W. J., Simonet, W. S., & Lacey, D. L. (2003). Osteoclast differentiation and activation. *Nature*, *423*(6937), 337–42. <http://doi.org/10.1038/nature01658>
- Bradshaw, D. H., Nakamura, Y., & Chapman, C. R. (2005). National Institutes of Health grant awards for pain, nausea, and dyspnea research: an assessment of funding patterns in 2003. *Journal of Pain*, *6*, 277–293.
- Brentani, R. R., Carraro, D. M., Verjovski-Almeida, S., Reis, E. M., Neves, E. J., De Souza, S. J., ... Reis, L. F. L. (2005). Gene expression arrays in cancer research: Methods and applications. *Critical Reviews in Oncology/Hematology*, *54*, 95–105. <http://doi.org/10.1016/j.critrevonc.2004.12.006>
- Brideau, C., Kargman, S., Liu, S., Dallob, a. L., Ehrich, E. W., Rodger, I. W., & Chan, C. C. (1996). A human whole blood assay for clinical evaluation of biochemical efficacy of cyclooxygenase inhibitors. *Inflammation Research*, *45*, 68–74. <http://doi.org/10.1007/BF02265118>
- Brooks, J., & Tracey, I. (2005). From nociception to pain perception: Imaging the spinal and supraspinal pathways. *Journal of Anatomy*. <http://doi.org/10.1111/j.1469-7580.2005.00428.x>
- Buckner, R. L., Andrews-Hanna, J. R., & Schacter, D. L. (2008). The Brain’s Default Network: Anatomy, Function, and Relevance to Disease. *Annals of the New York Academy of Sciences*, *1124*(1), 1–38. <http://doi.org/10.1196/annals.1440.011>
- Bullmore, E. T., Suckling, J., Overmeyer, S., Rabe-Hesketh, S., Taylor, E., & Brammer, M. J. (1999). Global, voxel, and cluster tests, by theory and permutation, for a difference between two groups of structural MR images of the brain. *IEEE Transactions on Medical Imaging*, *18*, 32–42. <http://doi.org/10.1109/42.750253>
- Bunge, M. (1963). A General Black Box Theory. *Philosophy of Science*, *30*(4), 346. <http://doi.org/10.1086/287954>
- Burr, M. L., Naseem, H., Hinks, A., Eyre, S., Gibbons, L. J., Bowes, J., ... Barton, A. (2010). PADI4 genotype is not associated with rheumatoid arthritis in a large UK Caucasian population. *Annals of the Rheumatic Diseases*, *69*, 666–670.

- <http://doi.org/10.1136/ard.2009.111294>
- Busch-Dienstfertig, M., & Stein, C. (2010). Opioid receptors and opioid peptide-producing leukocytes in inflammatory pain - Basic and therapeutic aspects. *Brain, Behavior, and Immunity*, 24(5), 683–694. <http://doi.org/10.1016/j.bbi.2009.10.013>
- Buse, D. C., Manack, a, Serrano, D., Turkel, C., & Lipton, R. B. (2010). Sociodemographic and comorbidity profiles of chronic migraine and episodic migraine sufferers. *Journal of Neurology, Neurosurgery, and Psychiatry*, 81, 428–432. <http://doi.org/10.1136/jnnp.2009.192492>
- Butler, R. W., Damarin, F. L., Beaulieu, C., Schwebel, A. I., & et al. (1989). Assessing cognitive coping strategies for acute postsurgical pain. *Psychological Assessment*. <http://doi.org/10.1037//1040-3590.1.1.41>
- Büttner, J. (1997). Diagnostic validity as a theoretical concept and as a measurable quantity. *Clinica Chimica Acta*, 260(April 1995), 131–143. [http://doi.org/10.1016/S0009-8981\(96\)06491-1](http://doi.org/10.1016/S0009-8981(96)06491-1)
- Caceres, A., Hall, D. L., Zelaya, F. O., Williams, S. C. R., & Mehta, M. A. (2009). Measuring fMRI reliability with the intra-class correlation coefficient. *NeuroImage*, 45, 758–768. <http://doi.org/10.1016/j.neuroimage.2008.12.035>
- Cahana, A., Carota, A., Montadon, M.-L., & Annoni, J. M. (2004). The Long-Term Effect of Repeated Intravenous Lidocaine on Central Pain and Possible Correlation in Positron Emission Tomography Measurements. *Anesthesia & Analgesia*, 1581–1584. <http://doi.org/10.1213/01.ANE.0000113258.31039.C8>
- Carr, E. C. J., Thomas, V. N., & Wilson-Barnet, J. (2005). Patient experiences of anxiety, depression and acute pain after surgery: A longitudinal perspective. *International Journal of Nursing Studies*, 42(5), 521–530. <http://doi.org/10.1016/j.ijnurstu.2004.09.014>
- Carter, R. W. G., & Woodroffe, C. D. (1997). *Coastal Evolution: Late Quaternary Shoreline Morphodynamics*. Cambridge, UK: Cambridge University Press.
- Cauda, F., Sacco, K., D'Agata, F., Duca, S., Cocito, D., Geminiani, G., ... Isoardo, G. (2009). Low-frequency BOLD fluctuations demonstrate altered thalamocortical connectivity in diabetic neuropathic pain. *BMC Neuroscience*, 10, 138. <http://doi.org/10.1186/1471-2202-10-138>
- Cauda, F., Sacco, K., Duca, S., Cocito, D., D'Agata, F., Geminiani, G. C., & Canavero, S. (2009). Altered resting state in diabetic neuropathic pain. *PLoS One*, 4, e4542. <http://doi.org/10.1371/journal.pone.0004542>
- Çavuşoğlu, M., Pfeuffer, J., Uğurbil, K., & Uludağ, K. (2009). Comparison of pulsed arterial spin labeling encoding schemes and absolute perfusion quantification. *Magnetic Resonance Imaging*, 27, 1039–1045. <http://doi.org/10.1016/j.mri.2009.04.002>
- Spielberger, C. D. (1983). *Manual for the State-Trait Anxiety Inventory*. Palo Alto, CA: Consulting Psychologists' Press.
- Ceko, M., Bushnell, M. C., Fitzcharles, M. A., & Schweinhardt, P. (2013). Fibromyalgia interacts with age to change the brain. *NeuroImage: Clinical*, 3, 249–260. <http://doi.org/10.1016/j.nicl.2013.08.015>
- Chalovich, J. M., & Eisenberg, E. (2009). Molecular Roles of Cdk5 in Pain Signaling. *Drug Discovery Today Therapeutic Strategies*, 6(3), 105–111. <http://doi.org/10.1016/j.immuni.2010.12.017>. Two-stage
- Chapman, C. R., Casey, K. L., Dubner, R., Foley, K. M., Gracely, R. H., & Reading, a E. (1985). Pain measurement: an overview. *Pain*, 22, 1–31. [http://doi.org/10.1016/S0885-3924\(86\)80031-8](http://doi.org/10.1016/S0885-3924(86)80031-8)
- Chau, C. H., Chen, K.-Y., Deng, H.-T., Kim, K.-J., Hosoya, K., Terasaki, T., ... Ann,

- D. K. (2002). Coordinating Etk/Bmx activation and VEGF upregulation to promote cell survival and proliferation. *Oncogene*, *21*(57), 8817–8829. <http://doi.org/10.1038/sj.onc.1206032>
- Chen, a C., Dworkin, S. F., Haug, J., & Gehrig, J. (1989). Human pain responsivity in a tonic pain model: psychological determinants. *Pain*, *37*, 143–160. [http://doi.org/10.1016/0304-3959\(89\)90126-7](http://doi.org/10.1016/0304-3959(89)90126-7)
- Chen, L.-C., Elliott, R. A., & Ashcroft, D. M. (2004). Systematic review of the analgesic efficacy and tolerability of COX-2 inhibitors in post-operative pain control. *Journal of Clinical Pharmacy and Therapeutics*, *29*, 215–229. <http://doi.org/10.1111/j.1365-2710.2004.00558.x>
- Chen, Y., Wang, D. J. J., & Detre, J. A. (2011). Test-retest reliability of arterial spin labeling with common labeling strategies. *Journal of Magnetic Resonance Imaging*, *33*, 940–949. <http://doi.org/10.1002/jmri.22345>
- Chizh, B. A., Priestley, T., Rowbotham, M., & Schaffler, K. (2009). Predicting therapeutic efficacy - Experimental pain in human subjects. *Brain Research Reviews*. <http://doi.org/10.1016/j.brainresrev.2008.12.016>
- Chudler, E. H., & Dong, W. K. (1995). The role of the basal ganglia in nociception and pain. *Pain*, *60*, 3–38. [http://doi.org/10.1016/0304-3959\(94\)00172-B](http://doi.org/10.1016/0304-3959(94)00172-B)
- Churchill, F. B. (1974). William Johannsen and the genotype concept. *Journal of the History of Biology*, *7*(1), 5–30. <http://doi.org/10.1007/BF00179291>
- Coghill, R. C., McHaffie, J. G., & Yen, Y.-F. (2003). Neural correlates of interindividual differences in the subjective experience of pain. *Proceedings of the National Academy of Sciences of the United States of America*, *100*, 8538–8542. <http://doi.org/10.1073/pnas.1430684100>
- Coghill, R. C., Talbot, J. D., Evans, a C., Meyer, E., Gjedde, a, Bushnell, M. C., & Duncan, G. H. (1994). Distributed processing of pain and vibration by the human brain. *The Journal of Neuroscience: The Official Journal of the Society for Neuroscience*, *14*(7), 4095–4108.
- Comings, D. E., Dietz, G., Gade-Andavolu, R., Blake, H., Muhleman, D., Huss, M., ... MacMurray, J. P. (2000). Association of the neutral endopeptidase (MME) gene with anxiety. *Psychiatric Genetics*, *(10)*, 91–94.
- Cox, J. J., Reimann, F., Nicholas, A. K., Thornton, G., Roberts, E., Springell, K., ... Woods, C. G. (2006). An SCN9A channelopathy causes congenital inability to experience pain. *Nature*, *444*(December), 894–898. <http://doi.org/10.1038/nature05413>
- Craft, R. M., Mogil, J. S., & Maria Aloisi, A. (2004). Sex differences in pain and analgesia: The role of gonadal hormones. *European Journal of Pain*, *8*, 397–411. <http://doi.org/10.1016/j.ejpain.2004.01.003>
- Cruccu, G., Anand, P., Attal, N., Garcia-Larrea, L., Haanpaa, M., Jorum, E., ... Jensen, T. S. (2004). EFNS guidelines on neuropathic pain assessment. *European Journal of Neurology*, *11*, 153–162.
- Dai, W., Garcia, D., De Bazelaire, C., & Alsop, D. C. (2008). Continuous flow-driven inversion for arterial spin labeling using pulsed radio frequency and gradient fields. *Magnetic Resonance in Medicine*, *60*, 1488–1497. <http://doi.org/10.1002/mrm.21790>
- Davis, K. D., Kwan, C. L., Crawley, a P., & Mikulis, D. J. (1998). Functional MRI study of thalamic and cortical activations evoked by cutaneous heat, cold, and tactile stimuli. *Journal of Neurophysiology*, *80*, 1533–1546.
- Davis, K. D., & Moayed, M. (2013). Central mechanisms of pain revealed through functional and structural MRI. *Journal of Neuroimmune Pharmacology: The Official Journal of the Society on NeuroImmune Pharmacology*, *8*(3), 518–34.

- <http://doi.org/10.1007/s11481-012-9386-8>
- Davis, K. D., Racine, E., & Collett, B. (2012). Neuroethical issues related to the use of brain imaging: Can we and should we use brain imaging as a biomarker to diagnose chronic pain? *Pain*. <http://doi.org/10.1016/j.pain.2012.02.037>
- Day-Williams, A. G., & Zeggini, E. (2011). The effect of next-generation sequencing technology on complex trait research. *European Journal of Clinical Investigation*, *41*, 561–567. <http://doi.org/10.1111/j.1365-2362.2010.02437.x>
- De Leeuw, R., Albuquerque, R., Okeson, J., & Carlson, C. (2005). The contribution of neuroimaging techniques to the understanding of supraspinal pain circuits: Implications for orofacial pain. *Oral Surgery, Oral Medicine, Oral Pathology, Oral Radiology and Endodontology*, *100*, 308–314.
- Derbyshire, S. W. G. (2006). Burning questions about the brain in pain. *Pain*, *122*, 217–218. <http://doi.org/10.1016/j.pain.2006.02.031>
- Derbyshire, S. W. G., & Jones, A. K. P. (1998). Cerebral responses to a continual tonic pain stimulus measured using positron emission tomography. *Pain*, *76*, 127–135. [http://doi.org/10.1016/S0304-3959\(98\)00034-7](http://doi.org/10.1016/S0304-3959(98)00034-7)
- Derbyshire, S. W. G., Jones, A. K. P., Collins, M., Feinmann, C., & Harris, M. (1999). Cerebral responses to pain in patients suffering acute post-dental extraction pain measured by positron emission tomography (PET). *European Journal of Pain*, *3*, 103–113. <http://doi.org/10.1053/eujp.1998.0102>
- Derbyshire, S. W. G., Jones, A. K. P., Gyulai, F., Clark, S., Townsend, D., & Firestone, L. L. (1997). Pain processing during three levels of noxious stimulation produces differential patterns of central activity. *Pain*, *73*, 431–445. [http://doi.org/10.1016/S0304-3959\(97\)00138-3](http://doi.org/10.1016/S0304-3959(97)00138-3)
- Derbyshire, S. W., Jones, A. K., Devani, P., Friston, K. J., Feinmann, C., Harris, M., ... Frackowiak, R. S. (1994). Cerebral responses to pain in patients with atypical facial pain measured by positron emission tomography. *J Neurol Neurosurg Psychiatry*, *57*, 1166–1172. Retrieved from http://www.ncbi.nlm.nih.gov/entrez/query.fcgi?cmd=Retrieve&db=PubMed&dopt=Citation&list_uids=7931375 LK - Link%7Chttp://www.ncbi.nlm.nih.gov/entrez/query.fcgi?cmd=Retrieve&db=PubMed&dopt=Citation&list_uids=7931375 %7C
- Derogatis, L. (2005). *SCL-90-R Symptom Checklist Revised*. Minneapolis: NCS Pearson, Inc.
- Desai, S. P., Kojima, K., Vacanti, C. A., & Kodama, S. (2008). Lidocaine inhibits NIH-3T3 cell multiplication by increasing the expression of cyclin-dependent kinase inhibitor 1A (p21). *Anesthesia and Analgesia*, *107*(5), 1592–1597. <http://doi.org/10.1213/ane.0b013e3181844cef>
- Dessem, D., Moritani, M., & Ambalavanar, R. (2007). Nociceptive craniofacial muscle primary afferent neurons synapse in both the rostral and caudal brain stem. *Journal of Neurophysiology*, *98*, 214–223. <http://doi.org/10.1152/jn.00990.2006>
- Devlin, B., & Roeder, K. (1999). Genomic control for association studies. *Biometrics*, *55*(December), 997–1004. <http://doi.org/10.1111/j.0006-341X.1999.00997.x>
- Devlin, B., Roeder, K., & Wasserman, L. (2001). Genomic control, a new approach to genetic-based association studies. *Theoretical Population Biology*, *60*, 155–166. <http://doi.org/10.1006/tpbi.2001.1542>
- Devor, M. (2010). What are “Pain Genes”, and Why Are They Interesting? In J. S. Mogil (Ed.), *Pain 2010 - An Updated Review: Refresher Course Syllabus* (pp. 227–237). Seattle: IASP Press.
- Devor, M., & Raber, P. (1990). Heritability of symptoms in an experimental model of neuropathic pain. *Pain*, *42*, 51–67.

- Di Piero, V., Jones, A. K., Iannotti, F., Powell, M., Perani, D., Lenzi, G. L., & Frackowiak, R. S. (1991). Chronic pain: a PET study of the central effects of percutaneous high cervical cordotomy. *Pain*, *46*, 9–12. [http://doi.org/10.1016/0304-3959\(91\)90026-T](http://doi.org/10.1016/0304-3959(91)90026-T)
- Diatchenko, L., Nackley, A. G., Slade, G. D., Bhalang, K., Belfer, I., Max, M. B., ... Maixner, W. (2006). Catechol-O-methyltransferase gene polymorphisms are associated with multiple pain-evoking stimuli. *Pain*, *125*, 216–224. <http://doi.org/10.1016/j.pain.2006.05.024>
- Diatchenko, L., Slade, G. D., Nackley, A. G., Bhalang, K., Sigurdsson, A., Belfer, I., ... Maixner, W. (2005). Genetic basis for individual variations in pain perception and the development of a chronic pain condition. *Human Molecular Genetics*, *14*, 135–143. <http://doi.org/10.1093/hmg/ddi013>
- DiMasi, J. a., Hansen, R. W., & Grabowski, H. G. (2003). The price of innovation: New estimates of drug development costs. *Journal of Health Economics*, *22*, 151–185. [http://doi.org/10.1016/S0167-6296\(02\)00126-1](http://doi.org/10.1016/S0167-6296(02)00126-1)
- Downar, J., Mikulis, D. J., & Davis, K. D. (2003). Neural correlates of the prolonged salience of painful stimulation. *NeuroImage*, *20*, 1540–1551. [http://doi.org/10.1016/S1053-8119\(03\)00407-5](http://doi.org/10.1016/S1053-8119(03)00407-5)
- Draghici, S., Khatri, P., Eklund, A. C., & Szallasi, Z. (2006). Reliability and reproducibility issues in DNA microarray measurements. *Trends in Genetics: TIG*, *22*(2), 101–9. <http://doi.org/10.1016/j.tig.2005.12.005>
- Dray, A. (1995). Inflammatory mediators of pain. *British Journal of Anaesthesia*, *75*, 125–131. <http://doi.org/10.1093/bja/75.2.125>
- Drummond, M. F., Wilson, D. a., Kanavos, P., Ubel, P. a., & Rovira, J. (2007). Assessing the economic challenges posed by orphan drugs: A response to McCabe et al., *1*, 36–42. <http://doi.org/10.1017/S0266462307071024>
- Duong, T. Q., Yacoub, E., Adriany, G., Hu, X., Ugurbil, K., Vaughan, J. T., ... Kim, S. G. (2002). High-resolution, spin-echo BOLD, and CBF fMRI at 4 and 7 T. *Magnetic Resonance in Medicine*, *48*(4), 589–593. <http://doi.org/10.1002/mrm.10252>
- Dworkin, R. H., Turk, D. C., Farrar, J. T., Haythornthwaite, J. a., Jensen, M. P., Katz, N. P., ... Witter, J. (2005). Core outcome measures for chronic pain clinical trials: IMMPACT recommendations. *Pain*, *113*(September 2004), 9–19. <http://doi.org/10.1016/j.pain.2004.09.012>
- Eccleston, C., Palermo, T. M., de, C. W. A. C., Lewandowski, A., Morley, S., Fisher, E., & Law, E. (2012). Psychological therapies for the management of chronic and recurrent pain in children and adolescents. [Review][Update of Cochrane Database Syst Rev. 2009;(2):CD003968; PMID: 19370592]. *Cochrane Database of Systematic Reviews (Online)*. Retrieved from <http://ovidsp.ovid.com/ovidweb.cgi?T=JS&CSC=Y&NEWS=N&PAGE=fulltext&D=medl&AN=23235601%5Cnhttp://ovidsp.ovid.com/ovidweb.cgi?T=JS&CSC=Y&NEWS=N&PAGE=fulltext&D=emed11&AN=23235601>
- Eccleston, C., Williams, A. C. de C., & Morley, S. (2009). Psychological therapies for the management of chronic pain (excluding headache) in adults. *Cochrane Database of Systematic Reviews (Online)*, CD007407. <http://doi.org/10.1002/14651858.CD007407.pub2>
- Einarsdottir, E., Carlsson, A., Minde, J., Toolanen, G., Svensson, O., Solders, G., ... Holmberg, M. (2004). A mutation in the nerve growth factor beta gene (NGFB) causes loss of pain perception. *Human Molecular Genetics*, *13*(8), 799–805. <http://doi.org/10.1093/hmg/ddh096>
- Emerson, N. M., Zeidan, F., Lobanov, O. V., Hadsel, M. S., Martucci, K. T., Quevedo,

- A. S., ... Coghill, R. C. (2014). Pain sensitivity is inversely related to regional grey matter density in the brain. *Pain*, *155*(3), 566–73. <http://doi.org/10.1016/j.pain.2013.12.004>
- Engel, H., Steinert, H., Buck, a, Berthold, T., Huch Böni, R. a, & von Schulthess, G. K. (1996). Whole-body PET: physiological and artifactual fluorodeoxyglucose accumulations. *Journal of Nuclear Medicine: Official Publication, Society of Nuclear Medicine*, *37*(3), 441–446.
- Esmond, R. W. (2001). The patenting of tools for drug discovery and development. *Journal of Clinical Pharmacology, Suppl*, 112S–115S. <http://doi.org/10.1177/009127001773744260>
- Ettlin, D. A., Zhang, H., Lutz, K., Järman, T., Meier, D., Gallo, L. M., ... Palla, S. (2004). Cortical activation resulting from painless vibrotactile dental stimulation measured by functional magnetic resonance imaging (fMRI). *Journal of Dental Research*, *83*, 757–761. <http://doi.org/10.1177/154405910408301004>
- Fillingim, R. B. (2000). Sex, gender, and pain: women and men really are different. *Current Review of Pain*, *4*(1), 24–30.
- Fillingim, R. B., Kaplan, L., Staud, R., Ness, T. J., Glover, T. L., Campbell, C. M., ... Wallace, M. R. (2005). The A118G single nucleotide polymorphism of the mu-opioid receptor gene (OPRM1) is associated with pressure pain sensitivity in humans. *The Journal of Pain: Official Journal of the American Pain Society*, *6*, 159–167. <http://doi.org/10.1016/j.jpain.2004.11.008>
- Finan, P. H., Zautra, A. J., Davis, M. C., & Lemery-chalfant, K. (2011). Genetic Influences on the Dynamics of Pain and Affect in Fibromyalgia. *Health Psychology*, *29*(2), 134–142. <http://doi.org/10.1037/a0018647>.Genetic
- Fishbain, D. (2000). Evidence-based data on pain relief with antidepressants. *Annals of Medicine*, *32*, 305–316. <http://doi.org/10.3109/07853890008995932>
- Fleiss, J. L., Levin, B., & Paik, M. C. (2003). *Statistical Methods for Rates and Proportions*. Hoboken, New Jersey: Wiley & Sons, Inc.
- Flor, H., Behle, D. J., & Birbaumer, N. (1993). Assessment of pain-related cognitions in chronic pain patients. *Behaviour Research and Therapy*, *31*(1), 63–73. [http://doi.org/10.1016/0005-7967\(93\)90044-U](http://doi.org/10.1016/0005-7967(93)90044-U)
- Flor, H., Braun, C., Elbert, T., & Birbaumer, N. (1997). Extensive reorganization of primary somatosensory cortex in chronic back pain patients. *Neuroscience Letters*, *224*, 5–8. [http://doi.org/10.1016/S0304-3940\(97\)13441-3](http://doi.org/10.1016/S0304-3940(97)13441-3)
- Flores, C. M., & Mogil, J. S. (2001). The pharmacogenetics of analgesia: toward a genetically-based approach to pain management. *Pharmacogenomics*, *2*, 177–194. <http://doi.org/10.1517/14622416.2.3.177>
- Floyd, T. F., Ratcliffe, S. J., Wang, J., Resch, B., & Detre, J. A. (2003). Precision of the CASL-Perfusion MRI Technique for the Measurement of Cerebral Blood Flow in Whole Brain and Vascular Territories. *Journal of Magnetic Resonance Imaging*, *18*, 649–655. <http://doi.org/10.1002/jmri.10416>
- Ford, D., Easton, D. F., Bishop, D. T., Narod, S. a., & Goldgar, D. E. (1994). Risks of cancer in BRCA1-mutation carriers. *Lancet*, *343*, 692–695. [http://doi.org/10.1016/S0140-6736\(94\)91578-4](http://doi.org/10.1016/S0140-6736(94)91578-4)
- Foster, A., Mobley, E., & Wang, Z. (2007). Complicated Pain Management in a CYP450 2D6 Poor Metabolizer. *Pain Practice*, *7*(4), 352–356.
- Fox, M. D., Snyder, A. Z., Vincent, J. L., Corbetta, M., Van Essen, D. C., & Raichle, M. E. (2005). The human brain is intrinsically organized into dynamic, anticorrelated functional networks. *Proceedings of the National Academy of Sciences of the United States of America*, *102*(27), 9673–8. <http://doi.org/10.1073/pnas.0504136102>

- Frampton, D., Kerr, J., Harrison, T. J., & Kellam, P. (2011). Assessment of a 44 gene classifier for the evaluation of chronic fatigue syndrome from peripheral blood mononuclear cell gene expression. *PLoS ONE*, *6*(3), 1–8. <http://doi.org/10.1371/journal.pone.0016872>
- Frank, R., & Hargreaves, R. (2003). Clinical biomarkers in drug discovery and development. *Nature Reviews. Drug Discovery*, *2*(July), 566–580. <http://doi.org/10.1038/nrd1130>
- Friebel, U., Eickhoff, S. B., & Lotze, M. (2011). Coordinate-based meta-analysis of experimentally induced and chronic persistent neuropathic pain. *NeuroImage*, *58*(4), 1070–80. <http://doi.org/10.1016/j.neuroimage.2011.07.022>
- Friston, K. J., Price, C. J., Fletcher, P., Moore, C., Frackowiak, R. S., & Dolan, R. J. (1996). The trouble with cognitive subtraction. *NeuroImage*, *4*, 97–104. <http://doi.org/10.1006/nimg.1996.0033>
- Galicia, J. C., Henson, B. R., Parker, J. S., & Khan, A. A. (2016). Gene expression profile of pulpitis. *Genes and Immunity*, *17*(4), 239–243. <http://doi.org/10.1038/gene.2016.14>
- Gandjakhch, F., Fajardy, I., Ferre, B., Dubucquoi, S., Flipo, R. M., Roger, N., & Solau-Gervais, E. (2009). A functional haplotype of PADI4 gene in rheumatoid arthritis: positive correlation in a French population. *Journal of Rheumatology*, *36*(5), 881–6.
- Ge, Y., Grossman, R. I., Babb, J. S., Rabin, M. L., Mannon, L. J., & Kolson, D. L. (2002). Age-related total gray matter and white matter changes in normal adult brain. Part I: volumetric MR imaging analysis. *AJNR. American Journal of Neuroradiology*, *23*(8), 1327–1333.
- Geisser, P. D. E. (1996). *Die Schmerzempfindungs-Skala (SES)*. Goettingen: Hogrefe Verlag GmbH & Co. KG.
- Gervil, M., Ulrich, V., Kyvik, K. O., Olesen, J., & Russell, M. B. (1999). Migraine without aura: A population-based twin study. *Annals of Neurology*, *46*, 606–611. [http://doi.org/10.1002/1531-8249\(199910\)46:4<606::AID-ANA8>3.0.CO;2-O](http://doi.org/10.1002/1531-8249(199910)46:4<606::AID-ANA8>3.0.CO;2-O)
- Gevers, S., Majoie, C. B. L. M., Van Den Tweel, X. W., Lavini, C., & Nederveen, A. J. (2009a). Acquisition time and reproducibility of continuous arterial spin-labeling perfusion imaging at 3T. *American Journal of Neuroradiology*, *30*, 968–971. <http://doi.org/10.3174/ajnr.A1454>
- Gevers, S., Majoie, C. B. L. M., Van Den Tweel, X. W., Lavini, C., & Nederveen, a. J. (2009b). Acquisition time and reproducibility of continuous arterial spin-labeling perfusion imaging at 3T. *American Journal of Neuroradiology*, *30*(5), 968–971. <http://doi.org/10.3174/ajnr.A1454>
- Gevers, S., van Osch, M. J., Bokkers, R. P. H., Kies, D. A., Teeuwisse, W. M., Majoie, C. B., ... Nederveen, A. J. (2011). Intra- and multicenter reproducibility of pulsed, continuous and pseudo-continuous arterial spin labeling methods for measuring cerebral perfusion. *Journal of Cerebral Blood Flow and Metabolism: Official Journal of the International Society of Cerebral Blood Flow and Metabolism*, *31*, 1706–1715. <http://doi.org/10.1038/jcbfm.2011.10>
- Gillet, J.-P., de Longueville, F., & Remacle, J. (2006). DualChip microarray as a new tool in cancer research. *Expert Review of Molecular Diagnostics*, *6*, 295–306. <http://doi.org/10.1586/14737159.6.3.295>
- Glover, G. H. (1999). Deconvolution of impulse response in event-related BOLD fMRI. *NeuroImage*, *9*(4), 416–429. <http://doi.org/10.1006/nimg.1998.0419>
- Gluud, L. L. (2006). Bias in clinical intervention research. *American Journal of Epidemiology*, *163*(6), 493–501. <http://doi.org/10.1093/aje/kwj069>
- Gommans, W. M., Haisma, H. J., & Rots, M. G. (2005). Engineering zinc finger

- protein transcription factors: The therapeutic relevance of switching endogenous gene expression on or off at command. *Journal of Molecular Biology*, 354(3), 507–519. <http://doi.org/10.1016/j.jmb.2005.06.082>
- Gonzalez, Y. M., Schiffman, E., Gordon, S. M., Seago, B., Truelove, E. L., Slade, G., & Ohrbach, R. (2011). Development of a brief and effective temporomandibular disorder pain screening questionnaire: reliability and validity. *Journal of the American Dental Association (1939)*, 142, 1183–91. Retrieved from <http://www.ncbi.nlm.nih.gov/pubmed/21965492>
- Gottesman, I. I., & Gould, T. D. (2003). The Endophenotype Concept in Psychiatry: Etymology and Strategic Intentions. *American Journal of Psychiatry*, 160, 636–645.
- Greenspan, J. D., Craft, R. M., LeResche, L., Arendt-Nielsen, L., Berkley, K. J., Fillingim, R. B., ... the Consensus Working Group of the Sex, Gender, and P. S. of the I. (2007). Studying sex and gender differences in pain and analgesia: A consensus report. *Pain, Supplement*, S26–S45.
- Gregersen, P. K., Amos, C. I., Lee, A. T., Lu, E., Elaine, F., Kastner, D. L., ... Siminovitch, K. A. (2009). REL, a member of the NF- κ B family of transcription factors, is a newly defined risk locus for rheumatoid arthritis. *Nature Genetics*, 41(7), 820–823. <http://doi.org/10.1038/ng.395.REL>
- Gulcher, J. R., Kong, a, & Stefansson, K. (2001). The role of linkage studies for common diseases. *Current Opinion in Genetics & Development*, 11, 264–267.
- Gündel, H., Valet, M., Sorg, C., Huber, D., Zimmer, C., Sprenger, T., & Tölle, T. R. (2008). Altered cerebral response to noxious heat stimulation in patients with somatoform pain disorder. *Pain*, 137, 413–421. <http://doi.org/10.1016/j.pain.2007.10.003>
- Halder, I., Shriver, M., Thomas, M., Fernandez, J. R., & Frudakis, T. (2008). A Panel of Ancestry Informative Markers for Estimating Individual Biogeographical Ancestry and Admixture From Four Continents: Utility and Applications. *Human Mutation*, 29(5), 648–658. <http://doi.org/10.1002/humu.20695>
- Hansson, P., Backonja, M., & Bouhassira, D. (2007). Usefulness and limitations of quantitative sensory testing: Clinical and research application in neuropathic pain states. *Pain*, 129, 256–259. <http://doi.org/10.1016/j.pain.2007.03.030>
- Hargreaves, K. M., Schmidt, E. a, Mueller, G. P., & Dionne, R. a. (1987). Dexamethasone alters plasma levels of beta-endorphin and postoperative pain. *Clinical Pharmacology and Therapeutics*, 42, 601–607. [http://doi.org/10.1016/0278-2391\(88\)90201-7](http://doi.org/10.1016/0278-2391(88)90201-7)
- Harper, P. S. (2005). William Bateson, human genetics and medicine. *Human Genetics*, 118, 141–151. <http://doi.org/10.1007/s00439-005-0010-3>
- Harris, R. E., Clauw, D. J., Scott, D. J., McLean, S. a, Gracely, R. H., & Zubieta, J.-K. (2007). Decreased central mu-opioid receptor availability in fibromyalgia. *The Journal of Neuroscience: The Official Journal of the Society for Neuroscience*, 27(37), 10000–6. <http://doi.org/10.1523/JNEUROSCI.2849-07.2007>
- Hastie, B. A., Riley, J. L., Kaplan, L., Herrera, D. G., Campbell, C. M., Virtusio, K., ... Fillingim, R. B. (2012). Ethnicity interacts with the OPRM1 gene in experimental pain sensitivity. *Pain*, 153, 1610–1619. <http://doi.org/10.1016/j.pain.2012.03.022>
- Hayasaka, S., & Nichols, T. E. (2003). Validating cluster size inference: Random field and permutation methods. *NeuroImage*, 20, 2343–2356. <http://doi.org/10.1016/j.neuroimage.2003.08.003>
- Head, H., & Holmes, G. (1911). Sensory disturbances from cerebral lesions. *Brain*, 34(102–254).
- Hermes, M., Hagemann, D., Britz, P., Lieser, S., Rock, J., Naumann, E., & Walter, C.

- (2007). Reproducibility of continuous arterial spin labeling perfusion MRI after 7 weeks. *Magnetic Resonance Materials in Physics, Biology and Medicine*, 20, 103–115. <http://doi.org/10.1007/s10334-007-0073-3>
- Hernandez-Avila, C. a, Wand, G., Luo, X., Gelernter, J., & Kranzler, H. R. (2003). Association between the cortisol response to opioid blockade and the Asn40Asp polymorphism at the mu-opioid receptor locus (OPRM1). *American Journal of Medical Genetics*, 118B(1), 60–5. <http://doi.org/10.1002/ajmg.b.10054>
- Herz, S. E. (1997). Don't test, do sell: legal implications of inclusion and exclusion of women in clinical drug trials. *Epilepsia*, 38 Suppl 4, S42-9. Retrieved from <http://www.ncbi.nlm.nih.gov/pubmed/9240240>
- Hill, R. (2000). NK1 (substance P) receptor antagonists - Why are they not analgesic in humans? *Trends in Pharmacological Sciences*, 21(July), 244–246. [http://doi.org/10.1016/S0165-6147\(00\)01502-9](http://doi.org/10.1016/S0165-6147(00)01502-9)
- Hillman-Jackson, J., Clements, D., Blankenberg, D., Taylor, J., Nekrutenko, A., & Team, G. (2007). Using Galaxy to Perform Large-Scale Interactive Data Analyses. *Current Protocols in Bioinformatics*, 1–77. <http://doi.org/10.1002/0471250953.bi1005s19.Using>
- Hodkinson, D. J., Khawaja, N., O'Daly, O., Thacker, M. a., Zelaya, F. O., Wooldridge, C. L., ... Howard, M. a. (2015a). Cerebral analgesic response to non-steroidal anti-inflammatory drug ibuprofen. *Pain*, 1. <http://doi.org/10.1097/j.pain.0000000000000176>
- Hodkinson, D. J., Khawaja, N., O'Daly, O., Thacker, M. A., Zelaya, F. O., Wooldridge, C. L., ... Howard, M. A. (2015b). Cerebral analgesic response to non-steroidal anti-inflammatory drug ibuprofen. *Pain*, April(3).
- Hodkinson, D. J., Veggeberg, R., Wilcox, S. L., Scrivani, S., Burstein, R., Becerra, L., & Borsook, D. (2015). Primary Somatosensory Cortices Contain Altered Patterns of Regional Cerebral Blood Flow in the Interictal Phase of Migraine. *Plos One*, 10(9), e0137971. <http://doi.org/10.1371/journal.pone.0137971>
- Holliday, R. (2006). Epigenetics: A historical overview. *Epigenetics*, 1(2), 76–80. <http://doi.org/10.4161/epi.1.2.2762>
- Howard, M. A., Krause, K., Khawaja, N., Massat, N., Zelaya, F., Schumann, G., ... Renton, T. F. (2011). Beyond patient reported pain: Perfusion magnetic resonance imaging demonstrates reproducible cerebral representation of ongoing post-surgical pain. *PLoS ONE*, 6(2).
- Howard, M. A., Sanders, D., Krause, K., O'Muircheartaigh, J., Fotopoulou, A., Zelaya, F., ... Williams, S. C. R. (2012). Alterations in resting-state regional cerebral blood flow demonstrate ongoing pain in osteoarthritis: An arterial spin-labeled magnetic resonance imaging study. *Arthritis and Rheumatism*, 64(12), 3936–46. <http://doi.org/10.1002/art.37685>
- Hsu, M. C., Harris, R. E., Sundgren, P. C., Welsh, R. C., Fernandes, C. R., Clauw, D. J., & Williams, D. A. (2009). No Consistent Difference in Gray Matter Volume between Individuals with Fibromyalgia and Age-Matched Healthy Subjects when Controlling for Affective Disorder. *Pain*, 143(3), 262–267. <http://doi.org/10.1111/j.1600-6143.2008.02497.x.Plasma>
- Huckins, D. S., Simon, H. K., Copeland, K., Spiro, D. M., Gogain, J., & Wandell, M. (2013). A novel biomarker panel to rule out acute appendicitis in pediatric patients with. *American Journal of Emergency Medicine*, 31(9), 1368–1375. <http://doi.org/10.1016/j.ajem.2013.06.016>
- Huehne, K., Schaal, U., Leis, S., Uebe, S., Gosso, M. F., van den Maagdenberg, A. M. J. M., ... Winterpacht, A. (2010). Lack of genetic association of neutral endopeptidase (NEP) with complex regional pain syndrome (CRPS).

- Neuroscience Letters*, 472, 19–23. <http://doi.org/10.1016/j.neulet.2010.01.044>
- Iannetti, G. D., & Mouraux, A. (2010). From the neuromatrix to the pain matrix (and back). *Experimental Brain Research*. <http://doi.org/10.1007/s00221-010-2340-1>
- Iannetti, G. D., Salomons, T. V., Moayed, M., Mouraux, A., & Davis, K. D. (2013). Beyond metaphor: contrasting mechanisms of social and physical pain. *Trends in Cognitive Sciences*, 17(8), 371–8. <http://doi.org/10.1016/j.tics.2013.06.002>
- Iannetti, G. D., Zambreanu, L., Wise, R. G., Buchanan, T. J., Huggins, J. P., Smart, T. S., ... Tracey, I. (2005). Pharmacological modulation of pain-related brain activity during normal and central sensitization states in humans. *Proceedings of the National Academy of Sciences of the United States of America*, 102(50), 18195–18200. <http://doi.org/10.1073/pnas.0506624102>
- Irizarry, R. a, Bolstad, B. M., Collin, F., Cope, L. M., Hobbs, B., & Speed, T. P. (2003). Summaries of Affymetrix GeneChip probe level data. *Nucleic Acids Research*, 31(4), e15. <http://doi.org/10.1093/nar/gng015>
- Irizarry, R. a, Hobbs, B., Collin, F., Beazer-Barclay, Y. D., Antonellis, K. J., Scherf, U., & Speed, T. P. (2003). Exploration, normalization, and summaries of high density oligonucleotide array probe level data. *Biostatistics (Oxford, England)*, 4, 249–264. <http://doi.org/10.1093/biostatistics/4.2.249>
- Bonica, J. (1953). *The Management of Pain*. Philadelphia: Lea & Febiger.
- Jääskeläinen, S. K., Rinne, J. O., Forssell, H., Tenovuo, O., Kaasinen, V., Sonninen, P., & Bergman, J. (2001). Role of the dopaminergic system in chronic pain - A fluorodopa-PET study. *Pain*, 90, 257–260. [http://doi.org/10.1016/S0304-3959\(00\)00409-7](http://doi.org/10.1016/S0304-3959(00)00409-7)
- Jacobsen, P. B., & Butler, R. W. (1996). Relation of cognitive coping and catastrophizing to acute pain and analgesic use following breast cancer surgery. *Journal of Behavioral Medicine*, 19(1), 17–29.
- Jahng, G.-H., Song, E., Zhu, X.-P., Matson, G. B., Weiner, M. W., & Schuff, N. (2005). Human brain: reliability and reproducibility of pulsed arterial spin-labeling perfusion MR imaging. *Radiology*, 234, 909–916. <http://doi.org/10.1148/radiol.2343031499>
- Jain, V., Duda, J., Avants, B., Giannetta, M., Xie, S. X., Roberts, T., ... Wang, D. J. J. (2012). Longitudinal Reproducibility and Accuracy of Pseudo-Continuous Arterial Spin-labeled Perfusion MR Imaging in Typically Developing Children. *Radiology*. <http://doi.org/10.1148/radiol.12111509>
- James, S. (2013). Human pain and genetics: some basics. *British Journal of Pain*, 7, 171–178. <http://doi.org/10.1177/2049463713506408>
- Jantsch, H. H. F., Kempainen, P., Ringler, R., Handwerker, H. O., & Forster, C. (2005). Cortical representation of experimental tooth pain in humans. *Pain*, 118, 390–399. <http://doi.org/10.1016/j.pain.2005.09.017>
- Jensen, M. P., Karoly, P., & Braver, S. (1986). The measurement of clinical pain intensity: a comparison of six methods. *Pain*, 27, 117–126. [http://doi.org/10.1016/0304-3959\(86\)90228-9](http://doi.org/10.1016/0304-3959(86)90228-9)
- Ji, R.-R., Gereau, R. W., Malcangio, M., & Strichartz, G. R. (2009). MAP kinase and pain. *Brain Research Reviews*, 60(1), 135–148. <http://doi.org/10.1016/j.biotechadv.2011.08.021>. Secreted
- Jiang, L., Kim, M., Chodkowski, B., Donahue, M. J., Pekar, J. J., Van Zijl, P. C. M., & Albert, M. (2010). Reliability and reproducibility of perfusion MRI in cognitively normal subjects. *Magnetic Resonance Imaging*, 28, 1283–1289. <http://doi.org/10.1016/j.mri.2010.05.002>
- Jones, A. K. P., Watabe, H., Cunningham, V. J., & Jones, T. (2004). Cerebral decreases in opioid receptor binding in patients with central neuropathic pain

- measured by [¹¹C]diprenorphine binding and PET. *European Journal of Pain*, 8, 479–485. <http://doi.org/10.1016/j.ejpain.2003.11.017>
- Joosten, L. a B., Netea, M. G., Kim, S.-H., Yoon, D.-Y., Oppers-Walgreen, B., Radstake, T. R. D., ... van den Berg, W. B. (2006). IL-32, a proinflammatory cytokine in rheumatoid arthritis. *Proceedings of the National Academy of Sciences of the United States of America*, 103(9), 3298–3303. <http://doi.org/10.1073/pnas.0511233103>
- Joseph, E. K., & Levine, J. D. (2003). Sexual dimorphism in the contribution of protein kinase C isoforms to nociception in the streptozotocin diabetic rat. *Neuroscience*, 120, 907–913. [http://doi.org/10.1016/S0306-4522\(03\)00400-7](http://doi.org/10.1016/S0306-4522(03)00400-7)
- Juhl, G. I., Jensen, T. S., Norholt, S. E., & Svensson, P. (2008). Central sensitization phenomena after third molar surgery: A quantitative sensory testing study. *European Journal of Pain*, 12, 116–127. <http://doi.org/10.1016/j.ejpain.2007.04.002>
- Jung, a C., Staiger, T., & Sullivan, M. (1997). The efficacy of selective serotonin reuptake inhibitors for the management of chronic pain. *Journal of General Internal Medicine*, 12, 384–389.
- Kalow, W. (2006). Pharmacogenetics and pharmacogenomics: origin, status, and the hope for personalized medicine. *The Pharmacogenomics Journal*, 6(November 2005), 162–165. <http://doi.org/10.1038/sj.tpj.6500361>
- Katz, J., & Melzack, R. (1999). Measurement of pain. *Surgical Clinics of North America*. [http://doi.org/10.1016/S0039-6109\(05\)70381-9](http://doi.org/10.1016/S0039-6109(05)70381-9)
- Kearney, P. M., Baigent, C., Godwin, J., Halls, H., Emberson, J. R., & Patrono, C. (2006). Do selective cyclo-oxygenase-2 inhibitors and traditional non-steroidal anti-inflammatory drugs increase the risk of atherothrombosis? Meta-analysis of randomised trials. *BMJ (Clinical Research Ed.)*, 332, 1302–1308. <http://doi.org/10.1136/bmj.332.7553.1302>
- Keller, P. J., Schmidt, A. D., Wittbrodt, J., & Stelzer, E. H. K. (2008). Reconstruction of zebrafish early embryonic development by scanned light sheet microscopy. *Science (New York, N.Y.)*, 322(November), 1065–1069. <http://doi.org/10.1126/science.1162493>
- Kerr, J. R. (2008). Gene profiling of patients with chronic fatigue syndrome/myalgic encephalomyelitis. *Current Rheumatology Reports*, 10(6), 482–491. <http://doi.org/10.1007/s11926-008-0079-5>
- Kesavapany, S., Lau, K.-F., Ackerley, S., Banner, S. J., Shemilt, S. J. a, Cooper, J. D., ... Miller, C. C. J. (2003). Identification of a novel, membrane-associated neuronal kinase, cyclin-dependent kinase 5/p35-regulated kinase. *The Journal of Neuroscience: The Official Journal of the Society for Neuroscience*, 23(12), 4975–83. <http://doi.org/23/12/4975> [pii]
- Kim, H., & Lee, H. (2009). GWAS of acute postsurgical pain in humans. *Pharmacogenomics*, 171–179.
- Kim, H., Lee, H., Rowan, J., Brahim, J., & Dionne, R. a. (2006). Genetic polymorphisms in monoamine neurotransmitter systems show only weak association with acute post-surgical pain in humans. *Molecular Pain*, 2, 24. <http://doi.org/10.1186/1744-8069-2-24>
- Kim, H., Mittal, D. P., Iadarola, M. J., & Dionne, R. a. (2006). Genetic predictors for acute experimental cold and heat pain sensitivity in humans. *Journal of Medical Genetics*. <http://doi.org/10.1136/jmg.2005.036079>
- Kim, H., Ramsay, E., Lee, H., Wahl, S., & Dionne, R. A. (2009). Genome-wide association study of acute post-surgical pain in humans. *Pharmacogenomics*, 10(2), 171–179. <http://doi.org/10.2217/14622416.10.2.171>. Genome-wide

- Klapa, M. I., & Quackenbush, J. (2003). The Quest for the Mechanisms of Life. *Biotechnology and Bioengineering*, *84*, 739–742. <http://doi.org/10.1002/bit.10858>
- Klomp, A., Caan, M. W. A., Denys, D., Nederveen, A. J., & Reneman, L. (2012). Feasibility of ASL-based pHMRI with a single dose of oral citalopram for repeated assessment of serotonin function. *NeuroImage*, *63*, 1695–1700. <http://doi.org/10.1016/j.neuroimage.2012.07.038>
- Knowler, W. C., Williams, R. C., Pettitt, D. J., & Steinberg, a G. (1988). Gm3;5,13,14 and type 2 diabetes mellitus: an association in American Indians with genetic admixture. *American Journal of Human Genetics*, *43*, 520–526.
- Kobayashi, Y., Kurata, J., Sekiguchi, M., Kokubun, M., Akaishizawa, T., Chiba, Y., ... Kikuchi, S. (2009). Augmented cerebral activation by lumbar mechanical stimulus in chronic low back pain patients: an FMRI study. *Spine*, *34*, 2431–2436. <http://doi.org/10.1097/BRS.0b013e3181b1fb76>
- Kupers, R., & Kehlet, H. (2006). Brain imaging of clinical pain states: a critical review and strategies for future studies. *Lancet Neurology*. [http://doi.org/10.1016/S1474-4422\(06\)70624-X](http://doi.org/10.1016/S1474-4422(06)70624-X)
- LaCroix-Fralish, M. L., Ledoux, J. B., & Mogil, J. S. (2007). The Pain Genes Database: An interactive web browser of pain-related transgenic knockout studies. *Pain*, *131*, 1–4. <http://doi.org/10.1016/j.pain.2007.04.041>
- Lafreniere, R. G., MacDonald, M. L. E., Dube, M.-P., MacFarlane, J., O'Driscoll, M., Brais, B., ... Samuels, M. E. (2004). Identification of a novel gene (HSN2) causing hereditary sensory and autonomic neuropathy type II through the Study of Canadian Genetic Isolates. *American Journal of Human Genetics*, *74*(Mim 256800), 1064–1073. <http://doi.org/10.1086/420795>
- Larsson, B., Bille, B., & Pedersen, N. L. (1995). Genetic influence in headaches: A Swedish Twin study. *Headache*, *35*, 513–519. <http://doi.org/10.1111/j.1526-4610.1995.hed3509513.x>
- Legrain, V., Iannetti, G. D., Plaghki, L., & Mouraux, A. (2011). The pain matrix reloaded: A salience detection system for the body. *Progress in Neurobiology*. <http://doi.org/10.1016/j.pneurobio.2010.10.005>
- Lesko, L. J., & Atkinson, A. J. (2001). Use of Biomarkers and Surrogate Endpoints in Drug Development and Regulatory Decision Making: Criteria, Validation, Strategies. *Annual Review of Pharmacology and Toxicology*, *41*, 347–366.
- Li, B.-Y., & Tun, X. (1990). Influence of morphine microinjected into head of caudate nucleus on electric activities of nociceptive neurons in parafascicular nucleus of rat thalamus. *Acta Pharmacologica Sinica*, *11*(2), 103–107.
- Lin, L.-D., Murray, G. M., & Sessle, B. J. (1993). The Effect of Bilateral Cold Block of the Primate Face Primary Somatosensory Cortex on the Performance of Trained Tongue-Protrusion Task and Biting Tasks. *Journal of Neurophysiology*, *70*(3), 985–996.
- Liu, J., Lan, L., Mu, J., Zhao, L., Yuan, K., Zhang, Y., ... Tian, J. (2015). Genetic contribution of catechol-O-methyltransferase in hippocampal structural and functional changes of female migraine sufferers. *Human Brain Mapping*, *0*(January), n/a-n/a. <http://doi.org/10.1002/hbm.22737>
- Lötsch, J., & Geisslinger, G. (2006). Relevance of frequent mu-opioid receptor polymorphisms for opioid activity in healthy volunteers. *The Pharmacogenomics Journal*, *6*(October 2005), 200–210. <http://doi.org/10.1038/sj.tpj.6500362>
- Lötsch, J., Geisslinger, G., & Tegeder, I. (2009a). Genetic modulation of the pharmacological treatment of pain. *Pharmacology and Therapeutics*, *124*(2), 168–184. <http://doi.org/10.1016/j.pharmthera.2009.06.010>
- Lötsch, J., Geisslinger, G., & Tegeder, I. (2009b). Genetic modulation of the

- pharmacological treatment of pain. *Pharmacology and Therapeutics*. <http://doi.org/10.1016/j.pharmthera.2009.06.010>
- Lötsch, J., Skarke, C., Grösch, S., Darimont, J., Schmidt, H., & Geisslinger, G. (2002). The polymorphism A118G of the human mu-opioid receptor gene decreases the pupil constrictory effect of morphine-6-glucuronide but not that of morphine. *Pharmacogenetics*, *12*, 3–9.
- Lötsch, J., Stuck, B., & Hummel, T. (2006). The human mu-opioid receptor gene polymorphism 118A > G decreases cortical activation in response to specific nociceptive stimulation. *Behavioral Neuroscience*, *120*(6), 1218–24. <http://doi.org/10.1037/0735-7044.120.6.1218>
- Lötsch, J., Zimmermann, M., Darimont, J., Marx, C., Dudziak, R., Skarke, C., & Geisslinger, G. Does the A118G polymorphism at the mu-opioid receptor gene protect against morphine-6-glucuronide toxicity?, *97Anesthesiology* 814–819 (2002). <http://doi.org/10.1097/00000542-200210000-00011>
- Luerding, R., Weigand, T., Bogdahn, U., & Schmidt-Wilcke, T. (2008). Working memory performance is correlated with local brain morphology in the medial frontal and anterior cingulate cortex in fibromyalgia patients: Structural correlates of pain-cognition interaction. *Brain*, *131*, 3222–3231. <http://doi.org/10.1093/brain/awn229>
- Luo, K., Yuan, J., Shan, Y., Li, J., Xu, M., Cui, Y., ... Yu, L. (2006). Activation of transcriptional activities of AP-1 and SRE by a new zinc finger protein ZNF641. *Biochemical and Biophysical Research Communications*, *339*(1–2), 1155–1164. <http://doi.org/10.1016/j.gene.2005.09.023>
- Luo, W., & Brouwer, C. (2013). Pathview: An R/Bioconductor package for pathway-based data integration and visualization. *Bioinformatics*, *29*(14), 1830–1831. <http://doi.org/10.1093/bioinformatics/btt285>
- Lutz, J., Jäger, L., De Quervain, D., Krauseneck, T., Padberg, F., Wichnalek, M., ... Schelling, G. (2008). White and gray matter abnormalities in the brain of patients with fibromyalgia: A diffusion-tensor and volumetric imaging study. *Arthritis and Rheumatism*, *58*(12), 3960–3969. <http://doi.org/10.1002/art.24070>
- Maarrawi, J., Peyron, R., Mertens, P., Costes, N., Magnin, M., Sindou, M., ... Garcia-Larrea, L. (2007). Differential brain opioid receptor availability in central and peripheral neuropathic pain. *Pain*, *127*, 183–194. <http://doi.org/10.1016/j.pain.2006.10.013>
- MacGregor, A. J., Griffiths, G. O., Baker, J., & Spector, T. D. (1997). Determinants of pressure pain threshold in adult twins: Evidence that shared environmental influences predominate. *Pain*, *73*, 253–257. [http://doi.org/10.1016/S0304-3959\(97\)00101-2](http://doi.org/10.1016/S0304-3959(97)00101-2)
- Maguire, E. a, Gadian, D. G., Johnsrude, I. S., Good, C. D., Ashburner, J., Frackowiak, R. S., & Frith, C. D. (2000). Navigation-related structural change in the hippocampi of taxi drivers. *Proceedings of the National Academy of Sciences of the United States of America*, *97*(8), 4398–4403. <http://doi.org/10.1073/pnas.070039597>
- Maihofner, C., Handwerker, H. O., Neundorfer, B., & Birklein, F. (2004). Cortical reorganization during recovery from complex regional pain syndrome. *Neurology*. <http://doi.org/10.1212/01.WNL.0000134661.46658.B0>
- Malats, N., & Calafell, F. (2003). Basic glossary on genetic epidemiology. *Journal of Epidemiology and Community Health*, *57*, 480–482. <http://doi.org/10.1136/jech.57.7.480>
- Maleki, N., Brawn, J., Barmettler, G., Borsook, D., & Becerra, L. (2013). Pain response measured with arterial spin labeling. *NMR in Biomedicine*, *26*, 664–

673. <http://doi.org/10.1002/nbm.2911>
- Malver, L. P., Brokjær, A., Staahl, C., Graversen, C., Andresen, T., & Drewes, A. M. (2014). Electroencephalography and analgesics. *British Journal of Clinical Pharmacology*, *77*, 72–95. <http://doi.org/10.1111/bcp.12137>
- Mardis, E. R. (2008). Next-generation DNA sequencing methods. *Annual Review of Genomics and Human Genetics*, *9*, 387–402. <http://doi.org/10.1146/annurev.genom.9.081307.164359>
- Marquand, A., Howard, M., Brammer, M., Chu, C., Coen, S., & Mourão-Miranda, J. (2010). Quantitative prediction of subjective pain intensity from whole-brain fMRI data using Gaussian processes. *NeuroImage*, *49*, 2178–2189. <http://doi.org/10.1016/j.neuroimage.2009.10.072>
- Martinsen, S., Flodin, P., Berrebi, J., Löfgren, M., Bileviciute-Ljungar, I., Ingvar, M., ... Kosek, E. (2014). Fibromyalgia Patients Had Normal Distraction Related Pain Inhibition but Cognitive Impairment Reflected in Caudate Nucleus and Hippocampus during the Stroop Color Word Test. *PLoS ONE*, *9*(10), e108637. <http://doi.org/10.1371/journal.pone.0108637>
- Max, M. B. (2000). Is mechanism-based pain treatment attainable? Clinical trial issues. *The Journal of Pain : Official Journal of the American Pain Society*, *1*(3), 2–9. <http://doi.org/10.1054/jpai.2000.9819>
- Max, M. B. (2008). Studying Common Genes that Contribute to Human Pain: An Introduction. In *Pain 2008 - An Updated Review: Refresher Course* (pp. 227–235). Seattle: IASP Press.
- Max, M. B., & Stewart, W. F. (2008a). The molecular epidemiology of pain: a New Discipline for Drug Discovery. *Nature Reviews. Drug Discovery*, *7*(august), 647–658.
- Max, M. B., & Stewart, W. F. (2008b). The molecular epidemiology of pain: a new discipline for drug discovery. *Nature Reviews. Drug Discovery*, *7*, 647–658. <http://doi.org/10.1038/nrd2595>
- May, A. (2008). Chronic pain may change the structure of the brain. *Pain*. <http://doi.org/10.1016/j.pain.2008.02.034>
- Mazzola, L., Isnard, J., Peyron, R., & Mauguire, F. (2012). Stimulation of the human cortex and the experience of pain: Wilder Penfield's observations revisited. *Brain*, *135*(2), 631–640. <http://doi.org/10.1093/brain/awr265>
- McCracken, L. M., Zayfert, C., & Gross, R. T. (1992). The pain anxiety symptoms scale: development and validation of a scale to measure fear of pain. *Pain*, *50*, 67–73. [http://doi.org/10.1016/0304-3959\(92\)90113-P](http://doi.org/10.1016/0304-3959(92)90113-P)
- McEwen, B. S., & Gianaros, P. J. (2011). Stress- and Allostasis-Induced Brain Plasticity. *Annual Review Medicine*, *62*, 431–445. <http://doi.org/10.1016/j.biotechadv.2011.08.021>. Secreted
- McHorney, C. A., Ware, J. E., & Raczek, A. E. (1993). The MOS 36-Item Short-Form Health Survey (SF-36): II. Psychometric and clinical tests of validity in measuring physical and mental health constructs. *Medical Care*, *31*, 247–263. <http://doi.org/10.2307/3765819>
- Mcneil, D. W. (1998). Development of the Fear of Pain Questionnaire — III. *Journal of Behavioral Medicine*, *21*(4), 389–410. <http://doi.org/10.1023/A:1018782831217>
- Mechelli, A., Price, C. J., Friston, K. J., & Ashburner, J. (2005). Voxel-based morphometry of the human brain: Methods and applications. *Current Medical Imaging Reviews*, *1*, 105–113. <http://doi.org/10.2174/1573405054038726>
- Melzack, R. (1975). The McGill pain questionnaire: major properties and scoring methods. *PAIN*, *1*, 277–299. [http://doi.org/10.1016/0304-3959\(75\)90044-5](http://doi.org/10.1016/0304-3959(75)90044-5)

- Melzack, R. (1999). From the gate to the neuromatrix. *Pain, Suppl* 6(1), S121–S126. [http://doi.org/10.1016/S0304-3959\(99\)00145-1](http://doi.org/10.1016/S0304-3959(99)00145-1)
- Melzack, R. (2001). Pain and the neuromatrix in the brain. *Journal of Dental Education*, 65, 1378–1382.
- Melzack, R. (2005). The McGill Pain Questionnaire. *Anesthesiology*, 103(1), 199–202. <http://doi.org/10.1097/00000542-200507000-00028>
- Melzack, R., & Casey, K. L. (1968). Sensory, motivational and central control determinants of chronic pain: A new conceptual model. In *The Skin Senses* (pp. 423–443). Charles C. Thomas.
- Mendel, G. (1866). *Versuche ueber Pflanzenhybriden. History*. Bruenn: Verhandlungen des Naturforschenden Vereins zu Brünn.
- Mersky, H., & Bogduk, N. (Eds.). (1994). Part III: Pain Terms, A Current List with Definitions and Notes on Usage. In *Classification of Chronic Pain* (Second Edition, pp. 209–214). Seattle: IASP Press.
- Metzker, M. L. (2010). Sequencing technologies - the next generation. *Nature Reviews. Genetics*, 11(1), 31–46. <http://doi.org/10.1038/nrg2626>
- Miezin, F. M., Maccotta, L., Ollinger, J. M., Petersen, S. E., & Buckner, R. L. (2000). Characterizing the hemodynamic response: effects of presentation rate, sampling procedure, and the possibility of ordering brain activity based on relative timing. *NeuroImage*, 11(6 Pt 1), 735–759. <http://doi.org/10.1006/nimg.2000.0568>
- Minde, J., Toolanen, G., Andersson, T., Nennesmo, I., Remahl, I. N., Svensson, O., & Solders, G. (2004). Familial insensitivity to pain (HSAN V) and a mutation in the NG2B gene. A neurophysiological and pathological study. *Muscle and Nerve*, 30(December), 752–760. <http://doi.org/10.1002/mus.20172>
- Mitsis, G. D., Iannetti, G. D., Smart, T. S., Tracey, I., & Wise, R. G. (2008). Regions of interest analysis in pharmacological fMRI: how do the definition criteria influence the inferred result? *NeuroImage*, 40(1), 121–32. <http://doi.org/10.1016/j.neuroimage.2007.11.026>
- Moayedi, M., Weissman-Fogel, I., Salomons, T. V., Crawley, A. P., Goldberg, M. B., Freeman, B. V., ... Davis, K. D. (2012). Abnormal gray matter aging in chronic pain patients. *Brain Research*, 1456, 82–93. <http://doi.org/10.1016/j.brainres.2012.03.040>
- Mogil, J. S. (2009). Animal models of pain: progress and challenges. *Nature Reviews. Neuroscience*, 10, 283–294. <http://doi.org/10.1038/nrn2606>
- Mogil, J. S. (2009). Are we getting anywhere in human pain genetics? *Pain*, 146, 231–232. <http://doi.org/10.1016/j.pain.2009.07.023>
- Mogil, J. S., & McCarter, K. E. (2000). Identifying pain genes: bottom-up and top-down approaches. *The Journal of Pain: Official Journal of the American Pain Society*, 1(3), 66–80. <http://doi.org/10.1054/jpai.2000.9821>
- Mogil, J. S., Wilson, S. G., Bon, K., Lee, S. E., Chung, K., Raber, P., ... Devor, M. (1999). Heritability of nociception II. “Types” of nociception revealed by genetic correlation analysis. *Pain*, 80, 83–93. [http://doi.org/10.1016/S0304-3959\(98\)00196-1](http://doi.org/10.1016/S0304-3959(98)00196-1)
- Mogil, J. S., Wilson, S. G., Chesler, E. J., Rankin, A. L., Nemmani, K. V. S., Lariviere, W. R., ... Fillingim, R. B. (2003). The melanocortin-1 receptor gene mediates female-specific mechanisms of analgesia in mice and humans. *Proceedings of the National Academy of Sciences of the United States of America*, 100(8), 4867–4872. <http://doi.org/10.1073/pnas.0730053100>
- Mogil, J. S., Yu, L., & Basbaum, A. I. (2000). Pain genes?: natural variation and transgenic mutants. *Annual Review of Neuroscience*, 23, 777–811.

- <http://doi.org/10.1146/annurev.neuro.23.1.777>
- Moncada, S., Ferreira, S. H., & Vane, J. R. (1975). Inhibition of Prostaglandin Biosynthesis as the Mechanism of Analgesia of Aspirin-Like Drugs in the Dog Knee Joint. *European Journal of Pharmacology*, *31*, 250–260. [http://doi.org/10.1016/0014-2999\(75\)90047-3](http://doi.org/10.1016/0014-2999(75)90047-3)
- Moore, R. A., Edwards, J. E., & McQuay, H. J. (2005). Acute pain: individual patient meta-analysis shows the impact of different ways of analysing and presenting results. *Pain*, *116*(3), 322–331.
- Moore, R. A., Gavaghan, D., Tramèr, M. R., Collins, S. L., & McQuay, H. J. (1998). Size is everything - Large amounts of information are needed to overcome random effects in estimating direction and magnitude of treatment effects. *Pain*, *78*, 209–216. [http://doi.org/10.1016/S0304-3959\(98\)00140-7](http://doi.org/10.1016/S0304-3959(98)00140-7)
- Mootha, V. K., Lindgren, C. M., Eriksson, K., Subramanian, A., Sihag, S., Lehar, J., ... Groop, L. C. (2003). PGC-1 α -responsive genes involved in oxidative phosphorylation are coordinately downregulated in human diabetes. *Nature Genetics*, *34*(3), 267–273. <http://doi.org/10.1038/nn1239>
- Morris-Yates, A., Talley, N. J., Boyce, P. M., Nandurkar, S., & Andrews, G. (1998). Evidence of a genetic contribution to functional bowel disorder. *American Journal of Gastroenterology*, *93*(8), 1311–1317. http://doi.org/10.1111/j.1572-0241.1998.440_j.x
- Moseley, G. L., & Flor, H. (2012). Targeting Cortical Representations in the Treatment of Chronic Pain: A Review. *Neurorehabilitation and Neural Repair*. <http://doi.org/10.1177/1545968311433209>
- Mountz, J. M., Bradley, L. a, Modell, J. G., Alexander, R. W., Triana-Alexander, M., Aaron, L. a, ... Mountz, J. D. (1995). Fibromyalgia in women. Abnormalities of regional cerebral blood flow in the thalamus and the caudate nucleus are associated with low pain threshold levels. *Arthritis and Rheumatism*, *38*(7), 926–938. <http://doi.org/10.1002/art.1780380708>
- Mura, E., Govoni, S., Racchi, M., Carossa, V., Ranzani, G. N., Allegri, M., & van Schaik, R. H. (2013). Consequences of the 118A>G polymorphism in the OPRM1 gene: translation from bench to bedside? *Journal of Pain Research*, *6*, 331–53. <http://doi.org/10.2147/JPR.S42040>
- Mutso, A. a, Radzicki, D., Baliki, M. N., Huang, L., Banisadr, G., Centeno, M. V, ... Apkarian, a V. (2012). Abnormalities in hippocampal functioning with persistent pain. *The Journal of Neuroscience: The Official Journal of the Society for Neuroscience*, *32*(17), 5747–56. <http://doi.org/10.1523/JNEUROSCI.0587-12.2012>
- Nash, P. G., Macefield, V. G., Klineberg, I. J., Murray, G. M., & Henderson, L. A. (2009). Differential activation of the human trigeminal nuclear complex by noxious and non-noxious orofacial stimulation. *Human Brain Mapping*, *30*, 3772–3782. <http://doi.org/10.1002/hbm.20805>
- Neely, G. G., Rao, S., Costigan, M., Mair, N., Racz, I., Milinkeviciute, G., ... Belfer, I. (2012). Construction of a Global Pain Systems Network Highlights Phospholipid Signaling as a Regulator of Heat Nociception. *PLoS Genetics*, *8*(12), e1003071. <http://doi.org/10.1371/journal.pgen.1003071>
- NICE/NHS. (2000). *Technology Appraisal Guidance No. 1 Guidelines for the Extraction of Wisdom Teeth*. London: National Institute for Clinical Excellence.
- Nichols, T. E., & Holmes, A. P. (2002). Nonparametric permutation tests for functional neuroimaging: a primer with examples. *Human Brain Mapping*, *15*, 1–25. <http://doi.org/10.1002/hbm.1058>
- Nieuwenhuys, R., Voogd, J., & Van Huijzen, C. (2008). *The Human Central Nervous*

- System*. Heidelberg: Springer Berlin Heidelberg.
- Nijman, I. J., Kuipers, S., Verheul, M., Guryev, V., & Cuppen, E. (2008). A genome-wide SNP panel for mapping and association studies in the rat. *BMC Genomics*, *9*, 95. <http://doi.org/10.1186/1471-2164-9-95>
- Nimnuan, C., Rabe-Hesketh, S., Wessely, S., & Hotopf, M. (2001). How many functional somatic syndromes? *Journal of Psychosomatic Research*, *51*, 549–557. [http://doi.org/10.1016/S0022-3999\(01\)00224-0](http://doi.org/10.1016/S0022-3999(01)00224-0)
- Norbury, T. A., MacGregor, A. J., Urwin, J., Spector, T. D., & McMahon, S. B. (2007). Heritability of responses to painful stimuli in women: A classical twin study. *Brain*, *130*, 3041–3049. <http://doi.org/10.1093/brain/awm233>
- Nussbaum, E. L., & Downes, L. (1998). Reliability of clinical pressure-pain algometric measurements obtained on consecutive days. *Physical Therapy*, *78*, 160–169. <http://doi.org/ptjournal.apta.org/content/78/2/160>
- Oertel, B. G., Preibisch, C., Wallenhorst, T., Hummel, T., Geisslinger, G., Lanfermann, H., & Loetsch, J. (2008). Differential Opioid Action on Sensory and Affective Cerebral Pain Processing. *Clinical Pharmacology and Therapeutics*, *83*(4), 577–588. <http://doi.org/10.1038/sj.clp>
- Oertel, B. G., Preibisch, C., Wallenhorst, T., Hummel, T., Geisslinger, G., Lanfermann, H., & Lötsch, J. (2008). Differential opioid action on sensory and affective cerebral pain processing. *Clinical Pharmacology and Therapeutics*, *83*, 577–588. <http://doi.org/10.1038/sj.clpt.6100441>
- Oertel, B., & Lötsch, J. (2008). Genetic mutations that prevent pain: implications for future pain medication. *Pharmacogenomics*, *9*, 179–194. <http://doi.org/10.2217/14622416.9.2.179>
- Ogawa, S., & Lee, T. (1990). Brain magnetic resonance imaging with contrast dependent on blood oxygenation. *Proceedings of the ...*, *87*(24), 9868–72. <http://doi.org/10.1073/pnas.87.24.9868>
- Ohrbach, R., & Gale, E. N. (1989a). Pressure pain thresholds, clinical assessment, and differential diagnosis: reliability and validity in patients with myogenic pain. *Pain*, *39*, 157–169. [http://doi.org/10.1016/0304-3959\(89\)90003-1](http://doi.org/10.1016/0304-3959(89)90003-1)
- Ohrbach, R., & Gale, E. N. (1989b). Pressure pain thresholds in normal muscles: reliability, measurement effects, and topographic differences. *Pain*, *37*, 257–263. [http://doi.org/10.1016/0304-3959\(89\)90189-9](http://doi.org/10.1016/0304-3959(89)90189-9)
- Olsen, M. B., Jacobsen, L. M., Schistad, E. I., Pedersen, L. M., Rygh, L. J., Roe, C., & Gjerstad, J. (2012). Pain intensity the first year after lumbar disc herniation is associated with the A118G polymorphism in the opioid receptor mu 1 gene: evidence of a sex and genotype interaction. *The Journal of Neuroscience*, *(32)*, 9831–9834. <http://doi.org/10.1523/JNEUROSCI.1742-12.2012>
- Owen, A., & Coleman, M. (2008). Functional neuroimaging of the vegetative state. *Nature Reviews Neuroscience*, *9*, 235–243. <http://doi.org/10.1038/nrn2330>
- Owen, D. G., Bureau, Y., Thomas, A. W., Prato, F. S., & Lawrence, K. S. S. (2008). Quantification of pain-induced changes in cerebral blood flow by perfusion MRI. *Pain*, *136*, 85–96. <http://doi.org/10.1016/j.pain.2007.06.021>
- Owen, D. G., Clarke, C. F., Bureau, Y., Ganapathy, S., Prato, F. S., & St. Lawrence, K. S. (2012). Measuring the neural response to continuous intramuscular infusion of hypertonic saline by perfusion MRI. *Journal of Magnetic Resonance Imaging*, *35*, 669–677. <http://doi.org/10.1002/jmri.22814>
- Owen, D. G., Clarke, C. F., Ganapathy, S., Prato, F. S., & St. Lawrence, K. S. (2010). Using perfusion MRI to measure the dynamic changes in neural activation associated with tonic muscular pain. *Pain*, *148*, 375–386. <http://doi.org/10.1016/j.pain.2009.10.003>

- Ozawa, S., Soyama, A., Saeki, M., Fukushima-Uesaka, H., Itoda, M., Koyano, S., ... Awada, J. S. (2004). Review Ethnic Differences in Genetic Polymorphisms of CYP2D6 , CYP2C19 , CYP3As and MDR1/ABCB1. *Drug Metabolism and Pharmacokinetics*, 19(2), 83–95.
- Paavonen, K., Ekamn, N., Wirzenius, M., Rajantie, I., Poutanen, M., & Alitalo, K. (2004). Bmx Tyrosine Kinase Transgene Induces Skin Hyperplasia, Inflammatory Angiogenesis, and Accelerated Wound Healing. *Molecular Biology of the Cell*, 15(1), 4226–4233. <http://doi.org/www.molbiolcell.org/cgi/doi/10.1091/mbc.E04-03-0241>.
- Palmer, C. D., Mutch, B. E., Page, T. H., Horwood, N. J., & Foxwell, B. M. J. (2008). Bmx regulates LPS-induced IL-6 and VEGF production via mRNA stability in rheumatoid synovial fibroblasts. *Biochemical and Biophysical Research Communications*, 370, 599–602. <http://doi.org/10.1016/j.bbrc.2008.03.142>
- Papworth, M., Kolasinska, P., & Minczuk, M. (2006). Designer zinc-finger proteins and their applications. *Gene*, 366(1), 27–38. <http://doi.org/10.1016/j.gene.2005.09.011>
- Pareek, T. K., Keller, J., Kesavapany, S., Pant, H. C., Iadarola, M. J., Brady, R. O., & Kulkarni, A. B. (2006). Cyclin-dependent kinase 5 activity regulates pain signaling. *Proceedings of the National Academy of Sciences of the United States of America*, 103(3), 791–796. <http://doi.org/10.1073/pnas.0510405103>
- Parkes, L. M., Rashid, W., Chard, D. T., & Tofts, P. S. (2004). Normal cerebral perfusion measurements using arterial spin labeling: reproducibility, stability, and age and gender effects. *Magn Reson Med*, 51, 736–743. <http://doi.org/10.1002/mrm.20023>
- Pasternak, G. W. (2010). Molecular insights into mu opioid pharmacology: From the clinic to the bench. *The Clinical Journal of Pain*, 26 Suppl 1, S3–S9. <http://doi.org/10.3109/03008200903019703>
- Penfield, W., & Boldrey, E. (1937). Somatic Motor and Sensory Representation in. *Brain: A Journal of Neurology*, 60, 389–443. <http://doi.org/10.1093/brain/60.4.389>
- Penfield, W., & Rasmussen, T. (1950). *The Cerebral Cortex of Man, A Clinical Study of Localization of Function*. New York: McMillan.
- Petersen, E. T., Mouridsen, K., & Golay, X. (2010). The QUASAR reproducibility study, Part II: Results from a multi-center Arterial Spin Labeling test-retest study. *NeuroImage*, 49, 104–113. <http://doi.org/10.1016/j.neuroimage.2009.07.068>
- Petersen, E. T., Zimine, I., Ho, Y. C. L., & Golay, X. (2006). Non-invasive measurement of perfusion: A critical review of arterial spin labelling techniques. *British Journal of Radiology*, 79, 688–701. <http://doi.org/10.1259/bjr/67705974>
- Peyron, R., Laurent, B., & García-Larrea, L. (2000). Functional imaging of brain responses to pain. A review and meta-analysis (2000). *Neurophysiologie Clinique = Clinical Neurophysiology*, 30, 263–88. [http://doi.org/10.1016/S0987-7053\(00\)00227-6](http://doi.org/10.1016/S0987-7053(00)00227-6)
- Petrokovski, J., & Massler, M. (1967). Alveolar ridge resorption following tooth extraction. *Journal of Prosthetic Dentistry*, 17(1), 21–7. [http://doi.org/10.1016/0022-3913\(67\)90046-7](http://doi.org/10.1016/0022-3913(67)90046-7)
- Plomin, R., & Crabbe, J. (2000). DNA. *Psychological Bulletin*. <http://doi.org/10.1037/0033-2909.126.6.806>
- Pogatzki-Zahn, E. M., Wagner, C., Meinhardt-Renner, A., Burgmer, M., Beste, C., Zahn, P. K., & Pfleiderer, B. (2010). *Coding of incisional pain in the brain: a functional magnetic resonance imaging study in human volunteers. Anesthesiology* (Vol. 112).

- Pogatzki-Zahn, E. M., Zahn, P. K., & Brennan, T. J. (2007). Postoperative pain-clinical implications of basic research. *Best Practice and Research: Clinical Anaesthesiology*. <http://doi.org/10.1016/j.bpa.2006.11.003>
- Pöpping, D. M., Zahn, P. K., Van Aken, H. K., Dasch, B., Boche, R., & Pogatzki-Zahn, E. M. (2008). Effectiveness and safety of postoperative pain management: A survey of 18 925 consecutive patients between 1998 and 2006 (2nd revision): A database analysis of prospectively raised data. *British Journal of Anaesthesia*, *101*, 832–840. <http://doi.org/10.1093/bja/aen300>
- Portenoy, R. K., & Hagen, N. A. (1990). Breakthrough pain: definition, prevalence and characteristics. *Pain*, *41*, 273–281.
- Price, D. (1999). *Psychological Mechanisms of Pain and Analgesia*. Seattle: IASP Press.
- Price, D., Bush, F., Long, S., & Harkins, S. (1994). A comparison of pain measurement characteristics of mechanical visual analog and simple numeric rating scales. *Pain*, *56*(1904), 217–226.
- Prichep, L. S., John, E. R., Howard, B., Merkin, H., & Hiesiger, E. M. (2011). Evaluation of the pain matrix using EEG source localization: a feasibility study. *Pain Med*, *12*, 1241–1248. <http://doi.org/10.1111/j.1526-4637.2011.01191.x>
- Purcell, S., Neale, B., Todd-Brown, K., Thomas, L., Ferreira, M. A. R., Bender, D., ... Sham, P. C. (2007). PLINK: a tool set for whole-genome association and population-based linkage analyses. *American Journal of Human Genetics*, *81*, 559–575. <http://doi.org/10.1086/519795>
- Raemaekers, M., Vink, M., Zandbelt, B., van Wezel, R. J. A., Kahn, R. S., & Ramsey, N. F. (2007). Test-retest reliability of fMRI activation during prosaccades and antisaccades. *NeuroImage*, *36*, 532–542. <http://doi.org/10.1016/j.neuroimage.2007.03.061>
- Raichle, M. E. (1998). Behind the scenes of functional brain imaging: a historical and physiological perspective. *Proceedings of the National Academy of Sciences of the United States of America*, *95*(3), 765–772. <http://doi.org/10.1073/pnas.95.3.765>
- Rainville, P., Feine, J. S., Bushnell, M. C., & Duncan, G. H. (1992). A psychophysical comparison of sensory and affective responses to four modalities of experimental pain. *Somatosensory & Motor Research*, *9*(4), 265–277. <http://doi.org/10.3109/08990229209144776>
- Ramasubbu, K., Gurm, H., & Litaker, D. (2001). Gender Bias in Clinical Trials: Do Double Standards Still Apply? *Journal of Women's Health and Gender-Based Medicine*, *10*(8), 757–764.
- Renton, T., Smeeton, N., & McGurk, M. (2001). Factors predictive of difficulty of mandibular third molar surgery. *British Dental Journal*, *190*, 607–610. <http://doi.org/10.1038/sj.bdj.4801052a>
- Rhead, B., Karolchik, D., Kuhn, R. M., Hinrichs, a. S., Zweig, a. S., Fujita, P. a., ... Kent, W. J. (2009). The UCSC Genome Browser database: update 2010. *Nucleic Acids Research*, *38*(Database), D613–D619. <http://doi.org/10.1093/nar/gkp939>
- Risch, N., & Merikangas, K. (1996). The future of genetic studies of complex human diseases. *Science (New York, N.Y.)*, *273*(September), 1516–1517. <http://doi.org/doi:10.1126/science.273.5281.1516>
- Roberts, S. B., MacLean, C. J., Neale, M. C., Eaves, L. J., & Kendler, K. S. (1999). Replication of linkage studies of complex traits: an examination of variation in location estimates. *American Journal of Human Genetics*, *65*(3), 876–884. <http://doi.org/10.1086/302528>

- Robinson, M. E., Craggs, J. G., Price, D. D., Perlstein, W. M., & Staud, R. (2011). Grey Matter Volumes of Pain Related Brain Areas are Decreased in Fibromyalgia Syndrome. *Journal of Pain*, *12*(4), 436–443. <http://doi.org/10.1016/j.jpain.2010.10.003>. Gray
- Robinson, M. E., Staud, R., & Price, D. D. (2013). Pain measurement and brain activity: Will neuroimages replace pain ratings? *Journal of Pain*, *14*, 323–327. <http://doi.org/10.1016/j.jpain.2012.05.007>
- Rodríguez-Muñoz, M., & Garzón, J. (2013). Nitric oxide and zinc-mediated protein assemblies involved in Mu opioid receptor signaling. *Molecular Neurobiology*, *48*(3), 769–782. <http://doi.org/10.1007/s12035-013-8465-z>
- Rodríguez-Raecke, R., Niemeier, A., Ihle, K., Ruether, W., & May, A. (2013a). Structural Brain Changes in Chronic Pain Reflect Probably Neither Damage Nor Atrophy. *PLoS ONE*, *8*. <http://doi.org/10.1371/journal.pone.0054475>
- Rodríguez-Raecke, R., Niemeier, A., Ihle, K., Ruether, W., & May, A. (2013b). Structural brain changes in chronic pain reflect probably neither damage nor atrophy. *PloS One*, *8*(2), e54475. <http://doi.org/10.1371/journal.pone.0054475>
- Rolke, R., Baron, R., Maier, C., Tölle, T. R., Treede, R. D., Beyer, A., ... Wasserka, B. (2006a). Quantitative sensory testing in the German Research Network on Neuropathic Pain (DFNS): Standardized protocol and reference values. *Pain*, *123*, 231–243. <http://doi.org/10.1016/j.pain.2006.01.041>
- Rolke, R., Baron, R., Maier, C., Tölle, T. R., Treede, R. D., Beyer, a., ... Wasserka, B. (2006b). Quantitative sensory testing in the German Research Network on Neuropathic Pain (DFNS): Standardized protocol and reference values. *Pain*, *123*, 231–243. <http://doi.org/10.1016/j.pain.2006.01.041>
- Rolke, R., Magerl, W., Campbell, K. A., Schalber, C., Caspari, S., Birklein, F., & Treede, R. D. (2006). Quantitative sensory testing: A comprehensive protocol for clinical trials. *European Journal of Pain*, *10*, 77–88. <http://doi.org/10.1016/j.ejpain.2005.02.003>
- Roques, B. P., Fournié-Zaluski, M.-C., & Wurm, M. (2012). Inhibiting the breakdown of endogenous opioids and cannabinoids to alleviate pain. *Nature Reviews Drug Discovery*, *11*(4), 292–310. <http://doi.org/10.1038/nrd3673>
- Rorden, C., & Brett, M. (2000). Stereotaxic display of brain lesions. *Behavioural Neurology*, *12*, 191–200. Retrieved from <http://www.ncbi.nlm.nih.gov/pubmed/11568431>
- Roses, A. D. (2000). Pharmacogenetics and future drug development and delivery. *Lancet*, *355*, 1358–1361. [http://doi.org/10.1016/S0140-6736\(00\)02126-7](http://doi.org/10.1016/S0140-6736(00)02126-7)
- Rosier, E. M., Iadarola, M. J., & Coghill, R. C. (2002). Reproducibility of pain measurement and pain perception. *Pain*, *98*, 205–216. [http://doi.org/10.1016/S0304-3959\(02\)00048-9](http://doi.org/10.1016/S0304-3959(02)00048-9)
- Roy, C. S., & Sherrington, C. S. (1890). On the Regulation of the Blood-supply of the Brain. *The Journal of Physiology*, *11*(1–2), 85–158.17. <http://doi.org/10.1152/japplphysiol.00257.2010>
- Ruiz, M. T., & Verbrugge, L. M. (1997). A two way view of gender bias in medicine. *Journal of Epidemiology and Community Health*, *51*, 106–109.
- Sanders, D., Krause, K., O’Muircheartaigh, J., Thacker, M. a., Huggins, J. P., Vennart, W., ... Howard, M. a. (2015). Pharmacologic Modulation of Hand Pain in Osteoarthritis: A Double-Blind Placebo-Controlled Functional Magnetic Resonance Imaging Study Using Naproxen. *Arthritis & Rheumatology*, *67*(3), 741–751. <http://doi.org/10.1002/art.38987>
- Schiavenato, M., & Craig, K. D. (2010). Pain assessment as a social transaction: Beyond the “gold standard.” *Clinical Journal of Pain*, *26*, 667–676.

- <http://doi.org/10.1097/AJP.0b013e3181e72507>
- Schmidt-Wilcke, T. (2008). Variations in brain volume and regional morphology associated with chronic pain. *Current Rheumatology Reports*, *10*(6), 467–474. <http://doi.org/10.1007/s11926-008-0077-7>
- Schmidt-Wilcke, T., Leinisch, E., Gänßbauer, S., Draganski, B., Bogdahn, U., Altmeppen, J., & May, A. (2006). Affective components and intensity of pain correlate with structural differences in gray matter in chronic back pain patients. *Pain*, *125*, 89–97. <http://doi.org/10.1016/j.pain.2006.05.004>
- Schmidt-Wilcke, T., Leinisch, E., Straube, A., Kämpfe, N., Draganski, B., Diener, H. C., ... May, A. (2005). Gray matter decrease in patients with chronic tension type headache. *Neurology*, *65*, 1483–1486. <http://doi.org/10.1212/01.wnl.0000183067.94400.80>
- Schmidt-Wilcke, T., Luerding, R., Weigand, T., Jürgens, T., Schuierer, G., Leinisch, E., & Bogdahn, U. (2007). Striatal grey matter increase in patients suffering from fibromyalgia--a voxel-based morphometry study. *Pain*, *132 Suppl*, S109–S116. <http://doi.org/10.1016/j.pain.2007.05.010>
- Schreiter, A., Gore, C., Labuz, D., Fournie-Zaluski, M. C., Roques, B. P., Stein, C., & Machelska, H. (2012). Pain inhibition by blocking leukocytic and neuronal opioid peptidases in peripheral inflamed tissue. *FASEB Journal*, *26*(12), 5161–5171. <http://doi.org/10.1096/fj.12-208678>
- Schropp, L., Wenzel, A., Kostopoulos, L., & Karring, T. (2003). Bone healing and soft tissue contour changes following single-tooth extraction: a clinical and radiographic 12-month prospective study. *The International Journal of Periodontics & Restorative Dentistry*, *23*(4), 313–23. <http://doi.org/10.1016/j.prosdent.2003.10.022>
- Schulz, E., Zherdin, A., Tiemann, L., Plant, C., & Ploner, M. (2012). Decoding an individual's sensitivity to pain from the multivariate analysis of EEG data. *Cerebral Cortex*, *22*, 1118–1123. <http://doi.org/10.1093/cercor/bhr186>
- Schweinhardt, P., & Bushnell, M. C. (2010). Pain imaging in health and disease--how far have we come? *The Journal of Clinical Investigation*, *120*, 3788–3797. <http://doi.org/10.1172/JCI43498>
- Shabalina, S. A., Zaykin, D. V., Gris, P., Ogurtsov, A. Y., Gauthier, J., Shibata, K., ... Diatchenko, L. (2009). Expansion of the human mu-opioid receptor gene architecture: novel functional variants. *Human Molecular Genetics*, *18*, 1037–1051. <http://doi.org/10.1093/hmg/ddn439>
- Shrout, P. E., & Fleiss, J. L. (1979). Intraclass correlations: uses in assessing rater reliability. *Psychological Bulletin*, *86*, 420–428. <http://doi.org/10.1037/0033-2909.86.2.420>
- Sikander, A., Rana, S. V., Sharma, S. K., Sinha, S. K., Arora, S. K., Prasad, K. K., & Singh, K. (2010). Association of alpha 2A adrenergic receptor gene (ADRA2A) polymorphism with irritable bowel syndrome, microscopic and ulcerative colitis. *Clinica Chimica Acta*, *411*(1–2), 59–63. <http://doi.org/10.1016/j.cca.2009.10.003>
- Sjöstrand, C., Duvefelt, K., Steinberg, A., Remahl, I. N., Waldenlind, E., & Hillert, J. (2006). Gene expression profiling in cluster headache: A pilot microarray study. *Headache*, *46*, 1518–1534. <http://doi.org/10.1111/j.1526-4610.2006.00611.x>
- Slade, G. D., Conrad, M., Diatchenko, L., Rashid, N., Zhong, S., Smith, S., ... Nackley, A. G. (2011). Cytokine Biomarkers and Chronic Pain: Association of Genes, Transcription, and Circulating Proteins with Temporomandibular Disorders and Widespread Palpation Tenderness. *Pain*, *152*(12), 2802–2812. <http://doi.org/10.1016/j.pain.2011.09.005>
- Smith, S. M., Jenkinson, M., Woolrich, M. W., Beckmann, C. F., Behrens, T. E. J.,

- Johansen-Berg, H., ... Matthews, P. M. (2004). Advances in functional and structural MR image analysis and implementation as FSL. *NeuroImage*, 23 Suppl 1, S208-19. <http://doi.org/10.1016/j.neuroimage.2004.07.051>
- Smith, S., & Maixner, D. (2012). Large candidate gene association study reveals genetic risk factors and therapeutic targets for fibromyalgia. *Arthritis & ...*, 64(2), 584–593. <http://doi.org/10.1002/art.33338>
- Sneider, W. (1997). The discovery of aspirin. *Pharmaceutical Journal*, 259(December), 614–617. <http://doi.org/10.1136/bmj.321.7276.1591>
- Solak, Ö., Erdoğan, M. Ö., Yıldız, H., Ulaşlı, A. M., Yaman, F., Terzi, E. S. A., ... Solak, M. (2014). Assessment of opioid receptor μ 1 gene A118G polymorphism and its association with pain intensity in patients with fibromyalgia. *Rheumatology International*, 1257–1261. <http://doi.org/10.1007/s00296-014-2995-1>
- Solak, O., Erdoğan, M. O., Yıldız, H., Ulaşlı, A. M., Yaman, F., Terzi, E. S. A., ... Solak, M. (2014). Assessment of opioid receptor μ 1 gene A118G polymorphism and its association with pain intensity in patients with fibromyalgia. *Rheumatology International*. <http://doi.org/10.1007/s00296-014-2995-1>
- Specht, K., Willmes, K., Shah, N. J., & Jancke, L. (2003). Assessment of reliability in functional imaging studies. *J Magn Reson Imaging*, 17, 463–471. Retrieved from http://www.ncbi.nlm.nih.gov/entrez/query.fcgi?cmd=Retrieve&db=PubMed&dopt=Citation&list_uids=12655586
- Spector, T. D., Cicuttini, F., Baker, J., Loughlin, J., & Hart, D. (1996). Genetic influences on osteoarthritis in women: a twin study. *BMJ (Clinical Research Ed.)*, 312, 940–943. <http://doi.org/10.1136/bmj.312.7036.940>
- Spencer, C. C., Su, Z., Donnelly, P., & Marchini, J. (2009). Designing genome-wide association studies: Sample size, power, imputation, and the choice of genotyping chip. *PLoS Genetics*, 5(5), 1–13. <http://doi.org/10.1371/journal.pgen.1000477>
- Sprenger, T., Berthele, A., Platzer, S., Boecker, H., & Tölle, T. R. (2005). What to learn from in vivo opioidergic brain imaging? *European Journal of Pain*, 9, 117–121. <http://doi.org/10.1016/j.ejpain.2004.07.010>
- Stamer, U. M., Zhang, L., & Stüber, F. (2010). Personalized therapy in pain management: where do we stand? *Pharmacogenomics*, 11, 843–864. <http://doi.org/10.2217/pgs.10.47>
- Starr, C. J., Sawaki, L., Wittenberg, G. F., Burdette, J. H., Oshiro, Y., Quevedo, A. S., ... Coghill, R. C. (2011). The contribution of the putamen to sensory aspects of pain: insights from structural connectivity and brain lesions. *Brain: A Journal of Neurology*, 134(Pt 7), 1987–2004. <http://doi.org/10.1093/brain/awr117>
- Steingrimsdóttir, O., Vøllestad, N., Røe, C., & Knardahl, S. (2004). Variation in reporting of pain and other subjective health complaints in a working population and limitations of single sample measurements. *Pain*, 110(1–2), 130–139.
- Sternbach, R. A. (1974). *Pain Patients: Traits and Treatment*. New York: Academic Press.
- Stevens, A. J., Jensen, J. J., Wyller, K., Kilgore, P. C., Chatterjee, S., & Rohrbaugh, M. L. (2011). The Role of Public-Sector Research in the Discovery of Drugs and Vaccines. *New England Journal of Medicine*, 364, 535–541. <http://doi.org/http://www.nejm.org/doi/full/10.1056/NEJMsa1008268>
- Stordeur, P., Zhou, L., Byl, B., Brohet, F., Burny, W., De Groote, D., ... Goldman, M. (2003). Immune monitoring in whole blood using real-time PCR. *Journal of Immunological Methods*, 276, 69–77. [http://doi.org/10.1016/S0022-1759\(03\)00074-7](http://doi.org/10.1016/S0022-1759(03)00074-7)

- Subramanian, A., Tamayo, P., & Mootha, V. (2014). GSEA: Gene set enrichment analysis Gene set enrichment analysis: A knowledge-based approach for interpreting genome-wide expression profiles. *Proceedings of the National Academy of Sciences of the United States of America*, *102*(43), 15545–15550.
- Sullivan, M. J. L., Bishop, S. R., & Pivik, J. (1995). The Pain Catastrophizing Scale : Development and Validation, *7*(4), 524–532.
- Szmyd, L., Shannon, I., & Mohnac, A. (1965). Control of postoperative sequelae in impacted third molar surgery. *Journal of Oral Therapy*, *21*, 491–496.
- Talbot, J. D., Marrett, S., Evans, a C., Meyer, E., Bushnell, M. C., & Duncan, G. H. (1991). Multiple representations of pain in human cerebral cortex. *Science (New York, N.Y.)*, *251*(4999), 1355–1358.
- Teepker, M., Peters, M., Vedder, H., Schepelmann, K., & Lautenbacher, S. (2010). Menstrual variation in experimental pain: Correlation with gonadal hormones. *Neuropsychobiology*, *61*, 131–140. <http://doi.org/10.1159/000279303>
- Than, M., Cullen, L., Reid, C. M., Lim, S. H., Aldous, S., Ardagh, M. W., ... Richards, a. M. (2011). A 2-h diagnostic protocol to assess patients with chest pain symptoms in the Asia-Pacific region (ASPECT): A prospective observational validation study. *The Lancet*, *377*(9771), 1077–1084. [http://doi.org/10.1016/S0140-6736\(11\)60310-3](http://doi.org/10.1016/S0140-6736(11)60310-3)
- The Wellcome Trust Case Control Consortium. (2007). Genome-wide association study of 14 , 000 cases of seven common diseases and 3 , 000 shared controls. *Nature*, *447*(7145), 661–678. <http://doi.org/10.1038/nature05911>. Genome-wide
- Thunberg, J., Lyskov, E., Korotkov, A., Ljubisavljevic, M., Pakhomov, S., Katayeva, G., ... Johansson, H. (2005). Brain processing of tonic muscle pain induced by infusion of hypertonic saline. *European Journal of Pain*, *9*, 185–194. <http://doi.org/10.1016/j.ejpain.2004.05.003>
- Tisserand, D. J., van Boxtel, M. P. J., Pruessner, J. C., Hofman, P., Evans, A. C., & Jolles, J. (2004). A voxel-based morphometric study to determine individual differences in gray matter density associated with age and cognitive change over time. *Cerebral Cortex*, *14*(September), 966–973. <http://doi.org/10.1093/cercor/bhh057>
- Tjandra, T., Brooks, J. C. W., Figueiredo, P., Wise, R., Matthews, P. M., & Tracey, I. (2005). Quantitative assessment of the reproducibility of functional activation measured with BOLD and MR perfusion imaging: Implications for clinical trial design. *NeuroImage*, *27*, 393–401. <http://doi.org/10.1016/j.neuroimage.2005.04.021>
- Tobler, A. R., Short, S., Andersen, M. R., Paner, T. M., Briggs, J. C., Lambert, S. M., ... Wenz, H. M. (2005). The SNPlex genotyping system: a flexible and scalable platform for SNP genotyping. *Journal of Biomolecular Techniques : JBT*, *16*, 398–406. <http://doi.org/10.1016/j.jbt.2005.04.001> [pii]
- Tracey, I. (2010). Getting the pain you expect: mechanisms of placebo, nocebo and reappraisal effects in humans. *Nature Medicine*, *16*, 1277–1283. <http://doi.org/10.1038/nm.2229>
- Tracey, I., & Bushnell, M. C. (2009a). How Neuroimaging Studies Have Challenged Us to Rethink: Is Chronic Pain a Disease? *Journal of Pain*. <http://doi.org/10.1016/j.jpain.2009.09.001>
- Tracey, I., & Bushnell, M. C. (2009b). How neuroimaging studies have challenged us to rethink: is chronic pain a disease? *The Journal of Pain : Official Journal of the American Pain Society*, *10*(11), 1113–20. <http://doi.org/10.1016/j.jpain.2009.09.001>
- Tracey, I., & Johns, E. (2010a). The pain matrix: Reloaded or reborn as we image

- tonic pain using arterial spin labelling. *Pain*, *148*, 359–360. <http://doi.org/10.1016/j.pain.2009.11.009>
- Tracey, I., & Johns, E. (2010b). The pain matrix: Reloaded or reborn as we image tonic pain using arterial spin labelling. *Pain*, *148*, 359–360.
- Treloar, S. a., Martin, N. G., & Heath, a. C. (1998). Longitudinal genetic analysis of menstrual flow, pain, and limitation in a sample of Australian twins. *Behavior Genetics*, *28*(2), 107–116. <http://doi.org/10.1023/A:1021419907305>
- Tsai, C.-A., Wang, S.-J., Chen, D.-T., & Chen, J. J. (2005). Sample size for gene expression microarray experiments. *Bioinformatics (Oxford, England)*, *21*(8), 1502–1508. <http://doi.org/10.1093/bioinformatics/bti162>
- Turk, D. C., Dworkin, R. H., Allen, R. R., Bellamy, N., Brandenburg, N., Carr, D. B., ... Witter, J. (2003). Core outcome domains for chronic pain clinical trials: IMMPACT recommendations. *Pain*, *106*, 337–345. <http://doi.org/10.1016/j.pain.2003.08.001>
- Turk, D. C., Flor, H., & Rudy, T. E. (1987). Pain and families. I. Etiology, maintenance, and psychosocial impact. *Pain*, *30*, 3–27.
- Ulett, G. A., D, E., & O'Leary, J. L. (1952). Survey of EEG findings in 1,000 patients with chief complaint of headache. *Electroencephalography and Clinical Neurophysiology*, *4*(4), 463–70.
- Ultsch, A., Kringel, D., Kalso, E., & Mogil, J. S. (2016). A data science approach to candidate gene selection of pain regarded as a process of learning and neural plasticity. *Pain*, *157*(12), 2747–2757.
- Vane, J. R. (1971). Inhibition of prostaglandin synthesis as a mechanism of action for aspirin-like drugs. *Nature: New Biology*, *231*, 232–235. <http://doi.org/10.1038/newbio231232a0>
- Vargas-Alarcón, G., Fragoso, J.-M., Cruz-Robles, D., Vargas, A., Vargas, A., Lao-Villadóniga, J.-I., ... Martínez-Lavín, M. (2007). Catechol-O-methyltransferase gene haplotypes in Mexican and Spanish patients with fibromyalgia. *Arthritis Research & Therapy*, *9*(5), R110. <http://doi.org/10.1186/ar2316>
- Vargas-Alarcón, G., Fragoso, J. M., Cruz-Robles, D., Vargas, A., Martinez, A., Lao-Villadóniga, J. I., ... Martínez-Lavín, M. (2009). Association of adrenergic receptor gene polymorphisms with different fibromyalgia syndrome domains. *Arthritis and Rheumatism*, *60*(7), 2169–2173. <http://doi.org/10.1002/art.24655>
- Venter, J. C., Adams, M. D., Myers, E. W., Li, P. W., Mural, R. J., Sutton, G. G., ... Zhu, X. (2001). The sequence of the human genome. *Science (New York, N.Y.)*, *291*(February), 1304–1351. <http://doi.org/10.1126/science.1058040>
- Victor, T. W., Jensen, M. P., Gammaitoni, A. R., Gould, E. M., White, R. E., & Galer, B. S. (2008). The Dimensions of Pain Quality: Factor Analysis of the Pain Quality Assessment Scale. *The Clinical Journal of Pain*. <http://doi.org/10.1097/AJP.0b013e31816b1058>
- Visser, E. J. (2006). Chronic post-surgical pain: Epidemiology and clinical implications for acute pain management. *Acute Pain*, *8*, 73–81. <http://doi.org/10.1016/j.acpain.2006.05.002>
- Vogt, B. A., Derbyshire, S., & Jones, A. K. P. (1996). Pain processing in four regions of human cingulate cortex localized with co-registered PET and MR imaging. *European Journal of Neuroscience*, *8*(February), 1461–1473. <http://doi.org/10.1111/j.1460-9568.1996.tb01608.x>
- Wada, T., Kobayashi, N., Takahashi, Y., Aoki, T., Watanabe, T., & Saitoh, S. (2002). Wide clinical variability in a family with a CACNA1A T666M mutation: Hemiplegic migraine, coma, and progressive ataxia. *Pediatric Neurology*, *26*(1), 47–50. [http://doi.org/10.1016/S0887-8994\(01\)00371-X](http://doi.org/10.1016/S0887-8994(01)00371-X)

- Wagner, K. J., Willoch, F., Kochs, E. F., Siessmeier, T., Tölle, T. R., Schwaiger, M., & Bartenstein, P. (2001). *Dose-dependent regional cerebral blood flow changes during remifentanyl infusion in humans: a positron emission tomography study*. *Anesthesiology* (Vol. 94).
- Walter, C., & Lötsch, J. (2009a). Meta-analysis of the relevance of the OPRM1 118A>G genetic variant for pain treatment. *Pain*, *146*, 270–275. <http://doi.org/10.1016/j.pain.2009.07.013>
- Walter, C., & Lötsch, J. (2009b). Meta-analysis of the relevance of the OPRM1 118A>G genetic variant for pain treatment. *Pain*, *146*(3), 270–5. <http://doi.org/10.1016/j.pain.2009.07.013>
- Wand, G. S., McCaul, M., Yang, X., Reynolds, J., Gotjen, D., Lee, S., & Ali, A. (2002). *The mu-opioid receptor gene polymorphism (A118G) alters HPA axis activation induced by opioid receptor blockade*. *Neuropsychopharmacology: official publication of the American College of Neuropsychopharmacology* (Vol. 26).
- Wang, G., Zhang, H., He, F., & Fang, X. (2006). Effect of the CYP2D6*10 C188T polymorphism on postoperative tramadol analgesia in a Chinese population. *European Journal of Clinical Pharmacology*, *62*, 927–931. <http://doi.org/10.1007/s00228-006-0191-2>
- Wang, X.-M., Wu, T.-X., Hamsa, M., Ramsay, E. S., Wahl, S. M., & Dionne, R. A. (2007). Rofecoxib modulates multiple gene expression pathways in a clinical model of acute inflammatory pain. *Pain*, *128*(1–2), 136–147.
- Wang, X., Wu, T., Hamza, M., Ramsay, E. S., Wahl, S. M., & Dionne, R. a. (2007). Rofecoxib modulates multiple gene expression pathways in a clinical model of acute inflammatory pain. *Pain*, *128*(1–2), 136–147.
- Wang, Z., Guo, Q., Wang, R., Xu, G., Li, P., Sun, Y., ... Wu, M. (2016). The D Domain of LRRC4 anchors ERK1/2 in the cytoplasm and competitively inhibits MEK/ERK activation in glioma cells. *Journal of Hematology & Oncology*, *9*(1), 130. <http://doi.org/10.1186/s13045-016-0355-1>
- Warburton, G., Nares, S., Angelov, N., Brahim, J. S., Dionne, R. a., & Wahl, S. M. (2005). Transcriptional events in a clinical model of oral mucosal tissue injury and repair. *Wound Repair and Regeneration*, *13*, 19–26. <http://doi.org/10.1111/j.1067-1927.2005.130104.x>
- Ware, J. E., & Sherbourne, C. D. (1992). The MOS 36-item Short Form Health Survey (SF-36). I. Conceptual framework and item selection. *Med Care*, *30*, 473–483.
- Wasan, A. D., Loggia, M. L., Chen, L. Q., Napadow, V., Kong, J., & Gollub, R. L. (2011). Neural correlates of chronic low back pain measured by arterial spin labeling. *Anesthesiology*, *115*, 364–374. <http://doi.org/10.1097/ALN.0b013e318220e880>
- Watson, J. B. (1913). Psychology as the Behaviorist Views It. *Psychological Review*, *20*, 158–177.
- Weigelt, A., Terekhin, P., Kemppainen, P., Dörfler, A., & Forster, C. (2010). The representation of experimental tooth pain from upper and lower jaws in the human trigeminal pathway. *Pain*, *149*, 529–538. <http://doi.org/10.1016/j.pain.2010.03.027>
- Weissman, M. M., Sholomskas, D., Pottenger, M., Prusoff, B. A., & Locke, B. Z. (1977). Assessing depressive symptoms in five psychiatric populations: a validation study. *American Journal of Epidemiology*, *106*, 203–214.
- Wenzel, R., Bartenstein, P., Dieterich, M., Danek, A., Weindl, A., Minoshima, S., ... Brandt, T. Deactivation of human visual cortex during involuntary ocular

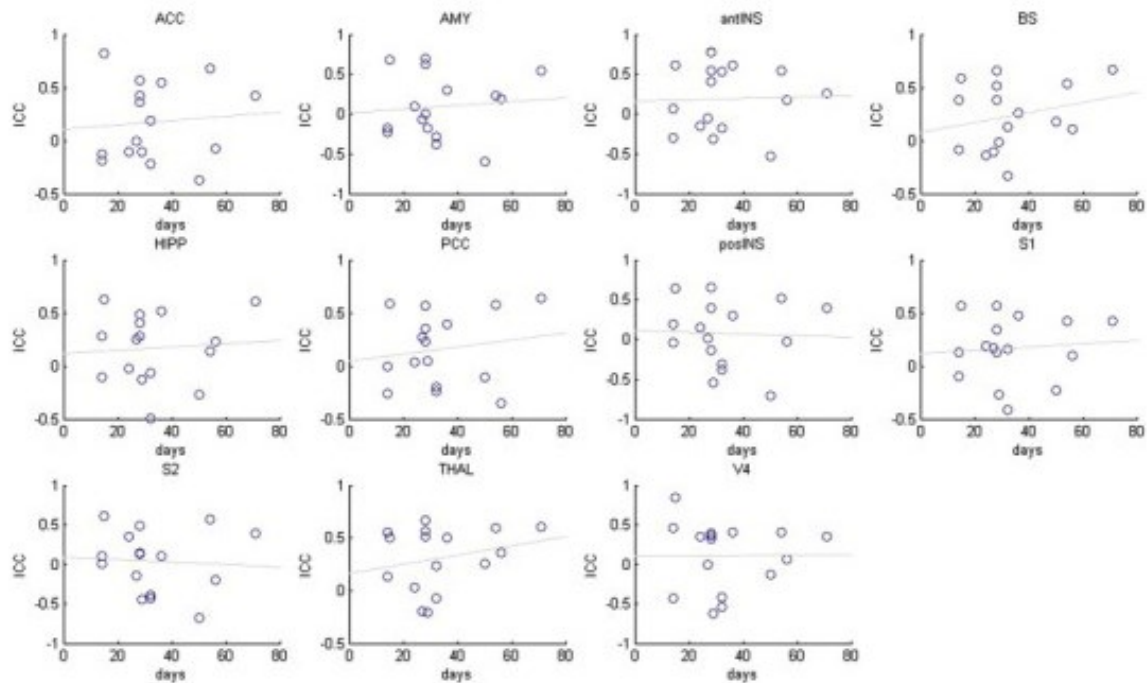
- oscillations. A PET activation study., 119 (Pt 1 Brain: a journal of neurology 101–110 (1996). <http://doi.org/10.1093/brain/119.1.101>
- Werber, a, & Schiltenswolf, M. (2012). [Chronic lower back pain]. *Der Nervenarzt*, 83(2), 243–57; quiz 258. <http://doi.org/10.1007/s00115-011-3421-5>
- Wey, H.-Y., Catana, C., Hooker, J. M., Dougherty, D. D., Knudsen, G. M., Wang, D. J. J., ... Kong, J. (2014). Simultaneous fMRI-PET of the opioidergic pain system in human brain. *NeuroImage*, 102, 275–282. <http://doi.org/10.1016/j.neuroimage.2014.07.058>
- WHO. (2010). *International Classification of Diseases 10th Revision*. Geneva: World Health Organization.
- Williams, D. S., Detre, J. A., Leigh, J. S., & Koretsky, A. P. (1992). Magnetic-Resonance-Imaging of Perfusion Using Spin Inversion of Arterial Water. *Proceedings of the National Academy of Sciences of the United States of America*, 89, 212–216. <http://doi.org/10.1073/pnas.89.1.212>
- Willoch, F., Schindler, F., Wester, H. J., Empl, M., Straube, A., Schwaiger, M., ... Tölle, T. R. (2004a). Central poststroke pain and reduced opioid receptor binding within pain processing circuitries: A [11C]diprenorphine PET study. *Pain*, 108, 213–220. <http://doi.org/10.1016/j.pain.2003.08.014>
- Willoch, F., Schindler, F., Wester, H. J., Empl, M., Straube, A., Schwaiger, M., ... Tölle, T. R. (2004b). Central poststroke pain and reduced opioid receptor binding within pain processing circuitries: a [11C]diprenorphine PET study. *Pain*, 108(3), 213–20. <http://doi.org/10.1016/j.pain.2003.08.014>
- Wing, J. K., Babor, T., Brugha, T., Burke, J., Cooper, J. E., Giel, R., ... Sartorius, N. (1990). SCAN. Schedules for Clinical Assessment in Neuropsychiatry. *Archives of General Psychiatry*, 47, 589–593. <http://doi.org/10.1001/archpsyc.1990.01810180089012>
- Wittgenstein, L. (2003). *Philosophische Untersuchungen* (Auflage: 6). Frankfurt am Main: Suhrkamp Verlag. Retrieved from http://www.amazon.de/Philosophische-Untersuchungen-Ludwig-Wittgenstein/dp/3518223720/ref=sr_1_1?s=books&ie=UTF8&qid=1422649131&sr=1-1&keywords=philosophische+untersuchungen
- Woda, A., Tubert-Jeannin, S., Bouhassira, D., Attal, N., Fleiter, B., Goulet, J. P., ... Albuissou, E. (2005). Towards a new taxonomy of idiopathic orofacial pain. *Pain*, 116, 396–406. <http://doi.org/10.1016/j.pain.2005.05.009>
- Wolfe, F., Clauw, D. J., Fitzcharles, M.-A., Goldenberg, D. L., Katz, R. S., Mease, P., ... Yunus, M. B. (2010). The American College of Rheumatology preliminary diagnostic criteria for fibromyalgia and measurement of symptom severity. *Arthritis Care & Research*, 62(5), 600–10. <http://doi.org/10.1002/acr.20140>
- Wolfe, F., Smythe, H. A., Yunus, M. B., Bennett, R. M., Bombardier, C., Goldenberg, D. L., ... Clark, P. (1990). The American College of Rheumatology 1990 Criteria for the Classification of Fibromyalgia. Report of the Multicenter Criteria Committee. *Arthritis and Rheumatism*, 33, 160–172. <http://doi.org/10.1002/art.1780330203>
- Wong, E. C. (2014). An introduction to ASL labeling techniques. *Journal of Magnetic Resonance Imaging*, 40(1), 1–10. <http://doi.org/10.1002/jmri.24565>
- Woodcock, J., Witter, J., & Dionne, R. A. (2007). Stimulating the development of mechanism-based, individualized pain therapies. *Nature Reviews. Drug Discovery*, 6, 703–710. <http://doi.org/10.1038/nrd2335>
- Woolf, C. J. (2004). Pain: Moving from Symptom Control toward Mechanism-Specific Pharmacologic Management. *Annals of Internal Medicine*, 140, 441–451. <http://doi.org/10.7326/0003-4819-140-8-200404200-00010>

- Woolf, C. J., Bennett, G. J., Doherty, M., Dubner, R., Kidd, B., Koltzenburg, M., ... Torebjork, E. (1998). Towards a mechanism-based classification of pain? *Pain*, *77*, 227–229. [http://doi.org/10.1016/S0304-3959\(98\)00099-2](http://doi.org/10.1016/S0304-3959(98)00099-2)
- Woolf, C. J., & Max, M. B. (2001). Mechanism-based pain diagnosis: issues for analgesic drug development. *Anesthesiology*, *95*(1), 241–249. <http://doi.org/10.1097/00000542-200107000-00034>
- Woolf Central Sensitization Pain and Plasticity. (n.d.).
- Worsley, K. J., Evans, A. C., Marrett, S., & Neelin, P. (1992). A three-dimensional statistical analysis for CBF activation studies in human brain. *J Cereb Blood Flow Metab*, *12*, 900–918. <http://doi.org/10.1038/jcbfm.1992.127>
- Wright, I. C., McGuire, P. K., Poline, J. B., Travere, J. M., Murray, R. M., Frith, C. D., ... Friston, K. J. (1995). A voxel-based method for the statistical analysis of gray and white matter density applied to schizophrenia. *NeuroImage*. <http://doi.org/10.1006/nimg.1995.1032>
- Xiao, Y., Jin, J., Chang, M., Chang, J., Hu, H., & Zhou, X. (2014). Peli1 promotes microglia-mediated CNS inflammation by regulating Traf3 degradation. *Nature Medicine*, *19*(5), 595–602. <http://doi.org/10.1038/nm.3111.Peli1>
- Xie, W. L., Chipman, J. G., Robertson, D. L., Erikson, R. L., & Simmons, D. L. (1991). Expression of a mitogen-responsive gene encoding prostaglandin synthase is regulated by mRNA splicing. *Proceedings of the National Academy of Sciences of the United States of America*, *88*(April), 2692–2696. <http://doi.org/10.1073/pnas.88.7.2692>
- Xu, G. F., Rowley, H. A., Wu, G. H., Alsop, D. C., Shankaranarayanan, A., Dowling, M., ... Johnson, S. C. (2010). Reliability and precision of pseudo-continuous arterial spin labeling perfusion MRI on 3.0 T and comparison with O-15-water PET in elderly subjects at risk for Alzheimer's disease. *Nmr in Biomedicine*, *23*, 286-293 ST-Reliability and precision of pseudo-. <http://doi.org/10.1002/nbm.1462>
- Xu, G., Rowley, H. A., Wu, G., Alsop, D. C., Shankaranarayanan, A., Dowling, M., ... Johnson, S. C. (2011). Reliability and Precision of Pseudo-continuous Arterial Spin Labeling Perfusion MRI on 3.0 T and Comparison with 15O-water PET in Elderly Subjects at Risk for Alzheimer's Disease. *NMR in Biomedicine*, *23*(3), 286–293. <http://doi.org/10.1002/nbm.1462.Reliability>
- Yarnitsky, D., Sprecher, E., Zaslansky, R., & Hemli, J. a. (1995). Heat pain thresholds: normative data and repeatability. *Pain*, *60*, 329–332. [http://doi.org/10.1016/0304-3959\(94\)00132-X](http://doi.org/10.1016/0304-3959(94)00132-X)
- Yen, Y. F., Field, A. S., Martin, E. M., Ari, N., Burdette, J. H., Moody, D. M., & Takahashi, A. M. (2002). Test-retest reproducibility of quantitative CBF measurements using FAIR perfusion MRI and acetazolamide challenge. *Magnetic Resonance in Medicine*, *47*, 921–928. <http://doi.org/10.1002/mrm.10140>
- Yu, M.-C., Huang, C.-M., Wu, M.-C., Wu, J.-Y., & Tsai, F.-J. (2004). Association of TAP2 gene polymorphisms in Chinese patients with rheumatoid arthritis. *Clinical Rheumatology*, *23*(2), 35–39. <http://doi.org/10.1007/s10067-003-0769-3>
- Yu, Y., Ricciotti, E., Scalia, R., Tang, S. Y., Grant, G., Yu, Z., ... Fitzgerald, G. A. (2012). Vascular COX-2 Modulates Blood Pressure and Thrombosis in Mice. *Science Translational Medicine*, *4*(132), 1–15. <http://doi.org/10.1126/scitranslmed.3003787.Vascular>
- Yunus, M. B. (2008). Central Sensitivity Syndromes: A New Paradigm and Group Nosology for Fibromyalgia and Overlapping Conditions, and the Related Issue of Disease versus Illness. *Seminars in Arthritis and Rheumatism*, *37*, 339–352.

- <http://doi.org/10.1016/j.semarthrit.2007.09.003>
- Zangen, A., Herzberg, U., Vogel, Z., & Yadid, G. (1998). Nociceptive stimulus induces release of endogenous beta-endorphin in the rat brain. *Neuroscience*, *85*, 659–662. [http://doi.org/S0306-4522\(98\)00050-5](http://doi.org/S0306-4522(98)00050-5) [pii]
- Zelaya, F. O., Zois, E., Christopher, M. P., Lythgoe, D. J., Lee, S., Andrews, C., ... Reed, L. J. (2012). The response to rapid infusion of fentanyl in the human brain measured using pulsed arterial spin labelling. *Magnetic Resonance Materials in Physics, Biology and Medicine*, *25*, 163–175. <http://doi.org/10.1007/s10334-011-0293-4>
- Zeng, Q. Y., Chen, R., Darmawan, J., Xiao, Z. Y., Chen, S. B., Wigley, R., ... Zhang, N. Z. (2008). Rheumatic diseases in China. *Arthritis Research & Therapy*, *10*(1), R17. <http://doi.org/10.1186/ar2368>
- Zhao, X., Tang, Z., Zhang, H., Atianjoh, F. E., Zhao, J.-Y., Liang, L., ... Tao, Y.-X. (2013). A long noncoding RNA contributes to neuropathic pain by silencing *Kcna2* in primary afferent neurons. *Nature Neuroscience*, *16*(8), 1024–1031. <http://doi.org/10.1038/nn.3438.A>
- Zondervan, K. T., & Cardon, L. R. (2007). Designing candidate gene and genome-wide case-control association studies. *Nature Protocols*, *2*(10), 2492–2501. <http://doi.org/10.1038/nprot.2007.366>
- Zubieta, J.-K., Bueller, J. a, Jackson, L. R., Scott, D.J., Xu, Y., Koeppe, R. a, ... Stohler, C. S. (2005). Placebo effects mediated by endogenous opioid activity on mu-opioid receptors. *The Journal of Neuroscience : The Official Journal of the Society for Neuroscience*, *25*(34), 7754–62. <http://doi.org/10.1523/JNEUROSCI.0439-05.2005>
- Zubieta, J.-K., Heitzeg, M. M., Smith, Y. R., Bueller, J. A., Xu, K., Xu, Y., ... Goldman, D. (2003). COMT val158met genotype affects mu-opioid neurotransmitter responses to a pain stressor. *Science (New York, N.Y.)*, *299*, 1240–1243. <http://doi.org/10.1126/science.1078546>
- Zubieta, J. K., Smith, Y. R., Bueller, J. A., Xu, Y., Kilbourn, M. R., Jewett, D. M., ... Stohler, C. S. (2001a). *Regional mu opioid receptor regulation of sensory and affective dimensions of pain. Science (New York, N.Y.)* (Vol. 293).
- Zubieta, J. K., Smith, Y. R., Bueller, J. a, Xu, Y., Kilbourn, M. R., Jewett, D. M., ... Stohler, C. S. (2001b). Regional mu opioid receptor regulation of sensory and affective dimensions of pain. *Science (New York, N.Y.)*, *293*(5528), 311–5. <http://doi.org/10.1126/science.1060952>

5 APPENDIX

5.1.1 Supplementary table II-1: Correlation table repeated measures interval and within-subject ICC



Supplementary figure II-1: No significant correlations were observed between the repeated measures interval and within-subject ICC. Abbreviations: amygdala (AMY), hippocampus (HIPP), brainstem (BS), thalamus (THAL), anterior insula (antINS), posterior insula (posINS), somatosensory cortex (primary, S1 and secondary, S2), posterior cingulate cortex (PCC), anterior cingulate cortex (ACC).

5.1.2 Supplementary table III-1: Differentially expressed genes post surgery

Probe Set ID	Gene Symbol	Ls mean Pain Ctrl	Ls mean Pain Pain	Difference (Pain)-(Ctrl)	t-Statistic Difference (Pain)-(Ctrl)	p-Value Difference (Pain)-(Ctrl)	Adjusted p-Value for Difference (Pain)-(Ctrl)
64397_at	ZNF106	7,685	7,976	0,291	7,132	8,84085E-11	2,14948E-06
660_at	BMX	3,784	4,220	0,436	6,800	4,67664E-10	5,68515E-06
23569_at	PADI4	4,707	5,220	0,513	6,142	1,15201E-08	7,00218E-05
63971_at	KIF13A	5,151	5,600	0,449	6,161	1,05244E-08	7,00218E-05
10123_at	ARL4C	7,638	7,277	-0,361	-5,879	3,98964E-08	0,000138572
353189_at	SLCO4C1	6,342	6,835	0,492	5,909	3,47132E-08	0,000138572
80183_at	KIAA0226L	5,874	6,531	0,658	5,880	3,96096E-08	0,000138572
535_at	ATP6V0A1	6,876	7,326	0,449	5,848	4,60853E-08	0,000139627
84255_at	SLC37A3	6,166	6,936	0,769	5,823	5,16861E-08	0,000139627
22853_at	LMTK2	4,909	5,218	0,309	5,791	6,00367E-08	0,000145967
2204_at	FCAR	5,000	5,547	0,547	5,750	7,24522E-08	0,000160139
4311_at	MME	8,373	9,071	0,698	5,726	8,11398E-08	0,000164396
1362_at	CPD	8,340	8,792	0,452	5,646	1,16727E-07	0,00016694
2005_at	ELK4	7,024	6,734	-0,291	-5,656	1,11493E-07	0,00016694
3930_at	LBR	9,114	9,455	0,341	5,686	9,73636E-08	0,00016694
5058_at	PAK1	8,813	9,083	0,271	5,651	1,14058E-07	0,00016694
57161_at	PELI2	5,882	6,216	0,333	5,693	9,43899E-08	0,00016694
57633_at	LRRN1	4,019	4,237	0,218	5,619	1,32213E-07	0,000169184
64101_at	LRRC4	5,090	5,555	0,465	5,630	1,25711E-07	0,000169184
5663_at	PSEN1	8,161	8,361	0,200	5,576	1,6033E-07	0,000194906
53346_at	TM6SF1	6,412	6,838	0,425	5,557	1,75242E-07	0,000202888
55526_at	DHTKD1	5,176	5,451	0,276	5,504	2,22634E-07	0,000246041
79660_at	PPP1R3B	5,048	5,480	0,432	5,474	2,54658E-07	0,000269196
101927873_at	LINC01508	3,560	3,658	0,098	5,449	2,84242E-07	0,000287949
50486_at	G0S2	4,991	5,404	0,414	5,437	3,00907E-07	0,000289322
57136_at	APMAP	7,294	7,713	0,419	5,431	3,09397E-07	0,000289322
4318_at	MMP9	5,351	5,883	0,532	5,397	3,58833E-07	0,000323122
407008_at	MIR223	8,321	8,935	0,613	5,370	4,04816E-07	0,000341871
6176_at	RPLP1	8,789	8,228	-0,560	-5,369	4,07776E-07	0,000341871
23604_at	DAPK2	5,043	5,263	0,220	5,349	4,45691E-07	0,000361203
83658_at	DYNLRB1	8,170	7,911	-0,260	-5,329	4,8615E-07	0,000381283
159013_at	CXorf38	5,356	5,696	0,340	5,294	5,68496E-07	0,000407574
51314_at	NME8	3,751	3,989	0,238	5,293	5,69964E-07	0,000407574
728558_at	ENTPD1-AS1	4,164	4,415	0,251	5,295	5,63823E-07	0,000407574
4358_at	MPV17	6,588	6,343	-0,245	-5,271	6,26999E-07	0,000435549
6655_at	SOS2	7,995	8,393	0,398	5,255	6,73647E-07	0,000454955
285521_at	COX18	5,826	5,599	-0,227	-5,225	7,69813E-07	0,00050585
23157_at	SEPT6	6,900	6,577	-0,323	-5,167	9,89876E-07	0,000633339
10057_at	ABCC5	4,587	4,809	0,222	5,136	1,13471E-06	0,000683084
285848_at	PNPLA1	4,470	4,659	0,189	5,132	1,15191E-06	0,000683084
6386_at	SDCBP	10,268	10,563	0,295	5,142	1,10601E-06	0,000683084
5836_at	PYGL	8,870	9,408	0,538	5,103	1,30816E-06	0,000757269
8655_at	DYNLL1	6,675	6,347	-0,327	-5,079	1,44892E-06	0,000819247
5218_at	CDK14	5,264	5,835	0,571	5,051	1,63191E-06	0,000856119
6222_at	RPS18	10,771	10,261	-0,510	-5,060	1,57245E-06	0,000856119
64757_at	MARC1	4,745	5,136	0,391	5,048	1,65498E-06	0,000856119
9975_at	NR1D2	5,822	5,533	-0,289	-5,052	1,63011E-06	0,000856119
2353_at	FOS	4,712	4,961	0,249	5,029	1,80017E-06	0,000893214
94097_at	SFXN5	4,600	4,747	0,148	5,031	1,78445E-06	0,000893214
154141_at	MBOAT1	6,354	6,638	0,284	4,992	2,10523E-06	0,001003618
55752_at	SEPT11	6,023	5,754	-0,269	-4,992	2,10215E-06	0,001003618

Appendix

84641_at	MFSD14B	6,624	7,098	0,474	4,984	2,17907E-06	0,001018842
729296_at	LOC729296	4,114	4,299	0,185	4,973	2,28077E-06	0,001046272
192670_at	AGO4	7,732	8,099	0,366	4,958	2,43172E-06	0,00109486
3087_at	HHEX	6,237	6,493	0,256	4,938	2,6492E-06	0,001171091
3560_at	IL2RB	4,993	4,766	-0,227	-4,932	2,71988E-06	0,001180864
83716_at	CRISPLD2	5,253	5,766	0,513	4,922	2,83834E-06	0,001210676
84674_at	CARD6	4,718	5,022	0,304	4,899	3,12011E-06	0,001307918
	LOC105375						
105375667_at	667	3,685	3,839	0,154	4,880	3,38268E-06	0,001326501
120425_at	JAML	10,620	10,883	0,264	4,890	3,24111E-06	0,001326501
3704_at	ITPA	5,048	4,890	-0,157	-4,881	3,36287E-06	0,001326501
9885_at	OSBPL2	6,966	7,264	0,299	4,886	3,30491E-06	0,001326501
57488_at	ESYT2	7,360	7,164	-0,196	-4,872	3,49995E-06	0,001350705
128646_at	SIRPD	5,381	5,798	0,417	4,862	3,65751E-06	0,001389456
222389_at	BEND7	3,700	3,845	0,145	4,843	3,95552E-06	0,001414273
338339_at	CLEC4D	5,471	6,218	0,748	4,849	3,86089E-06	0,001414273
6141_at	RPL18	10,211	9,909	-0,302	-4,844	3,93529E-06	0,001414273
7039_at	TGFA	4,720	4,936	0,216	4,849	3,84952E-06	0,001414273
170575_at	GIMAP1	8,220	7,909	-0,311	-4,839	4,02802E-06	0,001419323
10296_at	MAEA	4,846	5,035	0,189	4,832	4,13571E-06	0,001436451
2950_at	GSTP1	8,377	8,100	-0,277	-4,822	4,32159E-06	0,00147987
388011_at	LINC01550	6,394	5,972	-0,422	-4,812	4,50087E-06	0,001519855
54956_at	PARP16	4,481	4,657	0,176	4,807	4,59951E-06	0,001531888
2713_at	GK3P	6,998	7,666	0,669	4,800	4,72396E-06	0,001552076
1089_at	CEACAM4	5,462	5,792	0,330	4,791	4,90731E-06	0,001562724
22990_at	PCNX1	7,835	8,182	0,347	4,777	5,20629E-06	0,001562724
26053_at	AUTS2	4,316	4,197	-0,119	-4,787	4,9849E-06	0,001562724
51596_at	CUTA	7,022	6,776	-0,247	-4,778	5,19078E-06	0,001562724
6132_at	RPL8	8,704	8,340	-0,364	-4,777	5,20628E-06	0,001562724
6281_at	S100A10	9,871	9,625	-0,246	-4,781	5,12094E-06	0,001562724
731424_at	MIR3945HG	4,771	5,108	0,337	4,790	4,92688E-06	0,001562724
55692_at	LUC7L	6,258	6,043	-0,215	-4,771	5,33931E-06	0,001583105
23534_at	TNPO3	5,773	6,064	0,291	4,758	5,63457E-06	0,001650521
8500_at	PPFIA1	5,685	5,943	0,258	4,739	6,10409E-06	0,001766771
101927433_at	LINC01255	3,493	3,567	0,074	4,717	6,66954E-06	0,001842687
8993_at	PGLYRP1	4,404	4,715	0,311	4,722	6,53988E-06	0,001842687
9214_at	FCMR	7,870	7,599	-0,271	-4,718	6,66134E-06	0,001842687
978_at	CDA	5,962	6,455	0,492	4,724	6,49759E-06	0,001842687
3034_at	HAL	5,401	5,872	0,471	4,710	6,86344E-06	0,001874953
152007_at	GLIPR2	7,568	7,795	0,227	4,707	6,94792E-06	0,001876942
6792_at	CDKL5	5,055	5,398	0,342	4,699	7,17755E-06	0,001917669
3187_at	HNRNPH1	9,092	8,795	-0,297	-4,679	7,79488E-06	0,002059966
23074_at	UHRF1BP1L	6,684	7,079	0,395	4,667	8,21299E-06	0,002074221
3588_at	IL10RB	5,770	6,135	0,365	4,668	8,179E-06	0,002074221
366_at	AQP9	10,061	10,482	0,421	4,673	7,98892E-06	0,002074221
64745_at	METTL17	5,342	5,147	-0,195	-4,665	8,27538E-06	0,002074221
84188_at	FAR1	7,577	7,814	0,237	4,666	8,23276E-06	0,002074221
16_at	AARS	5,185	5,018	-0,167	-4,622	9,8571E-06	0,002396556
400863_at	NA	5,350	5,091	-0,258	-4,622	9,84159E-06	0,002396556
6223_at	RPS19	8,285	7,975	-0,310	-4,625	9,75087E-06	0,002396556
120892_at	LRRK2	9,331	9,715	0,384	4,611	1,02893E-05	0,002476859
6932_at	TCF7	5,185	5,032	-0,152	-4,604	1,06182E-05	0,002530983
6209_at	RPS15	8,680	8,330	-0,350	-4,592	1,11227E-05	0,002625503
8972_at	MGAM	7,980	8,677	0,697	4,589	1,1292E-05	0,002639838
154881_at	KCTD7	4,760	4,604	-0,156	-4,576	1,18595E-05	0,002686079
28504_at	IGHD2-8	3,305	3,392	0,087	4,575	1,19317E-05	0,002686079
57189_at	KIAA1147	5,313	5,119	-0,194	-4,577	1,18493E-05	0,002686079
6203_at	RPS9	5,315	5,049	-0,266	-4,581	1,16501E-05	0,002686079
	PCED1B-						
100233209_at	AS1	5,005	4,747	-0,258	-4,570	1,21879E-05	0,00269512

Appendix

10472_at	ZBTB18	5,950	6,238	0,288	4,567	1,23369E-05	0,00269512
353345_at	GPR141	5,179	5,593	0,414	4,563	1,2547E-05	0,00269512
4482_at	MSRA	4,647	4,824	0,177	4,564	1,2471E-05	0,00269512
54902_at	TTC19	6,692	6,507	-0,186	-4,560	1,26669E-05	0,00269512
58528_at	RRAGD	5,303	5,726	0,422	4,561	1,2641E-05	0,00269512
94241_at	TP53INP1	7,894	8,226	0,333	4,559	1,27479E-05	0,00269512
131118_at	DNAJC19	5,994	5,713	-0,281	-4,550	1,3191E-05	0,002697095
25797_at	QPCT	7,361	7,834	0,472	4,554	1,2972E-05	0,002697095
26648_at	OR7E24	3,820	3,999	0,179	4,551	1,31698E-05	0,002697095
81565_at	NDEL1	7,788	8,050	0,262	4,550	1,32009E-05	0,002697095
6434_at	TRA2B	7,316	7,062	-0,253	-4,537	1,38899E-05	0,0028142
254428_at	SLC41A1	4,709	4,603	-0,107	-4,531	1,4231E-05	0,002859481
23463_at	ICMT	5,000	4,858	-0,142	-4,528	1,44084E-05	0,002867269
27101_at	CACYBP	6,103	5,875	-0,228	-4,525	1,46079E-05	0,002867269
57542_at	KLHL42	4,737	4,602	-0,136	-4,523	1,47414E-05	0,002867269
9926_at	LPGAT1	7,014	7,297	0,283	4,524	1,46632E-05	0,002867269
6158_at	RPL28	4,791	4,555	-0,235	-4,507	1,56824E-05	0,003022315
8826_at	IQGAP1	9,694	9,900	0,206	4,505	1,57872E-05	0,003022315
11180_at	WDR6	4,708	4,601	-0,107	-4,497	1,63032E-05	0,003033602
5496_at	PPM1G	5,924	5,767	-0,157	-4,497	1,63452E-05	0,003033602
5936_at	RBM4	5,613	5,407	-0,205	-4,499	1,62343E-05	0,003033602
81671_at	VMP1	10,571	10,802	0,231	4,498	1,62989E-05	0,003033602
5813_at	PURA	7,392	7,185	-0,207	-4,493	1,66104E-05	0,003059466
842_at	CASP9	4,372	4,504	0,133	4,490	1,67934E-05	0,003069904
1431_at	CS	7,314	7,078	-0,236	-4,485	1,715E-05	0,003111694
4841_at	NONO	6,217	5,979	-0,239	-4,479	1,75641E-05	0,003163225
9761_at	MLEC	5,857	5,651	-0,205	-4,474	1,78764E-05	0,003195793
516_at	ATP5G1	6,355	6,099	-0,256	-4,454	1,9374E-05	0,003388784
5336_at	PLCG2	6,125	6,378	0,252	4,455	1,93084E-05	0,003388784
55784_at	MCTP2	7,074	7,498	0,424	4,456	1,92554E-05	0,003388784
6809_at	STX3	6,820	7,205	0,385	4,449	1,97748E-05	0,003434173
55276_at	PGM2	7,447	7,831	0,383	4,439	2,06213E-05	0,003555788
22978_at	NT5C2	7,428	7,796	0,367	4,432	2,12037E-05	0,003630465
51635_at	DHRS7	8,360	8,575	0,215	4,427	2,15488E-05	0,003663742
4723_at	NDUFV1	6,168	5,926	-0,243	-4,412	2,28972E-05	0,003865971
6604_at	SMARCD3	4,807	4,996	0,189	4,408	2,32524E-05	0,003898868
127829_at	ARL8A	5,306	5,641	0,335	4,403	2,37149E-05	0,003949173
100506144_at	ZMYM6NB	7,749	7,514	-0,235	-4,396	2,44453E-05	0,004015807
10147_at	SUGP2	5,005	4,897	-0,108	-4,396	2,43885E-05	0,004015807
121512_at	FGD4	5,110	5,407	0,296	4,391	2,49261E-05	0,004058016
1432_at	MAPK14	6,575	6,934	0,359	4,390	2,50361E-05	0,004058016
23210_at	JMJD6	5,012	5,183	0,171	4,380	2,59674E-05	0,004142935
283687_at	ST20-AS1	4,698	4,926	0,228	4,380	2,60436E-05	0,004142935
4783_at	NFIL3	7,977	8,353	0,376	4,379	2,61192E-05	0,004142935
51_at	ACOX1	7,294	7,671	0,377	4,378	2,62416E-05	0,004142935
55301_at	OLAH	3,420	3,466	0,046	4,367	2,74073E-05	0,004299049
5329_at	PLAUR	6,661	7,025	0,364	4,362	2,78541E-05	0,004341129
55718_at	POLR3E	5,292	5,169	-0,123	-4,360	2,81169E-05	0,004354178
23435_at	TARDBP	7,873	7,672	-0,201	-4,355	2,87288E-05	0,004420778
5256_at	PHKA2	5,187	5,330	0,143	4,346	2,97158E-05	0,004543901
207063_at	DHRSX	4,225	4,640	0,415	4,326	3,21139E-05	0,004790098
3695_at	ITGB7	4,915	4,779	-0,136	-4,326	3,20815E-05	0,004790098
5971_at	RELB	4,505	4,631	0,125	4,327	3,19952E-05	0,004790098
683_at	BST1	6,501	6,848	0,347	4,330	3,15782E-05	0,004790098
953_at	ENTPD1	7,520	7,790	0,270	4,320	3,29557E-05	0,004885687
662_at	BNIP1	3,972	3,880	-0,092	-4,314	3,36671E-05	0,004960896
10492_at	SYNCRIP	6,102	5,873	-0,228	-4,300	3,55755E-05	0,005187176
116369_at	SLC26A8	4,202	4,488	0,286	4,292	3,67255E-05	0,005187176
2091_at	FBL	9,470	9,138	-0,332	-4,295	3,62473E-05	0,005187176

Appendix

2153_at	F5	5,383	5,952	0,569	4,298	3,58956E-05	0,005187176
5997_at	RGS2	9,938	10,352	0,414	4,295	3,62819E-05	0,005187176
6693_at	SPN	4,876	4,752	-0,124	-4,298	3,58926E-05	0,005187176
7099_at	TLR4	9,173	9,575	0,403	4,290	3,69095E-05	0,005187176
9778_at	KIAA0232	5,305	5,621	0,316	4,291	3,69014E-05	0,005187176
51335_at	NGRN	5,814	5,621	-0,193	-4,286	3,75055E-05	0,005240644
1820_at	ARID3A	4,509	4,617	0,108	4,276	3,90332E-05	0,005422935
148145_at	LINC00906	3,971	4,213	0,241	4,263	4,11069E-05	0,005539336
5160_at	PDHA1	6,673	6,403	-0,270	-4,262	4,1238E-05	0,005539336
55754_at	TMEM30A	4,725	5,057	0,332	4,264	4,09307E-05	0,005539336
6304_at	SATB1	7,288	7,075	-0,213	-4,267	4,04029E-05	0,005539336
8086_at	AAAS	5,985	5,735	-0,250	-4,263	4,10398E-05	0,005539336
9880_at	ZBTB39	4,713	4,564	-0,148	-4,264	4,09835E-05	0,005539336
8445_at	DYRK2	6,945	6,711	-0,234	-4,253	4,26991E-05	0,005704078
254065_at	BRWD3	6,508	6,709	0,202	4,235	4,56931E-05	0,005999379
26253_at	CLEC4E	6,911	7,467	0,556	4,234	4,58966E-05	0,005999379
5209_at	PFKFB3	4,988	5,366	0,378	4,237	4,54896E-05	0,005999379
79817_at	MOB3B	4,694	4,555	-0,139	-4,235	4,57063E-05	0,005999379
201931_at	TMEM192	4,844	4,662	-0,182	-4,232	4,63622E-05	0,006014638
84078_at	KBTBD7	4,734	5,106	0,372	4,231	4,65081E-05	0,006014638
118932_at	ANKRD22	3,930	4,413	0,484	4,223	4,79082E-05	0,006086504
27236_at	ARFIP1	6,655	7,030	0,375	4,224	4,77907E-05	0,006086504
5580_at	PRKCD	7,896	8,228	0,332	4,222	4,80652E-05	0,006086504
84263_at	HSDL2	5,950	6,306	0,356	4,222	4,80529E-05	0,006086504
7409_at	VAV1	5,738	5,971	0,233	4,213	4,97085E-05	0,006201102
8563_at	THOC5	5,696	5,919	0,223	4,215	4,93747E-05	0,006201102
9448_at	MAP4K4	7,600	7,851	0,251	4,213	4,97353E-05	0,006201102
317_at	APAF1	7,193	7,480	0,287	4,201	5,21171E-05	0,006464917
8291_at	DYSF	5,048	5,418	0,370	4,197	5,28656E-05	0,006524469
55529_at	TMEM55A	7,803	8,184	0,381	4,182	5,61432E-05	0,006885715
606293_at	KLKP1	3,578	3,675	0,098	4,181	5,6359E-05	0,006885715
	LOC102724						
102724819_at	819	3,380	3,488	0,108	4,171	5,8483E-05	0,00710949
5004_at	ORM1	4,007	4,604	0,597	4,169	5,90022E-05	0,007112455
6950_at	TCP1	8,459	8,222	-0,237	-4,168	5,90925E-05	0,007112455
54893_at	MTMR10	6,995	7,266	0,272	4,164	6,00293E-05	0,007189622
9394_at	HS6ST1	10,456	10,139	-0,317	-4,162	6,04238E-05	0,007201388
4644_at	MYO5A	6,206	6,456	0,251	4,159	6,1271E-05	0,007266741
27131_at	SNX5	5,404	5,227	-0,177	-4,157	6,1773E-05	0,00729071
762_at	CA4	4,297	4,424	0,128	4,154	6,24061E-05	0,007329854
	LOC100287						
100287632_at	632	4,118	4,270	0,152	4,152	6,286E-05	0,007347673
79026_at	AHNAK	8,430	8,176	-0,255	-4,148	6,38471E-05	0,007391975
9874_at	TLK1	7,805	7,630	-0,175	-4,149	6,35935E-05	0,007391975
63939_at	FAM217B	4,288	4,567	0,279	4,139	6,61641E-05	0,007623928
2114_at	ETS2	5,588	5,857	0,269	4,131	6,81423E-05	0,007740176
340061_at	TMEM173	5,089	4,954	-0,135	-4,131	6,80277E-05	0,007740176
55652_at	SLC48A1	4,507	4,406	-0,102	-4,130	6,84464E-05	0,007740176
6400_at	SEL1L	7,370	7,533	0,163	4,131	6,81892E-05	0,007740176
100130460_at	CAND1.11	3,712	3,867	0,155	4,123	7,02426E-05	0,007833979
	LOC105373						
105373442_at	442	5,075	5,427	0,352	4,123	7,01535E-05	0,007833979
200185_at	KRTCAP2	5,188	4,930	-0,258	-4,123	7,01986E-05	0,007833979
328_at	APEX1	7,522	7,203	-0,319	-4,117	7,19348E-05	0,007936371
5432_at	POLR2C	4,397	4,501	0,104	4,116	7,21399E-05	0,007936371
79892_at	MCMBP	6,845	7,049	0,204	4,116	7,21109E-05	0,007936371
101927149_at	LINC01471	4,125	4,260	0,135	4,103	7,58248E-05	0,00822417
2180_at	ACSL1	8,910	9,543	0,633	4,102	7,59226E-05	0,00822417
57198_at	ATP8B2	5,245	5,121	-0,124	-4,101	7,64233E-05	0,00822417
6431_at	SRSF6	7,543	7,301	-0,242	-4,099	7,67855E-05	0,00822417

Appendix

84803_at	GPAT3	5,697	6,074	0,376	4,099	7,67438E-05	0,00822417
8825_at	LIN7A	5,976	6,522	0,546	4,102	7,61315E-05	0,00822417
101927018_at	LOC101927018	6,076	6,590	0,514	4,094	7,83306E-05	0,008280229
55239_at	OGFOD1	6,063	5,840	-0,223	-4,095	7,81937E-05	0,008280229
7185_at	TRAF1	4,363	4,273	-0,090	-4,094	7,8311E-05	0,008280229
57186_at	RALGAPA2	5,429	5,697	0,268	4,092	7,87953E-05	0,008293289
100151683_at	RNU4ATAC	3,943	4,222	0,279	4,090	7,95708E-05	0,008338811
10129_at	FRY	6,871	7,187	0,316	4,083	8,17849E-05	0,008534059
89857_at	KLHL6	6,040	5,814	-0,226	-4,076	8,36856E-05	0,008695073
266747_at	RGL4	4,595	4,758	0,163	4,071	8,54361E-05	0,008819607
91662_at	NLRP12	4,922	5,283	0,361	4,070	8,56096E-05	0,008819607
414778_at	HCG17	3,548	3,497	-0,051	-4,069	8,62103E-05	0,008835246
55152_at	DALRD3	5,275	5,107	-0,168	-4,068	8,64882E-05	0,008835246
11238_at	CA5B	6,142	5,817	-0,325	-4,063	8,79569E-05	0,008947687
400955_at	LINC01122	3,512	3,554	0,041	4,061	8,86304E-05	0,008964891
53838_at	C11orf24	5,027	4,889	-0,138	-4,061	8,88635E-05	0,008964891
54861_at	SNRK	7,022	7,188	0,165	4,057	9,0145E-05	0,009052716
85028_at	SNHG12	6,982	6,656	-0,326	-4,056	9,04788E-05	0,009052716
100129827_at	MRVI1-AS1	4,941	5,263	0,323	4,054	9,10731E-05	0,009074839
728290_at	LOC728290	3,337	3,419	0,082	4,050	9,23265E-05	0,009127225
79689_at	STEAP4	7,914	8,422	0,508	4,049	9,26966E-05	0,009127225
9378_at	NRXN1	3,702	3,746	0,043	4,049	9,27251E-05	0,009127225
30061_at	SLC40A1	6,704	7,042	0,338	4,047	9,33583E-05	0,009152504
4215_at	MAP3K3	5,251	5,484	0,233	4,043	9,50633E-05	0,009282225
5608_at	MAP2K6	4,536	4,791	0,255	4,039	9,64318E-05	0,009378184
26003_at	GORASP2	7,142	6,957	-0,185	-4,036	9,74004E-05	0,009434644
10606_at	PAICS	4,163	4,024	-0,138	-4,028	0,000100326	0,009617757
3772_at	KCNJ15	8,827	9,405	0,578	4,029	9,993E-05	0,009617757
8537_at	BCAS1	4,183	4,264	0,081	4,028	0,000100478	0,009617757
23287_at	AGTPBP1	8,282	8,540	0,258	4,022	0,000102784	0,009767434
29997_at	GLTSCR2	7,385	7,146	-0,239	-4,021	0,000103187	0,009767434
64211_at	LHX5	3,985	3,897	-0,088	-4,020	0,000103246	0,009767434
6515_at	SLC2A3	9,999	10,437	0,438	4,019	0,000103761	0,009778092
10613_at	ERLIN1	6,479	6,756	0,277	4,013	0,000106175	0,00985987
112398_at	EGLN2	6,412	6,089	-0,323	-4,013	0,000105982	0,00985987
344807_at	CD200R1L	3,393	3,444	0,051	4,015	0,000105507	0,00985987
55272_at	IMP3	8,891	8,652	-0,239	-4,013	0,000106251	0,00985987
6732_at	SRPK1	6,269	6,682	0,413	4,011	0,000106869	0,009879524
166_at	AES	5,203	5,011	-0,192	-4,007	0,000108586	0,010000239
55454_at	CSGALNAC T2	6,025	6,277	0,252	4,002	0,000110375	0,01012658
53827_at	FXYD5	7,644	7,385	-0,259	-3,997	0,000112425	0,01027594
93432_at	MGAM2	4,072	4,311	0,240	3,996	0,00011302	0,010291561
10765_at	KDM5B	5,793	6,033	0,240	3,994	0,000113837	0,01032728
9043_at	SPAG9	7,378	7,608	0,231	3,991	0,000114962	0,010390626
3326_at	HSP90AB1	7,582	7,284	-0,298	-3,990	0,000115534	0,010403582
51719_at	CAB39	6,739	6,971	0,232	3,989	0,000116115	0,01041737
54069_at	MIS18A	4,958	4,792	-0,165	-3,987	0,000117072	0,010438359
81539_at	SLC38A1	8,803	8,516	-0,287	-3,986	0,000117208	0,010438359
146691_at	TOM1L2	4,443	4,551	0,108	3,985	0,00011769	0,01044306
23046_at	KIF21B	4,719	4,842	0,123	3,984	0,000118343	0,010456066
83862_at	TMEM120A	4,665	4,830	0,165	3,983	0,000118697	0,010456066
10205_at	MPZL2	5,355	5,646	0,291	3,980	0,000120062	0,01053819
2113_at	ETS1	7,619	7,324	-0,295	-3,977	0,000121319	0,010610179
8556_at	CDC14A	6,427	6,208	-0,219	-3,972	0,000123531	0,010764944
10404_at	CPQ	7,063	7,370	0,307	3,969	0,000124954	0,010811383
91050_at	CCDC149	4,068	4,163	0,095	3,969	0,00012489	0,010811383
2182_at	ACSL4	6,272	6,588	0,316	3,966	0,000126202	0,010855801
83890_at	SPATA9	3,665	3,602	-0,063	-3,966	0,00012636	0,010855801

Appendix

1845_at	DUSP3	4,938	5,075	0,137	3,962	0,000128289	0,010953187
4670_at	HNRNPM	7,715	7,500	-0,215	-3,962	0,000128395	0,010953187
27347_at	STK39	5,942	5,713	-0,229	-3,960	0,00012896	0,01096293
125144_at	LRRC75A-AS1	5,074	4,920	-0,154	-3,958	0,000130081	0,010981418
57700_at	FAM160B1	6,777	7,028	0,252	3,958	0,00012998	0,010981418
337975_at	KRTAP20-1	4,255	4,045	-0,210	-3,955	0,000131369	0,011051829
101928143_at	LOC101928143	6,665	7,222	0,557	3,947	0,000135692	0,011328517
8493_at	PPM1D	5,961	6,144	0,183	3,946	0,000136056	0,011328517
90025_at	UBE3D	4,235	4,140	-0,095	-3,947	0,000135709	0,011328517
105373606_at	LOC105373606	5,389	5,917	0,528	3,943	0,000137659	0,011422882
5893_at	RAD52	5,117	5,005	-0,112	-3,941	0,000138622	0,01146364
55615_at	PRR5	5,019	4,892	-0,127	-3,939	0,00013964	0,011508714
101928551_at	LOC101928551	3,362	3,439	0,077	3,936	0,000140868	0,01153175
284757_at	MIR646HG	3,895	4,032	0,137	3,937	0,000140812	0,01153175
10941_at	UGT2A1	3,520	3,614	0,095	3,934	0,000142071	0,011591189
1378_at	CR1	6,936	7,452	0,516	3,931	0,000143598	0,011676593
121642_at	ALKBH2	4,494	4,372	-0,122	-3,929	0,000144754	0,011696877
26118_at	WSB1	9,319	9,528	0,209	3,929	0,00014481	0,011696877
9402_at	GRAP2	5,756	5,521	-0,234	-3,927	0,000145785	0,011736641
3340_at	NDST1	4,799	4,961	0,162	3,924	0,000147711	0,011815122
8073_at	PTP4A2	8,141	7,984	-0,157	-3,923	0,000147732	0,011815122
167555_at	FAM151B	4,079	4,298	0,219	3,914	0,000152803	0,012072244
26234_at	FBXL5	8,858	9,099	0,241	3,916	0,000151718	0,012072244
373156_at	GSTK1	6,762	6,547	-0,216	-3,913	0,000153413	0,012072244
5859_at	QARS	6,149	6,009	-0,139	-3,913	0,000153429	0,012072244
65265_at	C8orf33	4,789	4,681	-0,108	-3,915	0,000152495	0,012072244
3156_at	HMGCR	6,401	6,728	0,326	3,912	0,000154353	0,012105737
2926_at	GRSF1	6,130	5,982	-0,148	-3,910	0,000155386	0,012147613
101927950_at	LOC101927950	4,995	4,805	-0,190	-3,905	0,000157909	0,012282179
390195_at	OR5AN1	3,659	3,762	0,103	3,905	0,000158118	0,012282179
23186_at	RCOR1	7,063	7,265	0,202	3,901	0,000160186	0,012403174
51167_at	CYB5R4	7,335	7,632	0,297	3,895	0,000163964	0,012655394
54682_at	MANSC1	5,621	6,209	0,588	3,894	0,000164511	0,012657463
51490_at	C9orf114	4,656	4,576	-0,080	-3,891	0,000166553	0,012774171
101927124_at	LOC101927124	3,620	3,541	-0,079	-3,885	0,000170052	0,013001481
7016_at	TESK1	6,134	5,878	-0,256	-3,884	0,000170605	0,013002855
92170_at	MTG1	5,021	4,899	-0,122	-3,882	0,000172151	0,013079675
8893_at	EIF2B5	4,428	4,313	-0,115	-3,881	0,000172825	0,013089992
26031_at	OSBPL3	5,425	5,233	-0,192	-3,876	0,000175446	0,013242442
56005_at	MYDGF	5,712	5,510	-0,202	-3,876	0,000175927	0,013242442
122011_at	CSNK1A1L	5,555	5,923	0,367	3,874	0,000177195	0,013296716
645638_at	WFDC21P	4,203	4,066	-0,137	-3,870	0,000179422	0,013381242
972_at	CD74	8,943	8,646	-0,297	-3,870	0,000179419	0,013381242
60437_at	CDH26	3,931	4,002	0,071	3,869	0,000180395	0,013390047
646424_at	SPINK8	3,497	3,597	0,099	3,868	0,000180641	0,013390047
4267_at	CD99	7,284	7,060	-0,223	-3,867	0,000181332	0,013400368
104326191_at	LINC01336	5,919	5,601	-0,318	-3,865	0,000182547	0,013412337
8634_at	RTCA	7,171	6,999	-0,172	-3,865	0,000182597	0,013412337
6283_at	S100A12	9,888	10,409	0,521	3,859	0,000186686	0,013671371
29081_at	METTL5	5,776	5,554	-0,222	-3,858	0,000187511	0,013690527
837_at	CASP4	8,924	9,201	0,277	3,854	0,000190471	0,013823682
9096_at	TBX18	3,519	3,558	0,039	3,854	0,000190066	0,013823682
871_at	SERPINH1	4,369	4,287	-0,082	-3,852	0,000191927	0,01384663
9815_at	GIT2	8,474	8,607	0,133	3,852	0,00019143	0,01384663
596_at	BCL2	6,572	6,322	-0,250	-3,839	0,000200585	0,014428454

Appendix

7077_at	TIMP2	7,972	8,220	0,248	3,837	0,000202042	0,014490399
10783_at	NEK6	4,492	4,634	0,142	3,836	0,000203136	0,014495999
222487_at	ADGRG3	5,833	6,400	0,568	3,835	0,000203681	0,014495999
7311_at	UBA52	6,644	6,431	-0,213	-3,835	0,000203909	0,014495999
100302135_at	MIR320C1	6,234	6,647	0,413	3,825	0,000211107	0,014877204
518_at	ATP5G3	5,555	5,356	-0,199	-3,827	0,000210179	0,014877204
80777_at	CYB5B	7,818	7,564	-0,253	-3,826	0,000210827	0,014877204
79758_at	DHRS12	4,635	4,786	0,150	3,823	0,000212795	0,014924058
81833_at	SPACA1	3,437	3,412	-0,026	-3,822	0,000213613	0,014924058
8799_at	PEX11B	6,313	6,152	-0,162	-3,822	0,000213306	0,014924058
916_at	CD3E	8,382	7,998	-0,384	-3,819	0,000215596	0,015019474
53917_at	RAB24	6,268	6,480	0,212	3,816	0,000218349	0,015167796
4217_at	MAP3K5	6,188	6,470	0,282	3,810	0,0002229	0,015395948
9801_at	MRPL19	5,250	5,083	-0,167	-3,811	0,000222467	0,015395948
7136_at	TNNI2	4,978	5,149	0,171	3,808	0,000225014	0,015497919
25996_at	REXO2	5,567	5,348	-0,219	-3,806	0,000226553	0,015559841
64771_at	C6orf106	6,159	5,980	-0,179	-3,803	0,000228859	0,015668682
83759_at	RBM4B	6,549	6,315	-0,234	-3,802	0,000229427	0,015668682
2821_at	GPI	5,571	5,408	-0,162	-3,797	0,000233353	0,015847773
9870_at	AREL1	7,383	7,670	0,286	3,798	0,000232956	0,015847773
123720_at	WHAMM	5,329	5,156	-0,173	-3,792	0,000238064	0,016091765
4809_at	SNU13	6,455	6,259	-0,196	-3,791	0,000238931	0,016091765
55297_at	CCDC91	5,651	5,392	-0,259	-3,791	0,000238553	0,016091765
283635_at	FAM177A1	3,930	4,038	0,109	3,788	0,000241678	0,01614264
79918_at	SETD6	5,029	4,910	-0,119	-3,788	0,000241648	0,01614264
9520_at	NPEPPS	8,243	8,449	0,206	3,788	0,000241062	0,01614264
10794_at	ZNF460	7,443	7,268	-0,175	-3,785	0,000243868	0,016199895
3099_at	HK2	5,213	5,459	0,246	3,785	0,00024372	0,016199895
23001_at	WDFY3	7,292	7,731	0,439	3,775	0,00025298	0,0167594
88455_at	ANKRD13A	7,842	8,003	0,161	3,774	0,000253947	0,016777784
10572_at	SIVA1	5,021	4,905	-0,116	-3,773	0,000254932	0,016783751
116092_at	DNTTIP1	5,515	5,688	0,174	3,772	0,000255418	0,016783751
50650_at	ARHGEF3	5,909	5,719	-0,190	-3,768	0,00025918	0,016985026
5611_at	DNAJC3	7,101	7,455	0,354	3,766	0,000260743	0,016995809
729633_at	MRS2P2	3,851	4,055	0,205	3,767	0,000260452	0,016995809
11123_at	RCAN3	7,530	7,263	-0,267	-3,764	0,000262892	0,017090111
1937_at	EEF1G	7,318	7,071	-0,247	-3,761	0,000266235	0,017261242
1438_at	CSF2RA	4,423	4,627	0,204	3,758	0,000268814	0,017334255
399665_at	FAM102A	6,578	6,300	-0,279	-3,758	0,000268971	0,017334255
6799_at	SULT1A2	4,149	4,260	0,111	3,757	0,0002695	0,017334255
406954_at	MIR181A2	4,708	5,184	0,476	3,752	0,000274646	0,01761866
100873933_at	DPYD-AS2	4,300	4,555	0,255	3,748	0,000278184	0,017751927
23250_at	ATP11A	5,004	5,272	0,268	3,749	0,000277864	0,017751927
123879_at	DCUN1D3	4,367	4,555	0,188	3,743	0,00028313	0,018020273
55723_at	ASF1B	4,258	4,395	0,137	3,741	0,000285073	0,018096543
440944_at	THUMPD3- AS1	6,480	6,218	-0,262	-3,738	0,000288707	0,018279494
1785_at	DNM2	6,291	6,493	0,201	3,737	0,000289909	0,018307933
100130231_at	LINC00861	10,034	9,653	-0,381	-3,735	0,000291339	0,018350595
8994_at	LIMD1	4,912	4,806	-0,106	-3,734	0,000292438	0,01837219
101929664_at	HORMAD2- AS1	3,861	4,006	0,144	3,730	0,000297047	0,018518226
1955_at	MEGF9	9,111	9,407	0,297	3,731	0,000295634	0,018518226
389072_at	PLEKHM3	4,675	4,841	0,167	3,730	0,000296682	0,018518226
80762_at	NDFIP1	7,750	7,559	-0,191	-3,728	0,00029879	0,018579253
2355_at	FOSL2	5,117	5,271	0,154	3,725	0,000302305	0,018749832
101928161_at	LOC101928 161	3,737	3,638	-0,099	-3,722	0,000305058	0,018872438
10043_at	TOM1	4,778	4,935	0,157	3,720	0,000307002	0,018944507
51176_at	LEF1	8,241	7,909	-0,332	-3,719	0,000308148	0,018967073

Appendix

104384744_at	TET2-AS1	4,493	4,739	0,246	3,716	0,000311732	0,019139267
143384_at	CACUL1	7,345	7,533	0,188	3,714	0,000314534	0,019262659
6016_at	RIT1	7,068	7,330	0,262	3,712	0,000316678	0,019345225
407034_at	MIR30E	5,240	5,694	0,454	3,710	0,000318725	0,019421428
100885782_at	MYO16-AS1	4,133	4,548	0,414	3,709	0,000320049	0,019453408
5583_at	PRKCH	8,322	7,971	-0,351	-3,708	0,000320947	0,019459294
7852_at	CXCR4	9,566	9,736	0,170	3,706	0,000322844	0,019525627
23387_at	SIK3	5,758	5,962	0,204	3,705	0,000324125	0,019554457
1051_at	CEBPB	4,259	4,382	0,122	3,700	0,000329737	0,019843813
114885_at	OSBPL11	6,773	7,009	0,236	3,699	0,000331705	0,019912974
5037_at	PEBP1	7,573	7,279	-0,294	-3,696	0,000334212	0,020014045
353514_at	LILRA5	4,254	4,494	0,240	3,693	0,000337814	0,020180055
868_at	CBLB	6,917	6,636	-0,281	-3,689	0,000343129	0,020447285
151475_at	LOC151475	3,711	3,798	0,086	3,685	0,00034835	0,020707674
1610_at	DAO	3,890	3,981	0,092	3,683	0,000350781	0,020801319
101928523_at	LOC101928523						
5226_at	523	3,355	3,432	0,077	3,681	0,000352538	0,020826038
93190_at	PGD	8,873	9,171	0,298	3,681	0,000352911	0,020826038
1155_at	C1orf158	3,696	3,771	0,075	3,678	0,000356442	0,02098348
2314_at	TBCB	5,393	5,202	-0,191	-3,677	0,000357979	0,021005258
29914_at	FLII	4,857	4,991	0,133	3,675	0,000360051	0,021005258
9219_at	UBIAD1	5,497	5,344	-0,153	-3,676	0,000359142	0,021005258
7342_at	MTA2	6,229	6,058	-0,171	-3,675	0,000360268	0,021005258
9875_at	UBP1	6,605	6,455	-0,150	-3,672	0,000363627	0,021104099
26297_at	URB1	4,513	4,438	-0,075	-3,672	0,000363699	0,021104099
388695_at	SERGEF	5,488	5,319	-0,169	-3,669	0,000367723	0,021236204
3892_at	LYSMD1	4,386	4,575	0,189	3,669	0,000367374	0,021236204
347517_at	KRT86	4,388	4,249	-0,139	-3,668	0,000368983	0,021258465
8225_at	RAB41	3,776	3,707	-0,069	-3,666	0,000371336	0,021343452
102503427_at	GTPBP6	4,633	4,547	-0,086	-3,665	0,000372822	0,021378333
6402_at	LOC102503427						
6777_at	427	3,412	3,460	0,048	3,664	0,000374034	0,021397367
5052_at	SELL	10,076	10,315	0,239	3,655	0,000386306	0,022047572
55011_at	STAT5B	6,572	6,865	0,292	3,654	0,000388137	0,022100185
80212_at	PRDX1	6,984	6,754	-0,229	-3,649	0,00039406	0,022334272
80004_at	PIH1D1	5,193	5,034	-0,159	-3,649	0,000394086	0,022334272
10682_at	CCDC92	4,499	4,399	-0,099	-3,647	0,000397505	0,022475645
3936_at	ESRP2	4,347	4,292	-0,055	-3,645	0,0003997	0,022547359
646627_at	EBP	5,905	5,666	-0,238	-3,643	0,000403143	0,02268892
6756_at	LCP1	10,983	11,148	0,165	3,641	0,00040597	0,02271949
677840_at	LYPD8	4,459	4,550	0,091	3,641	0,000405849	0,02271949
137835_at	SSX1	3,504	3,577	0,073	3,640	0,000407424	0,02271949
100128770_at	SNORA71D	3,788	4,045	0,257	3,640	0,000406872	0,02271949
339448_at	TMEM71	8,189	8,465	0,276	3,639	0,0004091	0,022760743
57504_at	LOC100128770						
84628_at	770	3,940	4,037	0,096	3,637	0,000411988	0,022869121
2014_at	C1orf174	5,054	4,915	-0,139	-3,636	0,000413123	0,022879849
26469_at	MTA3	4,111	4,037	-0,074	-3,632	0,000418445	0,023069535
11060_at	NTNG2	4,371	4,448	0,077	3,633	0,000417766	0,023069535
161253_at	EMP3	7,887	7,582	-0,305	-3,629	0,00042318	0,023225228
116842_at	PTPN18	5,755	5,605	-0,150	-3,629	0,000422964	0,023225228
29065_at	WWP2	5,544	5,749	0,205	3,625	0,00042859	0,023416417
375341_at	REM2	4,350	4,498	0,148	3,626	0,000428006	0,023416417
80216_at	LEAP2	5,743	5,552	-0,192	-3,623	0,000431998	0,023546986
10673_at	ASAP1-IT1	5,337	5,729	0,392	3,622	0,000432917	0,023546986
3192_at	C3orf62	6,082	6,400	0,318	3,622	0,000434232	0,023565805
374907_at	ALPK1	6,728	7,068	0,339	3,620	0,000436458	0,023633872
	TNFSF13B	6,696	7,114	0,418	3,618	0,000439524	0,02366084
	HNRNPU	7,949	7,782	-0,167	-3,619	0,000438546	0,02366084
	B3GNT8	4,583	4,683	0,100	3,618	0,000439876	0,02366084

Appendix

55907_at	CMAS	5,784	5,616	-0,167	-3,616	0,000442081	0,023726965
498_at	ATP5A1	7,635	7,422	-0,214	-3,615	0,000444446	0,023801368
10972_at	TMED10	7,009	6,829	-0,180	-3,613	0,000446698	0,023869394
51571_at	FAM49B	7,966	8,115	0,149	3,612	0,000448262	0,023900444
8809_at	IL18R1	4,298	4,606	0,308	3,611	0,000450278	0,023955372
55129_at	ANO10	4,705	4,927	0,222	3,609	0,000454059	0,024103774
5435_at	POLR2F	7,168	6,942	-0,225	-3,607	0,000457039	0,02415648
79887_at	PLBD1	8,424	8,731	0,308	3,607	0,000456994	0,02415648
3182_at	HNRNPAB	8,284	8,063	-0,221	-3,604	0,000462267	0,02435213
8897_at	MTMR3	6,921	7,182	0,261	3,603	0,000462744	0,02435213
3554_at	IL1R1	4,286	4,592	0,306	3,602	0,000464964	0,024402391
360_at	AQP3	5,123	4,981	-0,142	-3,601	0,000465706	0,024402391
101930746_at	LINC00945	3,624	3,558	-0,066	-3,598	0,000471469	0,024555472
2000_at	ELF4	4,873	5,025	0,152	3,598	0,000471657	0,024555472
4001_at	LMNB1	5,453	5,742	0,289	3,598	0,000471118	0,024555472
23220_at	DTX4	4,627	4,731	0,104	3,597	0,000473091	0,024577485
84968_at	PNMA6A	4,273	4,548	0,275	3,593	0,00048023	0,024895184
10154_at	PLXNC1	8,247	8,531	0,284	3,591	0,000481915	0,024929377
286046_at	XKR6	4,149	4,088	-0,061	-3,591	0,000483012	0,024933064
84138_at	SLC7A6OS	6,812	6,628	-0,184	-3,589	0,000486027	0,025035524
1606_at	DGKA	6,640	6,429	-0,211	-3,586	0,000490722	0,025223963
8553_at	BHLHE40	5,266	5,119	-0,147	-3,585	0,000492677	0,025271013
538_at	ATP7A	6,498	6,682	0,184	3,583	0,00049686	0,025431932
1650_at	DDOST	6,385	6,221	-0,164	-3,581	0,000499596	0,025518222
23627_at	PRND	4,456	4,324	-0,132	-3,580	0,000501435	0,025558453
81554_at	WBSCR16	4,773	4,675	-0,098	-3,578	0,000504609	0,025612868
83853_at	ROPN1L	4,841	5,078	0,237	3,578	0,000504555	0,025612868
101928604_at	ZBTB46- AS1	4,180	4,322	0,142	3,575	0,000510962	0,025881288
9404_at	LPXN	5,780	5,599	-0,181	-3,574	0,000512521	0,025906273
23168_at	RTF1	5,078	5,260	0,182	3,572	0,000514939	0,025920724
6416_at	MAP2K4	5,889	6,128	0,239	3,572	0,000514881	0,025920724
84440_at	RAB11FIP4	4,940	5,048	0,108	3,569	0,000520455	0,026144253
10451_at	VAV3	6,416	6,664	0,248	3,566	0,000526004	0,02627587
339883_at	C3orf35	4,165	4,067	-0,098	-3,567	0,000524761	0,02627587
6484_at	ST3GAL4	4,183	4,270	0,087	3,566	0,000526317	0,02627587
10169_at	SERF2	6,086	5,917	-0,168	-3,564	0,000530375	0,026424172
7091_at	TLE4	7,015	7,254	0,238	3,561	0,000536016	0,026650608
58478_at	ENOPH1	5,510	5,366	-0,144	-3,560	0,000537294	0,026659667
10578_at	GNLY	6,733	6,362	-0,371	-3,557	0,000542109	0,026828361
399_at	RHOH	5,456	5,231	-0,225	-3,557	0,000542901	0,026828361
894_at	CCND2	5,151	4,983	-0,168	-3,554	0,000548197	0,027035138
6888_at	TALDO1	10,276	10,491	0,215	3,552	0,000551907	0,027162989
6774_at	STAT3	8,519	8,813	0,294	3,550	0,000556384	0,027244256
7259_at	TSPYL1	6,952	6,765	-0,187	-3,549	0,000558041	0,027244256
7587_at	ZNF37A	4,309	4,189	-0,120	-3,549	0,000557984	0,027244256
80301_at	PLEKHO2	6,027	6,262	0,235	3,550	0,000555233	0,027244256
202020_at	TAPT1-AS1	5,051	4,935	-0,116	-3,548	0,000559702	0,027270597
10008_at	KCNE3	4,700	4,891	0,191	3,546	0,000563629	0,027407027
101928517_at	LOC101928 517	3,673	3,747	0,074	3,540	0,000576116	0,027700124
26037_at	SIPA1L1	6,306	6,608	0,302	3,539	0,000577242	0,027700124
2876_at	GPX1	5,220	4,973	-0,247	-3,541	0,000572955	0,027700124
5191_at	PEX7	4,745	4,626	-0,120	-3,542	0,000571797	0,027700124
6280_at	S100A9	8,712	9,123	0,411	3,539	0,000577632	0,027700124
643036_at	SLED1	5,166	5,631	0,465	3,540	0,000575632	0,027700124
6555_at	SLC10A2	4,126	4,032	-0,094	-3,539	0,000576283	0,027700124
84898_at	PLXDC2	7,531	7,838	0,307	3,538	0,000579423	0,027731307
23593_at	HEBP2	7,418	7,626	0,207	3,533	0,000589046	0,028081343
8773_at	SNAP23	8,060	8,315	0,256	3,533	0,000588999	0,028081343

60685_at	ZFAND3	5,573	5,747	0,174	3,532	0,000590339	0,028087912
100874150_at	LINC00379	3,868	3,730	-0,138	-3,531	0,000593304	0,028173817
23357_at	ANGEL1	4,863	4,756	-0,107	-3,529	0,00059656	0,02823318
6748_at	SSR4	6,133	5,920	-0,213	-3,529	0,000596876	0,02823318
6248_at	RSC1A1	8,732	8,460	-0,272	-3,529	0,000598125	0,02823731
55739_at	NAXD	4,533	4,461	-0,073	-3,527	0,000601273	0,028276135
84226_at	C2orf16	3,700	3,771	0,071	3,527	0,000600563	0,028276135
79772_at	MCTP1	6,451	6,664	0,213	3,526	0,000604326	0,028364842
2176_at	FANCC	3,688	3,652	-0,036	-3,521	0,000612781	0,028656355
57217_at	TTC7A	4,662	4,584	-0,078	-3,521	0,000612895	0,028656355
9537_at	TP53I11	4,507	4,620	0,114	3,520	0,00061487	0,02869356
100505933_at	ADD3-AS1	3,871	3,970	0,099	3,518	0,000620904	0,028711085
11259_at	FILIP1L	4,568	4,417	-0,151	-3,518	0,000619124	0,028711085
23076_at	RRP1B	4,747	4,642	-0,106	-3,518	0,00062071	0,028711085
4660_at	PPP1R12B	5,482	5,755	0,273	3,520	0,000616682	0,028711085
55370_at	PPP4R1L	4,731	5,027	0,296	3,517	0,00062115	0,028711085
5818_at	NECTIN1	4,368	4,455	0,087	3,516	0,000624067	0,02879115
123606_at	NIPA1	5,444	5,251	-0,193	-3,512	0,00063371	0,029037235
23043_at	TNIK	5,915	5,647	-0,269	-3,512	0,000632129	0,029037235
28375_at	IGHVII-20-1	3,553	3,694	0,141	3,511	0,000634178	0,029037235
79961_at	DENND2D	6,654	6,471	-0,184	-3,512	0,000632219	0,029037235
	LOC105369						
105369535_at	535	4,386	4,692	0,306	3,511	0,000635986	0,029065256
7150_at	TOP1	6,781	6,971	0,190	3,510	0,000638096	0,029106994
26133_at	TRPC4AP	6,218	6,397	0,179	3,509	0,00063937	0,029110491
50484_at	RRM2B	5,262	5,473	0,211	3,506	0,000645095	0,029265244
8148_at	TAF15	9,184	8,929	-0,255	-3,506	0,000645176	0,029265244
51363_at	CHST15	5,730	6,001	0,271	3,505	0,000648228	0,029348903
100132341_at	CLUHP3	4,187	4,123	-0,063	-3,504	0,00065114	0,029371346
293_at	SLC25A6	9,072	8,847	-0,224	-3,504	0,000650459	0,029371346
9797_at	TATDN2	4,969	4,851	-0,118	-3,502	0,000653637	0,029429388
3309_at	HSPA5	6,862	6,680	-0,182	-3,502	0,000655559	0,029461366
5873_at	RAB27A	6,663	6,829	0,166	3,501	0,000657476	0,029492998
18_at	ABAT	4,965	5,140	0,175	3,498	0,000663087	0,029635352
6742_at	SSBP1	6,310	6,029	-0,281	-3,498	0,000662918	0,029635352
374899_at	ZNF829	4,038	3,928	-0,110	-3,496	0,000668443	0,029819939
114883_at	OSBPL9	5,783	5,956	0,173	3,494	0,000672235	0,029824927
3091_at	HIF1A	7,188	7,440	0,252	3,495	0,000671399	0,029824927
901_at	CCNG2	8,463	8,633	0,170	3,495	0,000671361	0,029824927
10130_at	PDIA6	6,005	5,776	-0,229	-3,491	0,000678923	0,029849265
	LOC101928						
101928386_at	386	3,728	3,867	0,139	3,492	0,000676511	0,029849265
112574_at	SNX18	5,604	5,791	0,188	3,492	0,000676262	0,029849265
54432_at	YIPF1	5,344	5,586	0,242	3,493	0,000674583	0,029849265
7873_at	MANF	6,996	6,750	-0,246	-3,492	0,000677912	0,029849265
54847_at	SIDT1	6,060	5,808	-0,252	-3,489	0,000683157	0,02998124
4691_at	NCL	8,653	8,273	-0,380	-3,488	0,00068715	0,030047988
994_at	CDC25B	5,396	5,270	-0,127	-3,488	0,000685959	0,030047988
114804_at	RNF157	4,974	4,851	-0,122	-3,487	0,00068957	0,030099687
2802_at	GOLGA3	4,424	4,369	-0,054	-3,483	0,000697464	0,030389683
10146_at	G3BP1	7,877	7,663	-0,214	-3,481	0,000702255	0,03050597
10335_at	MRV11	4,624	4,747	0,123	3,481	0,000703897	0,03050597
84945_at	ABHD13	5,148	5,352	0,204	3,481	0,000703417	0,03050597
914_at	CD2	7,965	7,561	-0,403	-3,479	0,000706763	0,030575665
689_at	BTF3	7,177	6,946	-0,231	-3,478	0,00070998	0,03066027
340578_at	DCAF12L2	4,115	3,978	-0,137	-3,476	0,000713907	0,030716905
751071_at	METTL12	5,067	4,886	-0,181	-3,475	0,000716345	0,030716905
84928_at	TMEM209	5,755	5,560	-0,195	-3,476	0,000715203	0,030716905
97_at	ACYP1	4,243	4,120	-0,123	-3,476	0,000715309	0,030716905
1912_at	PHC2	5,136	5,299	0,163	3,475	0,000717807	0,030725422

Appendix

55841_at	WWC3	5,054	5,217	0,163	3,472	0,000723856	0,030929897
55332_at	DRAM1	4,424	4,642	0,217	3,470	0,000728808	0,031050089
57689_at	LRRC4C	3,615	3,571	-0,045	-3,470	0,000729223	0,031050089
3703_at	STT3A	8,069	7,862	-0,207	-3,469	0,000732809	0,031081263
81553_at	FAM49A	7,846	8,066	0,219	3,468	0,00073379	0,031081263
8396_at	PIP4K2B	5,914	5,767	-0,147	-3,469	0,000731856	0,031081263
50862_at	RNF141	7,517	7,836	0,319	3,465	0,000741885	0,031262037
6626_at	SNRPA	4,494	4,392	-0,102	-3,465	0,000740754	0,031262037
96459_at	FNIP1	7,605	7,840	0,235	3,465	0,000741916	0,031262037
8668_at	EIF3I	7,964	7,706	-0,257	-3,464	0,000744762	0,031327676
116729_at	PPP1R27	3,785	3,843	0,058	3,463	0,000748244	0,031419803
550113_at	LOC550113	3,535	3,593	0,059	3,462	0,000750554	0,031462431
10553_at	HTATIP2	6,119	6,326	0,207	3,461	0,000752724	0,031499098
284067_at	C17orf105	3,473	3,519	0,046	3,459	0,00075821	0,03156567
7048_at	TGFBR2	8,093	8,266	0,172	3,459	0,00075764	0,03156567
9423_at	NTN1	4,775	4,646	-0,129	-3,459	0,000756706	0,03156567
401093_at	MBNL1-AS1	5,563	5,387	-0,176	-3,458	0,000760205	0,031594645
23095_at	KIF1B	5,364	5,651	0,287	3,453	0,000772643	0,03197024
29802_at	VPREB3	4,549	4,398	-0,151	-3,453	0,00077338	0,03197024
51466_at	EVL	5,535	5,391	-0,144	-3,452	0,000774502	0,03197024
54778_at	RNF111	5,771	5,955	0,184	3,453	0,000773627	0,03197024
54539_at	NDUFB11	7,482	7,221	-0,261	-3,451	0,000777234	0,032028626
54807_at	ZNF586	6,395	6,562	0,168	3,450	0,000779549	0,032069682
2870_at	GRK6	4,766	4,872	0,106	3,449	0,00078321	0,032165844
	LOC101927						
101927048_at	048	3,536	3,478	-0,059	-3,444	0,000796965	0,032501721
127833_at	SYT2	4,396	4,502	0,106	3,443	0,000798072	0,032501721
27141_at	CIDEB	5,816	6,045	0,229	3,444	0,000797474	0,032501721
286467_at	FIRRE	3,698	3,639	-0,059	-3,445	0,00079466	0,032501721
6421_at	SFPQ	8,762	8,558	-0,204	-3,445	0,00079324	0,032501721
56139_at	PCDHA10	3,670	3,617	-0,054	-3,442	0,0008006	0,032550142
101929212_at	SMIM2-AS1	3,596	3,653	0,057	3,441	0,000805475	0,032693699
51052_at	PRLH	5,251	5,036	-0,216	-3,440	0,000808284	0,032753015
140258_at	KRTAP13-1	3,627	3,548	-0,079	-3,438	0,000811853	0,032842896
255488_at	RNF144B	7,268	7,536	0,268	3,437	0,000815009	0,032915801
1396_at	CRIP1	7,510	7,234	-0,276	-3,436	0,000818239	0,032936831
390940_at	PINLYP	3,984	4,092	0,108	3,436	0,000817153	0,032936831
22849_at	CPEB3	4,106	4,220	0,114	3,433	0,000827435	0,033058445
25978_at	CHMP2B	5,870	6,134	0,264	3,432	0,000828107	0,033058445
51105_at	PHF20L1	6,967	7,192	0,226	3,433	0,000825799	0,033058445
5892_at	RAD51D	4,987	4,869	-0,118	-3,432	0,000827715	0,033058445
6472_at	SHMT2	5,350	5,210	-0,140	-3,432	0,000829418	0,033058445
690_at	BTF3P11	3,441	3,506	0,064	3,433	0,000826189	0,033058445
27018_at	BEX3	4,815	4,679	-0,136	-3,431	0,000831203	0,033075342
51433_at	ANAPC5	6,043	5,915	-0,128	-3,430	0,000834565	0,033079229
54536_at	EXOC6	5,690	6,007	0,317	3,430	0,000835382	0,033079229
79781_at	IQCA1	3,610	3,577	-0,033	-3,430	0,000833323	0,033079229
100507316_at	MINCR	4,451	4,321	-0,130	-3,424	0,000852564	0,033548073
	LOC102724						
102724612_at	612	3,490	3,551	0,061	3,425	0,000849679	0,033548073
1353_at	COX11	4,441	4,345	-0,096	-3,424	0,000852358	0,033548073
9462_at	RASAL2	3,865	3,824	-0,041	-3,424	0,000852742	0,033548073
79863_at	RBFA	4,487	4,408	-0,079	-3,423	0,000854786	0,033574152
727993_at	LOC727993	4,025	4,135	0,109	3,420	0,000864246	0,033890985
821_at	CANX	9,363	9,218	-0,145	-3,419	0,000867022	0,033945101
220004_at	PPP1R32	4,539	4,641	0,102	3,418	0,000868707	0,033956387
101927084_at	LINC01359	3,613	3,700	0,087	3,417	0,000872778	0,034060743
	LOC101928						
101928894_at	894	4,178	4,305	0,126	3,415	0,00087684	0,034164436
3454_at	IFNAR1	7,034	7,334	0,300	3,413	0,000883074	0,034235695

Appendix

4773_at	NFATC2	5,907	5,690	-0,218	-3,413	0,000884301	0,034235695
526_at	ATP6V1B2	9,912	10,058	0,146	3,413	0,000883731	0,034235695
606495_at	CYB5RL	4,355	4,272	-0,083	-3,413	0,000882993	0,034235695
9818_at	NUP58	6,419	6,622	0,203	3,411	0,000888778	0,034354294
100130155_at	MIR124-2HG	3,476	3,521	0,045	3,409	0,000894888	0,03453557
84253_at	GARNL3	3,775	3,733	-0,042	-3,408	0,000898373	0,034560335
84658_at	ADGRE3	8,614	8,994	0,380	3,408	0,000897341	0,034560335
100507266_at	STX18-AS1	4,339	4,216	-0,124	-3,405	0,000907124	0,034841884
100506134_at	TTC21B-AS1	3,759	3,897	0,139	3,404	0,000910462	0,034914908
5437_at	POLR2H	6,018	5,816	-0,203	-3,402	0,000915712	0,035060958
101928773_at	LINC01449	3,421	3,462	0,041	3,402	0,000917621	0,035078821
57458_at	TMCC3	5,676	5,959	0,284	3,401	0,000920238	0,035123626
9908_at	G3BP2	6,413	6,280	-0,133	-3,400	0,000921963	0,035134295
7084_at	TK2	4,535	4,658	0,123	3,399	0,000925017	0,035195517
55175_at	KLHL11	5,652	5,433	-0,219	-3,398	0,000927399	0,035231013
90673_at	PPP1R3E	4,887	4,770	-0,118	-3,398	0,000929135	0,035241914
81704_at	DOCK8	8,247	8,459	0,213	3,397	0,000932874	0,035328622
23468_at	CBX5	6,963	6,733	-0,230	-3,396	0,000936082	0,035394962
204801_at	NLRP11	3,565	3,535	-0,029	-3,394	0,000941063	0,035418068
5023_at	P2RX1	4,871	5,033	0,162	3,394	0,000940557	0,035418068
84148_at	KAT8	4,888	4,999	0,110	3,394	0,000941034	0,035418068
255725_at	OR52B2	3,990	4,164	0,174	3,393	0,000945007	0,035511527
220929_at	ZNF438	4,854	5,158	0,304	3,391	0,000949027	0,03555269
7507_at	XPA	5,950	5,748	-0,202	-3,391	0,000948938	0,03555269
84859_at	LRCH3	6,465	6,316	-0,149	-3,390	0,000952817	0,035639765
1521_at	CTSW	6,815	6,449	-0,366	-3,388	0,00095889	0,035811825
26502_at	NARF	6,052	6,232	0,179	3,387	0,000964105	0,035951345
284756_at	C20orf197	4,406	4,510	0,105	3,385	0,000971024	0,03609863
57096_at	RPGRIP1	3,774	3,847	0,073	3,385	0,000969957	0,03609863
10204_at	NUTF2	5,009	4,906	-0,103	-3,383	0,000976111	0,036182945
9025_at	RNF8	4,647	4,492	-0,155	-3,383	0,000977228	0,036182945
9677_at	PPIP5K1	4,432	4,330	-0,102	-3,382	0,000977757	0,036182945
347918_at	EP400NL	4,162	4,082	-0,080	-3,381	0,000982433	0,036300742
10330_at	CNPY2	5,286	5,126	-0,160	-3,378	0,000991083	0,036564785
147991_at	DPY19L3	4,478	4,767	0,289	3,370	0,001017747	0,037491652
26959_at	HBP1	7,992	8,180	0,188	3,369	0,001021048	0,037556335
10921_at	RNPS1	4,529	4,435	-0,094	-3,368	0,001025448	0,037614371
158158_at	RASEF	3,639	3,605	-0,034	-3,368	0,00102572	0,037614371
55350_at	VNN3	6,024	6,447	0,423	3,366	0,001032759	0,03775859
8218_at	CLTCL1	4,002	4,066	0,065	3,366	0,001031661	0,03775859
6619_at	SNAPC3	6,767	6,566	-0,201	-3,365	0,001034329	0,03775922
100130872_at	LOC100130872	5,040	4,856	-0,184	-3,363	0,001042936	0,037808222
116362_at	RBP7	6,736	7,202	0,467	3,365	0,001037435	0,037808222
127124_at	ATP6V1G3	3,418	3,460	0,042	3,364	0,001040376	0,037808222
3384_at	ICAM2	4,885	4,789	-0,096	-3,363	0,001043447	0,037808222
57658_at	CALCOCO1	4,975	5,115	0,140	3,364	0,001040539	0,037808222
10612_at	TRIM3	4,397	4,343	-0,054	-3,359	0,001055785	0,038111105
284391_at	ZNF844	3,890	4,044	0,154	3,359	0,001054874	0,038111105
7053_at	TGM3	4,203	4,320	0,117	3,359	0,001056508	0,038111105
5165_at	PDK3	6,339	6,597	0,258	3,356	0,001066062	0,038398759
283385_at	MORN3	4,190	4,277	0,086	3,355	0,001069972	0,038482584
140803_at	TRPM6	5,151	5,584	0,433	3,353	0,001078379	0,038556798
1588_at	CYP19A1	3,509	3,541	0,032	3,353	0,001076305	0,038556798
5236_at	PGM1	4,312	4,448	0,136	3,353	0,001077653	0,038556798
83442_at	SH3BGL3	8,213	7,968	-0,245	-3,354	0,001075326	0,038556798
64645_at	MFSD14A	6,796	7,030	0,234	3,352	0,001081689	0,038618374
5613_at	PRKX	6,097	5,966	-0,131	-3,351	0,001083881	0,038639896

Appendix

101928232_at	LINC01280	4,013	4,202	0,189	3,350	0,001087704	0,03866279
285335_at	SLC9C1	3,350	3,368	0,018	3,350	0,001087411	0,03866279
80012_at	PHC3	8,022	7,861	-0,161	-3,348	0,001093915	0,03882678
51530_at	ZC3HC1	4,522	4,432	-0,090	-3,347	0,001098256	0,038867388
51567_at	TDP2	7,945	8,222	0,277	3,348	0,001096835	0,038867388
3632_at	INPP5A	4,383	4,516	0,134	3,346	0,00110133	0,03889967
9654_at	TTLL4	4,945	5,118	0,173	3,346	0,001102368	0,03889967
	LOC100506						
100506470_at	470	4,114	3,959	-0,155	-3,345	0,001106609	0,038992729
26578_at	OSTF1	8,775	8,944	0,169	3,344	0,001110164	0,039061391
26152_at	ZNF337	4,917	4,817	-0,100	-3,342	0,001118255	0,039232511
28970_at	C11orf54	5,784	6,058	0,274	3,342	0,001117785	0,039232511
10981_at	RAB32	6,232	6,428	0,196	3,340	0,001123408	0,039299889
401494_at	HACD4	6,644	6,916	0,272	3,340	0,001122952	0,039299889
10898_at	CPSF4	4,578	4,488	-0,090	-3,338	0,001133017	0,039579093
246175_at	CNOT6L	8,259	8,081	-0,178	-3,336	0,001139195	0,039737796
102800310_at	HAGLROS	3,823	3,987	0,164	3,335	0,001143616	0,039834876
57696_at	DDX55	4,624	4,495	-0,129	-3,334	0,001146431	0,039875779
51727_at	CMPK1	5,935	5,778	-0,156	-3,330	0,001161407	0,040338977
64756_at	ATPAF1	5,132	4,995	-0,137	-3,326	0,001176094	0,040790836
677823_at	SNORA80E	5,649	5,975	0,326	3,325	0,001179803	0,040861166
241_at	ALOX5AP	9,133	9,428	0,296	3,323	0,001188181	0,041064602
79885_at	HDAC11	4,272	4,192	-0,080	-3,323	0,001189054	0,041064602
80339_at	PNPLA3	4,066	3,999	-0,068	-3,322	0,00119289	0,041138618
135935_at	NOBOX	4,060	4,120	0,060	3,320	0,001200436	0,041340211
10586_at	MAB21L2	4,788	4,627	-0,160	-3,319	0,001206595	0,041430784
1687_at	DFNA5	4,062	4,013	-0,049	-3,317	0,001211586	0,041430784
283951_at	C16orf91	5,230	5,060	-0,170	-3,318	0,001210326	0,041430784
54462_at	CCSER2	5,439	5,220	-0,219	-3,318	0,001209977	0,041430784
64332_at	NFKBIZ	6,791	7,025	0,234	3,317	0,0012112	0,041430784
29916_at	SNX11	5,383	5,566	0,183	3,316	0,001216903	0,041495869
51099_at	ABHD5	9,233	9,481	0,249	3,316	0,001216144	0,041495869
9051_at	PSTPIP1	5,330	5,494	0,164	3,315	0,001218719	0,041499613
51398_at	WDR83OS	7,312	7,111	-0,202	-3,314	0,001223325	0,04154007
80896_at	NPL	5,804	6,091	0,287	3,315	0,001222119	0,04154007
3920_at	LAMP2	8,510	8,785	0,275	3,314	0,001225481	0,041555254
254128_at	NIFK-AS1	5,167	5,036	-0,132	-3,312	0,001230799	0,041619509
3482_at	IGF2R	8,016	8,406	0,390	3,313	0,001229404	0,041619509
240_at	ALOX5	6,155	6,461	0,306	3,311	0,001235254	0,041712126
51614_at	ERGIC3	8,379	8,115	-0,264	-3,309	0,001243017	0,04191605
200315_at	APOBEC3A	7,677	8,108	0,431	3,307	0,001253148	0,04214077
6907_at	TBL1X	5,266	5,493	0,227	3,307	0,0012523	0,04214077
7014_at	TERF2	5,426	5,308	-0,118	-3,305	0,001262188	0,042386144
100131980_at	ZNF705G	3,612	3,722	0,111	3,303	0,001267562	0,042390962
10140_at	TOB1	7,368	7,202	-0,166	-3,304	0,001267084	0,042390962
10912_at	GADD45G	4,103	4,020	-0,082	-3,304	0,001264736	0,042390962
	LOC105376						
105376875_at	875	4,051	4,282	0,231	3,300	0,001280785	0,042460178
27284_at	SULT1B1	7,238	7,717	0,479	3,301	0,001276592	0,042460178
3952_at	LEP	3,990	4,085	0,095	3,302	0,001274807	0,042460178
3983_at	ABLIM1	5,408	5,225	-0,184	-3,300	0,001281856	0,042460178
81688_at	C6orf62	8,559	8,440	-0,118	-3,301	0,001276637	0,042460178
81846_at	SBF2	5,727	5,987	0,260	3,300	0,001280238	0,042460178
8562_at	DENR	6,169	5,963	-0,207	-3,302	0,001273973	0,042460178
	LOC101927						
101927196_at	196	3,484	3,554	0,070	3,292	0,001314695	0,043311912
4051_at	CYP4F3	6,730	7,138	0,408	3,293	0,001309822	0,043311912
64753_at	CCDC136	4,033	3,979	-0,054	-3,292	0,001313557	0,043311912
7351_at	UCP2	8,317	8,058	-0,259	-3,293	0,001312317	0,043311912
130013_at	ACMSD	3,604	3,643	0,039	3,291	0,001318263	0,043312078

Appendix

25873_at	RPL36	5,663	5,472	-0,191	-3,292	0,001316761	0,043312078
340156_at	MYLK4	4,427	4,344	-0,083	-3,290	0,00132269	0,043398857
100500829_at	MIR3943	4,078	3,899	-0,180	-3,289	0,001329121	0,043444763
154386_at	LINC01600	3,768	3,861	0,093	3,289	0,001328192	0,043444763
2649_at	NR6A1	4,175	4,257	0,082	3,289	0,001329449	0,043444763
1486_at	CTBS	7,789	8,028	0,239	3,288	0,001334189	0,043541126
94107_at	TMEM203	5,887	5,676	-0,210	-3,286	0,001339969	0,043671134
5272_at	SERPINB9	6,043	5,797	-0,246	-3,285	0,001345492	0,043792417
9686_at	VGLL4	4,826	4,740	-0,086	-3,283	0,001355492	0,044058936
6138_at	RPL15	7,652	7,460	-0,192	-3,282	0,001357835	0,044076145
2534_at	FYN	8,228	7,988	-0,239	-3,281	0,001361478	0,04413549
9839_at	ZEB2	6,607	6,485	-0,123	-3,281	0,001365108	0,044194242
22856_at	CHSY1	5,434	5,607	0,173	3,280	0,001368643	0,044249765
115426_at	UHRF2	6,031	5,828	-0,203	-3,279	0,001372864	0,044313976
116534_at	MRGPRES	4,651	4,870	0,219	3,276	0,00138402	0,044313976
2135_at	EXTL2	3,728	3,645	-0,083	-3,276	0,001383959	0,044313976
23360_at	FNBP4	6,042	5,834	-0,209	-3,278	0,00137528	0,044313976
3205_at	HOXA9	4,782	4,640	-0,142	-3,278	0,001378013	0,044313976
4818_at	NKG7	9,747	9,256	-0,491	-3,276	0,001385969	0,044313976
503538_at	A1BG-AS1	3,986	3,895	-0,091	-3,276	0,001387033	0,044313976
80067_at	DCAF17	4,894	4,758	-0,136	-3,277	0,001380334	0,044313976
81577_at	GFOD2	4,025	4,102	0,077	3,277	0,001381335	0,044313976
11235_at	PDCD10	7,386	7,186	-0,201	-3,275	0,001392242	0,044363807
1129_at	CHRM2	3,583	3,626	0,043	3,275	0,001391079	0,044363807
	LOC105375						
105375110_at	110	4,139	4,332	0,193	3,274	0,001395562	0,04441138
101409254_at	LINC00681	3,574	3,686	0,112	3,273	0,001399977	0,044493637
101927821_at	LINC01425	3,531	3,605	0,073	3,272	0,001405715	0,044559515
6224_at	RPS20	7,075	6,744	-0,331	-3,272	0,001405242	0,044559515
10938_at	EHD1	4,617	4,697	0,079	3,270	0,001411668	0,04468994
602_at	BCL3	5,090	5,296	0,206	3,270	0,001414633	0,044725596
9296_at	ATP6V1F	8,183	7,915	-0,267	-3,269	0,001419184	0,044811181
5036_at	PA2G4	9,073	8,853	-0,220	-3,268	0,001421196	0,044816528
10432_at	RBM14	5,027	4,893	-0,134	-3,267	0,001425375	0,04489008
388759_at	C1orf229	4,251	4,389	0,138	3,265	0,001433941	0,045101441
23062_at	GGA2	5,622	5,503	-0,119	-3,264	0,001442419	0,045309483
7203_at	CCT3	6,015	5,849	-0,166	-3,263	0,001445103	0,045335226
2237_at	FEN1	6,204	5,972	-0,232	-3,260	0,001457011	0,045635132
353323_at	KRTAP12-2	5,034	4,800	-0,235	-3,260	0,001458417	0,045635132
4600_at	MX2	7,189	7,475	0,286	3,259	0,001464083	0,045753539
645682_at	POU5F1P4	5,138	5,357	0,218	3,258	0,001468566	0,04583472
10327_at	AKR1A1	5,472	5,340	-0,132	-3,255	0,001483515	0,046117667
126231_at	ZNF573	3,980	3,870	-0,110	-3,255	0,001484551	0,046117667
79829_at	NAA40	4,440	4,343	-0,097	-3,255	0,001481404	0,046117667
9187_at	SLC24A1	4,361	4,299	-0,062	-3,255	0,001485219	0,046117667
101926950_at	LINC01570	4,406	4,271	-0,135	-3,253	0,001490761	0,046160423
389123_at	IQCF2	3,381	3,430	0,050	3,253	0,001492292	0,046160423
4134_at	MAP4	4,930	4,846	-0,084	-3,253	0,001491822	0,046160423
23530_at	NNT	5,907	5,763	-0,143	-3,252	0,001496814	0,046241462
91694_at	LONRF1	4,279	4,394	0,115	3,251	0,001500765	0,046304702
139067_at	SPANXN3	3,554	3,655	0,101	3,250	0,001505812	0,04640152
25791_at	NGEF	4,123	4,207	0,084	3,248	0,001515499	0,046582653
6583_at	SLC22A4	4,820	5,050	0,230	3,248	0,001515522	0,046582653
51504_at	TRMT112	7,069	6,921	-0,148	-3,245	0,001529637	0,046957165
28892_at	IGKV1D-42	3,668	3,566	-0,102	-3,244	0,001534535	0,046962093
4726_at	NDUFS6	8,028	7,813	-0,214	-3,244	0,001535593	0,046962093
57567_at	ZNF319	4,217	4,353	0,135	3,244	0,001535435	0,046962093
10541_at	ANP32B	9,275	9,028	-0,247	-3,243	0,001542828	0,047124105
3738_at	KCNA3	6,537	6,298	-0,239	-3,239	0,00155912	0,047561958

Appendix

3329_at	HSPD1	6,100	5,901	-0,198	-3,238	0,00156648	0,047690232
731789_at	LINC00202-2	3,858	3,918	0,060	3,238	0,001567248	0,047690232
400027_at	LINC00938	5,498	5,303	-0,195	-3,236	0,001578146	0,047961838
102723590_at	BMP7-AS1	4,058	4,184	0,125	3,234	0,001589022	0,04816276
124935_at	SLC43A2	4,849	5,008	0,158	3,233	0,00159286	0,04816276
4552_at	MTRR	6,417	6,210	-0,207	-3,232	0,00159858	0,04816276
64432_at	MRPS25	5,348	5,234	-0,115	-3,233	0,001592529	0,04816276
6503_at	SLA	7,950	8,171	0,221	3,233	0,001590492	0,04816276
84229_at	DRC7	3,894	3,938	0,044	3,232	0,001598177	0,04816276
90693_at	CCDC126	4,846	5,133	0,287	3,232	0,001598624	0,04816276
83544_at	DNAL1	3,577	3,534	-0,043	-3,230	0,001607021	0,048355809
254225_at	RNF169	6,909	7,074	0,165	3,229	0,001610801	0,048409652
133619_at	PRRC1	6,333	6,185	-0,148	-3,226	0,001627002	0,048536573
23358_at	USP24	7,052	6,870	-0,182	-3,228	0,00161952	0,048536573
5686_at	PSMA5	6,709	6,481	-0,228	-3,228	0,00161778	0,048536573
65220_at	NADK	5,463	5,649	0,185	3,226	0,00162695	0,048536573
79027_at	ZNF655	6,769	6,649	-0,120	-3,227	0,001625009	0,048536573
8867_at	SYNJ1	5,675	5,875	0,200	3,227	0,001625038	0,048536573
4942_at	OAT	4,374	4,580	0,206	3,225	0,001631704	0,048617175
22901_at	ARSG	5,246	5,428	0,181	3,225	0,001635543	0,048671932
101927411_at	LOC101927411	4,164	4,257	0,093	3,222	0,001648225	0,048818136
105376353_at	LOC105376353	4,620	4,945	0,325	3,223	0,001643471	0,048818136
25938_at	HEATR5A	4,822	4,987	0,165	3,223	0,001645181	0,048818136
5693_at	PSMB5	4,304	4,200	-0,104	-3,222	0,001649704	0,048818136
7386_at	UQCRFS1	4,694	4,941	0,247	3,222	0,001651012	0,048818136
9046_at	DOK2	5,067	4,917	-0,150	-3,221	0,001652504	0,048818136
148581_at	UBE2U	3,440	3,465	0,025	3,219	0,001665704	0,049128177
23195_at	MDN1	4,654	4,541	-0,114	-3,219	0,00166704	0,049128177
83640_at	FAM103A1	3,646	3,880	0,234	3,218	0,001669517	0,049141599
3142_at	HLX	5,189	5,316	0,127	3,217	0,001676153	0,049277267
100289473_at	LOC100289473	3,936	4,025	0,089	3,214	0,001690841	0,049469826
10550_at	ARL6IP5	8,255	8,075	-0,180	-3,214	0,001690739	0,049469826
54433_at	GAR1	4,759	4,623	-0,136	-3,214	0,001689988	0,049469826
93624_at	TADA2B	4,984	5,140	0,156	3,214	0,001690434	0,049469826
10808_at	HSPH1	5,539	5,273	-0,266	-3,213	0,001694555	0,0495189
10333_at	TLR6	6,995	7,345	0,350	3,213	0,001699337	0,049599005
11247_at	NXPH4	4,366	4,286	-0,080	-3,212	0,001704708	0,049666481
9031_at	BAZ1B	6,267	6,100	-0,167	-3,211	0,001705734	0,049666481
100996573_at	LOC100996573	4,194	4,424	0,230	3,210	0,001711278	0,049708832
64854_at	USP46	3,993	3,927	-0,066	-3,211	0,00171034	0,049708832

5.1.3 Supplementary Table III-2a: ES and rank scores for genes in the osteoclast differentiation pathway

PROBE	GENE SYMBOL	GENE TITLE	RANK IN GENE LIST	RANK METRIC SCORE	RUNNING ES
3554	IL1R1	interleukin 1 receptor type 1	65	0.171	0.03331613
5608	MAP2K6	mitogen-activated protein kinase 6	138	0.141	0.059910223
353514	LILRA5	leukocyte immunoglobulin like receptor A5	147	0.136	0.088175714
1432	MAPK14	mitogen-activated protein kinase 14	166	0.131	0.1149766
79168	LILRA6	leukocyte immunoglobulin like receptor A6	176	0.130	0.14188443
11027	LILRA2	leukocyte immunoglobulin like receptor A2	189	0.128	0.1681944
2353	FOS	FBJ murine osteosarcoma viral oncogene homolog	196	0.126	0.1944211
9846	GAB2	GRB2 associated binding protein 2	300	0.109	0.21313561
4689	NCF4	neutrophil cytosolic factor 4	303	0.109	0.23599717
3454	IFNAR1	interferon alpha and beta receptor subunit 1	348	0.104	0.2560934
5336	PLCG2	phospholipase C gamma 2	378	0.101	0.276099
3460	IFNGR2	interferon gamma receptor 2 (interferon gamma transducer 1)	620	0.084	0.28368548
7040	TGFB1	transforming growth factor beta 1	628	0.083	0.3008908
1147	CHUK	conserved helix-loop-helix ubiquitous kinase	633	0.083	0.31816998
3553	IL1B	interleukin 1 beta	831	0.074	0.32554778
2355	FOSL2	FOS like antigen 2	875	0.072	0.33900252
5595	MAPK3	mitogen-activated protein kinase 3	938	0.070	0.35114598
5971	RELB	v-rel avian reticuloendotheliosis viral oncogene homolog B	998	0.068	0.3629658
11025	LILRB3	leukocyte immunoglobulin like receptor B3	1007	0.068	0.37683624
10326	SIRPB1	signal regulatory protein beta 1	1083	0.065	0.38731176
2213	FCGR2B	Fc fragment of IgG receptor IIb	1260	0.059	0.39250892
3726	JUNB	jun B proto-oncogene	1424	0.056	0.39744228
11024	LILRA1	leukocyte immunoglobulin like receptor A1	1428	0.055	0.40898195
3455	IFNAR2	interferon alpha and beta receptor subunit 2	1451	0.055	0.4196273
7048	TGFBR2	transforming growth factor beta receptor II	1622	0.051	0.42340788
4688	NCF2	neutrophil cytosolic factor 2	1718	0.050	0.42992634
5879	RAC1	ras-related C3 botulinum toxin substrate 1 (rho family, small GTP binding protein Rac1)	1847	0.048	0.4346525
10288	LILRB2	leukocyte immunoglobulin like receptor B2	1864	0.048	0.44397527
9021	SOCS3	suppressor of cytokine signaling 3	1868	0.047	0.45382264
126014	OSCAR	osteoclast associated immunoglobulin-like receptor	1875	0.047	0.46352413
6688	SPI1	Spi-1 proto-oncogene	1892	0.047	0.472775
5603	MAPK13	mitogen-activated protein kinase 13	2005	0.046	0.47772962
4791	NFKB2	nuclear factor of kappa light polypeptide gene enhancer in B-	2331	0.041	0.4729852

cells 2					
5594	MAPK1	mitogen-activated protein kinase 1	2386	0.041	0.47931698
5530	PPP3CA	protein phosphatase 3 catalytic subunit alpha	2388	0.041	0.48783866
140885	SIRPA	signal regulatory protein alpha	2443	0.040	0.4940357
207	AKT1	v-akt murine thymoma viral oncogene homolog 1	2494	0.040	0.50027627
2885	GRB2	growth factor receptor bound protein 2	2495	0.040	0.50858384
5290	PIK3CA	phosphatidylinositol-4,5-bisphosphate 3-kinase catalytic subunit alpha	2875	0.036	0.5003934
5294	PIK3CG	phosphatidylinositol-4,5-bisphosphate 3-kinase catalytic subunit gamma	2905	0.035	0.5066097
3459	IFNGR1	interferon gamma receptor 1	2912	0,035	0.5137642
5291	PIK3CB	phosphatidylinositol-4,5-bisphosphate 3-kinase catalytic subunit beta	3347	0.031	0.5023933
695	BTK	Bruton tyrosine kinase	3363	0.031	0.50832057
6850	SYK	spleen tyrosine kinase	3543	0.030	0.5072015
23533	PIK3R5	phosphoinositide-3-kinase regulatory subunit 5	3572	0.030	0.5122718
4792	NFKBIA	NFKB inhibitor alpha	3611	0.029	0.51688164
23118	TAB2	TGF-beta activated kinase 1/MAP3K7 binding protein 2	3759	0.028	0.5167917
11006	LILRB4	leukocyte immunoglobulin like receptor B4	4079	0.026	0.50916827
3552	IL1A	interleukin 1 alpha	4735	0.023	0.48688638
5293	PIK3CD	phosphatidylinositol-4,5-bisphosphate 3-kinase catalytic subunit delta	4877	0.022	0.48569188
1436	CSF1R	colony stimulating factor 1 receptor	4895	0.022	0.48961207
1435	CSF1	colony stimulating factor 1	5131	0.021	0.48429412
2212	FCGR2A	Fc fragment of IgG receptor IIa	5183	0.021	0.48653117
2354	FOSB	FBJ murine osteosarcoma viral oncogene homolog B	5227	0.020	0.489058
1513	CTSK	cathepsin K	5313	0.020	0.4897568
23547	LILRA4	leukocyte immunoglobulin like receptor A4	5338	0.020	0.49295676
6773	STAT2	signal transducer and activator of transcription 2	5357	0.020	0.4963886
8600	TNFSF11	tumor necrosis factor superfamily member 11	5429	0.020	0.49756795
7124	TNF	tumor necrosis factor	5491	0.019	0.49910983
8517	IKBKG	inhibitor of kappa light polypeptide gene enhancer in B-cells. kinase gamma	5925	0.018	0.4848992
7132	TNFRSF1A	tumor necrosis factor receptor superfamily member 1A	6076	0.017	0.48227096
10859	LILRB1	leukocyte immunoglobulin like receptor B1	6626	0.015	0.46270847
5602	MAPK10	mitogen-activated protein kinase 10	6914	0.014	0.45378423
9020	MAP3K14	mitogen-activated protein kinase kinase kinase 14	7306	0.013	0.44028223
5468	PPARG	peroxisome proliferator activated receptor gamma	7382	0.012	0.4397952
7297	TYK2	tyrosine kinase 2	7497	0.012	0.4376258
5296	PIK3R2	phosphoinositide-3-kinase regulatory subunit 2	8233	0.010	0.4093378

7046	TGFBR1	transforming growth factor beta receptor I	8247	0.010	0.41089284
54	ACP5	acid phosphatase 5, tartrate resistant	8331	0.010	0.40949705
5604	MAP2K1	mitogen-activated protein kinase kinase 1	8566	0.009	0.4017148
1536	CYBB	cytochrome b-245, beta polypeptide	8994	0.008	0.38569617
3716	JAK1	Janus kinase 1	9242	0.007	0.37696484
27035	NOX1	NADPH oxidase 1	9245	0.007	0.37836218
6772	STAT1	signal transducer and activator of transcription 1	9809	0.006	0.35626137
7189	TRAF6	TNF receptor associated factor 6	10091	0.005	0.34565714
10990	LILRB5	leukocyte immunoglobulin like receptor B5	10289	0.004	0.33840805
10454	TAB1	TGF-beta activated kinase 1/MAP3K7 binding protein 1	10722	0.003	0.32122055
4286	MITF	microphthalmia-associated transcription factor	10752	0.003	0.3206776
3937	LCP2	lymphocyte cytosolic protein 2	11148	0.002	0.30478245
5609	MAP2K7	mitogen-activated protein kinase kinase 7	11217	0.002	0.30236506
5970	RELA	v-rel avian reticuloendotheliosis viral oncogene homolog A	11324	0.002	0.29832092
50508	NOX3	NADPH oxidase 3	11453	0.001	0.29330757
799	CALCR	calcitonin receptor	11690	676501775160.431	0.28369245
7305	TYROBP	TYRO protein tyrosine kinase binding protein	11734	580195977818.220	0.28203657
5534	PPP3R1	protein phosphatase 3 regulatory subunit B, alpha	12668	-0.002	0.24382015
7186	TRAF2	TNF receptor associated factor 2	12718	-0.002	0.24217357
5601	MAPK9	mitogen-activated protein kinase 9	12958	-0.002	0.23281395
1535	CYBA	cytochrome b-245, alpha polypeptide	13154	-0.003	0.22538179
5599	MAPK8	mitogen-activated protein kinase 8	13156	-0.003	0.22597149
5532	PPP3CB	protein phosphatase 3 catalytic subunit beta	13268	-0.003	0.22207832
4772	NFATC1	nuclear factor of activated T-cells, cytoplasmic, calcineurin-dependent 1	13278	-0.003	0.22240824
3551	IKBKB	inhibitor of kappa light polypeptide gene enhancer in B-cells, kinase beta	13462	-0.004	0.21565863
8792	TNFRSF11A	tumor necrosis factor receptor superfamily member 11a	13917	-0.005	0.19794624
10379	IRF9	interferon regulatory factor 9	14897	-0.008	0.15908806
3725	JUN	jun proto-oncogene	15414	-0.009	0.13970372
2214	FCGR3A	Fc fragment of IgG receptor IIIa	15528	-0.010	0.13704884
5535	PPP3R2	protein phosphatase 3 regulatory subunit B, beta	15735	-0.010	0.13069208
4790	NFKB1	nuclear factor of kappa light polypeptide gene enhancer in B-cells 1	16234	-0.012	0.11257468
208	AKT2	v-akt murine thymoma viral oncogene homolog 2	16396	-0.012	0.10849883
1540	CYLD	CYLD lysine 63 deubiquitinase	16402	-0.012	0.11088098
6300	MAPK12	mitogen-activated protein kinase 12	16696	-0.013	0.101556025
1385	CREB1	cAMP responsive element binding protein 1	16888	-0.014	0.09659159
7042	TGFB2	transforming growth factor beta 2	17253	-0.015	0.08476528

4982	TNFRSF11B	tumor necrosis factor receptor superfamily member 11b	18244	-0.019	0.047831133
5600	MAPK11	mitogen-activated protein kinase 11	18296	-0.019	0.049762312
8061	FOSL1	FOS like antigen 1	18329	-0.019	0.05251048
54209	TREM2	triggering receptor expressed on myeloid cells 2	18434	-0.020	0.05238389
8878	SQSTM1	sequestosome 1	18660	-0.021	0.047468197
3690	ITGB3	integrin subunit beta 3	18670	-0.021	0.05149536
3456	IFNB1	interferon, beta 1, fibroblast suppressor of cytokine signaling 1	18854	-0.022	0.04850237
8651	SOCS1		18962	-0.022	0.04874891
2274	FHL2	four and a half LIM domains 2	19338	-0.024	0.038252965
29760	BLNK	B-cell linker	20260	-0.029	0.006221308
8503	PIK3R3	phosphoinositide-3-kinase regulatory subunit 3	20858	-0.033	-0.011581848
6885	MAP3K7	mitogen-activated protein kinase kinase 7	21388	-0.037	-0.025740072
5533	PPP3CC	protein phosphatase 3 catalytic subunit gamma	21783	-0.040	-0.03358892
7006	TEC	tec protein tyrosine kinase	22629	-0.050	-0.05809652
3458	IFNG	interferon, gamma	22656	-0.050	-0.04864443
814	CAMK4	calcium/calmodulin-dependent protein kinase IV	22717	-0.051	-0.040421534
3727	JUND	jun D proto-oncogene	22846	-0.053	-0.034606956
55423	SIRPG	signal regulatory protein gamma	23277	-0.060	-0.039750647
5295	PIK3R1	phosphoinositide-3-kinase regulatory subunit 1	23370	-0.063	-0.030401625
3932	LCK	LCK proto-oncogene, Src family tyrosine kinase	23498	-0.066	-0.02180087
2534	FYN	FYN proto-oncogene, Src family tyrosine kinase	23689	-0.072	-0.014592583
4773	NFATC2	nuclear factor of activated T-cells, cytoplasmic, calcineurin-dependent 2	24078	-0.091	-0.011586786
10000	AKT3	v-akt murine thymoma viral oncogene homolog 3	24179	-0.101	0.005498807

5.1.4 Supplementary Table III-2b: Es and rank scores for genes in the MAP kinase signaling pathway

PROBE	GENE SYMBOL	GENE TITLE	RANK IN GENE LIST	RANK METRIC SCORE	RUNNING ES
3554	IL1R1	interleukin 1 receptor type 1	65	0,171	0.020782057
5608	MAP2K6	mitogen-activated protein kinase kinase 6	138	0.141	0.0370774
7850	IL1R2	interleukin 1 receptor type 2	143	0.138	0.055797216
1432	MAPK14	mitogen-activated protein kinase 14	166	0.131	0.07284942
2353	FOS	FBJ murine osteosarcoma viral oncogene homolog	196	0.126	0.08891255
6655	SOS2	SOS Ras/Rho guanine nucleotide exchange factor 2	218	0.121	0.104645476
4215	MAP3K3	mitogen-activated protein kinase kinase kinase 3	286	0.111	0.11709238
4217	MAP3K5	mitogen-activated protein kinase kinase kinase 5	294	0.110	0.13186273
1843	DUSP1	dual specificity phosphatase 1	359	0.103	0.1433498
6416	MAP2K4	mitogen-activated protein kinase kinase 4	418	0.099	0.15444621
9693	RAPGEF2	Rap guanine nucleotide exchange factor 2	505	0.091	0.16338848
10746	MAP3K2	mitogen-activated protein kinase kinase kinase 2	570	0.086	0.17257577
7040	TGFB1	transforming growth factor beta 1	628	0.083	0.18161775
1147	CHUK	conserved helix-loop-helix ubiquitous kinase	633	0.083	0.19282994
9448	MAP4K4	mitogen-activated protein kinase kinase kinase kinase 4	653	0.082	0.20326643
9252	RPS6KA5	ribosomal protein S6 kinase A5	659	0.082	0.21423402
785	CACNB4	calcium voltage-gated channel auxiliary subunit beta 4	662	0.081	0.22530486
115727	RASGRP4	RAS guanyl releasing protein 4	751	0.077	0.23226441
5058	PAK1	p21 protein (Cdc42/Rac)-activated kinase 1	801	0.075	0.24050967
3553	IL1B	interleukin 1 beta	831	0.074	0.24942917
5595	MAPK3	mitogen-activated protein kinase 3	938	0.070	0.25461605
5971	RELB	v-rel avian reticuloendotheliosis viral oncogene homolog B	998	0.068	0.26146445
1845	DUSP3	dual specificity phosphatase 3	1047	0.066	0.26854336
5894	RAF1	Raf-1 proto-oncogene, serine/threonine kinase	1185	0.062	0.27131084
9261	MAPKAPK2	mitogen-activated protein kinase-activated protein kinase 2	1187	0.062	0.27971923
3310	HSPA6	heat shock protein family A (Hsp70) member 6	1257	0.059	0.28500193
4763	NF1	neurofibromin 1	1590	0.052	0.27833423
7048	TGFBR2	transforming growth factor beta receptor II	1622	0.051	0.28409615
8569	MKMK1	MAP kinase interacting serine/threonine kinase 1	1744	0.049	0.28582168
5879	RAC1	ras-related C3 botulinum toxin substrate 1 (rho family, small GTP binding protein Rac1)	1847	0.048	0.28811663
8822	FGF17	fibroblast growth factor 17	2001	0.046	0.2880137

51776	ZAK	sterile alpha motif and leucine zipper containing kinase AZK	2003	0.046	0.29422808
5603	MAPK13	mitogen-activated protein kinase 13	2005	0.046	0.30043858
2872	MKNK2	MAP kinase interacting serine/threonine kinase 2	2024	0.045	0.30591595
1649	DDIT3	DNA damage inducible transcript 3	2093	0.044	0.30917093
8649	LAMTOR3	late endosomal/lysosomal adaptor, MAPK and MTOR activator 3	2151	0.044	0.3127749
5606	MAP2K3	mitogen-activated protein kinase kinase 3	2165	0.043	0.31818688
4791	NFKB2	nuclear factor of kappa light polypeptide gene enhancer in B-cells 2	2331	0.041	0.31699857
4616	GADD45B	growth arrest and DNA damage inducible beta	2381	0.041	0.32055372
5594	MAPK1	mitogen-activated protein kinase 1	2386	0.041	0.3259737
5530	PPP3CA	protein phosphatase 3 catalytic subunit alpha	2388	0.041	0.33151746
3305	HSPA1L	heat shock protein family A (Hsp70) member 1 like	2440	0.040	0.33489907
207	AKT1	v-akt murine thymoma viral oncogene homolog 1	2494	0.040	0.338115
2885	GRB2	growth factor receptor bound protein 2	2495	0.040	0.34353375
7867	MAPKAPK3	mitogen-activated protein kinase-activated protein kinase 3	2524	0.039	0.3477451
5495	PPM1B	protein phosphatase, Mg ²⁺ /Mn ²⁺ dependent 1B	2635	0.038	0.34840533
1398	CRK	v-crk avian sarcoma virus CT10 oncogene homolog	2855	0.036	0.3442015
5321	PLA2G4A	phospholipase A2 group IVA	2924	0.035	0.34619147
6788	STK3	serine/threonine kinase 3	3129	0.033	0.34227455
777	CACNA1E	calcium voltage-gated channel subunit alpha1 E	3257	0.032	0.34138742
1326	MAP3K8	mitogen-activated protein kinase kinase kinase 8	3336	0.031	0.3424407
8491	MAP4K3	mitogen-activated protein kinase kinase kinase kinase 3	3688	0.029	0.33181953
23118	TAB2	TGF-beta activated kinase 1/MAP3K7 binding protein 2	3759	0.028	0.33281556
998	CDC42	cell division cycle 42	3976	0.027	0.3275475
100506012	PPP5D1	PPP5 tetratricopeptide repeat domain containing 1	4494	0.024	0.30936128
3552	IL1A	interleukin 1 alpha	4735	0.023	0.30251586
4909	NTF4	neurotrophin 4	4793	0.023	0.30323958
5494	PPM1A	protein phosphatase, Mg ²⁺ /Mn ²⁺ dependent 1A	4811	0.022	0.30561456
5922	RASA2	RAS p21 protein activator 2	4950	0.022	0.30286506
57551	TAOK1	TAO kinase 1	5188	0.021	0.29584628
776	CACNA1D	calcium voltage-gated channel subunit alpha1 D	5260	0.020	0.29568303
6195	RPS6KA1	ribosomal protein S6 kinase A1	5269	0.020	0.2981331
5566	PRKACA	protein kinase cAMP-activated catalytic subunit alpha	5305	0.020	0.29943135
1647	GADD45A	growth arrest and DNA damage inducible alpha	5394	0.020	0.29847705
4914	NTRK1	neurotrophic tyrosine kinase, receptor, type 1	5417	0.020	0.30025205
51347	TAOK3	TAO kinase 3	5455	0.019	0.30138317

7124	TNF	tumor necrosis factor	5491	0.019	0.3025791
5062	PAK2	p21 protein (Cdc42/Rac)-activated kinase 2	5807	0.018	0.2919633
8517	IKBKG	inhibitor of kappa light polypeptide gene enhancer in B-cells, kinase gamma	5925	0.018	0.28950813
5871	MAP4K2	mitogen-activated protein kinase kinase kinase 2	6029	0.017	0.28758138
9064	MAP3K6	mitogen-activated protein kinase kinase kinase 6	6064	0.017	0.28850526
7132	TNFRSF1A	tumor necrosis factor receptor superfamily member 1A	6076	0.017	0.29037887
6789	STK4	serine/threonine kinase 4	6110	0.017	0.29131868
2261	FGFR3	fibroblast growth factor receptor 3	6142	0.017	0.29232207
23162	MAPK8IP3	mitogen-activated protein kinase 8 interacting protein 3	6216	0.016	0.2915352
1852	DUSP9	dual specificity phosphatase 9	6222	0.016	0.29357326
773	CACNA1A	calcium voltage-gated channel subunit alpha1 A	6323	0.016	0.2916168
2318	FLNC	filamin C	6459	0.015	0.28812844
6197	RPS6KA3	ribosomal protein S6 kinase A3	6613	0.015	0.2838213
4137	MAPT	microtubule associated protein tau	6864	0.014	0.2753741
5602	MAPK10	mitogen-activated protein kinase 10	6914	0.014	0.2752562
3304	HSPA1B	heat shock protein family A (Hsp70) member 1B	6916	0.014	0.27713326
22808	MRAS	muscle RAS oncogene homolog	6955	0.014	0.2774519
4214	MAP3K1	mitogen-activated protein kinase kinase kinase 1, E3 ubiquitin protein ligase	6999	0.014	0.2775414
2250	FGF5	fibroblast growth factor 5	7016	0.014	0.2787467
23542	MAPK8IP2	mitogen-activated protein kinase 8 interacting protein 2	7106	0.013	0.27686986
5923	RASGRF1	Ras protein specific guanine nucleotide releasing factor 1	7245	0.013	0.27289912
5536	PPP5C	protein phosphatase 5 catalytic subunit	7261	0.013	0.27403453
9020	MAP3K14	mitogen-activated protein kinase kinase kinase 14	7306	0.013	0.27394313
786	CACNG1	calcium voltage-gated channel auxiliary subunit gamma 1	7332	0.013	0.27462947
123745	PLA2G4E	phospholipase A2 group IVE	7375	0.012	0.2745915
779	CACNA1S	calcium voltage-gated channel subunit alpha1 S	7444	0.012	0.27344596
51295	ECSIT	ECSIT signalling integrator	7501	0.012	0.27277595
2264	FGFR4	fibroblast growth factor receptor 4	7521	0.012	0.27363333
255189	PLA2G4F	phospholipase A2 group IVF	7725	0.011	0.26675865
7043	TGFB3	transforming growth factor beta 3	7767	0.011	0.2666023
3845	KRAS	Kirsten rat sarcoma viral oncogene homolog	7881	0.011	0.26341197
3303	HSPA1A	heat shock protein family A (Hsp70) member 1A	7924	0.011	0.26315668
6722	SRF	serum response factor	8002	0.011	0.26141968
5579	PRKCB	protein kinase C beta	8045	0.011	0.26111805
27091	CACNG5	calcium voltage-gated channel auxiliary subunit gamma 5	8222	0.010	0.25517792
7046	TGFBR1	transforming growth factor beta receptor I	8247	0.010	0.25554523

1850	DUSP8	dual specificity phosphatase 8	8272	0.010	0.25589928
781	CACNA2D1	calcium voltage-gated channel auxiliary subunit alpha2delta 1	8450	0.009	0.24981655
5604	MAP2K1	mitogen-activated protein kinase kinase 1	8566	0.009	0.24627095
5582	PRKCG	protein kinase C gamma	8656	0.009	0.24377425
5598	MAPK7	mitogen-activated protein kinase 7	8937	0.008	0.23322345
3164	NR4A1	nuclear receptor subfamily 4 group A member 1	9087	0.007	0.22805755
355	FAS	Fas cell surface death receptor	9102	0.007	0.22849573
5159	PDGFRB	platelet derived growth factor receptor beta	9167	0.007	0.22683215
5155	PDGFB	platelet derived growth factor subunit B	9402	0.007	0.21801947
6196	RPS6KA2	ribosomal protein S6 kinase A2	9453	0.006	0.21683216
10369	CACNG2	calcium voltage-gated channel auxiliary subunit gamma 2	9578	0.006	0.21252409
1950	EGF	epidermal growth factor	9891	0.005	0.20028965
5906	RAP1A	RAP1A, member of RAS oncogene family	9912	0.005	0.20018657
5778	PTPN7	protein tyrosine phosphatase, non-receptor type 7	9954	0.005	0.19919538
7189	TRAF6	TNF receptor associated factor 6	10091	0.005	0.19420373
4296	MAP3K11	mitogen-activated protein kinase kinase kinase 11	10155	0.005	0.1922232
7786	MAP3K12	mitogen-activated protein kinase kinase kinase 12	10230	0.004	0.18975316
5801	PTPRR	protein tyrosine phosphatase, receptor type R	10265	0.004	0.18893495
25780	RASGRP3	RAS guanyl releasing protein 3	10428	0.004	0.18274246
1956	EGFR	epidermal growth factor receptor	10477	0.004	0.18126664
2259	FGF14	fibroblast growth factor 14	10495	0.004	0.18107389
2249	FGF4	fibroblast growth factor 4	10589	0.004	0.17768899
2255	FGF10	fibroblast growth factor 10	10657	0.003	0.17536317
59284	CACNG7	calcium voltage-gated channel auxiliary subunit gamma 7	10666	0.003	0.17548849
8823	FGF16	fibroblast growth factor 16	10685	0.003	0.17519331
8605	PLA2G4C	phospholipase A2 group IVC	10702	0.003	0.17497443
10454	TAB1	TGF-beta activated kinase 1/MAP3K7 binding protein 1	10722	0.003	0.17462389
673	BRAF	B-Raf proto-oncogene, serine/threonine kinase	10732	0.003	0.17468572
9344	TAOK2	TAO kinase 2	10905	0.003	0.16790885
778	CACNA1F	calcium voltage-gated channel subunit alpha1 F	11063	0.002	0.16169725
27330	RPS6KA6	ribosomal protein S6 kinase A6	11077	0.002	0.16146623
409	ARRB2	arrestin, beta 2	11155	0.002	0.15854761
5609	MAP2K7	mitogen-activated protein kinase kinase 7	11217	0.002	0.15626918
4342	MOS	v-mos Moloney murine sarcoma viral oncogene homolog	11244	0.002	0.15543768
8986	RPS6KA4	ribosomal protein S6 kinase A4	11249	0.002	0.15551914
1846	DUSP4	dual specificity phosphatase 4	11319	0.002	0.15287302
5970	RELA	v-rel avian reticuloendotheliosis viral oncogene homolog A	11324	0.002	0.15292749
10368	CACNG3	calcium voltage-gated channel auxiliary subunit gamma 3	11336	0.002	0.15268724
5568	PRKACG	protein kinase cAMP-activated catalytic subunit gamma	11476	0.001	0.14708045

8074	FGF23	fibroblast growth factor 23	11491	0.001	0.14666532
1386	ATF2	activating transcription factor 2	11560	0.001	0.14397849
8912	CACNA1H	calcium voltage-gated channel subunit alpha1 H	11822	359000000000.000	0.13317935
1844	DUSP2	dual specificity phosphatase 2	11865	268000000000.000	0.13147035
2252	FGF7	fibroblast growth factor 7	12005	-293000000000.000	0.1256969
2122	MECOM	MDS1 and EVI1 complex locus	12351	-895000000000.000	0.11147986
8911	CACNA1I	calcium voltage-gated channel subunit alpha1 I	12371	-950000000000.000	0.110820375
84867	PTPN5	protein tyrosine phosphatase, non-receptor type 5	12426	-0.001	0.10872375
5534	PPP3R1	protein phosphatase 3 regulatory subunit B, alpha	12668	-0.002	0.09894022
2256	FGF11	fibroblast growth factor 11	12712	-0.002	0.09739785
7186	TRAF2	TNF receptor associated factor 2	12718	-0.002	0.097437434
627	BDNF	brain-derived neurotrophic factor	12831	-0.002	0.09307656
774	CACNA1B	calcium voltage-gated channel subunit alpha1 B	12953	-0.002	0.08838522
5601	MAPK9	mitogen-activated protein kinase 9	12958	-0.002	0.08855926
5156	PDGFRA	platelet derived growth factor receptor alpha	12970	-0.003	0.088446036
408	ARRB1	arrestin, beta 1	13040	-0.003	0.085947625
5599	MAPK8	mitogen-activated protein kinase 8	13156	-0.003	0.08157931
8817	FGF18	fibroblast growth factor 18	13158	-0.003	0.0819501
5532	PPP3CB	protein phosphatase 3 catalytic subunit beta	13268	-0.003	0.07787359
4772	NFATC1	nuclear factor of activated T-cells, cytoplasmic, calcineurin-dependent 1	13278	-0.003	0.0779574
4208	MEF2C	myocyte enhancer factor 2C	13444	-0.004	0.07162491
3551	IKBKB	inhibitor of kappa light polypeptide gene enhancer in B-cells, kinase beta	13462	-0.004	0.07145085
5881	RAC3	ras-related C3 botulinum toxin substrate 3 (rho family, small GTP binding protein Rac3)	13610	-0.004	0.06592801
784	CACNB3	calcium voltage-gated channel auxiliary subunit beta 3	13910	-0.005	0.054186627
836	CASP3	caspase 3	13927	-0.005	0.054217048
2263	FGFR2	fibroblast growth factor receptor 2	13965	-0.005	0.053389404
4915	NTRK2	neurotrophic tyrosine kinase, receptor, type 2	14153	-0.006	0.046392094
9965	FGF19	fibroblast growth factor 19	14163	-0.006	0.046795897
3306	HSPA2	heat shock protein family A (Hsp70) member 2	14436	-0.006	0.036369722
9254	CACNA2D2	calcium voltage-gated channel auxiliary subunit alpha2delta 2	14605	-0.007	0.030336963
2253	FGF8	fibroblast growth factor 8	14787	-0.007	0.02382762
2257	FGF12	fibroblast growth factor 12	14946	-0.008	0.018339701
2317	FLNB	filamin B	14952	-0.008	0.019213421
2246	FGF1	fibroblast growth factor 1	15035	-0.008	0.016920274
2251	FGF6	fibroblast growth factor 6	15046	-0.008	0.017624982
5605	MAP2K2	mitogen-activated protein kinase kinase 2	15068	-0.008	0.017882572
3725	JUN	jun proto-oncogene	15414	-0.009	0.0048143677
7157	TP53	tumor protein p53	15485	-0.009	0.0032063094

8913	CACNA1G	calcium voltage-gated channel subunit alpha1 G	15498	-0.010	0.004012888
27006	FGF22	fibroblast growth factor 22	15562	-0.010	0.0027241355
5535	PPP3R2	protein phosphatase 3 regulatory subunit B, beta	15735	-0.010	-0.003015929
2258	FGF13	fibroblast growth factor 13	15853	-0.011	- 0.0064195893
9175	MAP3K13	mitogen-activated protein kinase kinase kinase 13	15930	-0.011	-0.008082654
59283	CACNG8	calcium voltage-gated channel auxiliary subunit gamma 8	15935	-0.011	- 0.0067516705
3925	STMN1	stathmin 1	15986	-0.011	- 0.0073111122
283748	PLA2G4D	phospholipase A2 group IVD	16072	-0.011	-0.009293311
4893	NRAS	neuroblastoma RAS viral (v-ras) oncogene homolog	16097	-0.011	-0.008728041
929	CD14	CD14 molecule	16137	-0.011	-0.008775188
4790	NFKB1	nuclear factor of kappa light polypeptide gene enhancer in B-cells 1	16234	-0.012	-0.011152871
208	AKT2	v-akt murine thymoma viral oncogene homolog 2	16396	-0.012	-0.016161518
6300	MAPK12	mitogen-activated protein kinase 12	16696	-0.013	-0.026770143
55799	CACNA2D3	calcium voltage-gated channel auxiliary subunit alpha2delta 3	16828	-0.014	-0.0303306
5154	PDGFA	platelet derived growth factor subunit A	17163	-0.015	-0.04216443
7042	TGFB2	transforming growth factor beta 2	17253	-0.015	-0.043761365
775	CACNA1C	calcium voltage-gated channel subunit alpha1 C	17345	-0.016	-0.045399915
2260	FGFR1	fibroblast growth factor receptor 1	17433	-0.016	-0.046826407
783	CACNB2	calcium voltage-gated channel auxiliary subunit beta 2	17523	-0.016	-0.048285425
356	FASLG	Fas ligand	17675	-0.017	-0.052241728
1847	DUSP5	dual specificity phosphatase 5	17817	-0.017	-0.05571387
5921	RASA1	RAS p21 protein activator 1	17902	-0.018	-0.056783155
2248	FGF3	fibroblast growth factor 3	17997	-0.018	-0.058220573
5880	RAC2	ras-related C3 botulinum toxin substrate 2 (rho family, small GTP binding protein Rac2)	18039	-0.018	-0.057432074
3265	HRAS	Harvey rat sarcoma viral oncogene homolog	18212	-0.019	-0.06198983
5600	MAPK11	mitogen-activated protein kinase 11	18296	-0.019	-0.06280471
93589	CACNA2D4	calcium voltage-gated channel auxiliary subunit alpha2delta 4	18463	-0.020	-0.066966355
2002	ELK1	ELK1, ETS transcription factor	18612	-0.021	-0.07028573
26291	FGF21	fibroblast growth factor 21	18656	-0.021	-0.06921322
782	CACNB1	calcium voltage-gated channel auxiliary subunit beta 1	19411	-0.024	-0.09723639
27092	CACNG4	calcium voltage-gated channel auxiliary subunit gamma 4	19460	-0.024	-0.09588268
11221	DUSP10	dual specificity phosphatase 10	19490	-0.025	-0.09372384
4149	MAX	MYC associated factor X	19730	-0.026	-0.1001044
2768	GNA12	G protein subunit alpha 12	19786	-0.026	-0.09879063
2316	FLNA	filamin A	19849	-0.027	-0.097732104
80824	DUSP16	dual specificity phosphatase 16	19874	-0.027	-0.09507861
4908	NTF3	neurotrophin 3	20061	-0.028	-0.099036135

6654	SOS1	SOS Ras/Rac guanine nucleotide exchange factor 1	20067	-0.028	-0.0954683
2247	FGF2	fibroblast growth factor 2	20865	-0.033	-0.12410476
55970	GNG12	G protein subunit gamma 12	20973	-0.033	-0.12396019
9479	MAPK8IP1	mitogen-activated protein kinase 8 interacting protein 1	21026	-0.034	-0.121482514
1616	DAXX	death-domain associated protein	21057	-0.034	-0.11806048
8550	MAPKAPK5	mitogen-activated protein kinase-activated protein kinase 5	21337	-0.036	-0.12468304
6885	MAP3K7	mitogen-activated protein kinase kinase kinase 7	21388	-0.037	-0.12173034
1848	DUSP6	dual specificity phosphatase 6	21523	-0.038	-0.12211614
4775	NFATC3	nuclear factor of activated T-cells, cytoplasmic, calcineurin-dependent 3	21541	-0.038	-0.11762262
5533	PPP3CC	protein phosphatase 3 catalytic subunit gamma	21783	-0.040	-0.12213398
51701	NLK	nemo-like kinase	21823	-0.041	-0.11820009
4803	NGF	nerve growth factor	21850	-0.041	-0.11369464
5908	RAP1B	RAP1B, member of RAS oncogene family	21950	-0.042	-0.11211199
2254	FGF9	fibroblast growth factor 9	21957	-0.042	-0.10665579
1399	CRKL	v-crk avian sarcoma virus CT10 oncogene homolog-like	22015	-0.042	-0.103234515
11184	MAP4K1	mitogen-activated protein kinase kinase kinase 1	22226	-0.044	-0.1058782
26281	FGF20	fibroblast growth factor 20	22234	-0.045	-0.100065276
1849	DUSP7	dual specificity phosphatase 7	22435	-0.047	-0.10194425
10912	GADD45G	growth arrest and DNA damage inducible gamma	22725	-0.051	-0.10696277
5613	PRKX	protein kinase, X-linked	22746	-0.051	-0.100766316
10235	RASGRP2	RAS guanyl releasing protein 2	22764	-0.052	-0.094406635
5607	MAP2K5	mitogen-activated protein kinase kinase 5	22776	-0.052	-0.08776823
468	ATF4	activating transcription factor 4	22810	-0.052	-0.08197386
3727	JUND	jun D proto-oncogene	22846	-0.053	-0.076184146
4216	MAP3K4	mitogen-activated protein kinase kinase kinase 4	22904	-0.054	-0.07119045
5578	PRKCA	protein kinase C alpha	23050	-0.056	-0.06953261
3312	HSPA8	heat shock protein family A (Hsp70) member 8	23066	-0.056	-0.062442154
4609	MYC	v-myc avian myelocytomatosis viral oncogene homolog	23176	-0.058	-0.059011027
994	CDC25B	cell division cycle 25B	23215	-0.059	-0.052543826
22800	RRAS2	related RAS viral (r-ras) oncogene homolog 2	23250	-0.059	-0.04581202
6237	RRAS	related RAS viral (r-ras) oncogene homolog	23415	-0.064	-0.043904167
3315	HSPB1	heat shock protein family B (small) member 1	23488	-0.066	-0.03790336
5567	PRKACB	protein kinase cAMP-activated catalytic subunit beta	23795	-0.076	-0.040178865
5924	RASGRF2	Ras protein specific guanine nucleotide releasing factor 2	23835	-0.078	-0.03115253
10125	RASGRP1	RAS guanyl releasing protein 1	23842	-0.078	-0.020726288
59285	CACNG6	calcium voltage-gated channel auxiliary subunit gamma 6	24026	-0.087	-0.016403418
10000	AKT3	v-akt murine thymoma viral oncogene homolog 3	24179	-0.101	-0.008880179
2005	ELK4	ELK4, ETS transcription factor	24204	-0.105	0.0044891406

5.1.5 Supplementary Table III-2c: ES and rank scores for genes in the chemokine signaling pathway

PROBE	GENE SYMBOL	GENE TITLE	RANK IN GENE LIST	RANK METRIC SCORE	RUNNING ES
6655	SOS2	SOS Ras/Rho guanine nucleotide exchange factor 2	218	0.121	0.011438798
6777	STAT5B	signal transducer and activator of transcription 5B	314	0.107	0.025648568
3717	JAK2	Janus kinase 2	326	0.106	0.04311809
5580	PRKCD	protein kinase C delta	367	0.102	0.058749933
7409	VAV1	vav guanine nucleotide exchange factor 1	411	0.099	0.07365365
10451	VAV3	vav guanine nucleotide exchange factor 3	444	0.096	0.08849276
3055	HCK	HCK proto-oncogene, Src family tyrosine kinase	512	0.091	0.10106315
58191	CXCL16	C-X-C motif chemokine ligand 16	593	0.085	0.11215416
6774	STAT3	signal transducer and activator of transcription 3 (acute-phase response factor)	626	0.083	0.124904655
1147	CHUK	conserved helix-loop-helix ubiquitous kinase	633	0.083	0.13868468
3576	CXCL8	C-X-C motif chemokine ligand 8	652	0.082	0.15178001
3577	CXCR1	chemokine (C-X-C motif) receptor 1	756	0.077	0.16056749
5058	PAK1	p21 protein (Cdc42/Rac)-activated kinase 1	801	0.075	0.17142072
1230	CCR1	chemokine (C-C motif) receptor 1	882	0.072	0.18030214
5595	MAPK3	mitogen-activated protein kinase 3	938	0.070	0.18984975
2185	PTK2B	protein tyrosine kinase 2 beta	963	0.069	0.20055221
2783	GNB2	G protein subunit beta 2	970	0.069	0.21195896
57580	PREX1	phosphatidylinositol-3,4,5-trisphosphate-dependent Rac exchange factor 1	983	0.068	0.2230366
94235	GNG8	G protein subunit gamma 8	999	0.068	0.2338696
5894	RAF1	Raf-1 proto-oncogene, serine/threonine kinase	1185	0.062	0.23663521
1794	DOCK2	dedicator of cytokinesis 2	1367	0.057	0.23871137
7454	WAS	Wiskott-Aldrich syndrome	1396	0.056	0.24701689
54331	GNG2	G protein subunit gamma 2	1462	0.055	0.25356865
10344	CCL26	C-C motif chemokine ligand 26	1501	0.054	0.26109427
2870	GRK6	G protein-coupled receptor kinase 6	1507	0.054	0.26997265
6366	CCL21	C-C motif chemokine ligand 21	1557	0.053	0.27685428
1237	CCR8	chemokine (C-C motif) receptor 8	1719	0.050	0.27857915
4067	LYN	LYN proto-oncogene, Src family tyrosine kinase	1740	0.049	0.2860978
156	ADRBK1	adrenergic, beta, receptor kinase 1	1789	0.049	0.2923229
5879	RAC1	ras-related C3 botulinum toxin substrate 1 (rho family, small GTP binding protein Rac1)	1847	0.048	0.29801714
2826	CCR10	chemokine (C-C motif) receptor 10	1873	0.047	0.30498856
9844	ELMO1	engulfment and cell motility 1	1977	0.046	0.30849022

2932	GSK3B	glycogen synthase kinase 3 beta	2042	0.045	0.31345806
10850	CCL27	C-C motif chemokine ligand 27	2116	0.044	0.3178718
59345	GNB4	G protein subunit beta 4	2172	0.043	0.3229155
5330	PLCB2	phospholipase C beta 2	2209	0.043	0.32867756
7852	CXCR4	chemokine (C-X-C motif) receptor 4	2288	0.042	0.33254147
5594	MAPK1	mitogen-activated protein kinase 1	2386	0.041	0.33540875
207	AKT1	v-akt murine thymoma viral oncogene homolog 1	2494	0.040	0.33765525
2885	GRB2	growth factor receptor bound protein 2	2495	0.040	0.34433612
23236	PLCB1	phospholipase C beta 1	2637	0.038	0.34494045
2919	CXCL1	C-X-C motif chemokine ligand 1	2688	0.038	0.34923044
2784	GNB3	G protein subunit beta 3	2838	0.036	0.34912714
1398	CRK	v-crk avian sarcoma virus CT10 oncogene homolog	2855	0.036	0.35450387
5290	PIK3CA	phosphatidylinositol-4,5-bisphosphate 3-kinase catalytic subunit alpha	2875	0.036	0.35973102
5294	PIK3CG	phosphatidylinositol-4,5-bisphosphate 3-kinase catalytic subunit gamma	2905	0.035	0.3644924
5829	PXN	paxillin	2949	0.035	0.3686076
2787	GNG5	G protein subunit gamma 5	2970	0.035	0.37363783
2773	GNAI3	G protein subunit alpha i3	3027	0.034	0.3770849
51764	GNG13	G protein subunit gamma 13	3062	0.034	0.38139
2309	FOXO3	forkhead box O3	3194	0.033	0.38147116
196883	ADCY4	adenylate cyclase 4	3284	0.032	0.38315174
5291	PIK3CB	phosphatidylinositol-4,5-bisphosphate 3-kinase catalytic subunit beta	3347	0.031	0.3858678
23533	PIK3R5	phosphoinositide-3-kinase regulatory subunit 5	3572	0.030	0.3815928
6346	CCL1	C-C motif chemokine ligand 1	3577	0.030	0.38643363
6093	ROCK1	Rho associated coiled-coil containing protein kinase 1	3601	0.029	0.39046004
4792	NFKBIA	NFKB inhibitor alpha	3611	0.029	0.3950577
2869	GRK5	G protein-coupled receptor kinase 5	3673	0.029	0.3974369
998	CDC42	cell division cycle 42	3976	0.027	0.3894948
3579	CXCR2	chemokine (C-X-C motif) receptor 2	4221	0.026	0.38372058
6375	XCL1	X-C motif chemokine ligand 1	4311	0.025	0.38428256
2920	CXCL2	C-X-C motif chemokine ligand 2	4392	0.025	0.38512826
6357	CCL13	C-C motif chemokine ligand 13	4448	0.024	0.38696355
5590	PRKCZ	protein kinase C zeta	4520	0.024	0.3880743
2793	GNGT2	G protein subunit gamma transducin 2	4557	0.024	0.3906022
6370	CCL25	C-C motif chemokine ligand 25	4647	0.023	0.39084518
6369	CCL24	C-C motif chemokine ligand 24	4711	0.023	0.39210945
5293	PIK3CD	phosphatidylinositol-4,5-bisphosphate 3-kinase catalytic subunit delta	4877	0.022	0.3889987
7410	VAV2	vav guanine nucleotide exchange factor 2	4971	0.022	0.38880992
6714	SRC	SRC proto-oncogene, non-receptor tyrosine kinase	5039	0.021	0.3896404

2791	GNG11	G protein subunit gamma 11	5080	0.021	0.39155492
729230	CCR2	chemokine (C-C motif) receptor 2	5156	0.021	0.39196363
5566	PRKACA	protein kinase cAMP-activated catalytic subunit alpha	5305	0.020	0.3892242
6773	STAT2	signal transducer and activator of transcription 2	5357	0.020	0.3904689
7074	TIAM1	T-cell lymphoma invasion and metastasis 1	5382	0.020	0.3928156
8517	IKBKG	inhibitor of kappa light polypeptide gene enhancer in B-cells, kinase gamma	5925	0.018	0.3733217
114	ADCY8	adenylate cyclase 8 (brain)	5980	0.017	0.3740253
6367	CCL22	C-C motif chemokine ligand 22	6170	0.017	0.36899358
10563	CXCL13	C-X-C motif chemokine ligand 13	6344	0.016	0.36452243
5331	PLCB3	phospholipase C beta 3	6392	0.016	0.36523885
3718	JAK3	Janus kinase 3	6470	0.015	0.36465907
2770	GNAI1	G protein subunit alpha i1	6689	0.015	0.3581151
3627	CXCL10	C-X-C motif chemokine ligand 10	6817	0.014	0.35527328
6376	CX3CL1	C-X3-C motif chemokine ligand 1	7008	0.014	0.3497077
53358	SHC3	SHC (Src homology 2 domain containing) transforming protein 3	7035	0.014	0.3509181
6355	CCL8	C-C motif chemokine ligand 8	7050	0.013	0.35261673
2931	GSK3A	glycogen synthase kinase 3 alpha	7108	0.013	0.3525012
6356	CCL11	C-C motif chemokine ligand 11	7316	0.013	0.34605935
6363	CCL19	C-C motif chemokine ligand 19	7355	0.013	0.3466018
111	ADCY5	adenylate cyclase 5	7380	0.012	0.34771082
6372	CXCL6	C-X-C motif chemokine ligand 6	7790	0.011	0.332659
131890	GRK7	G protein-coupled receptor kinase 7	7843	0.011	0.33237827
6351	CCL4	C-C motif chemokine ligand 4	7869	0.011	0.333206
3845	KRAS	Kirsten rat sarcoma viral oncogene homolog	7881	0.011	0.33460745
108	ADCY2	adenylate cyclase 2 (brain)	7906	0.011	0.3354586
5579	PRKCB	protein kinase C beta	8045	0.011	0.33151978
5296	PIK3R2	phosphoinositide-3-kinase regulatory subunit 2	8233	0.010	0.32545877
2833	CXCR3	chemokine (C-X-C motif) receptor 3	8555	0.009	0.31368193
5604	MAP2K1	mitogen-activated protein kinase kinase 1	8566	0.009	0.3147893
5332	PLCB4	phospholipase C beta 4	8628	0.009	0.31375664
2788	GNG7	G protein subunit gamma 7	8852	0.008	0.30589187
25759	SHC2	SHC (Src homology 2 domain containing) transforming protein 2	8886	0.008	0.30588698
4283	CXCL9	C-X-C motif chemokine ligand 9	9001	0.008	0.30247337
2771	GNAI2	G protein subunit alpha i2	9066	0.008	0.3010968
6011	GRK1	G protein-coupled receptor kinase 1	9380	0.007	0.28925955
9547	CXCL14	C-X-C motif chemokine ligand 14	9646	0.006	0.27929038
6772	STAT1	signal transducer and activator of transcription 1	9809	0.006	0.27352232
5906	RAP1A	RAP1A, member of RAS	9912	0.005	0.27019283

oncogene family					
387	RHOA	ras homolog family member A	10036	0.005	0.26593232
113	ADCY7	adenylate cyclase 7	10039	0.005	0.2666855
6359	CCL15	C-C motif chemokine ligand 15	10219	0.004	0.26002115
8976	WASL	Wiskott-Aldrich syndrome-like	10581	0.004	0.24565682
2786	GNG4	G protein subunit gamma 4	10726	0.003	0.24022906
673	BRAF	B-Raf proto-oncogene, serine/threonine kinase	10732	0.003	0.24055928
2782	GNB1	G protein subunit beta 1	10923	0.003	0.23313293
409	ARRB2	arrestin, beta 2	11155	0.002	0.2239069
6347	CCL2	C-C motif chemokine ligand 2	11281	0.002	0.21901819
5970	RELA	v-rel avian reticuloendotheliosis viral oncogene homolog A	11324	0.002	0.21754967
6361	CCL17	C-C motif chemokine ligand 17	11411	0.001	0.21422556
5568	PRKACG	protein kinase cAMP-activated catalytic subunit gamma	11476	0.001	0.2117836
6846	XCL2	X-C motif chemokine ligand 2	11557	0.001	0.20864157
115	ADCY9	adenylate cyclase 9	11968	40600000000.000	0.19165644
399694	SHC4	SHC (Src homology 2 domain containing) family member 4	12309	-81400000000.000	0.17770317
408	ARRB1	arrestin, beta 1	13040	-0.003	0.14790472
1234	CCR5	chemokine (C-C motif) receptor 5 (gene/pseudogene)	13443	-0.004	0.13189231
109	ADCY3	adenylate cyclase 3	13460	-0.004	0.13188377
3551	IKBKB	inhibitor of kappa light polypeptide gene enhancer in B-cells, kinase beta	13462	-0.004	0.1324989
6374	CXCL5	C-X-C motif chemokine ligand 5	13672	-0.004	0.124585435
2921	CXCL3	C-X-C motif chemokine ligand 3	13713	-0.005	0.12369324
6354	CCL7	C-C motif chemokine ligand 7	14434	-0.006	0.09493738
2785	GNG3	G protein subunit gamma 3	14542	-0.007	0.09163805
643	CXCR5	chemokine (C-X-C motif) receptor 5	14694	-0.007	0.086586766
6387	CXCL12	C-X-C motif chemokine ligand 12	14804	-0.007	0.083330095
6360	CCL16	C-C motif chemokine ligand 16	15905	-0.011	0.039571855
2790	GNG10	G protein subunit gamma 10	15970	-0.011	0.03878284
4893	NRAS	neuroblastoma RAS viral (v-ras) oncogene homolog	16097	-0.011	0.035487734
56288	PARD3	par-3 family cell polarity regulator	16112	-0.011	0.03684071
4790	NFKB1	nuclear factor of kappa light polypeptide gene enhancer in B-cells 1	16234	-0.012	0.033814088
107	ADCY1	adenylate cyclase 1 (brain)	16333	-0.012	0.03179537
5747	PTK2	protein tyrosine kinase 2	16352	-0.012	0.03310246
208	AKT2	v-akt murine thymoma viral oncogene homolog 2	16396	-0.012	0.033395663
9475	ROCK2	Rho associated coiled-coil containing protein kinase 2	16677	-0.013	0.024024887
6464	SHC1	SHC (Src homology 2 domain containing) transforming protein 1	16835	-0.014	0.019848317
9564	BCAR1	breast cancer anti-estrogen resistance 1	17243	-0.015	0.005563962
6364	CCL20	C-C motif chemokine ligand 20	17262	-0.015	0.0074141626
2268	FGR	FGR proto-oncogene, Src family tyrosine kinase	17474	-0.016	0.0013939511

112	ADCY6	adenylate cyclase 6	17643	-0.017	-0.0027322304
6373	CXCL11	C-X-C motif chemokine ligand 11	17720	-0.017	-0.0029982238
4793	NFKBIB	NFKB inhibitor beta	17845	-0.017	-0.0051811957
5880	RAC2	ras-related C3 botulinum toxin substrate 2 (rho family, small GTP binding protein Rac2)	18039	-0.018	-0.010106646
2868	GRK4	G protein-coupled receptor kinase 4	18178	-0.019	-0.012657629
3265	HRAS	Harvey rat sarcoma viral oncogene homolog	18212	-0.019	-0.010830374
56477	CCL28	C-C motif chemokine ligand 28	18321	-0.019	-0.012042116
9560	CCL4L2	chemokine (C-C motif) ligand 4-like 2	18413	-0.020	-0.012476725
10681	GNB5	G protein subunit beta 5	18422	-0.020	-0.009464691
6362	CCL18	C-C motif chemokine ligand 18	19436	-0.024	-0.047339834
2792	GNGT1	G protein subunit gamma transducin 1	19444	-0.024	-0.043516282
2829	XCR1	chemokine (C motif) receptor 1	19618	-0.025	-0.046407893
6348	CCL3	C-C motif chemokine ligand 3	19870	-0.027	-0.052312125
5473	PPBP	pro-platelet basic protein	19878	-0.027	-0.048095997
6654	SOS1	SOS Ras/Rac guanine nucleotide exchange factor 1	20067	-0.028	-0.05123237
1235	CCR6	chemokine (C-C motif) receptor 6	20479	-0.030	-0.063173026
414062	CCL3L3	C-C motif chemokine ligand 3 like 3	20678	-0.032	-0.06605019
8503	PIK3R3	phosphoinositide-3-kinase regulatory subunit 3	20858	-0.033	-0.06793623
55970	GNG12	G protein subunit gamma 12	20973	-0.033	-0.06699931
157	ADRBK2	adrenergic, beta, receptor kinase 2	21587	-0.038	-0.08592737
1232	CCR3	chemokine (C-C motif) receptor 3	21687	-0.039	-0.083379544
10803	CCR9	chemokine (C-C motif) receptor 9	21808	-0.040	-0.08151908
5908	RAP1B	RAP1B, member of RAS oncogene family	21950	-0.042	-0.08033809
1399	CRKL	v-crk avian sarcoma virus CT10 oncogene homolog-like	22015	-0.042	-0.07585135
5197	PF4V1	platelet factor 4 variant 1	22069	-0.043	-0.07082176
6368	CCL23	C-C motif chemokine ligand 23	22305	-0.045	-0.07289121
5196	PF4	platelet factor 4	22562	-0.049	-0.07526246
5613	PRKX	protein kinase, X-linked	22746	-0.051	-0.07418207
10235	RASGRP2	RAS guanyl releasing protein 2	22764	-0.052	-0.06617448
5295	PIK3R1	phosphoinositide-3-kinase regulatory subunit 1	23370	-0.063	-0.080670804
10663	CXCR6	chemokine (C-X-C motif) receptor 6	23489	-0.066	-0.07445463
1524	CX3CR1	chemokine (C-X3-C motif) receptor 1	23618	-0.069	-0.06806984
5567	PRKACB	protein kinase cAMP-activated catalytic subunit beta	23795	-0.076	-0.06248832
1233	CCR4	chemokine (C-C motif) receptor 4	23964	-0.083	-0.055463944
3702	ITK	IL2 inducible T-cell kinase	24051	-0.089	-0.043997724
10000	AKT3	v-akt murine thymoma viral oncogene homolog 3	24179	-0.101	-0.032196235
1236	CCR7	chemokine (C-C motif) receptor 7	24186	-0.103	-0.015113599
6352	CCL5	C-C motif chemokine ligand 5	24257	-0.120	0.002279398

6 CURRICULUM VITAE

PERSONAL DETAILS

Name and Surname: Kristina Geraldine Krause
Date of birth: 17.12.1977
Place of birth: Düsseldorf, Nordrhein-Westfalia, Germany
Marital status: single
Father: Hans-Joachim Krause
Mother: Elvira Renate Krause (née Kant)

SECONDARY EDUCATION

1988-1997 Gymnasium an der Koblenzer Straße, Düsseldorf, Germany
20/06/1997 Abitur

TERTIARY EDUCATION

WS 1997/98 Subject: Psychology
Justus-Liebig-University Gießen, Germany
12/04/2000 *Vordiplom* (BSc) in psychology at Justus-Liebig-University, Gießen, Germany
SS 2000-2002 *Diplom* (MSc) in Psychology at Justus-Liebig-University, Gießen, Germany
• **Title of thesis:** Personal Initiative in the Work Place – A Behavior-Oriented Questionnaire
23/10/2002 Diplom
WS 2003/2005 Subject: Psychology
New School University, Graduate Faculty of Political and Social Science, New York City, NY, USA
Title of research paper: Personal Initiative and Attachment Styles
31/01/2005 Master of Arts in Psychology

7 DEDICATION AND ACKNOWLEDGEMENTS

Scientific work is hardly ever achieved by one individual alone, but develops and evolves in discussion, critical analysis and evaluation with fellow scientists. Hence, I would like to seize this opportunity to extend my gratitude to all those who enabled and inspired this achievement along the way.

First and foremost my heartfelt gratitude extends to my supervisor Prof. Dr. Herta Flor at the Institute of Cognitive and Clinical Neuroscience of the Central Institute for Mental Health of Ruprecht-Karls-University, Heidelberg, Germany for kind support, mentorship and guidance in planning and implementing the projects that make up this doctoral thesis.

Furthermore, I want to thank Martin Diers Ph.D. for mining the imaging and psychometric data for the VBM study, Stephanie Witt Ph.D. and her team from the molecular genetics lab for additional genotyping.

Special thanks go out to my fellow scientists at Kings College London, England. Professor Steven C. R. Williams Ph.D. at the Centre of Neuroimaging Science (CNS) for the opportunity to be part of the pain research unit and Matthew Howard Ph.D. and professor Mick Thacker Ph.D. for mentorship, advice, stimulating discussions and inspiring power breakfast sessions with a steady supply hash browns and HP sauce.

Moreover, I would like to thank professor Tara F. Renton MD and Nadine Khawaja MD for advice and support with all things relating to dental surgery. Special thanks also to professor Fernando Zelaya Ph.D. for mentorship on all things ASL, Duncan Sanders Ph.D. for great teamwork, Stephanie Stephenson for being a phlebotomy genius and the lovely team of radiographers for making the third molar extraction study possible by accommodating the need for flexible scanning time on Friday afternoons.

Further acknowledgement and thanks go to professor Dr. Gunter Schumann and Sylvane Desrivieres Ph.D. at the Social, Genetic and Developmental Psychiatry Centre (SGDP) for mentorship on planning and implementing the gene expression part of the third molar extraction study and genotyping, Anbarasu Lourdusamy Ph.D. and Dr. Carsten Sticht for support and advice on biostatistics, Toni Kim Clarke Ph.D. for advice and support with SNP selection and genotyping and last but not least professor professor Dr. Miriam Kunz for moral support and helpful discussions of the manuscripts.

Finally, I want to thank my family who enabled me to pursue some extraordinary educational opportunities and all the friends who supported me through the whole of it. You know who you are.